A STUDY OF STRAIGHT STABLE CHANNELS AND THEIR INTERACTIONS WITH BRIDGE STRUCTURES
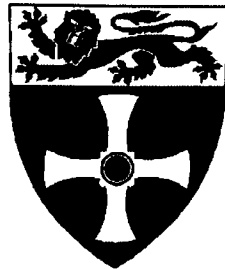
A DISSERTATION SUBMITTED IN PARTIAL FULFILMENT
FOR THE DEGREE OF DOCTOR OF PHILOSOPHY
IN CIVIL ENGINEERING

by:

Kourosh Babaeyan-Koopaei

DEPARTMENT OF CIVIL ENGINEERING
THE UNIVERSITY OF NEWCASTLE UPON TYNE

Abstract

This thesis concerns a carefully controlled set of experiments, to study in detail the characteristics of straight stable channels and the alterations occurring in these channels due to the presence of hydraulic structures e.g. bridge piers, and abutments. A unique feature of the experiments is the mobility of the entire cross-section.

The experimental data from present study are used to verify the characteristics of straight stable channels and the validity of the White et al (1981) theory and other published formulae for the prediction of the characteristics of these channels. The results show that the White et al (1981) theory is a useful tool for prediction of the hydraulic and geometric dimensions of stable straight channels. However, this theory underpredicts the water surface width, cross-sectional area, and sediment concentration of the laboratory channels for the range of applied discharges. It also overpredicts mean depth and water surface slopes. A bank profile investigation of the developed channels show that, for the prediction of bank profile, the fifth-degree polynomial of Diplas and Vigilar (1992) results in a better approximation than that obtained from the normal-depth method and the cosine profile. A hyperbolic function has been fitted to the bank profile data. This function approximates the bank profile even closer than the fifth-degree polynomial of Diplas and Vigilar (1992).

The effect of the introduction of hydraulic structures e.g. bridge piers or abutments into the bed of developed channels and the instabilities produced was investigated. The interaction of piers and developed channels reveals that the main abrupt change in channel bed and bank is because of scour hole formation. An increase in channel width downstream of piers is observed. The rate of this increase is high initially and reduces thereafter. A mathematical model has been proposed to predict the temporal variation of scour depth in clear water and live bed scour conditions. This model, when compared with available data, predicts satisfactory results for most conditions.

Scour topography due to the interaction of abutments and developed straight channels shows that the channel bank upstream of abutments was mainly scoured because of slowly circulating water ahead of the abutment. An equation is proposed to predict this scoured area.

TABLE OF CONTENTS

Contents   **Page**

Chapter One
Introduction

Chapter Two
Literature Review

Chapter Three
Rational Approaches to the Design of Stable Channels

i

Contents   Page

Chapter Four
Experimental Design and Data Description

Chapter Five
Self-Formed Laboratory Straight Stable Channels

Contents   Page

Chapter Six
The Characteristics of Alternate Bars in Alluvial Channels with Loose Boundaries

Chapter Seven
Interaction of Bridge Piers with Laboratory Channels

Contents   Page

Chapter Eight
Interaction of Abutments with Laboratory Channels

Chapter Nine
Conclusions and Recommendations for Future Work

Notation

The following symbols are used in this thesis :

A	Area of cross section, a constant
A_s	Area of scour hole
a	Abutment length, scoured length upstream of abutment
a'	Length of abutment projected normal to flow
B	Water surface width of channel
B_s	Stable width of alluvial stream
b	Pier width, scour width upstream of abutment
b_s	Bottom width of scour hole
b'	Projected pier width
C	Sediment concentration
C_D	Drag coefficient of particle
C_L	Lift coefficient
D	Mean depth of channel, pier diameter, sediment diameter
D_c	Channel depth in bed region
D_{g_r}	Dimensionless particle size
D_v	Diameter of primary vortex
d	Sediment size of bed material, flow depth
d_{av}	Average scour depth
d_S	Scour depth
d_{smax}	Maximum scour depth
$d*_{se}$	Maximum equilibrium scour depth
d_{50}	Mean bed material size
d_n	Sediment size of bed material (n% finer)
F	Froude number
F_b	Bed factor and equal to $1.9\sqrt{d}$
F_{g_o}	Critical grain Froude number
F_{g_r}	Dimensionless particle mobility
F_r	Froude number
F_{rc}	Critical Froude number
f	Silt factor
f'	Friction factor
G_{g_r}	Dimensionless sediment transport rate
g	Gravitational acceleration
H_B	Bar height
h	Water depth
K_d	Sediment size factor
K_I	Flow intensity factor
K_{ps}	Pier spacing factor

K_S	Pier shape coefficient
K_y	Flow depth factor
$K\alpha$	Pier alignment coefficient, shape factor
K_σ	Sediment gradation factor
K_Φ	Skew factor
κ	von Karman constant
k_s	Equivalent sand grain roughness
L	Pier length, abutment length, bar wavelength
n	Manning's roughness coefficient
P	Wetted perimeter, Total stream power of a channel reach
$P_{o,t}$	Average probability of movement of particle at time t
P_b	channel bed wetted perimeter
P_n	Boundary cross sectional length
P_w	channel wall wetted perimeter
Q	Water discharge
Q_s	Sediment discharge
q	Water discharge per unit width
q_S	Sediment discharge per unit width
R	Hydraulic radius
R_s	Submerged specific gravity of sediment
r	A ratio which defines downstream flow depth
r_o	Radius of vortex core
S	Hydraulic gradient
SF_b	Shear force acting on a channel bed
SF_w	Shear force acting on channel side walls
S_f	Energy gradient
S_v	Valley slope
SD	Standard deviation
S^*	Maximum scour depth
s	Specific gravity of the sediment
t^*	Time required by single sediment to move by vortex action
U	Average flow velocity of the channel
U_a	Mean approach flow velocity at armour peak
U_c	Mean approach flow velocity at threshold condition
U_{ca}	Mean approach flow velocity beyond which armouring of bed is impossible
U_o	Mean approach flow velocity
U_{oc}	Critical mean velocity for particle entrainment
U_*	Shear velocity
U_{*c}	Critical Shear velocity
$U_{*,t}$	Shear velocity at time t
u_{max}	Surface velocity
u_y	Mean velocity at elevation y

V	Velocity of flow
V_s	Volume of scour hole
V_*	Shear velocity
V_{max}	Downflow velocity
X	Sediment concentration
$\overline{X}$	Average sediment concentration
x	Transverse co-ordinate
Y	Approach flow depth
y	Lateral distance from the centre of channel on horizontal plane, vertical co-ordinate
y_1	Average depth in main channel
y_2	Average depth in contracted section
y_e	Equilibrium contraction depth
y_O	Uniform flow depth
y_r	Regime flow depth
y_S	Scour depth
Z	Side slope of a trapezoidal section (Z horizontal to 1 vertical)
z	vertical co-ordinate
W_{c_1}	Bottom width of main channel
W_{c_2}	Bottom width of contracted section
W_s	Top width of scour hole
w	Width of abutment in flow direction
α	Angle of attack , Bridge opening ratio, slope of scour hole
β	Ratio of hydrodynamic lift and drag forces, $\dfrac{B}{2h}$
β_c	Critical value of β
γ	Specific weight of fluid
γ_s	Specific weight of sediment
Δ	relative density of sediment particle in water
Δ_{AB}	Total height of alternate bar
Λ_D	Dune wavelength
Λ_M	Meander wavelength
λ	Transverse spacing of sand ribbons
ρ	Density of water
ρ_s	Density of sediment
τ_o	Shear stress
τ_c	Critical shear stress
τ_*	Shear stress, Shield stress
τ_b	Bed shear stress
$\overline{\tau}_b$	Average bed shear stress
σ_g	Geometric standard deviation of bed material, equal to $\dfrac{d_{84.1}}{d_{50}} = \dfrac{d_{50}}{d_{15.9}}$
ν	Kinematic viscosity

θ	Lateral inclination of element, Shield's parameter
θ_c	Critical Shield's parameter
η_B	Equal to $\dfrac{\theta_B}{\theta_c}$, ratio of Shield's factor characterising bar forming to critical Shield's factor
Γ_o	Circulation around the vortex core
Φ	Dimensionless sediment discharge, angle of repose of bed material
μ	submerged static coefficient of coulomb friction
ω	Fall velocity of sediment

Acknowledgements

Chapter One
Introduction

1.1 Background

Rivers have always been at the centre of human attention. As Man found that rivers can supply water necessary for irrigation, consumption, and washing, he began to establish the first societies near rivers. As Mankind's utilisation of the water of the rivers increased, he started to change the configuration of them without any appreciation of their intrinsic nature. Since the time when man first encountered problems associated with the effects of using these rivers, he began to tackle these problems. Thus, Hydraulic Engineering has been for many centuries, concerned with the problems of river utilisation. Attempts to understand the nature of rivers, in order to use them properly, have a long history. It has been found that using rivers without proper knowledge of their intrinsic natures not only does not profit human beings but also can cause loss of life and property.

Among those problems that hydraulic engineers have focused on, are those that have been connected with introducing manmade structures into rivers. Structures like bridge piers, abutments, spurs, dikes, etc. affect the velocity distribution and flow pattern across the river. They can therefore change the geometry of rivers as they flow over a loose bed. Determining the alterations caused in river geometry, by the interaction of rivers and man-made structures, has been the subject of much research during recent decades.

Among man-made hydraulic structures, bridges and their hydraulic problems have been given specific attention by hydraulic engineers. In earlier times, hydraulic problems of bridges were avoided as much as possible by providing generous lengths for bridges and selecting bridge sites where rivers were generally stable. Nowadays these policies have changed toward a minimum possible length for bridges because increasing the width and the height of the bridges makes their construction cost higher. The need to keep the bridge length as small as possible

has resulted in the encroachment of road embankments into the river channel. This encroachment constricts the flow and intensifies erosion problems at bridge sites. Erosion or scouring is a natural phenomenon caused by water running over the loose boundary of a river bed and bank. The water transports loose material along with it. This effect is more intense in alluvial rivers and past experience has shown that progressive scouring can gradually undermine the foundation of a bridge pier or its abutments. It can result in failure of the bridge.

In order to conquer scour problems which may arise from the interaction of bridge structures and rivers, it is necessary to understand the nature of rivers and different conditions for their stability as well as the effect of the bridge piers on stream flow and river geometry. A great deal of research has been carried out in the area of river mechanics. Efforts have been made to establish relationships between different values of flow and sediment load from one side and geometric quantities of the rivers from another side. The various achievements with this problem are divided in two major groups, regime and rational methods.

Regime relationships are those that have been established between various geometric parameters of rivers or laboratory channels and their sediment size and discharge when they have been stable or, in other words, when no major problems of siltation or scouring have occurred. Among pioneers in developing this kind of formula were Kennedy (1895), Lindley (1919), and Lacey (1929).

Regime theory was initially based on field measurements of the geometry of canal cross sections at nearly constant discharge mixed with a constant amount of sediment load. So this theory is thoroughly empirical.

In rational approaches, the researchers' efforts have focused on finding a theoretical basis for regime equations. A number of rational equations have been established based on combinations of sediment transport formulae and flow resistance equations with some other empirical relationships [Henderson (1961), Ackers (1964), Kellerhals (1967), Gill (1968), Stevens and Nordin (1990), Farias (1991)].

2

Some of the most recently discussed rational approaches to the design of stable channels are based on the combination of a sediment transport equation, a flow resistance equation and some extremal hypothesis, such as minimisation of energy dissipation rate [Yang and Song (1979)], stream power minimisation [Chang (1980)] or sediment transport maximisation [White, Paris, and Bettess (1981)].

In considering the effect of structures, it should be noted that two different phenomena can be distinguished at bridges sites. The first one is the scour caused by the presence of the bridge piers or abutments on the river bed. Local scour that occurs around bridge piers or abutments is caused by the local obstruction to flow. It can occur in one of two ways: (a) clear water scour and (b) live bed scour. In clear water scour the upstream bed materials are at rest and in live bed scour the bed materials are in transport with water.

The second phenomena is general scour which is due to the imbalance in sediment transport. General scour refers to the changes in river channel geometry caused by sediment imbalance due to natural or manmade causes. This kind of scour may include constriction scour at a bridge site or aggradation and degradation of the stream bed.

Aggradation and degradation are those processes that occur in a river system because of imbalance between sediment transportation in the considered reach and sediment supply from upstream. In degradation the river bed level decreases but in aggradation an increase of bed elevation occurs.

Since at a bridge site different kinds of scour take place, in order to consider scour problems, one should inspect each case separately and then consider their combined effect at a bridge site. At present, because of the complexity of scour phenomena, there is no unique theory which would enable engineers to estimate the depth of scour at bridge sites confidently.

The present research is carried out in order to investigate the alterations occurring in a channel due to presence of bridge structures. The objectives of the investigation are explained in the following.

1.2 Objectives of this study

The broad objective of this research is to conduct a carefully controlled set of experiments, to study in detail the characteristics of straight stable channels and the alterations occurring in these channels due to presence of hydraulic structures e.g. bridge piers, abutments. A unique feature of the experiments in the present study is the presence in the cross-section of mobile bank material. The experiments are carried out with the following major aims:

a) To examine the characteristics of self-formed straight channels in the laboratory.

b) To examine the effect of the introduction of hydraulic structures e.g. bridge piers or abutments into the bed of developed channels and the instabilities produced.

The collected data in part (a) play an important role in study of straight stable channels. These data are used to verify the validity of the WPB [White et. al (1981)] theory, and other published formulae e.g. Parker (1978), Ikdea et al. (1988), for the prediction of the characteristics of straight stable channels. This data is also used to study the bank profile of the developed channels and compare them with recently published numerical approaches, and the velocity and shear stress distributions in them.

To achieve the aim in part (b) the results of part (a) have been used. Bridge piers or abutments are introduced to the bed of the channels in part (a). Without changing the imposed conditions, e.g. discharge, sediment load, the channels are allowed to develop freely, until the rates of change in bed and banks of channels are insignificant. The changes due to presence of the hydraulic structures are evaluated by comparing the data in parts (a) and (b).

It is hoped that the completion of this experimental investigation will provide a precise data set on geometrical characteristics of straight stable channels and also more information on the instabilities of these channels at bridge sites due to the presence of bridge structures.

Chapter Two
Literature Review

2.1 Introduction

The scour phenomena at bridge sites are very complex and involve a combination of different factors e.g. river stability, and general and localised scour. In the following literature survey, topics related to the stability of rivers at bridge sites, are reviewed.

2.2 Alluvial channel stability

In river engineering projects, most of the problems are concerned with determining the cross sectional area, the shape and the slope of the stable channel which will carry a given water and sediment discharge.

There are many definitions for channel stability which are given by different researchers. Lindley's (1919) definition for a stable channel is "when an artificial channel carries silty water, its bed and banks scour or fill, change depth and width until a balanced state is attained". Lane (1953) defined the stable channel as "an unlined earth channel which (a) carries water, (b) its banks and bed are not scoured by water, and (c) there is no sediment deposition in it". Blench (1957) considers a channel "in regime" to be one in which the average values that constitute regime such as discharge, width, depth, slope and meander pattern do not show any definite trend of variation over some time interval.

An enormous effort by different researchers has been carried out on the prediction of the stable channel geometry and the slope of alluvial channels. The various achievements in dealing with the problem can be grouped as (a) regime concepts and (b) rational concepts. In the following paragraphs only recent approaches using rational methods which are of concern to the present work will be considered.

2.2.1 Recent rational methods

In recent years, two major rational approaches have contributed to the work on river regime. They are based on independent equations for the prediction of the cross section of regime channels. The first method is due to Chang (1980) and the second to White, Paris and Bettess (1981). A brief description of each method is given below.

2.2.2 The Chang method

Chang (1980) used three independent conditions for straight channel analysis (1) a sediment discharge formula, (2) a flow resistance formula and (3) the concept of minimum stream power.

For his analytical model he used three different sediment discharge formulae i.e. the Engelund-Hansen (1967) formula, the Einstein-Brown (1950) formula and the Duboys (1879) formula. He used the first formula for stable canals with ripple or dune beds. The other two were used both for canals and rivers. For flow resistance, he also used three formulae: (a) one which was developed by Lacy (1958) for stable canals which are in the lower flow regime (b) the resistance formula of Engelund and Hansen (1967) which covers both lower and upper flow regimes for rivers and (c) the formula of Simons and Richardson (1966) for the transition between the lower and upper flow regimes.

The third independent condition, which was used by Chang (1980), was the concept of minimum stream power. His description of the concept is as follows "for an alluvial channel, the necessary and sufficient condition of equilibrium occurs when the stream power per unit channel length γQS is a minimum subject to given constraints. Hence an alluvial channel with water discharge Q and sediment load Q_S as the independent variables, tends to establish its width, depth and slope such that $\gamma Q S$ is a minimum. Since Q is a given parameter, minimum $\gamma Q S$ also means minimum channel slope S. According to the described conditions, Chang (1980)

developed a computer program which may be used to predict the width, depth and channel slope of regime rivers for a given set of Q and Q_S.

The concept of minimum stream power stated by Chang (1980) was similar to the concept of minimum unit stream power proposed previously by Yang (1971, 1976). In his work, the unit stream power which is the product of velocity and slope ,VS, is minimised. Stream power is the unit stream power integrated over the channel cross-sectional area.

2.2.3 The White, Paris & Bettess (WPB) method

White, Paris and Bettess (1981) developed rational regime relationships for the width, depth and slope of a channel in equilibrium using the Ackers and White (1973) sediment transport formula and the White, Paris and Bettess (1980) friction relationships, together with the principle of maximum sediment transport rate. It was shown in their work that the two principles of maximising transport rate and minimising slope are equivalent and therefore it was concluded that the work relating minimising stream power to minimising the rate of energy dissipation could be used to support the principle of maximising the transport rate.

They declared that if one imposes values of discharge and slope but does not impose the condition of the maximum sediment transport, then there are a family of solutions each with different values of B, X, V and d, only one of them provides the maximum sediment rate.

A computer program was developed to determine the hydraulic and geometric characteristics of alluvial channels which for given values of water discharge, sediment concentration, bed material size, and water temperature the width, depth, velocity, and slope are calculated. It was assumed that the shape of the channel was approximately trapezoidal in cross section, and the hydraulic radius R was used in place of depth D so the values of width and depth were then adjusted to give values corresponding to a trapezoidal section of the same cross section area,

7

where the side slope, Z (Z horizontal to 1 vertical), of the trapezoid was given by Smith's (1974) empirically determined relationship:

$Z=0.5$ For $Q < 1 \ \text{m}^3/\text{s}$

$Z=0.5Q^{0.25}$ For $Q > 1 \ \text{m}^3/\text{s}$

They claimed because the width to depth ratio is generally large, errors introduced by this simplification were not significant. Bettess (Personal Communication) has since discussed the disadvantages of the adjusting procedure. For verification of the WPB method they compared their analytical results with available data and with existing empirical regime relationships derived by fitting curves to data. For comparison, they chose the field data of the Punjab canals, the CHOP canals and Sind canals, the Pakistan canals (ACOP), and the Simons and Bender data for American canals. These field data provided a total of 213 observations. They also used the laboratory data of Ackers (1964), Ackers and Charlton (1970), and Ranga-Raju et al (1977). After comparison, they concluded that:

(a) The predicted slopes or sediment concentrations show scatter when compared with observations, which is not necessarily a deficiency in the method, just that there is a slight tendency toward overestimation of the slopes and underestimation of sediment concentrations.

(b) The prediction of widths are excellent but for very large sand and meandering laboratory channels there is a tendency to underpredict.

2.3 Scouring

Scouring is a natural phenomenon induced by the erosive action of water in rivers and streams. At a bridge site scouring can cause reduction in strength of the

foundation of a bridge. Different types of scour, which may occur at a bridge site, can be classified as follows: (a) Local Scour ,(b) General Scour and (c) Constriction Scour.

Local Scour which may occur by the interference of the piers and abutments with the flow is a result of the interaction between the high velocity flow and the loose bed and consequent modification in the flow pattern. This scour is superimposed on the general and constriction scour.

General scour which may occur because of the increased flow capacity of a river during flood flows or as a consequence of various man made structures or alterations, is a response to flow regime and it may occur whether a structure like a bridge is built or not.

Constriction scour may occur if a structure causes the narrowing of the waterway or channel.

In the following paragraphs previous studies on different types of scour are summarised.

2.3.1 Local scour at bridge piers

As mentioned, the local scour at bridge piers should be added to general scour and constriction scour to obtain the maximum scour depth which is a necessary design parameter for bridge piers. Local scour can occur as clear water scour or live bed scour.

Clear water scour occurs when the bed material upstream of the scour area is at rest, therefore, the bed shear stress outside the scour area is equal to or less than the critical or threshold shear stress for the initiation of particle movement. In clear water scour the maximum scour depth is reached when the flow can no longer remove particles from the scour hole.

Live bed scour occurs when the bed materials are in motion by flow action. In this situation equilibrium scour depths are reached when over a specific period of

time the amount of material removed from the scour hole by the flow equals the amount of the material supplied to the scour hole from upstream.

2.3.2 Live bed scour

Chabert and Engeldinger (1956) appear to have been the first to describe the behavioural pattern of scour at a cylindrical pier in terms of time and velocity, Fig. 2.1. They showed that the clear water scour approaches equilibrium asymptotically, over a period of days, where as the live bed scour develops rapidly and its depth fluctuates in response to the passage of bed features. Shen et al (1969) suggested that the mean value of the live bed scour depth was about 10% less than the maximum clear water scour depth. Raudkivi (1981) suggested that a second peak exists, as shown by the dashed line in Fig. 2.1.
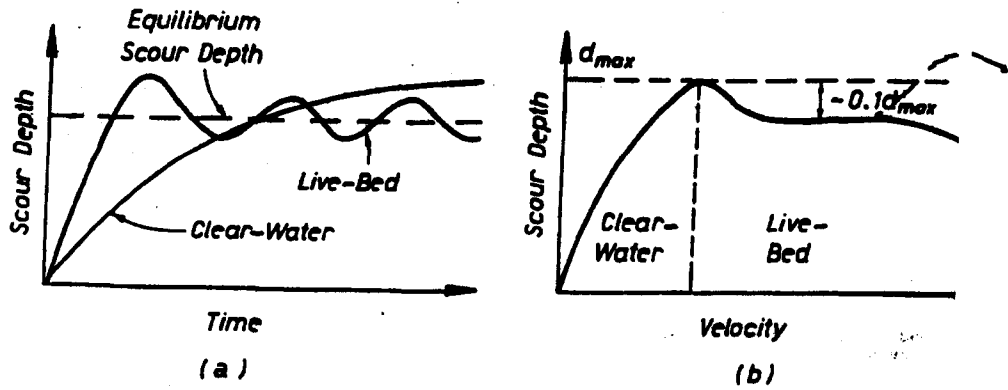
Figure 2.1. Scour depth for a specific pier and sediment size, (a) as a function of time, (b) as a function of shear or approach velocity [after Chabert and Engeldinger (1956)].

The consideration of scour problems, during past investigations, usually started by examining different parameters which characterise the fluid, bed material,

flow and bridge pier. These parameters can be described as follows.

$$d_S = f (\rho , \nu , g , d , \rho_S , y_O , U , b)$$ (2.1)

or in a dimensionless form:

$$\frac{d_s}{b} = f (\frac{U_b}{\nu} , \frac{U^2}{gb} , \frac{y_o}{b} , \frac{d}{b} , \Delta)$$ (2.2)

$$= f (\frac{u_* b}{\nu} , \frac{u_*^2}{g\Delta d} , \frac{y_o}{b} , \frac{d}{b} , \Delta)$$ (2.3)

where d_s is scour depth, $u_* = \sqrt{gy_o S}$ is the shear velocity, y_o is uniform flow depth, Δ is relative density of sediment, d is grain size, and b is pier width.

The published formulae for bridge scour are based on various combinations of the parameters in equation 2.1. Some of these formulae are for clear water scour and some for live bed scour and some may be used for both. Using scour prediction formulae to calculate the depth of scour, for a specified condition, may produce results which differ by a factor of five or more (Raudkivi and Sutherland 1981). The following paragraphs describe a brief summary of published formulae for live bed scour.

2.3.3 Live bed scour formulae

The following equation resulted from the collection of prototype scour data at various bridge sites in India and was proposed by Inglis (1949).

$$d_s = 0.946(\frac{Q}{f})^{\frac{1}{3}} \qquad\qquad (2.4)$$

where d_s is scour depth from the water surface in metres, Q is flood discharge in m³/s, f is a silt factor which is equal to $1.76\sqrt{d}$, and d is mean diameter of bed material in mm. Equation (2.4) is a statement of the fact that the maximum depth around the piers is equal to twice the Lacy regime depth.

Laursen and Toch (1956) from laboratory data with sediment grain sizes of 0.44 mm to 2.25 mm and average velocity of 0.31 to 0.76 m/s proposed a design curve for a square nosed pier aligned with the flow, which Neill (1964) expressed as:

$$d_s = 1.5kb^{0.7}y_o^{0.3} \qquad\qquad (2.5)$$

where $k = k_\alpha k_s$ are the values of the alignment and shape coefficients, y_o is depth of approach flow, and b is pier width.

Laursen's second formula (1958) which was based on analysis of the long contraction solution under conditions of balanced sediment transport in the approach and contracted sections has the following form:

$$\frac{b}{y_o} = 5.5\frac{d_s}{y_o}[(\frac{d_s}{ry_o}+1)^{1.7}-1] \qquad\qquad (2.6)$$

where r is a ratio which defines downstream flow depth as $\frac{1}{r}d_s + y_o$.

Callander (Personal Communication) showed that, by using some approximations, the second Laursen (1958) formula for $r \approx 11.5$ can be simplified to:

$$\frac{d_s}{b} = 1.11(\frac{y_o}{b})^{0.5} \qquad\qquad (2.7)$$

Garde (1961), from a dimensional analysis of the special case when the pier is aligned with the flow, developed the following formula:

$$\frac{d_s}{y_o} = (\frac{4.0\eta_1\eta_2\eta_3}{\alpha})F_r^n - 1 \qquad (2.8)$$

where η_1, η_2, and η_3 are respectively functions of the particle drag coefficient C_D, Froude number and pier shape. The drag coefficient and Froude number are expressed as:

$$C_D = \frac{4}{3}[\frac{(S_s - 1)\rho g d}{r\omega^2}] \qquad (2.9)$$

$$F_r = \frac{U_o}{\sqrt{gy_o}} \qquad (2.10)$$

where ω is the fall velocity of the grain of diameter d, y_o is the depth of approach flow, U_O is the mean approach velocity, $\alpha = (\frac{B-b}{B})$ is the opening ratio, where B is the width at the bridge of the clear channel, and b is the pier width.

The Larras equation (1963) which was based principally on the model experiments of Chabert and Engeldinger (1956) is as follows:

$$d_{se}^* = 1.05Kb^{0.75} \qquad (2.11)$$

where d_{se}^* is the maximum equilibrium scour measured from the mean bed elevation in metres, b is pier width in metres, and K is a multiplying factor which accounts for the shape of the pier and the angle of attack.

Breusers (1965) from laboratory data with 0.1 mm sand and using circular pier proposed the following equation:

$$d_{se}^* = 1.4b \qquad\qquad (2.12)$$

where d_{se}^* is maximum equilibrium scour depth measured from the mean bed elevation and b is the diameter of a circular pier.

Arunachalam (1965) reanalysed the data given by Inglis (1949) and proposed the following formula:

$$\frac{d_s}{y} = 1.95(\frac{b}{y})^{\frac{1}{6}} - 1 \qquad\qquad (2.13)$$

where d_s is the scour depth below the ambient bed level in metres, $y = 1.33(\frac{q^2}{f})^{\frac{1}{3}}$, q is the average discharge intensity in m²/s, f is the silt factor and equal $1.76\sqrt{d}$ where d is the mean diameter of bed material in millimetres.

Blench (1965) used F_b, the bed factor, in place of Lacey's silt factor and presented the following equation:

$$\frac{D_s}{y_r} = 1.8(\frac{b}{y_r})^{\frac{1}{4}} \qquad\qquad \text{For } b < y_r \qquad\qquad (2.14)$$

where D_s is scour depth below the water surface in metres, y_r is regime flow depth and is equal to $1.48(\frac{q^2}{F_b})^{\frac{1}{3}}$, F_b is equal to $1.9\sqrt{d}$, q is the average discharge intensity in m² /s, and d is the mean bed particle diameter in mm.

Shen et al (1969) used laboratory data from other investigators, such as Chabert and Engeldinger (1956), Maza Alvarez and Sanches (1964), Bata (1960), Knezevic (1960), Tison (1960), Chitale (1962) and field data from Neil (1964), Laursen and Toch (1956), and Larras (1963) to present an equation obtained by a least square fit to the data which has the following form:

$$\frac{d_s}{y_o} = 3.4 F_r^{\frac{2}{3}} (\frac{b}{y_o})^{\frac{2}{3}}$$

(2.15)

where F_r is pier Froude number and equal to $\frac{U_o}{\sqrt{gb}}$.

Coleman (1971) from laboratory data with 0.1 mm sand and based on circular piers suggested a correlation between two parameters, the scour Euler number$= \frac{U_o}{\sqrt{2gd_s}}$ and the pier Reynolds number$= \frac{U_o \rho l}{\mu}$, to predict scour. He suggested the following equation:

$$\frac{U_o}{\sqrt{2gd_s}} = 0.6(\frac{U_o}{\sqrt{gb}})^{0.9}$$

(2.16)

where U_O is the mean approach velocity, d_s is the scour depth below the upstream bed level and b is width of the circular pier.

Hancu (1971), from laboratory data with d in the range from 0.5 mm to 5.0 mm and circular piers proposed the following equation:

$$\frac{d_s}{y_o} = 2.42 F_{r_c}^{\frac{2}{3}} (\frac{b}{y_o})^{\frac{2}{3}}$$

(2.17)

$$U_c = C \sqrt{gd(\frac{\rho_s - \rho}{\rho})} (\frac{y_o}{d})^{0.2}$$

(2.18)

where $F_{r_c} = \frac{U_c}{\sqrt{gy_o}}$ and U_c is the velocity at the threshold of grain movement.

Bonasoundas' (1973) comprehensive investigation about scour at circular piers involved both theoretical and experimental work. The experimental work involved a series of model experiments based on the Froude similarity law. His formula for live bed scour is as follows:

15

$$\frac{d_s}{y_o} = a_i (\frac{b}{y_o} - 0.3)^n f_* \tag{2.19}$$

$$\frac{U_c}{U} = \frac{1.285}{F_r} (\frac{b}{y_o})^{0.7} \tag{2.20}$$

where $a_i = 2.0 - 0.88 \frac{U_c}{U}$ for $\frac{U_c}{U} < 1$, b is the pier diameter and f_* is a time factor and a function of $\frac{U_c}{U}$, U_c is the velocity at the threshold of grain movement. Bonasoundas declared that in order to obtain the maximum scour depth the following experiment durations are required.

For $\quad \frac{U_c}{U} > 1 \qquad$ (Clear water condition) $\qquad$ 72 - 96 hours $\qquad$ (2.21)

For $\quad \frac{U_c}{U} < 1 \qquad$ (Live bed condition) $\qquad$ 1 $\quad$ hour $\qquad$ (2.22)

The Colorado State University (CSU) formula (1975) which was derived from the best fit line to the data of Chabert and Engeldinger for sediment sizes between 0.52 and 0.26 mm and the data of CSU for sediment size of 0.24 mm has the following form:

$$\frac{d_s}{y_o} = 2.0 K_1 K_2 (\frac{b}{y_o})^{0.65} F_r^{0.43} \tag{2.23}$$

where d_s is the scour depth, y_o is the flow depth just upstream of the pier, K_1 is a correction for pier shape, K_2 a correction for the angle of attack of the flow, b is the pier width, $F = \frac{V_1}{\sqrt{g y_o}}$ is the Froude number and V_1 is the average velocity just upstream of the pier.

Breusers et al (1977) presented a review of local scour around cylindrical piers and recommended the following relationship:

$$\frac{d_s}{b} = [2.0 Tanh(\frac{y_o}{b})][f_1(\frac{U}{U_c})][f_2(Piershape)][f_3(\alpha, \frac{l}{b})]$$ (2.24)

where U_c is the critical velocity for the initiation of motion given by:

$$U_c = 1.54 d_{50}^{0.3} y_o^{0.2} g^{0.5}$$ (2.25)

The function f_1 is used to differentiate between clear water scour and scour with sediment motion and takes the following form:

$$f_1 = 0 \qquad \text{for} \qquad \frac{U}{U_c} \le 0.5$$ (2.26)

$$f_1 = 2(\frac{U}{U_c}) - 1.0 \qquad \text{for} \qquad 0.5 \le \frac{U}{U_c} \le 1.0$$ (2.27)

$$f_1 = 1.0 \qquad \text{for} \qquad \frac{U}{U_c} \ge 1.0$$ (2.28)

The functions f_2 and f_3 are essentially correction factors for shape and skewness.

Jain and Fischer (1980) conducted a series of experiments on scour at high flow velocities. They used different sizes of circular piers (b=5.08, 10.16 cm) and sand (d_{50} =0.25, 1.5, 2.5 mm). They observed that scour depth did increase at higher flow velocities. From the results of their experiments and dimensional analysis they proposed the following equation for live bed scour:

$$\frac{d_s}{b} = 1.86(\frac{y_o}{b})^{0.5}(F_r - F_{r_c})^{0.2}$$ (2.29)

in which,

$$F_{r_c} = \frac{U_c}{\sqrt{g y_o}}.$$ (2.30)

where U_c is the critical mean velocity for the initiation of the bed particle motion, b is the pier width, and y_o is the approach flow depth.

Raudkivi and Sutherland (1981) compared different live bed formula graphically. This comparison which was made in terms of the Froude number showed that the Coleman formula is more sensitive to relative flow depth ($\frac{b}{y_o}$) than the others. This comparison is shown in Fig 2.2.

Jones (1984) compared several prediction equations for bridge pier and abutment scour. In his comparison he divided the investigated equations into three groups. The first group was based on research, primarily in Pakistan and India, the second group was those of University of Iowa, and the third group was developed at Colorado State University (CSU). The Figs. 2.3 and 2.4 show the comparison.

Fig. 2.3 is for an average depth ratio ($\frac{y}{b}$) of 2.0 and Fig. 2.4 is for an average Froude number of 0.3.

According to the National Co-operative Highway Research Program (NCHRP) synthesis report (1970), to select the most appropriate equations for design, one should use two approaches. First, the equations should be compared to determine which one best matches with field data. Second, in the lack of these data, the conditions under which the equations were derived should be evaluated and the one which matches best with the design conditions should be utilised.

In order to take advantage of the NCHRP recommendation, Jones (1984) compared the indicated three groups of pier scour equations with Louisiana field measurements and at the end he recommended the equations of Laursen (1958), Jain and Fischer (1979), Shen et al (1969) and CSU(1975).

Froehlich (1987), by using the data of 83 field measurements on pier scour, developed the following live bed scour formula:

$$\frac{ds}{b} = 0.32 K_1 (\frac{b'}{b})^{0.62} (\frac{y_o}{b})^{0.46} F_r^{0.2} (\frac{b}{d_{50}})^{0.08} + 1.0 \tag{2.31}$$

in which K_1 is the coefficient of pier type, b is the projected pier width and equal to $b\cos\alpha + L\sin\alpha$, α is the angle of attack, L is the pier length, b is the pier width, y_o is the flow depth, F_r is the Froude number, and d_{50} is the mean bed material size.

Melville and Sutherland (1988) proposed a design method for the estimation of equilibrium depths of local scour at bridge piers based on envelope curves drawn to experimental data derived mostly from laboratory experiments. According to the method, the equilibrium scour depth d_s at a pier can be written in the following form:

$$\frac{d_s}{b} = K_I K_y K_d K_\sigma K_s K_\alpha \qquad (2.32)$$

where the K values are expressions describing the influence of different parameters on the scour depth. K_I is for the flow intensity, K_y is for the flow depth, K_d is for the sediment size, K_σ is for the sediment gradation, and K_s and K_α is for shape and alignment.

In the Federal Highway Administration report (FHWA, 1991), "Evaluating scour at bridges", for the computation of local scour at piers, it referred to the results of Jones' comparison (1984) of scour prediction equations and it is shown that the Colorado State University (CSU) equation encloses all the points when it is compared with field data measurements. Fig. 2.5 shows the results of this comparison. The equations illustrated in Fig. 2.5 do not take into account the possibility that larger sediment sizes in the bed material could armour the scour hole.

The significance of armouring of the scour hole over the long term and during floods is not clear. Therefore, in the report, it is recommended not to use these equations for the indicated situations.

In the FHWA report, the CSU equation is recommended for both live bed and clear water scour. It is also indicated that in the unusual situation where a dune
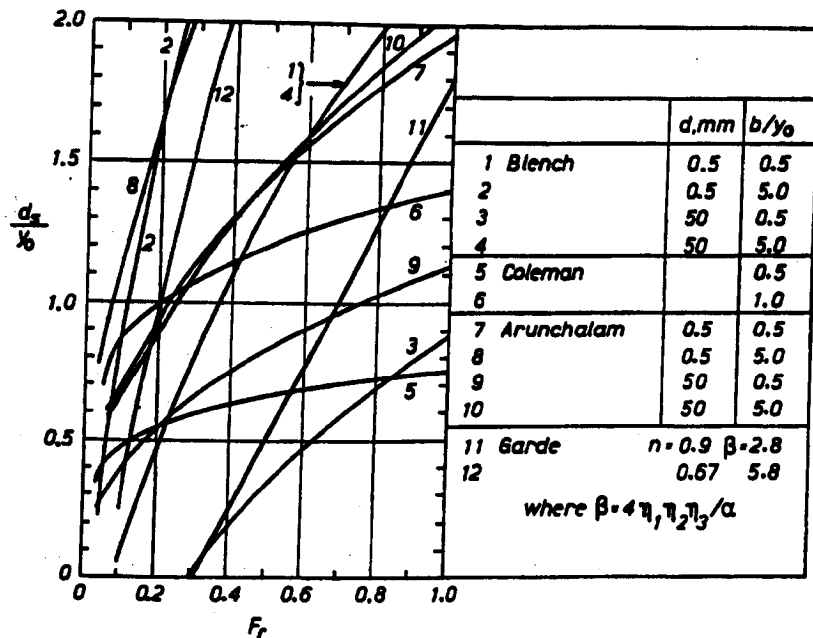
Figure 2.2. Comparison of predictions made using selected live bed scour formulae expressed in terms of the Froude number [after Raudkivi and Sutherland (1981)].
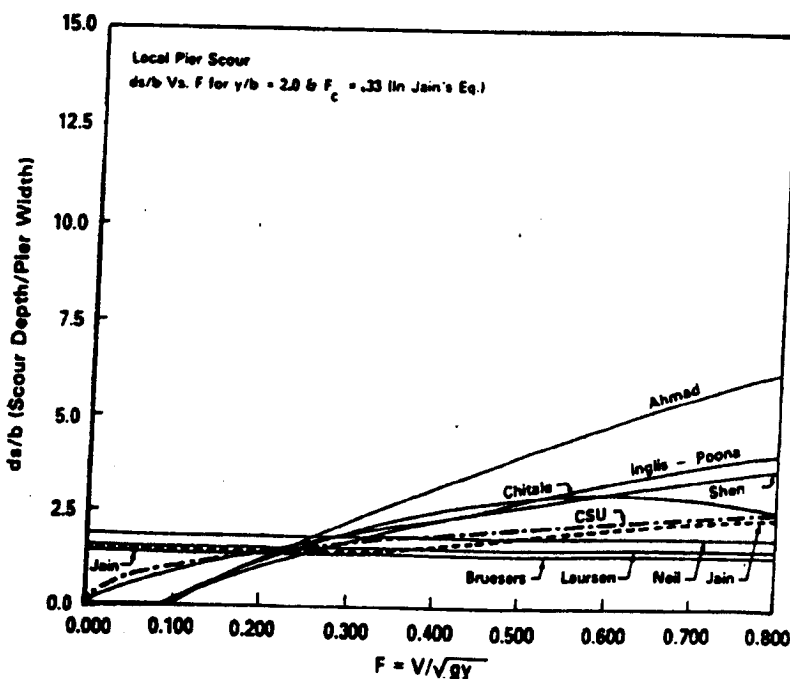

Figure 2.3. Graphical comparison of scour formulae for variable Froude numbers[after Jones (1984)].

20
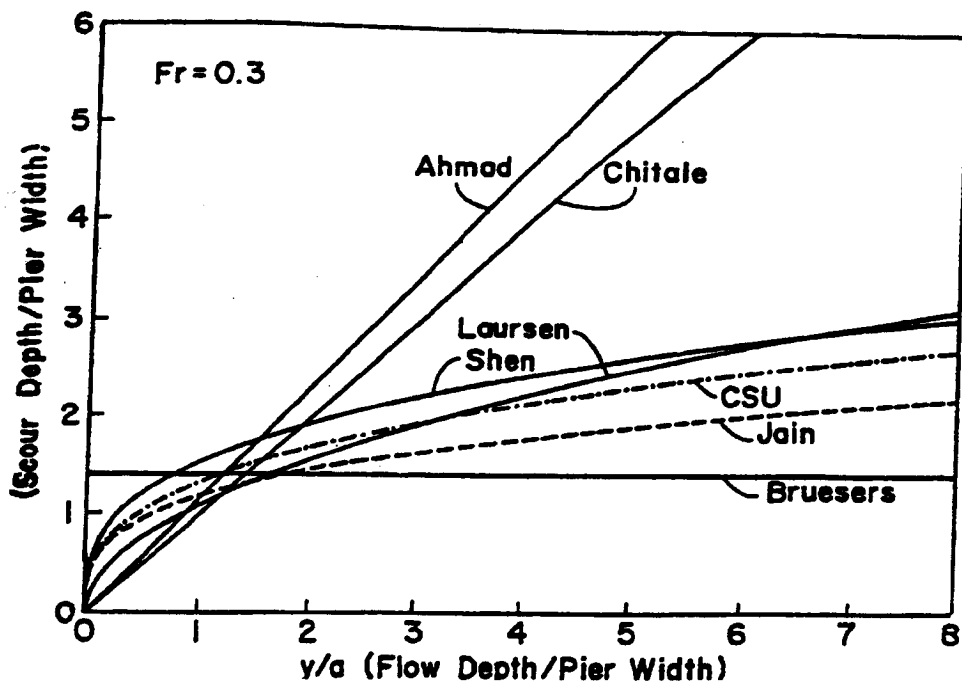
Figure 2.4. Comparison of scour formulae for variable depth ratio (y/a) [after Jones (1984)].
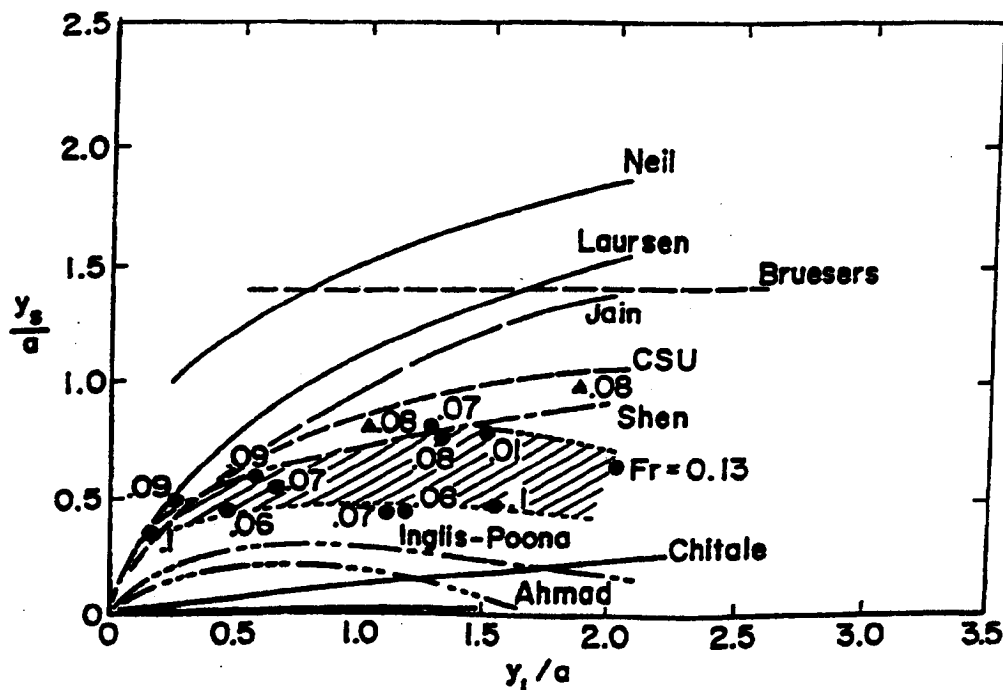

Figure 2.5. Comparison of scour formulae with field scour measurements [after Jones (1984)].

bed configuration exists at a site during flood flows, the maximum scour will be 30 percent greater than the predicted equation value and for the plane bed configuration, which is typical of the most bridge sites for the flood frequencies employed in scour design, the maximum scour may be 10 percent greater than computed with CSU's equation.

2.3.4 Effect of different parameters on scour depth

As has been stated, the variables which characterise the fluid, bed material, flow and bridge pier can affect the scour depth. The following paragraphs summarizes the previous research which has been carried out to examine these effects.

2.3.5 Effect of pier and sediment sizes

The pier size itself affects the time taken for the equilibrium scour depth to be achieved since the volume of the scour hole formed around the upstream half of the perimeter is proportional to the cube of the pier diameter. The larger the pier, the larger the scour volume and the longer is the time required for the scour to develop at a given shear stress ratio. Laboratory data for uniform grain sizes have shown that the relation between scour depth and pier size is as follows [Breusers & Raudkivi (1991)]:

$$\frac{y_s}{b} = A \ln[(\frac{d_{50}v}{b^3})t] + B \tag{2.33}$$

where A and B are constants. In clear water scour, it may take three or four days to establish equilibrium conditions at $U_*/U_{*c} \cong 0.9$ to 0.95 but in a live bed situation, $U_* > U_{*c}$, steady state conditions can be reached after a few minutes [Breusers & Raudkivi (1991)].

Chiew and Melville (1987) investigated live bed local scour experimentally in uniform cohesionless sediment. They claimed that for the live bed condition, the local scour depth does not remain constant but fluctuates with respect to the movement of bed features past the scour hole. Since the size of bed features is not a function of the size of the bridge pier, data should be presented as the equilibrium or average scour depth, d_{av}, rather than the maximum scour depth, d_{smax}.

The range between the maximum and minimum values of local scour depths is equal to the height of bed features under given flow conditions, i.e. the maximum depth is the sum of the average depth and half of the dune height.

Chiew and Melville (1987) showed that when the relative equilibrium scour depth, $\dfrac{d_{av}}{D}$, is plotted as a function of the velocity excess, $\dfrac{U_o}{U_{oc}}$, under the condition where the approach flows were subcritical and the Froude number less than unity, an initial reduction in scour depth for condition just exceeding the threshold velocity of the bed sediment exists. The reduction continues until a minimum scour depth is reached at $\dfrac{U_o}{U_{oc}} = 2.0$. Thereafter the local scour depth increases again but at a decreasing rate, until a second peak is reached at $\dfrac{U_o}{U_{oc}} = 4.0$, which corresponds to the condition where a transition flat bed is formed. The results of their experiment are shown in Fig. 2.6.

Chiew and Melville (1987) claimed that the scour depth and its variations for velocities greater than threshold are related to the rate of sediment transported into and out of the scour hole. They also found that two separate $\dfrac{d_{av}}{D}$ versus $\dfrac{U_o}{U_{oc}}$ curves exists for ripple forming, $d < 0.7$ mm, and non ripple forming, $d > 0.7$ mm, sediment respectively and the value of $\dfrac{d_{av}}{D}$ associated with ripple forming sediment is lower than that associated with non ripple forming sediments for velocities at and around threshold. This was consistent with the result obtained by Chee (1982).

Considering the effect of bed sediment size on scour depth, by plotting results of their experiments with those of Ettema (1980) for clear water scour and

those of Chee (1982), Chiew and Melville (1987) confirmed that $\frac{d_{av}}{D}$ increases almost linearly with increasing value of $\frac{D}{d_{50}}$ until a maximum at $\frac{D}{d_{50}}$ equals to 50. This fact indicates that the scour depth is independent of the ratio of pier to sediment size, i.e. $(\frac{D}{d_{50}})$, for values greater than 50.

Chiew and Melville (1987) used the limiting values of $\frac{d_{av}}{D}$ obtained in their study for high values of $\frac{D}{d_{50}}$ to normalise the results and showed that influence of $\frac{D}{d_{50}}$ on the depth of scour is independent of the stage of flow, whether it is clear water or the live bed condition. For low values of $\frac{D}{d_{50}}$, they offered the following equation:

$$\frac{d_{av}}{D}(\frac{D}{d_{50}}) = K(D/d) \; \frac{d_{av}}{D}(\frac{D}{d_{50}} \geq 50) \tag{2.34}$$

where $\frac{d_{av}}{D}(\frac{D}{d_{50}})$ is the relative equilibrium scour depth at a particular value of $\frac{U_o}{U_{oc}}$ and $\frac{D}{d_{50}}$, $\frac{d_{av}}{D}(\frac{D}{d_{50}} \geq 50)$ is the relative equilibrium scour depth at the same values of $\frac{U_o}{U_{oc}}$ and $\frac{D}{d_{50}} \geq 50$, $K(D/d)$ is the sediment size adjustment factor obtained from Fig. 2.7.

2.3.6 Effect of flow depth

Many researchers e.g. Laursen and Toch (1956), Laursen (1958-1970), Cunha (1970), Neil (1973) stated that scour depth increases as the ratio of relative flow depth, $\frac{y_o}{D}$, increases until a certain limiting value after which the scour depth is independent of $\frac{y_o}{D}$. The limit expressed ranges from $\frac{y_o}{D} = 1$ to 3. i.e. the scour depth becomes independent of flow depth when the depth is greater than three pier diameters. For shallow flows the scour depth increases with depth of flow and that is because a pier causes a surface roller, like a bow wave to a boat, and a horseshoe

24

vortex shaped at the base of the pier. These two rollers have opposite senses of rotation and as long as the two rollers do not interfere, the local scour depth is insensitive to depth of flow. With decreasing depth of flow, the surface roller becomes the more dominant and interferes with the down flow and reduces its strength.

The influence of flow depth affects both clear water and live bed scour depths. For clear water scour, Bonasoundas (1973) concluded that the effects of flow depth become insignificant for $\frac{y_o}{D}$ > 1 to 3.

Ettema (1980) claimed that the influence of flow depth is affected by the relative size of the pier and sediment, $\frac{D}{d_{50}}$. He concluded that, for high values of $\frac{D}{d_{50}}$, the development of local scour is almost independent of flow depths for $\frac{y_o}{D}$ > 1 while for low values of $\frac{D}{d_{50}}$, it is still dependent on flow depths even when the value of $\frac{y_o}{D}$ is as high as 6. He stated that the interference of the surface roller and the horseshoe vortex causes a reduction in the equilibrium scour depths for shallow flows and was especially significant for coarse sediment. This is because the surface roller is a function of the approach velocity and for a constant value of U_*/U_{*c}, the approach velocity for a fine sediment is less than the approach velocity of a coarse sediment. Hence, at the same $\frac{y_o}{D}$, the stagnation pressure which is related to the surface roller, for a coarse sediment is higher than the stagnation pressure for a fine sediment. Thus the influence of $\frac{y_o}{D}$ is more pronounced for the coarse sediment than the fine sediment.

Basak (1975) showed that the flow depth has a similar effect on live bed scour condition as a clear water scour. Jain and Fischer (1979) also showed that the live bed scour depth is lower for lower values of $\frac{y_o}{D}$. Chee (1982), by super imposing the results of Chabert and Engeldinger (1956), Hancu (1971), and White (1975) on his results, showed that, for live bed scour, with decreasing value of $\frac{y_o}{D}$, a decrease in scour depth exists.
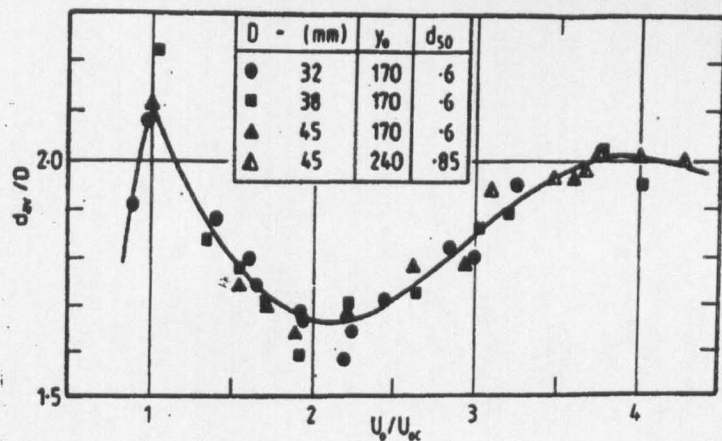
Figure 2.6 Relative equilibrium scour depth, d_{av}/D, versus velocity excess, U_0/U_{oc}, for d_{50} = 0.6 and 0.85 mm [after Chiew and Melville (1987)].
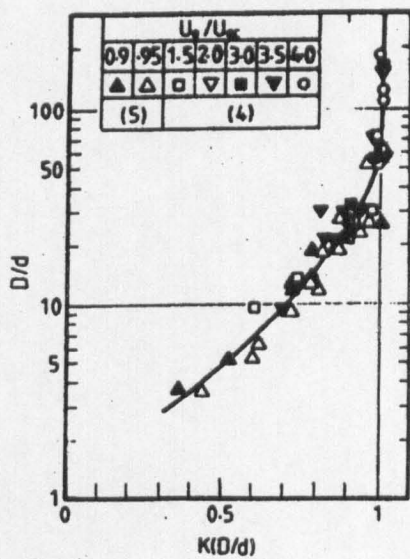

Figure 2.7 The pier to sediment size parameter (D/d) versus the sediment size adjustment factor $K(D/d)$ [after Chiew & Melville (1987)].

To consider the effect of the relative flow parameter, $\frac{y_o}{D}$, on the local scour

depth, Chiew and Melville (1987) plotted the data of Chee (1982), Ettema (1980)

and those of their study and showed that the effect of $\frac{y_o}{D}$ on the depth of scour is

independent of $\frac{D}{d_{50}}$, when this ratio is greater than or equal to 50, whether it is clear

water or live bed scour.

In summary, they inferred that the empirically determined relationship for

flow depth effects on clear water scour depth can be applied to live bed scour so for

estimating the equilibrium scour depth for any value of $\frac{y_o}{D}$, they proposed the

following equation:

$$\frac{d_{av}}{D}(\frac{y_o}{D}) = K(\frac{y_o}{D})\frac{d_{av}}{D} \qquad (2.35)$$

where $\frac{d_{av}}{D}(\frac{y_o}{D})$ is the relative equilibrium scour depth at a particular value of $\frac{U_o}{U_{oc}}$

and a relatively low $\frac{y_o}{D}$ such that the flow depth effects are present, $\frac{d_{av}}{D}$ is the

relative equilibrium scour depth at the same value of $\frac{U_o}{U_{oc}}$ but a relatively high $\frac{y_o}{D}$

such that flow depth effects are absent, and $K(\frac{y_o}{D})$ is a flow depth adjustment factor

obtained from Fig. 2.8. The flow depth adjustment factor for $\frac{b}{d_{50}} > 75$ and $\frac{y_o}{D} < 3$ is

approximately given by:

$$K(\frac{y_o}{b}) = 0.77(\frac{y_o}{b})^{0.21} \qquad (2.36)$$

2.3.7 Effect of sediment grading

The effect of sediment grading on the depth of local scour is still a subject

for research. This effect is more complex in live bed scour than clear water scour.

Fig. 2.9 shows the effect of sediment grading on the depth of live bed scour. The

curve for non-uniform sediment is obtained by using the data of Chiew (1984) with a 45 mm diameter pier, sediment with $d_{50} = 0.8$ mm, $\sigma_g = \dfrac{d_{84.1}}{d_{50}} = \dfrac{d_{50}}{d_{15.9}}$ is equal to 3.5, and a flow depth of 170 mm and the one for uniform sediment is obtained by using sediments with $d_{50} > 0.7$ mm and $\sigma_g < 1.3$.

The d_{50} size of a non-uniform sediment is only a rough indicator; some of the sediment grain transport commences at lower values of U_{*c} than indicated by the d_{50} size and some grains will resist substantially higher shear stresses. For a bed composed of non-uniform sediment, the armouring process of the bed surface begins when sediment transport starts. Armouring is a phenomena that happens in graded bed materials. During the armouring process, the fine materials of the mixture are washed out, the rate of sediment transport is decreased because less and less moveable material is available for transport and the top layer of bed material becomes coarser. This process increases the effective critical shear velocity that the bed surface can resist and the local scour depth increases up to a limiting or critical value of the shear velocity U_{*a}, or velocity U_a, of the armour layer for the specific sediment. At this shear stress the local scour in non-uniform sediment reaches the first peak. The full line in Fig. 2.9 for non-uniform sediment shows the armour peak.

At shear velocities $U_{*c} < U_* \leq U_{*a}$ the sediment transport can be unsteady, approaching zero as the armor layer stablizes, or have a dynamic equilibrium state.

The unsteady state of the armouring, for $U_* \approx 0.95\, U_{*a}$, leads to the similar scouring conditions and scour depths for the first scour peak as for clear water scour peak if the limiting equilibrium condition is reached. On passing the critical shear stress, τ_{ca}, the surface layer breaks down leading to increase of sediment transport rate and an initial decrease of local scour depth.

After the initial decrease, with increasing applied shear stress to the transition flat bed condition the scour depth increases again. First, the coarser fractions of sediment are still effective in armouring the local scour hole bed but with increasing
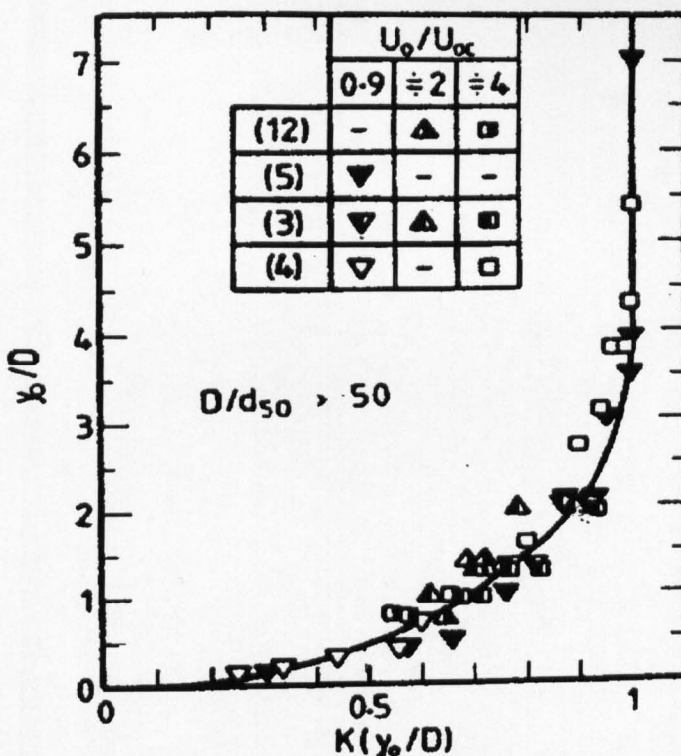
Figure 2.8 : y_O/D versus flow depth adjustment factor, $K(y_O/D)$.

[after Chiew and Melville (1987)]
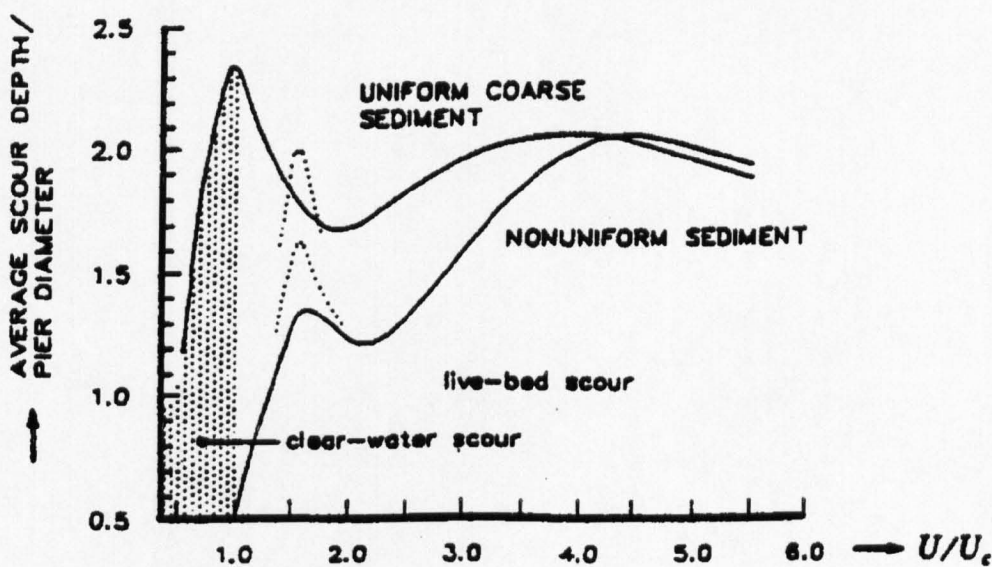
Figure 2.9 : d_{av}/D versus U/U_c in uniform and non-uniform sediment.

[after Breusers and Raudkivi (1991)]

bed shear stress their effectiveness decreases and at last vanishes at the transition flat bed conditions.

Limited laboratory data show that the effect of sediment grading is too small to be separated from the usual scatter present when $\sigma_g < 2$ and the data show the same trend of alteration as uniform sediment.

The critical velocity over a limiting armour layer, U_{ca}, can be estimated by using, d_{50} size of this armour layer, d_{50a}. Chin (1985) showed that the maximum value of d_{50a} is:

$$d_{50a} = d_{max} / 1.8 \qquad (2.37)$$

where d_{max} is the characteristic maximum size of the bed material. The d_{max} value is estimated by using two sieves, such that all particles just pass the coarser sieve. If the sieves used are in the $2^{1/4}$ series the error made by assuming that the d_{max} is equal to the coarser sieve is less than 20%, i.e. $(2^{1/4} - 1)$.

By using *the d_{50a}* size and the Shields diagram $U*_{ca}$ can be estimated and the corresponding critical mean velocity could be estimated from the following equation:

$$U_{ca} = U_{*_{ca}} [5.75 \log(\frac{y_o}{2d_{50a}}) + 6] \qquad (2.38)$$

Baker (1986) found that the critical velocity at which the armour peak occurs, for a situation that there is some sediment transport over the armour layer, is about $0.8U_{ca}$. Then the armour peak occurs at $\frac{[U - (0.8U_{ca} - U_c)]}{U_c} = 1$ where U_c is the critical velocity for the bed material with d_{50}.

Abdu (1993) carried out research to investigate the effect of sediment gradation on local pier scour. He conducted a series of experiments in a laboratory flume using six different sediment mixtures. The mean grain size, d_{50}, was kept

constant at 0.75 mm for the six bed materials. He concluded that the maximum local scour depth in clear water scour for uniform materials is much larger than those for graded material. He also concluded that the sizes of bed material fractions above d_{85} play an important role in reducing scour depth as does increasing the gradation coefficient σ_g.

2.3.8 The flow field around a circular pier

This type of flow has many different aspects which are complexly interrelated. The presence of the pier in the flow sets up a strong adverse pressure gradient in the plane of symmetry upstream of the pier. Since in the approach flow the flow velocity decreases from the water surface downwards, the stagnation pressures also decreases from the surface, i.e. there is a pressure gradient downwards. The downflow is caused by the pressure gradient. It acts somehow like a vertical jet in eroding the bed material. Ettema (1980) measured the downflow velocity at a 65mm pier in an air flow with approach velocity of 12.2 m/sec and a pier Reynolds number 5.4×10^4. Fig. 2.10 shows this data together with the data obtained by Melville (1975) in a water flow and the relationship proposed by Shen et al (1963) for the strength of the downflow impinging on a planar bed at the base of a cylinder pier.

To explain the discrepancy between measured values and predicted values by using the Shen et al equation, Ettema (1980) stated that the equation which is based on inviscid flow theory neglects the lateral leakage of downflow to the sides of the pier. He also noted that the velocity of the downflow increases as the scour hole forms and deepens.

Ettema (1980) stated that the downflow velocity reaches its maximum when the scour depth ratio $\frac{d_s}{D}$ is approximately 1 and that maximum value reaches 0.8 times the mean approach flow velocity.

When a hole has been excavated by the downflow, the oncoming flow separates at the edge of the hole, creating a roller within the scour hole. If the pressure field is strong enough a three dimensional separation of the boundary layer takes place at the base of the pier. The boundary layer rolls up in to a vortex ahead and along the sides of the pier and, because of its shape, it is called a horseshoe vortex.

Raudkivi and Sutherland (1981) described the horseshoe vortex in local scour as "resembling a very thick rope caught by the pier with its ends trailing downstream". The rotation is in the downward direction adjacent to the front of the pier. The vortex trails at either side, increases in cross sectional area in the downstream direction and decreases in intensity. Fig. 2.11 illustrates the flow field components around a circular pier.

Shen et al (1969) identified two general pier shapes, blunt nosed and sharp nosed. A blunt nosed pier is defined as a pier which is capable of inducing a large pressure gradient, enough to initiate the process described above. They claimed that since the horseshoe vortex does not form in the case of a sharp nosed pier it follows that the maximum scour depth is less for a sharp nosed pier than the maximum scour depth caused by a blunt nosed pier.

The wake vortices are generated when the flow separates at the sides of the pier. Separation is a result of the dissipation of the kinetic energy of the fluid particles moving along the surface by the frictional forces. Such particles do not have the kinetic energy to move into the region of increasing pressure and the flow separates from the surface.

Goldstein (1965) claimed that the time required for separation to take place is directly proportional to the radius of the circular pier and inversely proportional to the flow velocity. The position of the point of separation depends on the pier Reynolds number, $\frac{Ub}{v}$, surface roughness and the level of upstream turbulence intensity. If the flow in the boundary layer is laminar the separation point along the
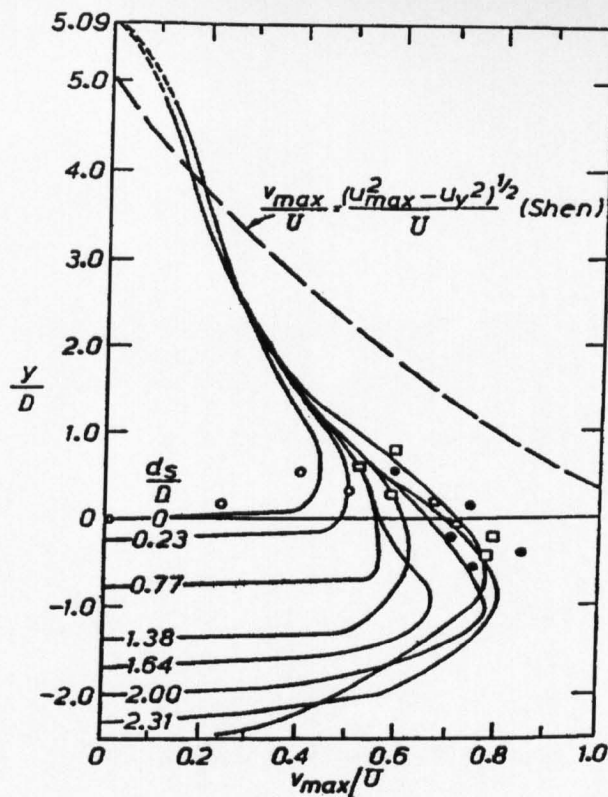
Figure 2.10. Pier downflow velocity V_{max} as measured in front of a 65 mm diameter pier in an air flow.

[after Raudkivi & Sutherland (1981)]
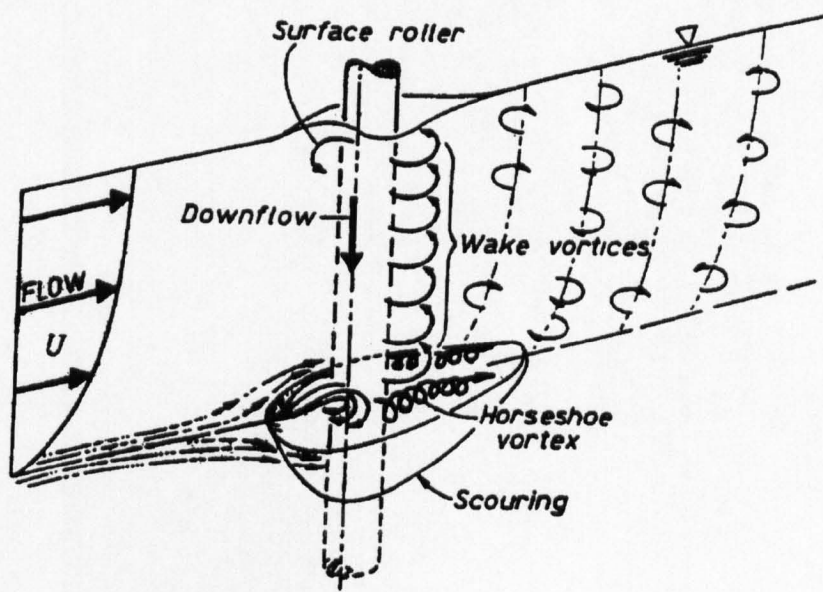
Figure 2.11. Diagrammatic representation of the flow pattern adjacent to a cylindrical pier.

[after Raudkivi & Sutherland (1981)]

sides of the circular pier is located at about 80 degrees from the forward stagnation point.

The unstable shear layer formed from the separated flow rolls up into an eddy structures to form the wake vortex system. The character of the wake vortex system depends on the Reynolds number. Near the bed these vortices interact with the horseshoe vortex causing the trailing parts to oscillate laterally and vertically at the frequency of vortex shedding. In a two dimensional flow the vortex shedding occurs at a constant Strouhal number $\frac{nb}{U}$ of 0.2 where n is frequency of vortex shedding, b is diameter of the pier and U is velocity of the flow.

Melville (1975) claimed that in an equilibrium scour hole the Strouhal number increased by about 15% from that of the two dimensional case. Shen et al (1965) reported that previous researchers such as Roper (1965), Dalton and Masch (1964) and Tison (1940) had observed an upflow existing behind the pier and that the wake vortex system is related to this upflow. This upflow has a suction effect on the bed. It acts like a vacuum cleaner and picks up the material from the bed. The material which is picked up is swept downstream by the flow. The wake vortices with their vertical low pressure centres erode the bed material like tornadoes. Generally, the sediment removed by the wake vortex system is minor compared to that removed by the horseshoe vortex system.

The development of the scour hole commences at the sides of the pier. Ettema (1980) observed that the initial small indentations occurred at about ±45 degrees to the direction of the undisturbed flow. This corresponds closely to the location of the maximum bed shear stress measured by Hjorth (1975) on a fixed plane bed surface around a cylinder pier but Melville (1975) indicated that the maximum bed shear stress occurs at ±100 degrees to the undisturbed flow direction.

After propagating rapidly upstream around the perimeter of the pier, these tiny holes, on either side of the pier, meet on the upstream centreline of the pier and form a shallow hole in front of the pier. When the hole is formed, the downflow and the horseshoe vortex begin to erode the bed materials. The downflow acts like a

vertical jet eroding a groove in front of the pier. The downflow is turned 180 degrees in the groove and the upward flow is deflected by the horseshoe vortex in the upstream direction, up the slope of the scour hole.

Melville (1975) claimed that, with the formation of the scour hole, the vortex rapidly grows in size and strength as additional fluid attains a downward component and the strength of the downflow increases. The horseshoe vortex moves down into the developing scour hole and expands as the hole enlarges. The upstream part of the scour hole develops rapidly and has the shape of the frustum of an inverted cone. The slope of the cone is equal to the angle of repose of bed material at erosion conditions.

2.4 Chapter summary

In this chapter, a literature survey on different topics related to the stability of rivers at bridge sites is presented. Different approaches of previous researchers for prediction of stable channel geometry and it's slope are described. Two major rational approaches, the Chang (1980) method and the White, Paris and Bettess (1981) method are highlighted. Local scour at bridge piers and the live bed scour formulae for scour depth prediction are described. The effects of various parameters on scour depth and the flow field around piers are also reviewed in the chapter. Most of the investigators, who have studied the problem of scour around bridge piers have proposed empirical equations for the estimation of scour depth. Most of these equations are based on limited data obtained from experiments in laboratory flumes with moveable bed and fixed walls.

Chapter Three
Rational Approaches to the Design of Stable Channels

3.1 Introduction

It is important in the design and operation of alluvial channels to determine their geometrical characteristics in dynamic equilibrium. Some of the most recent rational approaches to the design of stable channels are established on the combination of a sediment transport equation, a flow resistance equation and some extremal hypothesis. This chapter describes these approaches for the design of stable channels.

The most important parameters that describe the channel system are water discharge, slope, velocity, sediment concentration, water surface width, and depth. To achieve a dynamically stable condition a channel adjusts its slope, depth and width to carry the required amount of sediment and water to reach a stable form. Therefore, these three parameters may be used to describe the stable condition of an alluvial channel. In order to solve the channel system to get these three unknowns, one would need three equations. (1) A sediment transport formula (2) A flow resistance equation (3) An extremal hypothesis. The essential assumption of this hypothesis, for the third condition, is that a channel achieves a stable condition when a specified function of the physical variables, subject to environmental constraints, attains an extreme value e.g. minimum rate of energy dissipation [Yang and Song(1979)], minimum stream power [Chang(1980)], or maximisation of sediment transport [White et al.(1981)] etc.

In the following paragraphs, a number of extremal hypotheses, discussed in the literature, will be explained.

3.2 Minimisation Hypotheses

3.2.1 Minimum energy dissipation rate

Song and Yang (1980) stated that a river may adjust its flow as well as its boundary such that the total energy loss (or, for a fixed bed, the total stream power) is minimised. The principal means of adjusting the boundary is sediment transport. If there is no sediment transport, then the river can only adjust its velocity distribution. In achieving the condition of minimum stream power, the river is constrained by the law of conservation of mass and the sediment transport relations.

They used the hypothesis of minimum energy dissipation rate to explain measured hydraulic parameters from laboratory flumes and the Rio Grande river, for sediment concentrations below 1000 mg/l.

3.2.2 Minimum stream power

Chang (1980b) described this hypothesis with the following words. " For an alluvial channel, the necessary and sufficient condition of equilibrium occurs when the stream power per unit length of channel γQS is a minimum subject to given constraints. Hence an alluvial channel with water discharge Q and sediment load Qs as independent variables, tends to establish its width, depth and slope such that γQS is a minimum. Since Q is a given parameter, minimum γQS also means minimum channel slope S".

Chang [1979 a,b; 1980 a,b] used this hypothesis to explain the width depth ratios of rivers and alluvial canals in regime and the channel pattern of natural rivers.

3.2.3 Minimum unit stream power

Yang and Song (1979) stated the minimum unit stream power hypothesis as follows. For subcritical flow in an alluvial channel, the channel will adjust its velocity, slope, roughness and geometry in such a manner that a minimum amount of unit stream power is used to transport a given sediment and water discharge. The value of minimum unit stream power depends on the constraints applied to the channel. If the flow deviates from its equilibrium condition, it will adjust its velocity, slope, roughness and channel geometry in such a manner that the unit stream power is minimised until the equilibrium condition can be regained.

Song and Yang (1980) explained that the minimum unit stream power hypothesis is somehow different from but of a similar nature to that of minimum stream power and both are special cases of the general hypothesis of minimum energy dissipation rate.

3.3 Maximisation Hypotheses

3.3.1 Maximum friction factor

Davies and Sutherland (1980) described this hypothesis as follows. If the flow of a fluid past an originally plane boundary is able to deform the boundary to a non planar shape, it will do so in such a way that the friction factor increases. The deformation will cease when the shape of the boundary is that which gives rise to a local maximum of friction factor. Thus the equilibrium shape of a non planar self formed flow boundary or channel corresponds to a local maximum of friction factor.

Davies (1980) tested this hypothesis for the particular case of lower flow regime bedforms.

3.3.2 Maximum sediment transport

White et al. (1981) explained the hypothesis in the following words. For a particular water discharge and slope, the width of the channel adjusts to maximise the sediment transport rate.

They used the sediment transport formula of Ackers and White (1973), the frictional relationships of White, Paris, and Bettess (1980) combined with the principle of maximum sediment concentration capacity. Additionally they showed that maximum sediment transport hypothesis is equivalent to minimum channel slope hypothesis.

White et al. (1981) compared the proposed method with available field data and existing empirical regime relationships derived by fitting curves to data.

3.4 Formulation of present study

As it is the aim of the present study to test the White et al (1981) theory, only the external hypothesis of maximum sediment transport has been used. In order to examine the effects of using different sediment transport and flow resistance formulae on predictions of the White et al (1981) theory, the following formulae have been used.

The flow resistance formulae of Brownlie (1982) and Dabkowski (1991), and the sediment transport formulae of Brownlie (1982) have been used for their easy to program. Ackers and White (1973) for its' important role in the predictions of White et al (1981) theory. Engelund and Hansen (1967) for its' common use. The following paragraphs describe the equations used.

3.4.1 Brownlie's flow resistance equation

Brownlie (1982) evaluated six different available methods for predicting friction factor in sand bed rivers and proposed a new method based on dimensional

analysis, a statistical analysis of a large number of laboratory and field data, and basic principles of hydraulics.

In Brownlie's approach, sediment properties are described by the median size d, specific weight $\rho_s g$, and the geometric standard deviation σ_g under the assumption of log normal distribution. Using the π-theorem, he arranged the variables into dimensionless groups in the form

$$\frac{RS}{d} = \frac{\rho_s - \rho}{\rho}\tau_* = F\left(\frac{q}{\sqrt{gd_{50}^3}}, S, \sigma_g\right) \tag{3.1}$$

where q is the unit discharge, S is the channel slope, R is the hydraulic radius, and $\tau*$ is the shear stress. By using different assumptions and assuming $q_* = \dfrac{q}{\sqrt{gd_{50}^3}}$, he arranged Eq. 3.1 as follows.

$$\left(\frac{\rho_s - \rho}{\rho}\right)\tau_* = w(q_*S)^x S^y \sigma_g^z \tag{3.2}$$

where w, x, y, z are constants to be fitted empirically. Brownlie by taking logarithms of both sides of Eq. (3.2) and using multiple regression determined the constants. He used two different set of data for the lower flow regime and the upper flow regime and proposed the following equations.

For lower flow regime:

$$\frac{R}{d} = 0.3724(q_*)^{0.6539} S^{-0.2542} (\sigma_g)^{0.1050} \tag{3.3}$$

For upper flow regime:

$$\frac{R}{d} = 0.2836(q_*)^{0.6248} S^{-0.2877} (\sigma_g)^{0.0813} \tag{3.4}$$

The data used in his analysis had the discharge range of 0.0032-22000 m³/s, slope range of 0.000003-0.037, hydraulic radius range of 0.025-17.0 m, and median particle size range of 0.088-2.8 mm.

Determination of flow regime in Brownlie's approach is based on the forces on bed sediment particles to which bed deformation related. He considered F_g, $\frac{d}{\delta}$, and S as dimensionless parameters to be indicative of flow regime.

$$F_g = \frac{U\sqrt{\rho}}{\sqrt{(\rho_s - \rho)gd}} \tag{3.5}$$

$$\frac{d}{\delta} = \frac{dU'_*}{11.6\nu} \tag{3.6}$$

where U is the mean velocity, δ is the thickness of the laminar sublayer, ν is the kinematic viscosity and U'_* is the shear velocity for the upper regime and would occur where no dunes are present.

Brownlie (1983) showed that for slopes greater than 0.006 only upper regime flow exists. For lower values of S, an approximate dividing line was given by

$$F_g = F_g^* = 1.74S^{\frac{-1}{3}} \tag{3.7}$$

where F_g^* is the F_g value along this line. He then refined the overlap of both flow regimes along this line by the ratios $\frac{F_g}{F_g^*}$ and $\frac{d}{\delta}$ as follows:

For upper limit of lower regime:

$$\log\frac{F_g}{F_g^*} = \begin{cases} -0.2026+0.07026\log\frac{d}{\delta}+0.9330(\log\frac{d}{\delta})^2 & \text{for } \frac{d}{\delta}<2 \\ \\ \log 0.8 & \text{for } \frac{d}{\delta}\geq 2 \end{cases} \tag{3.8}$$

For lower limit of the upper flow regime

$$\log \frac{F_g}{F_g^*} = \begin{cases} -0.02469 + 0.1517\log\frac{d}{\delta} + 0.8381(\log\frac{d}{\delta})^2 & \text{for } \frac{d}{\delta} < 2 \\ \\ \log 1.25 & \text{for } \frac{d}{\delta} \geq 2 \end{cases} \qquad (3.9)$$

Brownlie (1982) compared his method with the data of the Rio Grande conveyance channel and the Mississippi River at Tar Bert landing, Louisiana where the results were good.

3.4.2 Dabkowski's flow resistance equation

Dabkowski (1991) used six dimensionless quantities and expressed the general form of mean depth in sandy bed rivers as follows:

$$\frac{h}{d_{50}} = F\{ \frac{q}{\sqrt{gd_{50}^3}}, \frac{B}{d_{50}}, \frac{gd_{50}^3}{v^2}, S, \sigma_g, s \} \qquad (3.10)$$

where $q = \frac{Q}{B}$ is the discharge per unit width, B is the water surface width, S is the hydraulic slope, v is the kinematic viscosity, s is the specific gravity and σ_g is the bed material geometric standard deviation.

By using multiple step wise regression and a set of measurement data including 212 observations, Dabkowski (1991) introduced the following equation.

$$h = 1.0683 Q^{0.6386} B^{-0.6629} d_{50}^{-0.1313} S^{-0.1202} v^{0.1318} \sigma_g^{0.1180} s^{0.3063} \qquad (3.11)$$

where Q is given in $\dfrac{m^3}{s}$, B in m, d_{50} in m, and v in $\dfrac{m^2}{s}$. The initial data to establish the regression equation were from 44 cross sections of 10 water courses with the width range of 1.7-589.0 m, discharge range of 0.067-1880 m³/s, and slope range 0f 0.000041-0.0034.

Dabkowski (1991) evaluated his proposed method with a new set of data which was not included in the initial set of data. He concluded that for flows with Froude number between 0.15 and 0.2 the error between the measured and calculated values is ±20%. The errors are smaller than in other authors' formulae.

3.4.3 Brownlie's sediment transport formula

Brownlie (1982), for his approach, used dimensional analysis. The dimensionless groups in his approach are the following.

$$C = F(F_g, \frac{R}{d_{50}}, S, \sigma_g, R_g, \frac{\rho_s - \rho}{\rho}) \qquad (3.12)$$

where

$$\text{Grain Froude number}, F_g = \frac{U}{\sqrt{g d_{50}\left(\dfrac{\rho_s - \rho}{\rho}\right)}} \text{ and the} \qquad (3.13)$$

$$\text{Grain Reynolds number}, R_g = \frac{\sqrt{g d_{50}^3}}{v} \qquad (3.14)$$

Multiple regression analysis was used to develop an equation with the general form of equation (3.12) which resulted in the following formula.

$$C = 7115 C_F \left(F_g - F_{g_o}\right)^{1.978} S^{0.6601} \left(\frac{R}{d_{50}}\right)^{-0.3301} \qquad (3.15)$$

where C_F is the coefficient for data given as:

$$C_F = 1 \qquad\qquad \text{for lab data}$$

$$C_F = 1.268 \qquad\qquad \text{for field data}$$

F_{g_o} is the critical grain Froude number given by

$$F_{g_o} = 4.596 \tau_{*_o}^{0.5293} S^{-0.1405} \sigma_g^{-0.1606} \qquad (3.16)$$

where

$$\tau_{*_o} = 0.22Y + 0.06(10)^{-7.7Y} \qquad (3.17)$$

$$Y = \left(\sqrt{\frac{\rho_s - \rho}{\rho}} R_g \right)^{-0.6} \qquad (3.18)$$

Brownlie (1982) compared his proposed method with existing methods and described the result as satisfactory.

3.4.4 Ackers and White sediment transport formula

Ackers and White (1973) described the movement of sediment in terms of three dimensionless groups. (a) particle mobility, F_{gr} (b) sediment transport G_{gr} and (c) dimensionless particle size D_{gr}.

The particle mobility definition is

$$F_{gr} = \frac{V_*^n}{\sqrt{gd(s-1)}} \left(\frac{V}{\sqrt{32} \log_{10}\left(\frac{10d}{D} \right)} \right)^{1-n} \qquad (3.19)$$

The dimensionless particle size definition is:

$$D_{gr} = D \left(\frac{g(s-1)}{v^2} \right)^{\frac{1}{3}} \qquad (3.20)$$

In their method the expression for sediment transport is based on the stream power concept. By combining the efficiency of transport with the mobility number, they defined a transport parameter as:

$$G_{gr} = \frac{Xd}{sD}\left(\frac{V_*}{V}\right)^n$$ (3.21)

They assumed a general transport equation in the form:

$$G_{gr} = C\left(\frac{F_{gr}}{A} - 1\right)^m$$ (3.22)

where C, m, and n are coefficients depending on D_{gr} ,determined from best fit curves of almost 1000 sets of data with sediment size greater than 0.04 mm and Froude number less than 0.8.

For transitional sizes, $1 \leq D_{gr} \leq 60$

$$n = 1.0 - 0.56\log_{10} D_{gr}$$
$$m = \frac{9.66}{D_{gr}} + 1.34$$
$$\log C = 2.86\log_{10} D_{gr} - \log_{10}^2 D_{gr} - 3.53$$ (3.23)
$$A = \frac{0.23}{D_{gr}} + 0.14$$

For coarse sediments, $D_{gr} > 60$

$$n = 0.0$$
$$m = 1.5$$ (3.24)
$$C = 0.025$$
$$A = 0.17$$

3.4.5 Engelund and Hansen sediment transport formula

Engelund and Hansen (1967) obtained their sediment transport formula by applying Bagnold's stream power concept and similarity principal as follows.

$$f' \Phi = 0.1(\tau_*)^{\frac{5}{2}}$$ (3.25)

with

$$f' = \frac{2gRS}{U^2}$$ (3.26)

$$\Phi = \frac{q_s}{\gamma_s \left[(s-1)gd^3 \right]^{\frac{1}{2}}}$$

$$\tau_* = \frac{\tau_o}{(\gamma_s - \gamma)d}$$ (3.27)

where f' is the friction factor, d is the median fall diameter of the bed material, Φ is the dimensionless sediment discharge, s is the specific gravity of sediment, and τ_* is dimensionless shear stress or the Shield stress. Substituting Eqs. 3.27 and 3.26 in Eq. 3.25 yields

$$C = 0.05 \left(\frac{s}{s-1} \right) \frac{US}{\left[(s-1)gd \right]^{\frac{1}{2}}} \left[\frac{RS}{(s-1)d} \right]^{\frac{1}{2}}$$ (3.28)

where C is the sediment concentration by weight, U is the mean flow velocity, R is the hydraulic radius, S is the hydraulic gradient slope, and s is the specific gravity of the sediment.

3.5 Effect of combining different formulae

In order to investigate the effect of combining different formulae, on predictions of the WPB (1981) theory, the following combinations have been used. The combinations are Brownlie (1982) equations, Brownlie (1982) and Ackers and White (1973) [Brownlie-White], Brownlie (1982) and Engelund and Hansen (1967) [Brownlie-Engelund], Dabkowski (1991) and Brownlie(1982) [Dabkowski-Brownlie], Dabkowski (1991) and Ackers and White (1973) [Dabkowski-White], Dabkowski (1991) and Engelund and Hansen (1967) [Dabkowski-Engelund].

The indicated combinations have been used with the hypothesis of sediment transport maximisation. A computer program has been developed which, for a specified discharge and slope, gives those values of depth, width, velocity and friction factor that maximise the sediment concentration in the channel.

In order to verify the proposed method, it has been compared with available laboratory and field data. The chosen data are from ACOP canal data of Mahmood, et al. (1979), CHOP canal data of Chaudhry, et al. (1970), American canal data of Simons (1957), laboratory data of Ranga-Raju, et al. (1977). This provided a total of 201 observations. From the above chosen data set the ACOP data have been used in the derivation of Brownlie's (1982) formulae. The laboratory data of Ranga-Raju et al (1977) are beyond applicability range of Dabkowski's (1991) equation, therefore they have not been used for its' verification. The following paragraphs address the effects of combining different formulae on predictions of WPB (1981) hypothesis i.e. sediment concentration, mean depth, water surface width, and slope.

3.6 Sediment Concentration

The Brownlie (1982) flow resistance and sediment transport equations have been used with sediment maximisation hypothesis. The results for sediment concentrations, from the developed computer program, for the data used are shown in Fig. 3.1.

Fig. 3.1 compares the amount of calculated and measured sediment concentrations. The comparison shows that the predictions of the method for the ACOP data are equally distributed around the 100% agreement line. The method mostly underpredicts the concentrations for CHOP data. It also underpredicts concentrations for the data of Simon and Ranga-Raju. The discrepancy ratio $(=\dfrac{\text{Calculated Value}}{\text{Observed Value}})$ for the sediment concentrations are shown in Fig. 3.2. It shows that the maximum discrepancy ratio is 11.5 and the minimum is 0.04. The mean value of the plotted discrepancy ratios is 1.2 with the standard deviation of 1.5.

The results for the combination of Brownlie (1982) and Ackers and White (1973) equations are shown in Fig. 3.3. It shows the amount of calculated and observed sediment concentrations. The comparison shows that the prediction of the method for the ACOP data equally distributed around 100% agreement line. It mostly overpredicts the concentrations for CHOP data. It also underpredicts concentrations for data of Simon and Ranga-Raju. The discrepancy ratio for the sediment concentrations are shown in Fig. 3.4. It shows that the maximum discrepancy ratio is 201.3 and the minimum is 0.03. The mean value of the plotted discrepancy ratios is 3.8 with the standard deviation of 18.5.

The results for the combination of Brownlie (1982) and Engelund and Hansen (1967) equations are presented in Figs. 3.5. It shows the amount of calculated and observed sediment concentrations. It shows that the prediction of the method for ACOP and CHOP data are roughly distributed equally around the 100% agreement line. It underpredicts the concentration for data of Simon and Ranga-Raju. The discrepancy ratio for the sediment concentrations are shown in Fig. 3.6. It shows that the maximum discrepancy ratio is 11.9 and the minimum is 0.04. The mean value of the plotted discrepancy ratios is 1.7 with the standard deviation of 1.9.

The results for the combination of Dabkowski (1991) and Brownlie (1982) equations are presented in Fig.3.7. It compares the amount of calculated and

observed sediment concentrations. It shows that the method mostly underpredicts the concentrations for all sets of data. The discrepancy ratio for the sediment concentrations are shown in Fig. 3.8. It shows that the maximum discrepancy ratio is 3.8 and the minimum is 0.008. The mean value of the plotted discrepancy ratios is 0.52 with the standard deviation of 0.5.

For the combination of Dabkowski (1991) and Ackers and White (1973) equations, the results are presented in Fig. 3.9. It shows the calculated and observed sediment concentrations. It declares that the method mostly underpredicts the concentrations for all sets of data. The discrepancy ratio for the sediment concentrations are shown in Fig. 3.10. It shows that the maximum discrepancy ratio is 36.8 and the minimum is 0.01. The mean value of the plotted discrepancy ratios is 1.1 with the standard deviation of 3.5.

The results for the combination of Dabkowski (1991) and Engelund and Hansen (1967) equations are presented in Fig. 3.11. It compares the calculated and observed sediment concentrations. The comparison shows that the predictions of the method for ACOP and CHOP data are roughly distributed equally around the 100% agreement line. The method underpredicts the concentration for data of Simon. The discrepancy ratio for the sediment concentrations are shown in Fig. 3.12. It shows that the maximum discrepancy ratio is 8.6 and the minimum is 0.04. The mean value of the plotted discrepancy ratios is 1.2 with the standard deviation of 1.4. The best combination of the used equations are those with mean discrepancy ratio close to 1.0 and standard deviation close to 0.0.
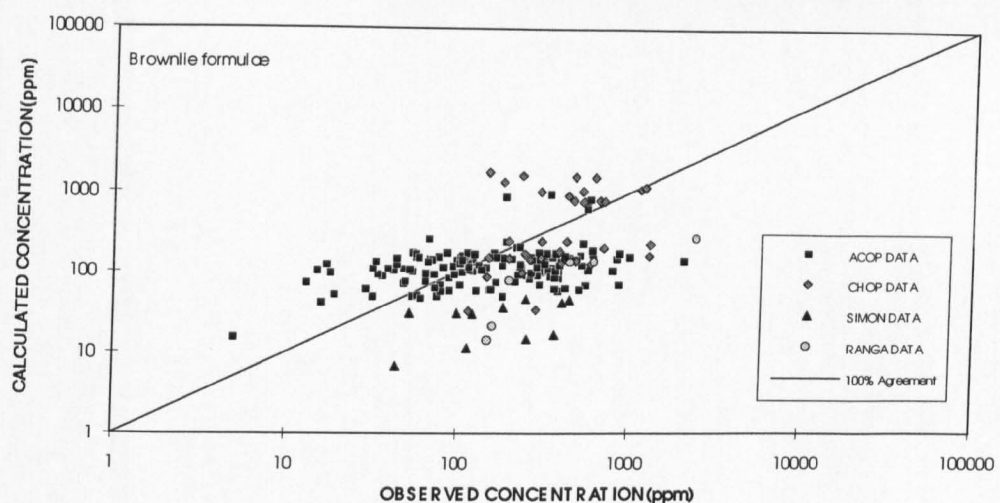
Figure 3.1. Calculated against observed sediment concentration using observed slopes
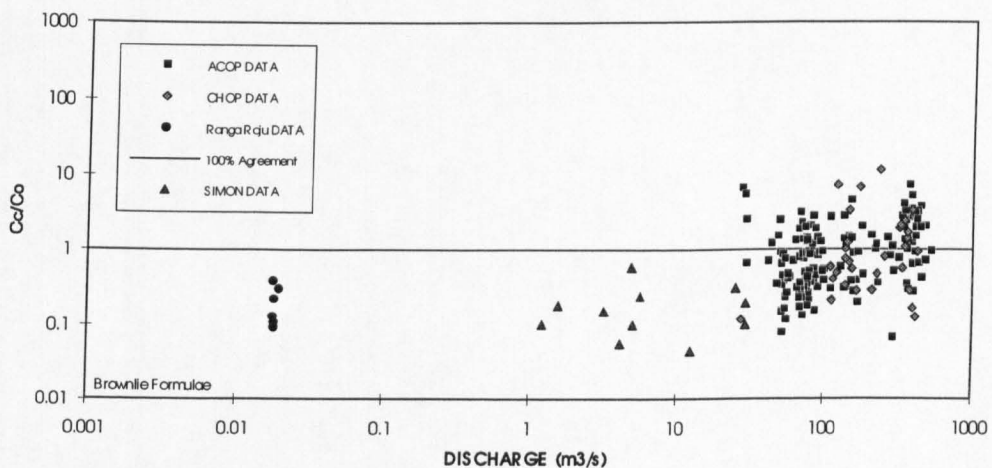
Figure 3.2. Discrepancy ratio for sediment concentration using observed slopes
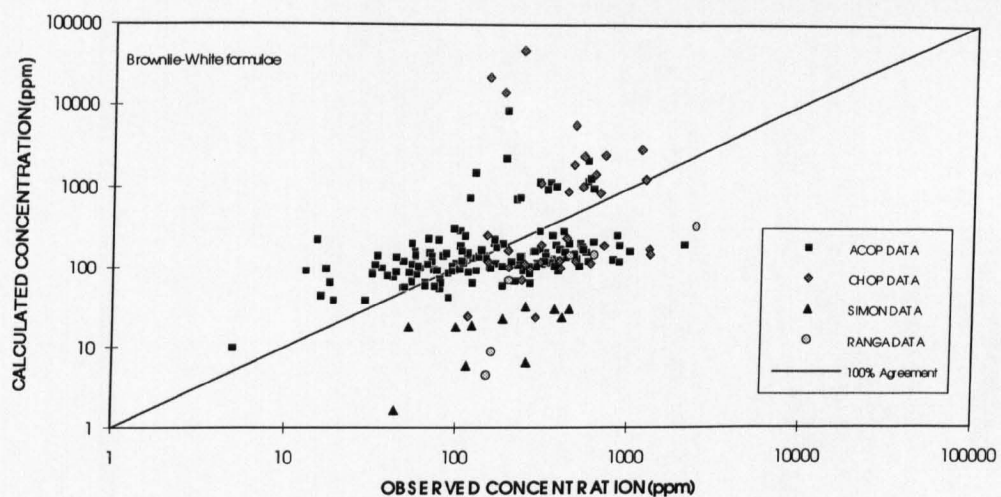
Figure 3.3. Calculated against observed sediment concentration using observed slopes

DISCREPANCY RATIO FOR SEDIMENT CONCENTRATION USING
OBSERVED SLOPES
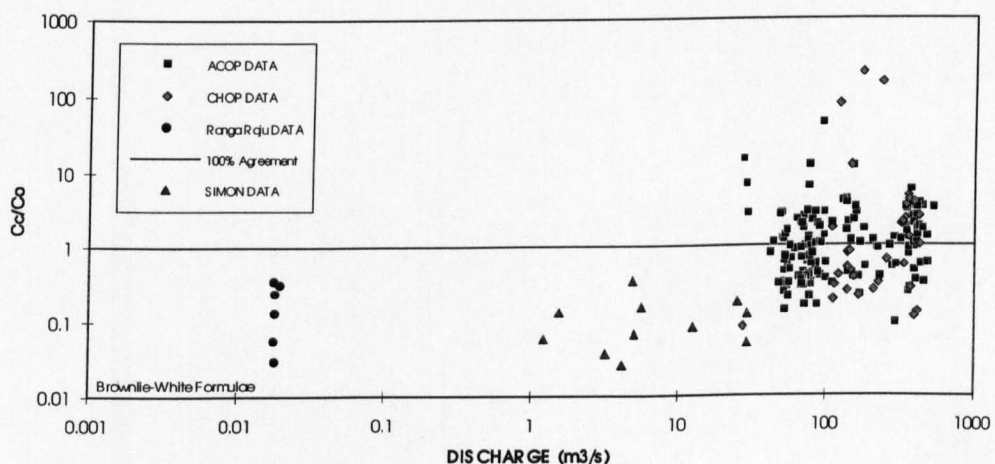
Figure 3.4. Discrepancy ratio for sediment concentration using observed slopes

COMPARISON OF THE OBSERVED AND CALCULATED CONCENTRATION
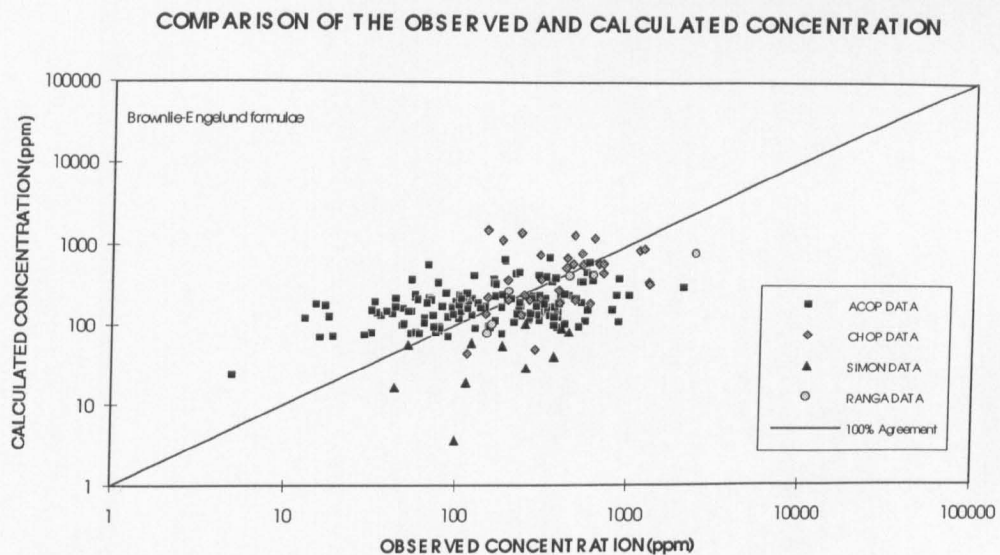
Figure 3.5. Calculated against observed sediment concentration using observed slopes

DISCREPANCY RATIO FOR SEDIMENT CONCENTRATION USING
OBSERVED SLOPES
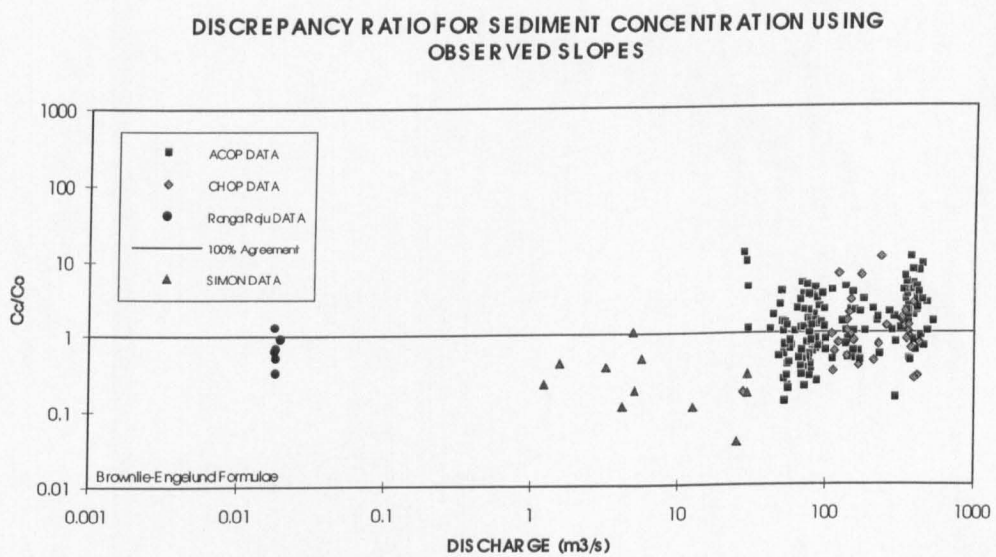
Figure 3.6. Discrepancy ratio for sediment concentration using observed slopes

COMPARISON OF THE OBSERVED AND CALCULATED CONCENTRATION USING OBSERVED SLOPES
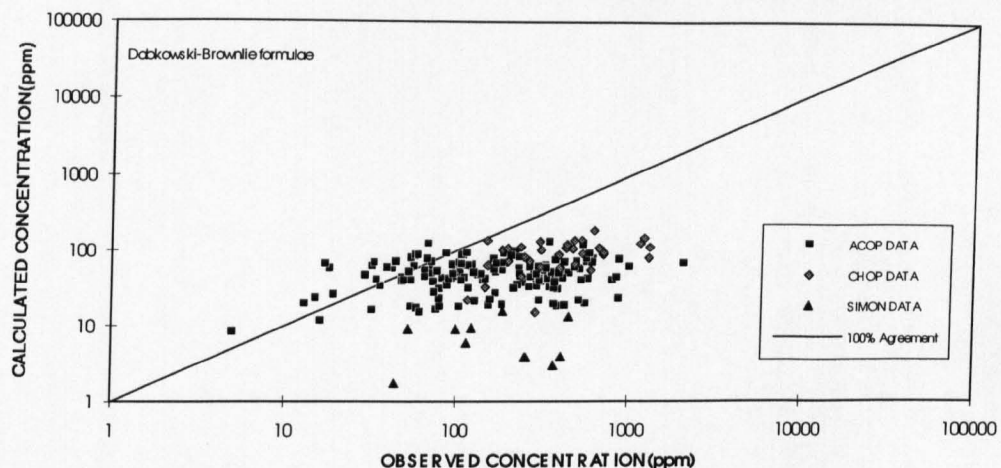
Figure 3.7. Calculated against observed sediment concentration using observed slopes

**DISCREPANCY RATIO FOR SEDIMENT CONCENTRATION USING OBSERVED SLOPES**
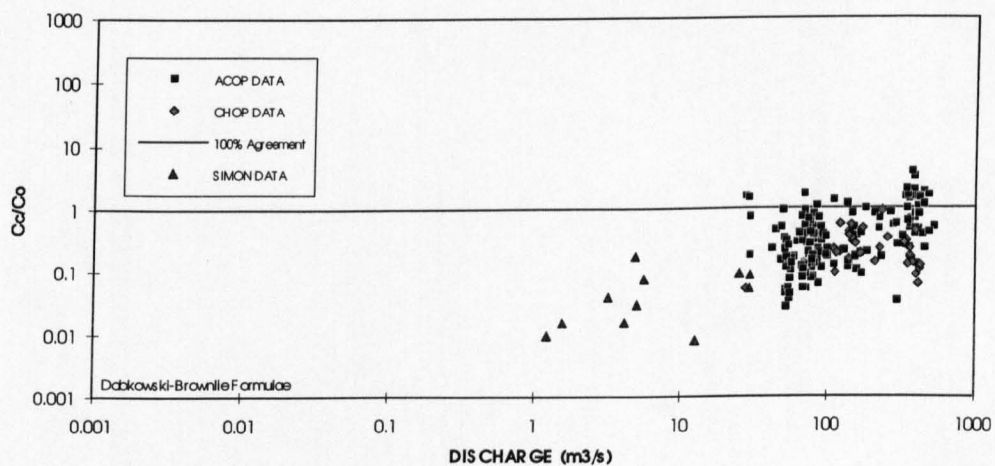
Figure 3.8. Discrepancy ratio for sediment concentration using observed slopes

COMPARISON OF THE OBSERVED AND CALCULATED CONCENTRATION
USING OBSERVED SLOPES
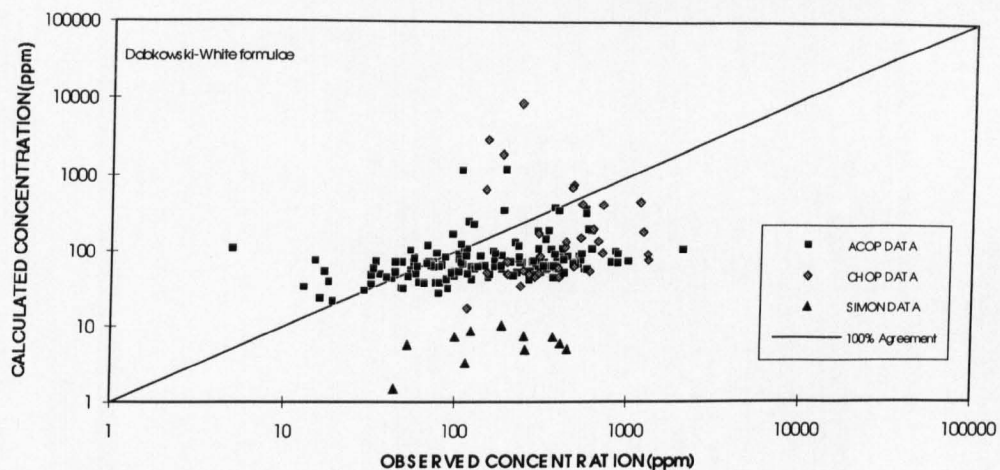
Figure 3.9. Calculated against observed sediment concentration using observed slopes

DISCREPANCY RATIO FOR SEDIMENT CONCENTRATION USING
OBSERVED SLOPES
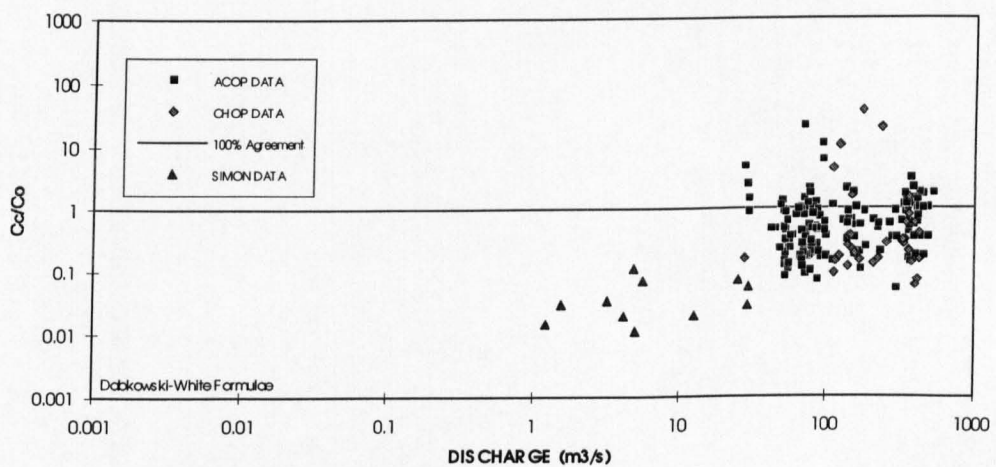
Figure 3.10. Discrepancy ratio for sediment concentration using observed slopes

COMPARISON OF THE OBSERVED AND CALCULATED CONCENTRATION
USING OBSERVED SLOPES
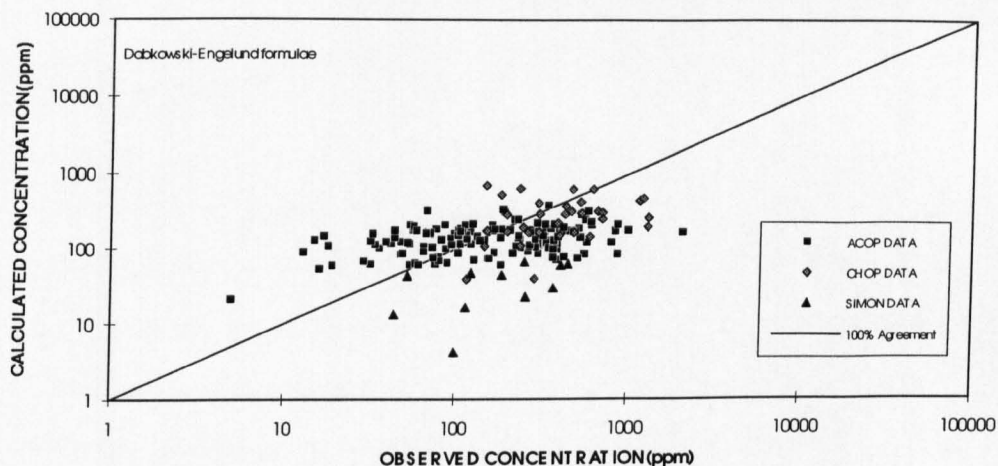
Figure 3.11. Calculated against observed sediment concentration using observed slopes

DISCREPANCY RATIO FOR SEDIMENT CONCENTRATION USING
OBSERVED SLOPES
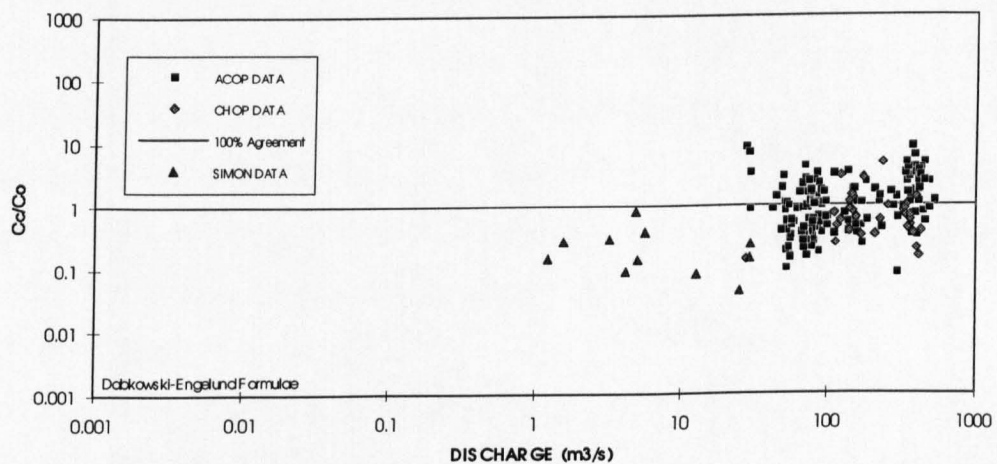
Figure 3.12. Discrepancy ratio for sediment concentration using observed slopes

The comparison shows that the best combinations for prediction of sediment concentration are [Brownlie] and [Dabkowski-Engelund].

3.7 Mean depth

For the combination of Brownlie (1982) equations, Fig. 3.13 shows the calculated and observed depths for the observed slope of data sets. The results show that the combination used mostly overpredicts the flow depth for the ACOP data and CHOP data. It mostly underpredicts the Simon data. The predicted values of depth for Ranga-Raju data are equally distributed around the 100% agreement line. The discrepancy ratio for the mean depths are shown in Fig. 3.14. It shows that the maximum discrepancy ratio is 2.8 and the minimum is 0.4. The mean value of the plotted discrepancy ratios is 1.5 with the standard deviation of 0.4.

For the next combination, the Brownlie (1982) flow resistance and Ackers and White (1973) have been used with sediment transport maximisation hypothesis. The results for depth prediction using observed slope are shown in Fig. 3.15. It shows that the combination used mostly overpredicts the flow depths for ACOP and CHOP data. It mostly underpredicts the data of Simon. The method overpredicts the depth for Ranga-Raju data. The discrepancy ratio for the mean depths are shown in Fig. 3.16. It shows that the maximum discrepancy ratio is 4.8 and the minimum is 0.4. The mean value of the plotted discrepancy ratios is 1.8 with the standard deviation of 0.6.

For the combination of Brownlie (1982) and Engelund and Hansen (1967), the results for flow depth prediction of the data used are shown in Fig. 3.17. It shows that the method overpredicts the flow depth for all sets of data. The discrepancy ratio for the mean depths are shown in Fig. 3.18. It shows that the maximum discrepancy ratio is 4.5 and the minimum is 1.09. The mean value of the plotted discrepancy ratios is 2.4 with the standard deviation of 0.6.

For the combination of Dabkowski (1991) and Brownlie (1982) equations, the results are shown in Fig. 3.19. It shows that the method overpredicts the flow depth for ACOP and CHOP data. It mostly overpredicts the flow depth for the data of Simon. The discrepancy ratio for the mean depths is shown in Fig. 3.20. It shows that the maximum discrepancy ratio is 3.6 and the minimum is 0.5. The mean value of the plotted discrepancy ratios is 1.8 with the standard deviation of 0.5.

For the Dabkowski-White combination, the method also overpredicts the depth for data sets of ACOP, CHOP, and Simon. The results for the calculated and observed data are shown in Fig. 3.21. The discrepancy ratio for the mean depths are shown in Fig. 3.22. It shows that the maximum discrepancy ratio is 4.1 and the minimum is 0.7. The mean value of the plotted discrepancy ratios is 1.9 with the standard deviation of 0.5.

For the Dabkowski-Engelund combination, the method shows the same behaviour for depth prediction. It overpredicts depth for all sets of data. Fig 3.23 shows the comparison results. The discrepancy ratio for the mean depths are shown in Fig. 3.24. It shows that the maximum discrepancy ratio is 5.9 and the minimum is 1.24. The mean value of the plotted discrepancy ratios is 2.9 with the standard deviation of 0.7.

The comparison shows that the best combinations for prediction of mean depth are [Brownlie] and [Dabkowski-Brownlie]. It also shows that the calculated results from all the combinations have the same order of sensitivity as the observed variation. This sensitivity is less pronounced for the calculated values of sediment concentration.

**COMPARISON OF OBSERVED DEPTH WITH CALCULATED DEPTH USING OBSERVED SLOPES**
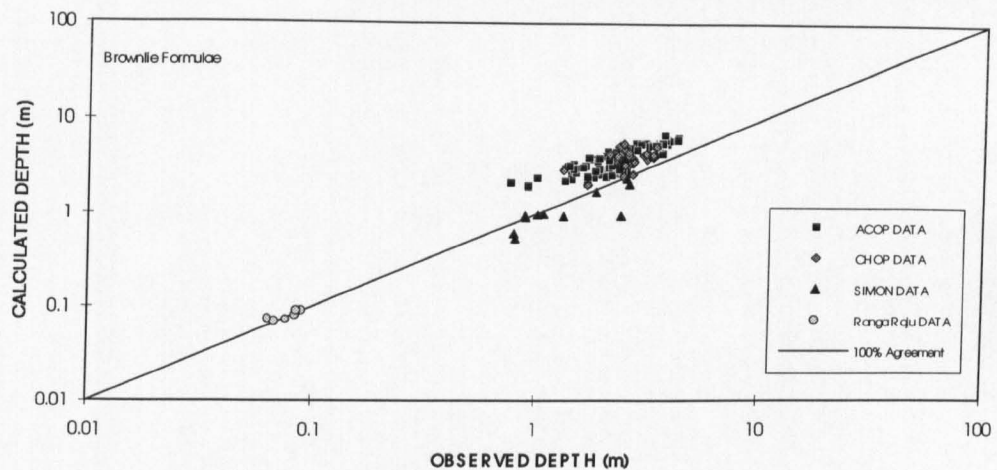
Figure 3.13. Calculated against observed depth using observed slopes

DISCREPANCY RATIO FOR DEPTH USING OBSERVED SLOPES
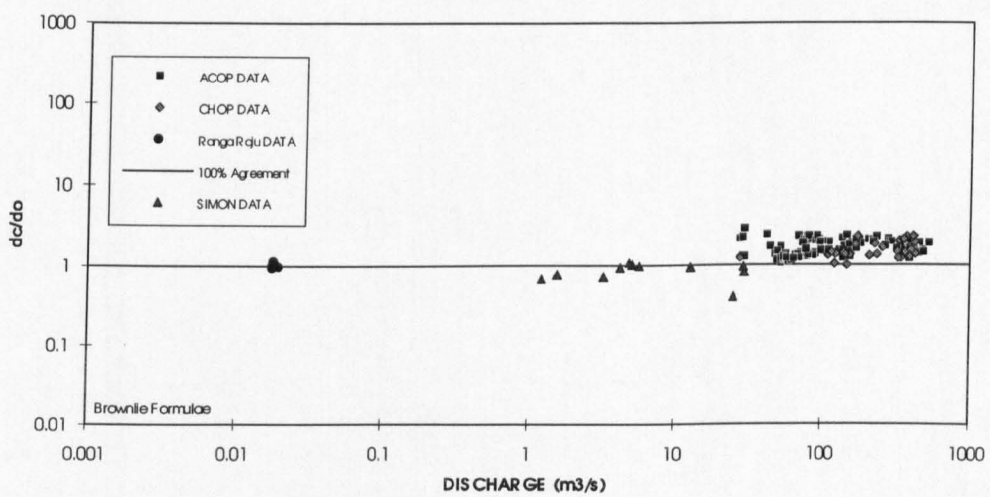
Figure 3.14. Discrepancy ratio for depth using observed slopes

COMPARISON OF OBSERVED DEPTH WITH CALCULATED DEPTH
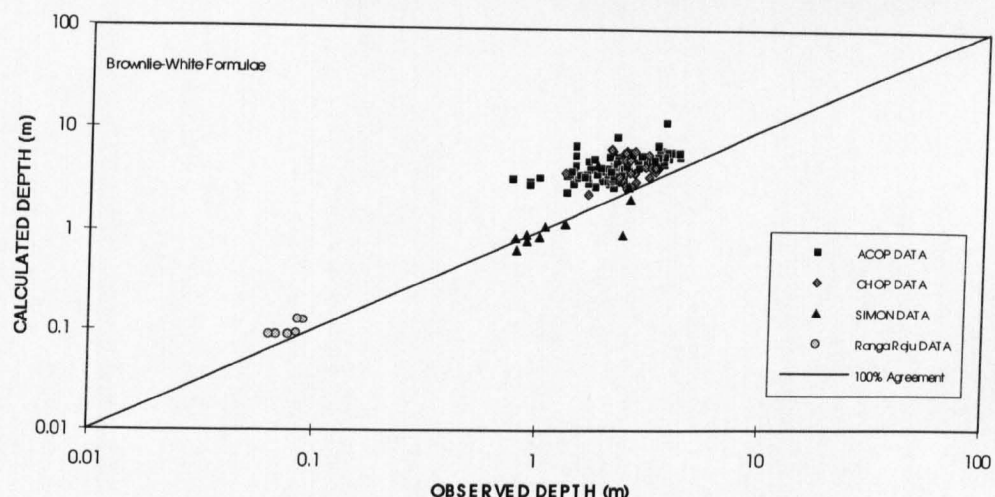
Figure 3.15. Calculated against observed depth using observed slopes

DISCREPANCY RATIO FOR DEPTH USING OBSERVED SLOPES
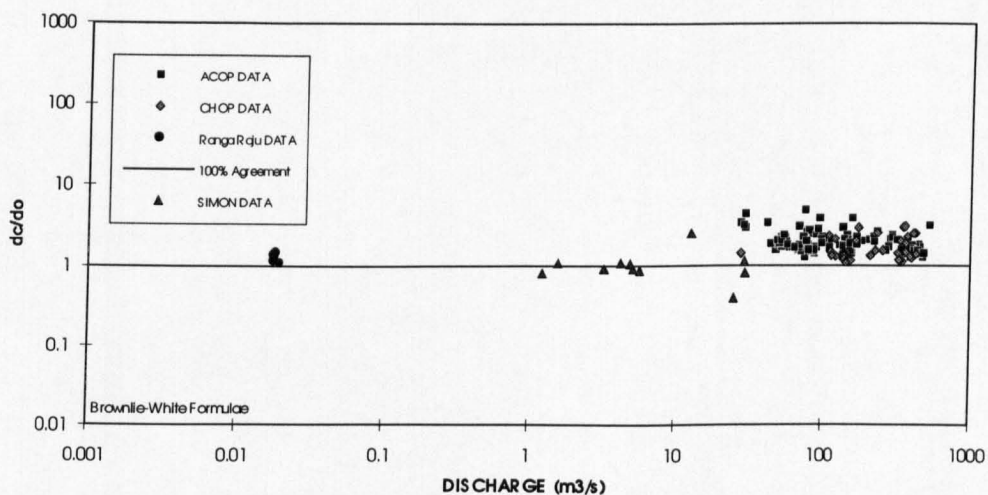
Figure 3.16. Discrepancy ratio for depth using observed slopes

COMPARISON OF OBSERVED DEPTH WITH CALCULATED DEPTH
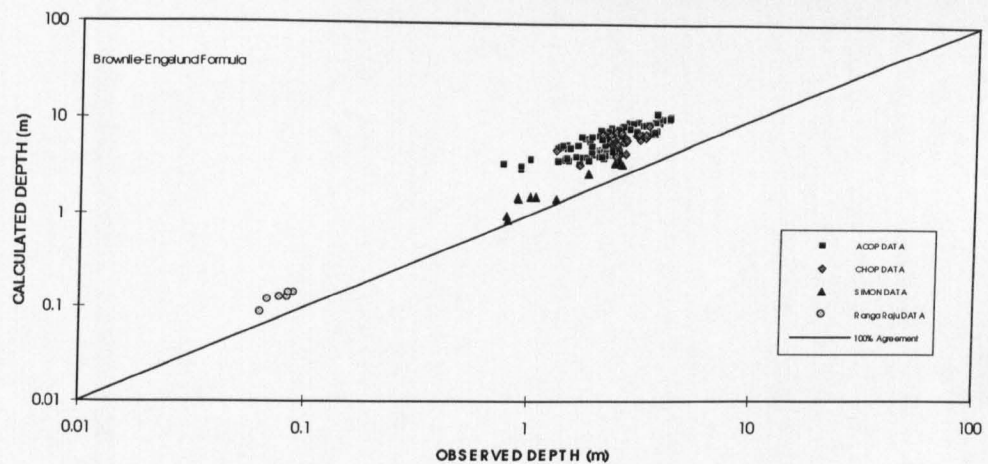
Figure 3.17. Calculated against observed depth using observed slopes

DISCREPANCY RATIO FOR DEPTH USING OBSERVED SLOPES
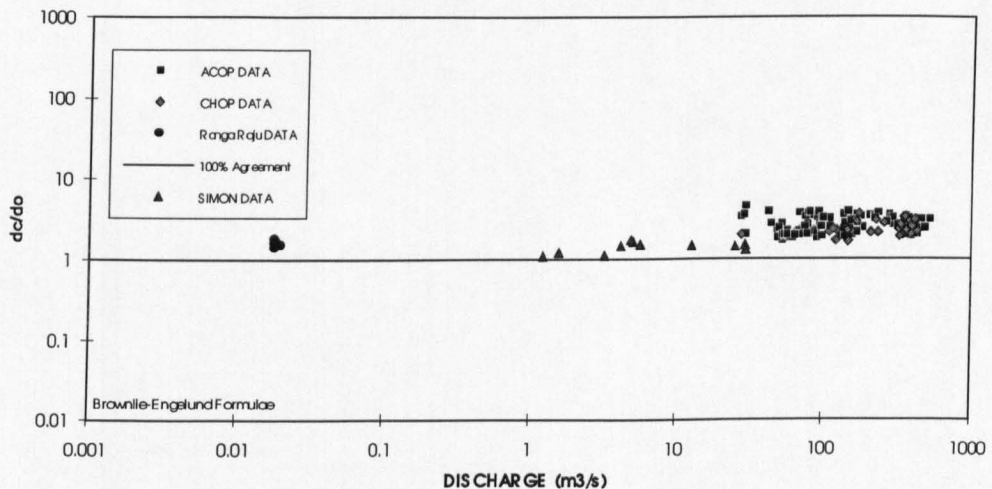
Figure 3.18. Discrepancy ratio for depth using observed slopes
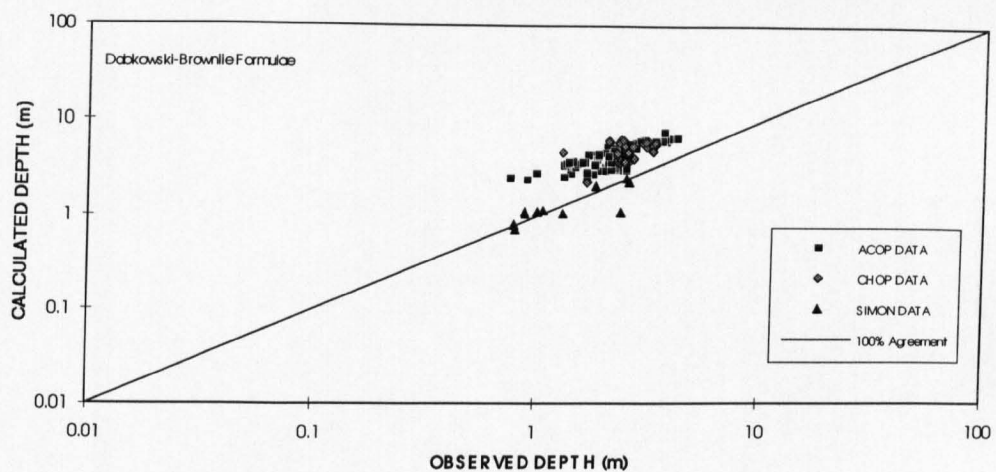
Figure 3.19. Calculated against observed depth using observed slopes
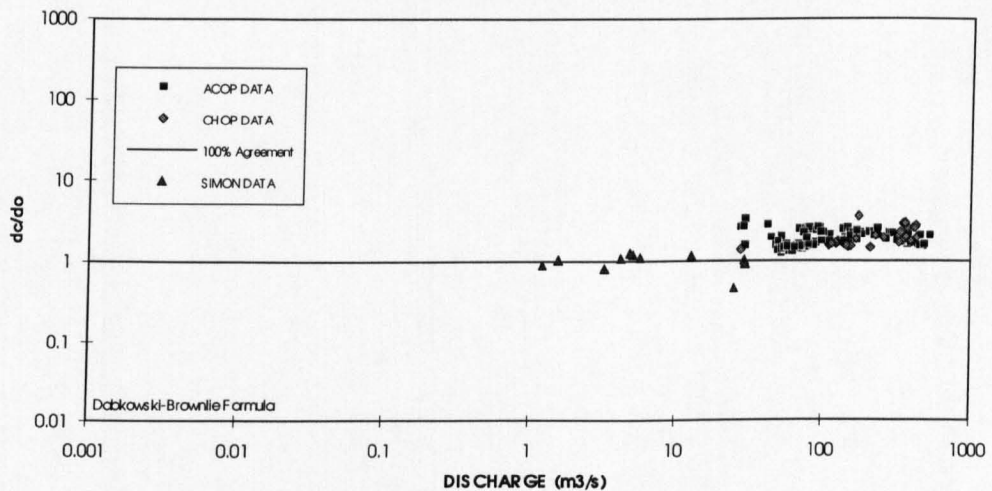

Figure 3.20. Discrepancy ratio for depth using observed slopes

COMPARISON OF OBSERVED DEPTH WITH CALCULATED DEPTH USING OBSERVED SLOPES
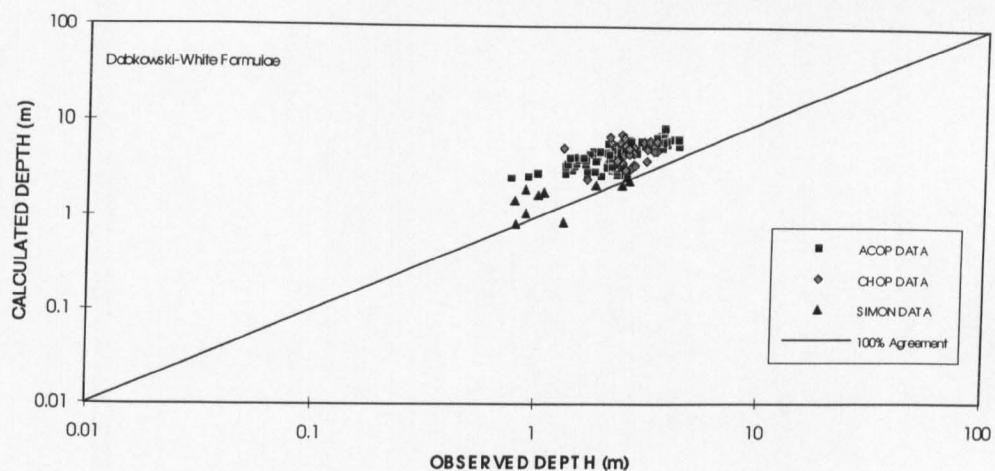
Figure 3.21. Calculated against observed depth using observed slopes

**DISCREPANCY RATIO FOR DEPTH USING OBSERVED SLOPES**
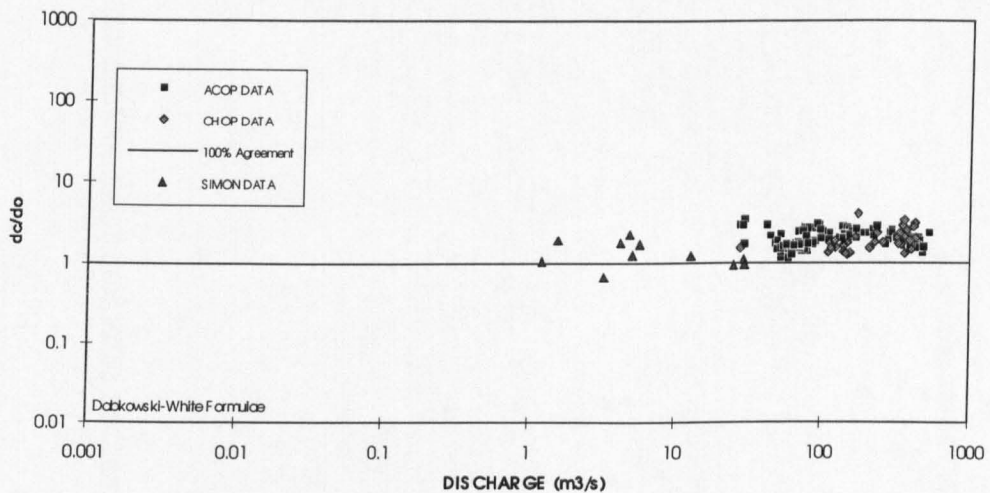
Figure 3.22. Discrepancy ratio for depth using observed slopes

COMPARISON OF OBSERVED DEPTH WITH CALCULATED DEPTH USING OBSERVED SLOPES
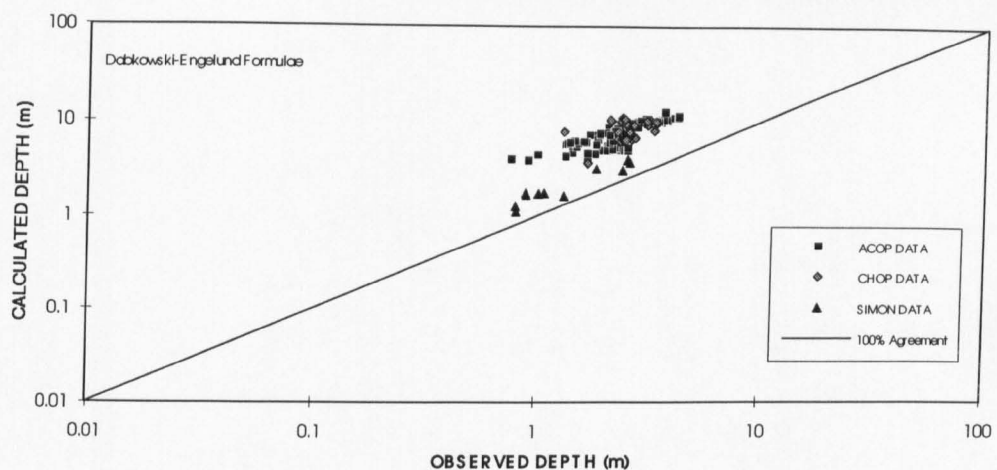

Figure 3.23. Calculated against observed depth using observed slopes

## DISCREPANCY RATIO FOR DEPTH USING OBSERVED SLOPES
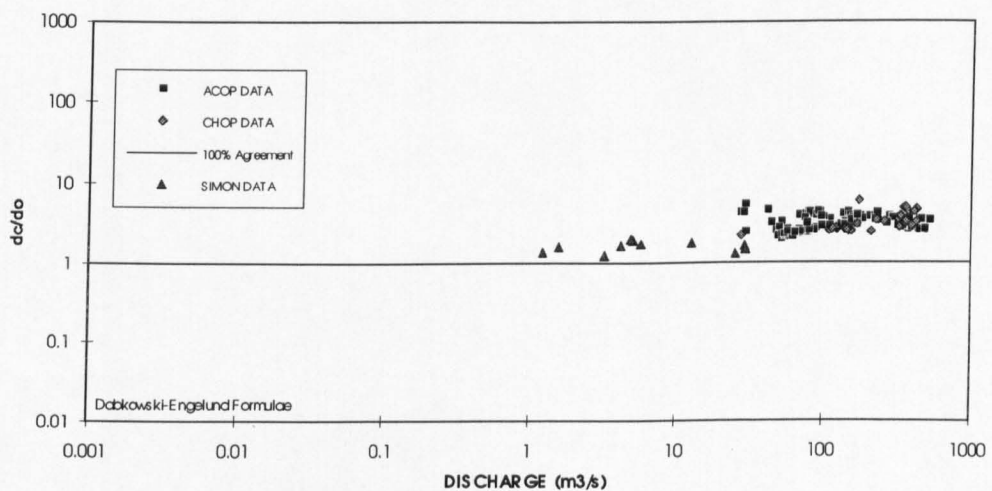
Figure 3.24. Discrepancy ratio for depth using observed slopes

3.8 Water surface width

For the combination of Brownlie (1982) equations, Fig. 3.25 shows the calculated and observed widths for the data sets used. The results show that the combination used mostly underpredicts the width for the ACOP data, CHOP data, and Ranga-Raju data. It overpredicts the width for Simon's data. The discrepancy ratio for the widths are shown in Fig. 3.26. It shows that the maximum discrepancy ratio is 2.6 and the minimum is 0.3. The mean value of the plotted discrepancy ratios is 0.7 with the standard deviation of 0.3.

For the next combination, the Brownlie (1982) flow resistance and Ackers and White (1973) have been used with sediment transport maximisation hypothesis. The results for width prediction are shown in Fig. 3.27. It shows that the combination used mostly underpredicts the width for the ACOP data, CHOP data, and Ranga-Raju data but it overpredicts the width for the data of Simon. The discrepancy ratio for the widths are shown in Fig. 3.28. It shows that the maximum discrepancy ratio is 2.1 and the minimum is 0.2. The mean value of the plotted discrepancy ratios is 0.6 with the standard deviation of 0.3.

For the combination of Brownlie (1982) and Engelund and Hansen (1967), the results for width prediction of the data used are shown in Fig. 3.29. It shows that the method underpredicts the width for the data of ACOP, CHOP, and Ranga-Raju. It mostly overpredicts the width for the data of Simon. The discrepancy ratio for the widths are shown in Fig. 3.30. It shows that the maximum discrepancy ratio is 1.8 and the minimum is 0.2. The mean value of the plotted discrepancy ratios is 0.4 with the standard deviation of 0.2.

For the combination of Dabkowski (1991) and Brownlie (1982) equations, the results are shown in Fig. 3.31. It shows that the method underpredicts the width for the data of ACOP, and CHOP. It overpredicts the width for the data of Simon. The discrepancy ratio for the widths are shown in Fig. 3.32. It shows that the

maximum discrepancy ratio is 3.0 and the minimum is 0.23. The mean value of the plotted discrepancy ratios is 0.8 with the standard deviation of 0.3.

For the Dabkowski-White combination, the method underpredicts the width for the data sets of ACOP, and CHOP. It overpredicts the width for Simon's data. The results for the calculated and observed data are shown in Fig. 3.33. The discrepancy ratio for the widths are shown in Fig. 3.34. It shows that the maximum discrepancy ratio is 14.1 and the minimum is 0.3. The mean value of the plotted discrepancy ratios is 0.9 with the standard deviation of 1.1.

For the Dabkowski-Engelund combination, the method shows the same behaviour for width prediction. It underpredicts the width for the data set of ACOP, and CHOP but mostly overpredicts the width for the data of Simon. Fig 3.35 shows the comparison results. The discrepancy ratio for the widths are shown in Fig. 3.36. It shows that the maximum discrepancy ratio is 2.1 and the minimum is 0.2. The mean value of the plotted discrepancy ratios is 0.5 with the standard deviation of 0.2.

The comparison shows that the best combinations for prediction of width are [Brownlie], [Brownlie-White], and [Dabkowski-Engelund]. It also indicates that the calculated widths, from all the combinations, have the same order of sensitivity as the observed variation.

COMPARISON OF OBSERVED WIDTH WITH CALCULATED WIDTH USING
OBSERVED SLOPES
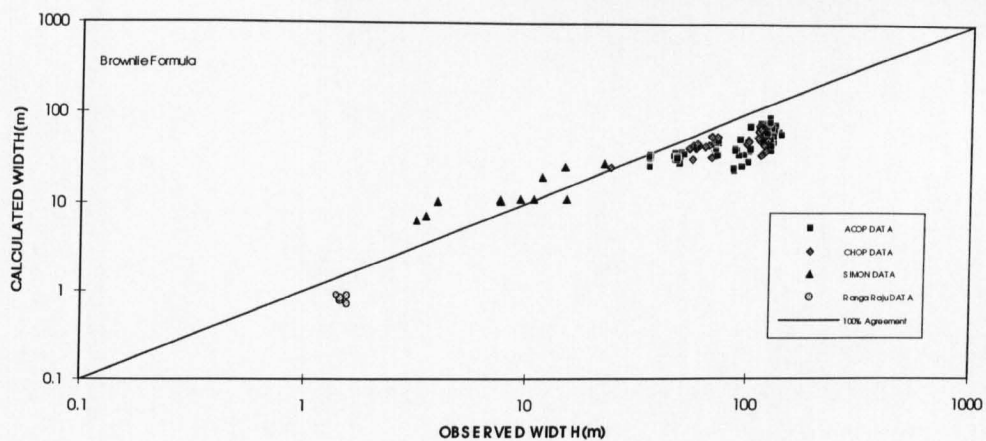
Figure 3.25. Calculated against observed width using observed slopes.

DISCREPANCY RATIO FOR WIDTH USING OBSERVED SLOPES
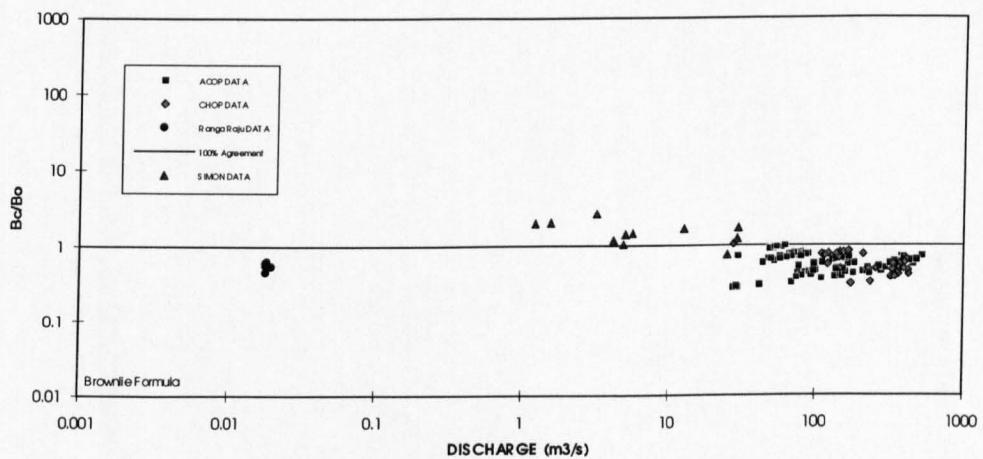
Figure 3.26. Discrepancy ratio for width using observed slopes.
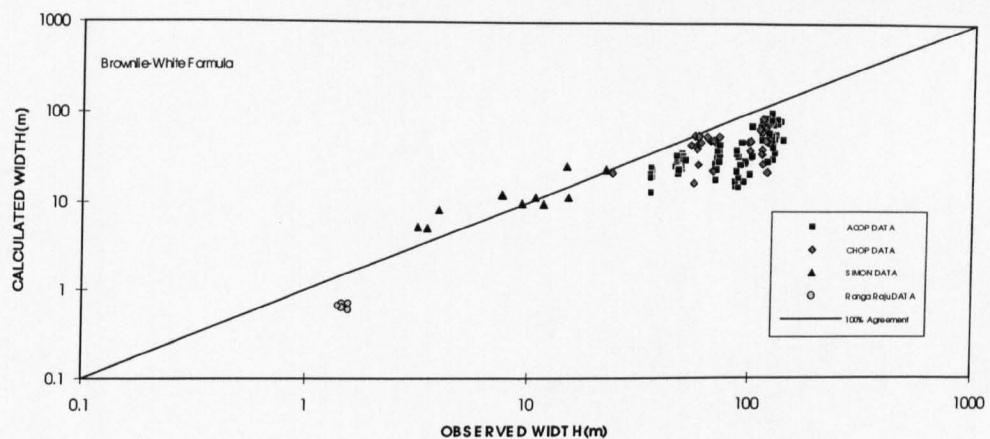
Figure 3.27. Calculated against observed width using observed slopes.
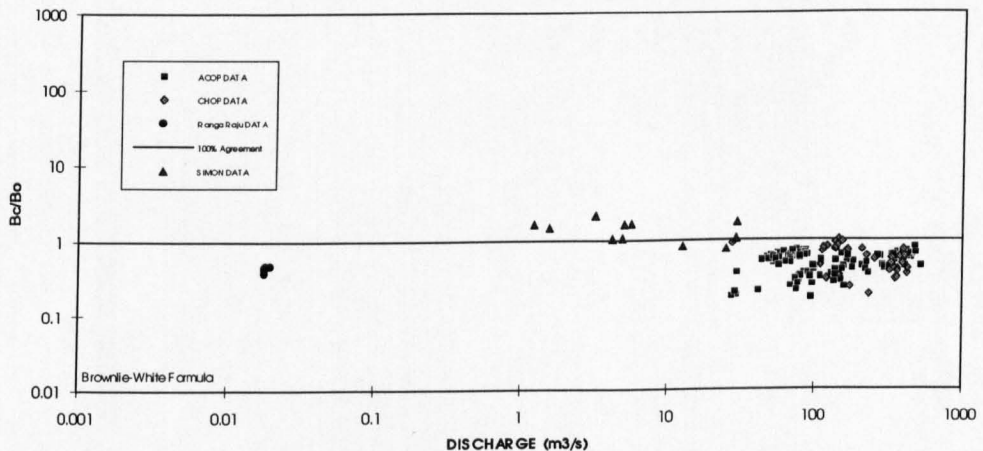
Figure 3.28. Discrepancy ratio for width using observed slopes.
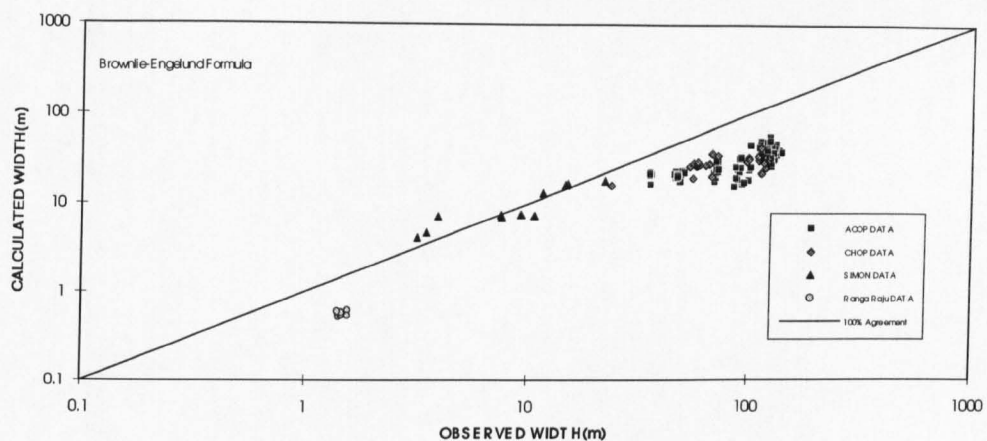
Figure 3.29. Calculated against observed width using observed slopes.
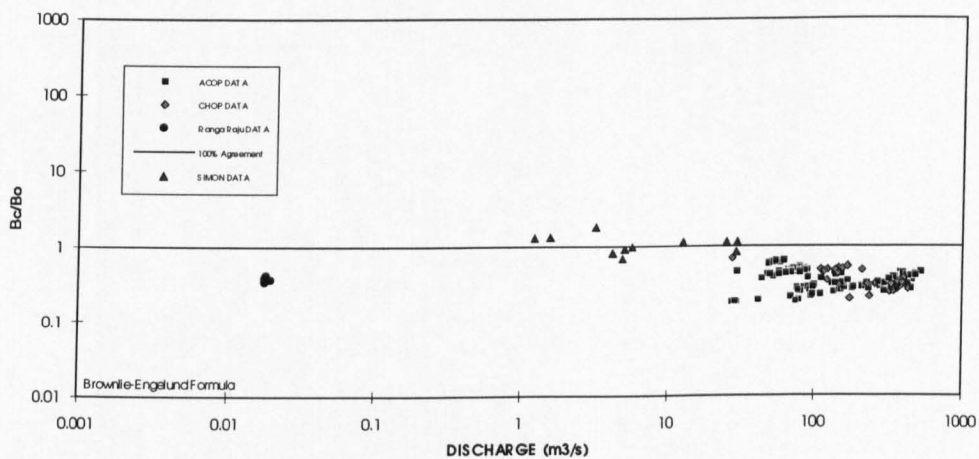
Figure 3.30. Discrepancy ratio for width using observed slopes.

Figure 3.31. Calculated against observed width using observed slopes.
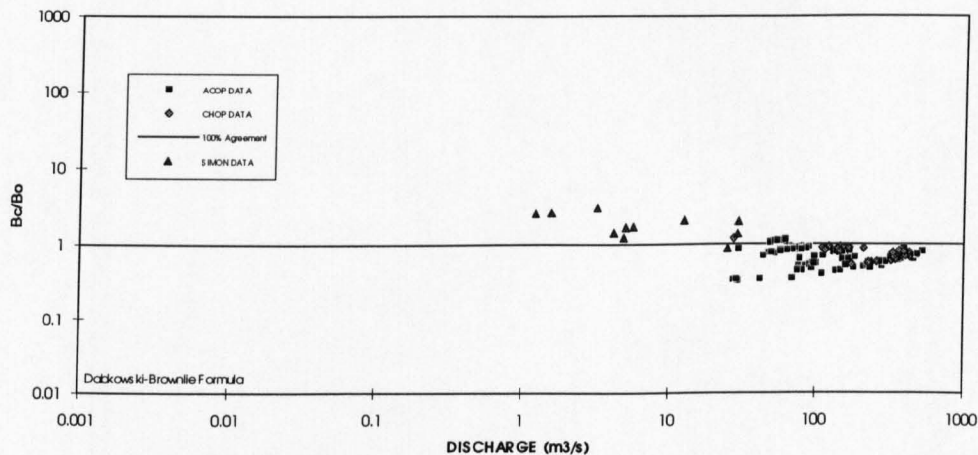
Figure 3.32. Discrepancy ratio for width using observed slopes.

Figure 3.33. Calculated against observed width using observed slopes.
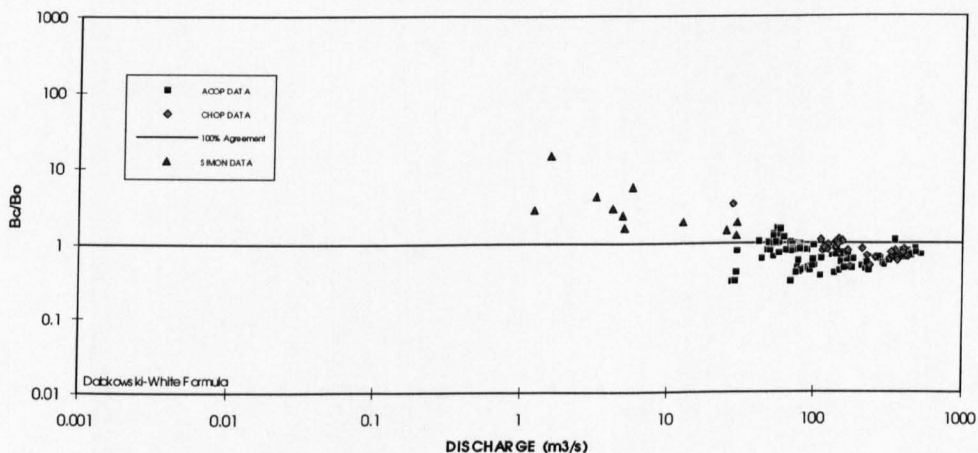
Figure 3.34. Discrepancy ratio for width using observed slopes.

Figure 3.35. Calculated against observed width using observed slopes.

DISCREPANCY RATIO FOR WIDTH USING OBSERVED SLOPES
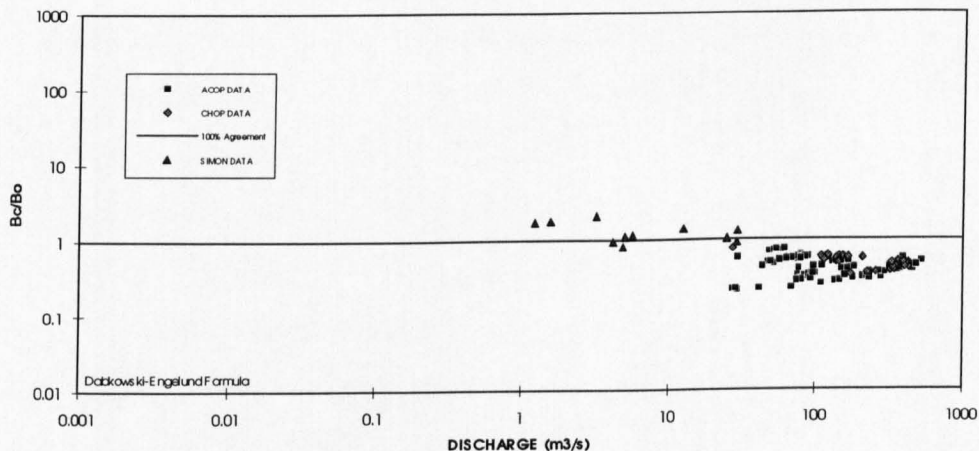
Figure 3.36. Discrepancy ratio for width using observed slopes.

3.9 Channel slope

For the combination of Brownlie (1982) equations, Fig. 3.37 shows the amount of calculated and observed slope using observed sediment concentration of the data sets. The results show that this combination mostly underpredicts the slope for the ACOP data, CHOP data, and Simon data. It overpredicts the slope for the Ranga-Raju data. The discrepancy ratio for the slopes are shown in Fig. 3.38. It shows that the maximum discrepancy ratio is 58.3 and the minimum is 0.0009. The mean value of the plotted discrepancy ratios is 0.6 with the standard deviation of 4.4.

For the next combination, the Brownlie (1982) flow resistance and Ackers and White (1973) have been used with channel slope minimisation hypothesis. The results for slope prediction are shown in Fig. 3.39. It shows that the combination used mostly underpredicts the slope for the ACOP data, CHOP data, and Simon data but it overpredicts the slope for the data of Ranga-Raju. The discrepancy ratio for the slopes are shown in Fig. 3.40. It shows that the maximum discrepancy ratio is 23.6 and the minimum is 0.008. The mean value of the plotted discrepancy ratios is 0.5 with the standard deviation of 1.9.

For the combination of Brownlie (1982) and Engelund and Hansen (1967), the results for slope prediction of the data used are shown in Fig. 3.41. It shows that the method mostly underpredicts the slope for the data of ACOP, CHOP, and Simon. It overpredicts the slope for the data of Ranga-Raju. The discrepancy ratio for the slope are shown in Fig. 3.42. It shows that the maximum discrepancy ratio is 7.0 and the minimum is 0.05. The mean value of the plotted discrepancy ratios is 0.8 with the standard deviation of 0.7.

For the combination of Dabkowski (1991) and Brownlie (1982) equations, the results are shown in Fig. 3.43. It shows that slope prediction of the method is equally distributed around the 100% agreement line for the data of ACOP, CHOP. It overpredicts the slope for the data of Simon. The discrepancy ratio for the slopes

are shown in Fig. 3.44. It shows that the maximum discrepancy ratio is 97.3 and the minimum is 0.03. The mean value of the plotted discrepancy ratios is 5.04 with the standard deviation of 10.4.

For the [Dabkowski-White] combination, the method mostly overpredicts the slope for the data sets of ACOP, CHOP, and Simon. The results for the calculated and observed data are shown in Fig. 3.45. The discrepancy ratio for the slopes are shown in Fig. 3.46. It shows that the maximum discrepancy ratio is 53.7 and the minimum is 0.12. The mean value of the plotted discrepancy ratios is 2.6 with the standard deviation of 4.4.

For the [Dabkowski-Engelund] combination, It shows the slope prediction of the method is equally distributed around the 100% agreement line for the data of ACOP, and CHOP. It overpredicts the slope for the data of Simon. Fig. 3.47 shows the comparison results. The discrepancy ratio for the slopes are shown in Fig. 3.48. It shows that the maximum discrepancy ratio is 7.3 and the minimum is 0.1. The mean value of the plotted discrepancy ratios is 1.1 with the standard deviation of 0.9.

The comparison shows that the best combinations for prediction of slope are [Brownlie-Engelund], and [Dabkowski-Engelund]. For all the considered combinations, the order of sensivity for the calculated slopes is higher than the observed variation.
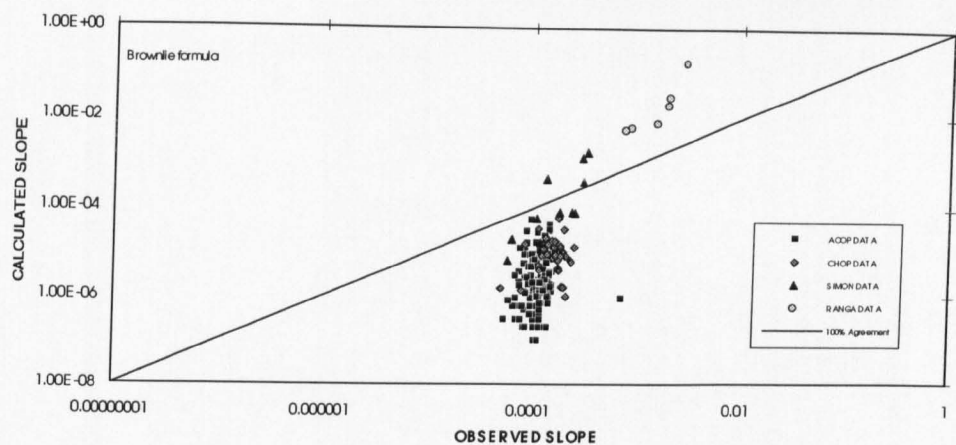
Figure 3.37. Calculated against observed slope using observed sediment concentrations.
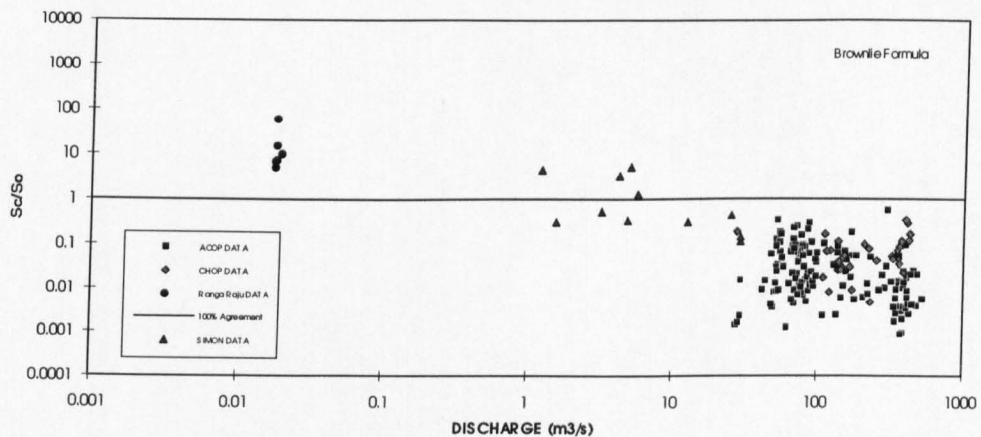
Figure 3.38. Discrepancy ratio for slope using observed sediment concentrations.

74
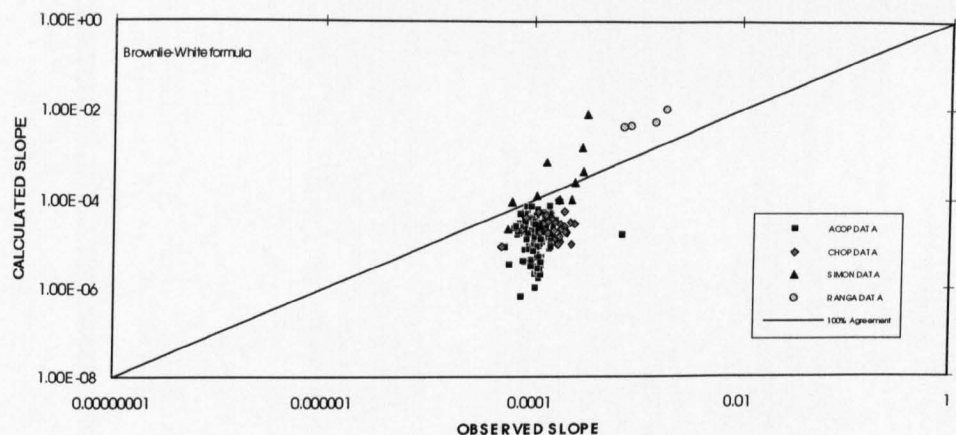
Figure 3.39. Calculated against observed slope using observed sediment concentrations.
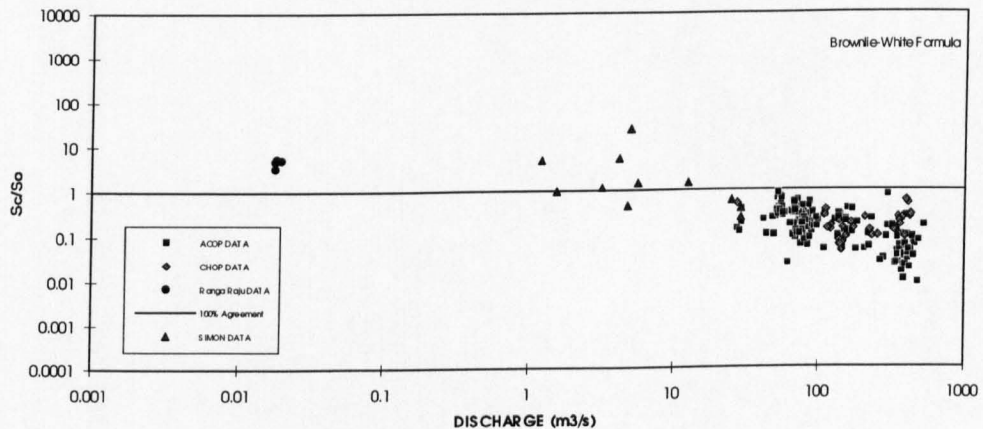
Figure 3.40. Discrepancy ratio for slope using observed sediment concentrations.
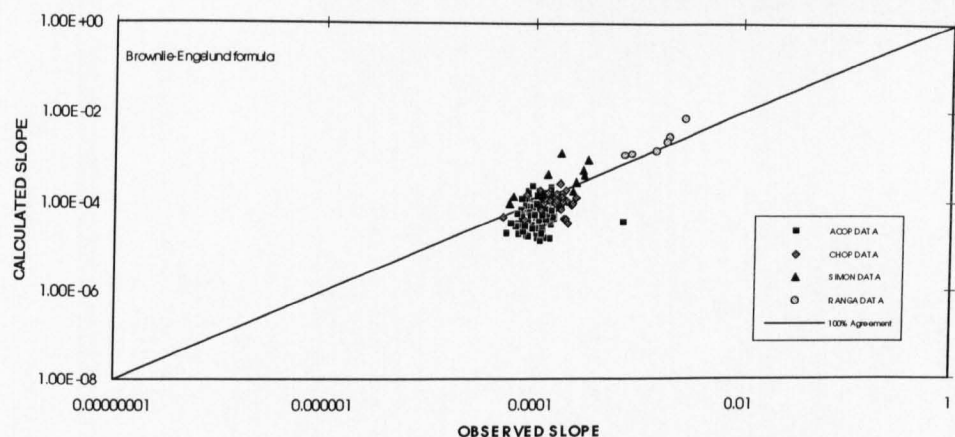
Figure 3.41. Calculated against observed slope using observed sediment concentrations.

DISCREPANCY RATIO FOR SLOPE USING OBSERVED SEDIMENT
CONCENTRATIONS
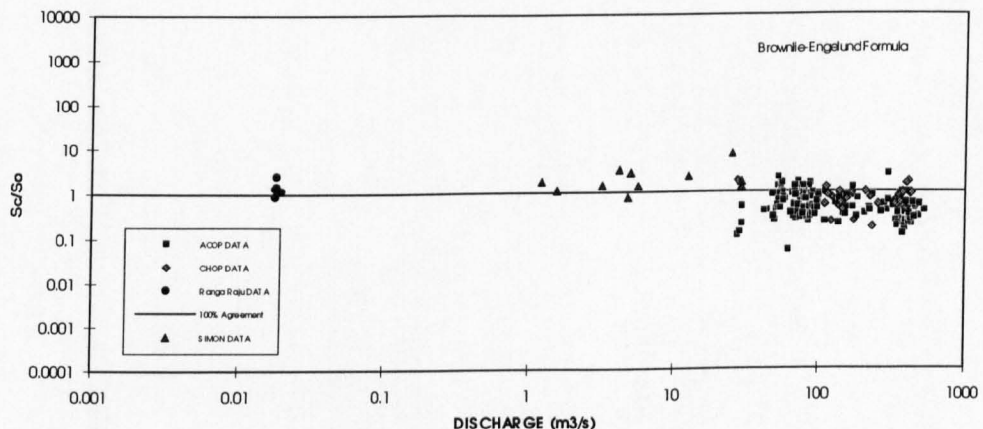
Figure 3.42. Discrepancy ratio for slope using observed sediment concentrations.
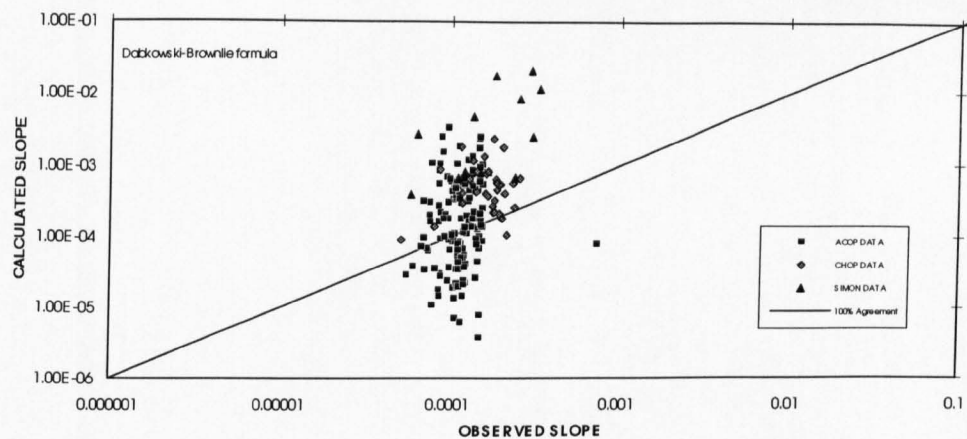
Figure 3.43. Calculated against observed slope using observed sediment concentrations.
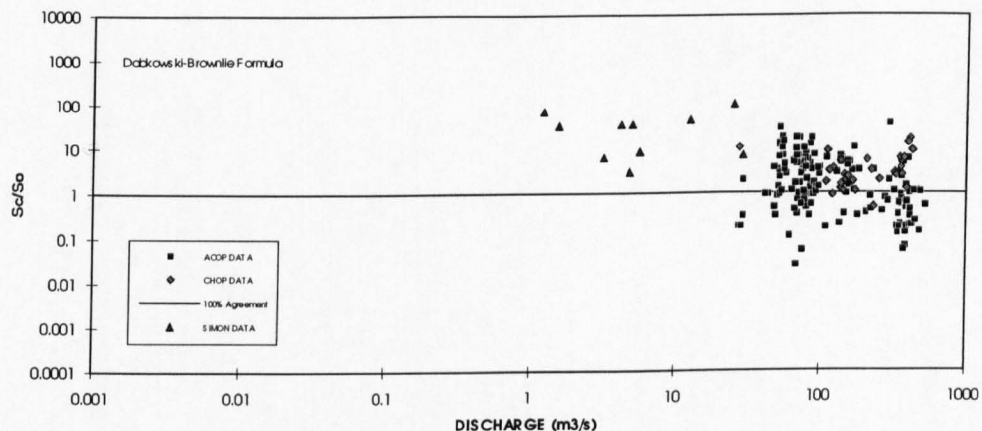
Figure 3.44. Discrepancy ratio for slope using observed sediment concentrations.
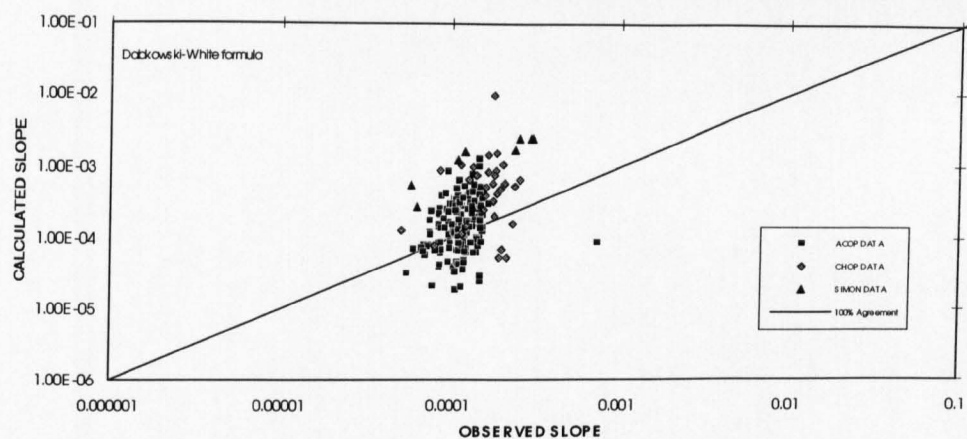
Figure 3.45. Calculated against observed slope using observed sediment concentrations.
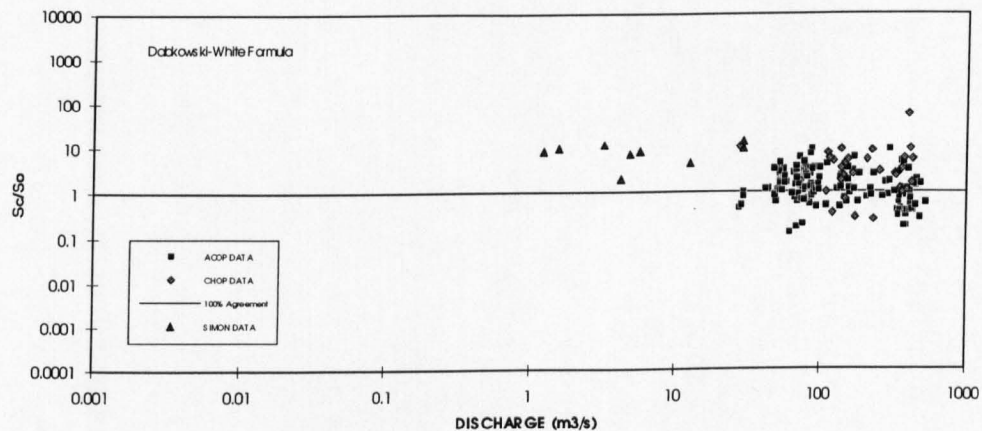
Figure 3.46. Discrepancy ratio for slope using observed sediment concentrations.
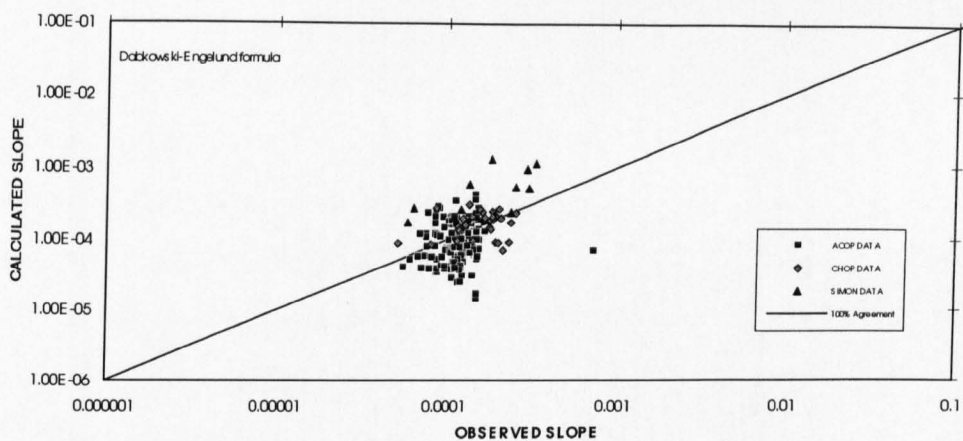
Figure 3.47. Calculated against observed slope using observed sediment concentrations.

DISCREPANCY RATIO FOR SLOPE USING OBSERVED SEDIMENT
CONCENTRATIONS
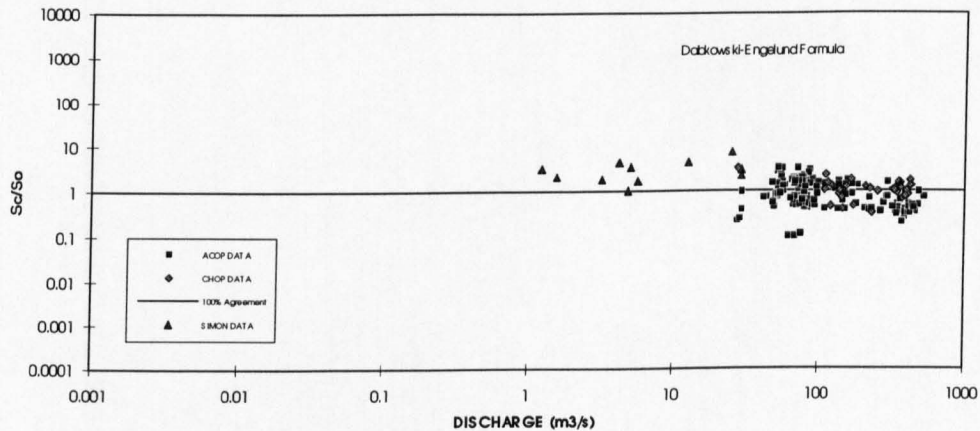
Figure 3.48. Discrepancy ratio for slope using observed sediment concentrations.

3.10 Chapter summary

In this chapter different extremal hypotheses have been reviewed. The maximum sediment concentration hypothesis for the design of stable alluvial channels has been used. This hypothesis has been combined with different flow resistance and sediment transport equations. A computer program has been developed which for specified discharge and slope gives those values of depth, width, velocity, and friction factor that maximise the sediment concentration in the channel. The output of the program has been verified with different field and lab data. The results show that the success of the method is dependent on the equations adopted. In other words, the use of different sediment transport and flow resistance equations may lead to different predictions. Among the different combinations considered the combination which provided the best agreement with the data were the Brownlie (1982) formulae.

Chapter Four
Experimental Design and Data Description

4.1 Introduction

This chapter describes the experimental design and equipment used in this study. It includes the details of different series of experiments, which have been carried out in this research. It also describes the facilities, apparatus, and equipment used in the experiments. All the experiments were carried out in the "regime flume" of the hydraulics laboratory of the Department of Civil Engineering of the University of Newcastle upon Tyne.

4.2 Experimental Design

The experimental programme was designed to examine the instabilities which may occur in a stable channel when interacted by hydraulic structures, e.g. bridge piers or abutments. The experiments were carried out in three series as explained below.

Series A: Development of straight stable channels. (Experiments 1 to 18, 19A to 39A)

These experiments have been carried out to examine the validity of the White et al (1981) theory in prediction of characteristics of straight stable channels. They also have been a basis for further experiments on interaction of piers and abutments with stable channels.

Series B: Interaction of straight stable channels with bridge piers (Experiments 19B to 28B, 34B, 36B, and 38B).

The aim of this series of experiments was to test the interaction between straight stable channels and bridge piers. The piers used in the experiments were cylindrical.

<u>Series C:</u> Interaction of straight stable channels with Abutments. (Experiments 29C to 33C, 35C, 37C, and 39C)

The aim of this series of experiments was to test the interaction between straight stable channels and abutments. The abutments used in the experiments had a vertical wall with semicircular nose.

The first series (i.e. series A) was designed to develop straight stable channels in the laboratory. The imposed initial conditions in the experiments were based on the predictions of the WPB theory. In this series, discharges in the range of Q=2-4 l/s were used. Sediment was fed to the upstream end of the carved channel, at the rate predicted by the WPB theory. The same slope, approximately, was imposed i.e. the slope of the carved channel for the fed sediment concentration. The initial cross sectional dimensions were also estimated using WPB theory. The channels were allowed to develop freely, without imposing any constraints, until the rates of change in bed and banks of channels were insignificant and a stable channel plan form was reached.

The series B of the experiments was designed to investigate the interaction between bridge piers and straight stable channels. In this series of experiments the developed straight stable channels of series A, i.e. 19A to 28A, 34A, 36A, and 38A, were used as a first part of the experiments. For the second part, bridge piers were located in the bed of the developed channels. Without changing the imposed conditions, e.g. discharge, sediment load, the channels were allowed to develop freely, until the rates of change in bed and banks of channels were insignificant. In the experiments, cylindrical piers were used. Single pier and groups of piers with different spacing were used in the experiments.

The purpose of the last series of the experiments i.e. series C, was to study the variations which occurred in the developed channels when interacting with abutments. The abutments used for the purpose of this study were vertical wall with semicircular nose. In this series of experiments, the developed straight stable channels of series A, i.e. 29A to 33A, 35A, 37A, and 39A, were used as the

82

foundation part of the experiments. For the next part, abutments were located in the bed of the developed channels. With abutments in place, the channels were allowed to develop freely until the rates of change in bed and banks of the channels were insignificant.

4.3 The description of experimental set-up

This section describes the details of the "regime flume" which has been used for the purpose of this research. A brief description and function of each part of the experimental set-up is described in the following paragraphs. Fig. 4.1 shows the schematic layout of the regime flume.

The flume in which the experiments were carried out is 22 metres long and 2.5 metres wide. The depth of the flume, which is filled with a uniform sand is, 600 mm. The d_{50} of the sand is 1 mm. The model channels were carved in the sand using a wooden former fixed on the carriage. The slope of the channel was imposed by using the rails and adjusting them to the desired slope.

For imposing different sediment concentrations in the experiments, a screw type sediment feeder was used. The feeder location is above the inlet box and in the centre of the flume and allows the sand to be fed over the full width of the model channels. The uniformity of sand feeding rate of the instrument was tested. The tests showed that the rate of feed of sand remained uniform even with varying head in the hopper. The feeder calibrated for different dial settings. Using the calibration curve it was possible to set the dial of the sand feeder in order to feed any required value of the sediment rate into the flume. It is possible to feed sand up to 1100 g/min using different dial settings.

There are two rails on both sides of the flume on which a carriage can be moved along the channel. The side rails are supported on mild steel angle, which are located at 1m intervals. These rails are used to provide the required channel slope by changing the location of the screw inside each support.
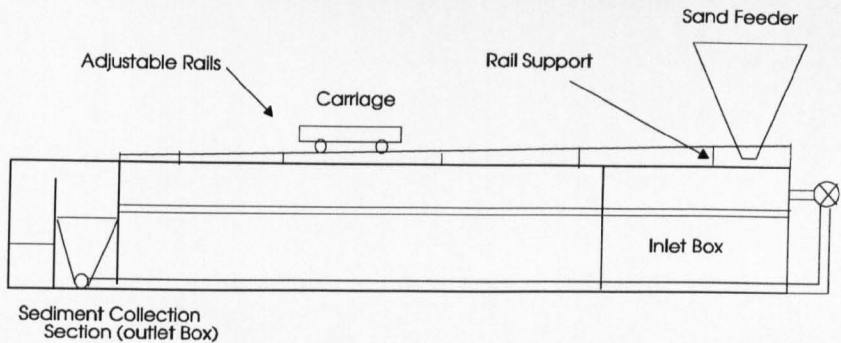
b) Section
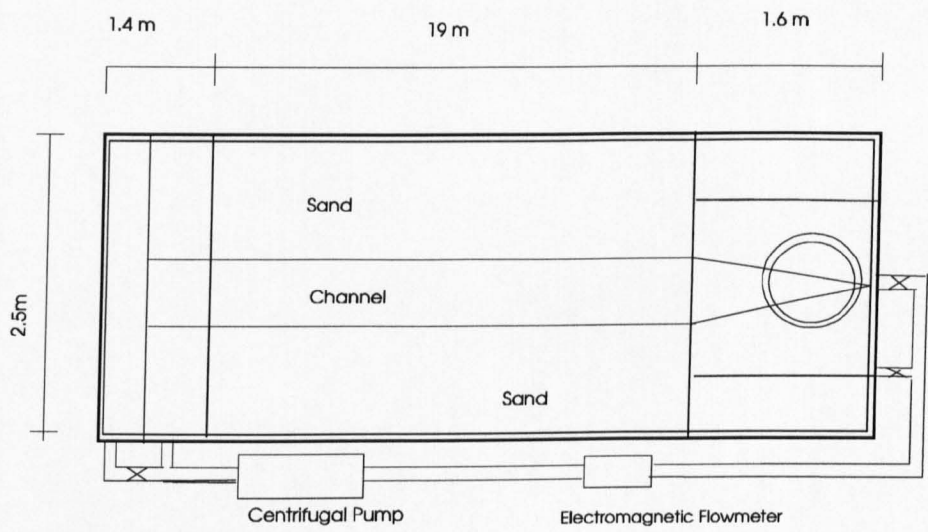
b) Plan

Figure 4.1. Schematic a) Plan and b) Section of the regime flume (Not to scale)

The inlet box acts as an upstream reservoir, a guide channel diverging gradually to the width of the prepared channel is located above the inlet box and conducts water towards the model channels. The honey-comb shaped metal inside the guide channel dissipates the excessive energy of the pumped water to allow free flow of water and sediment mixture.

The outlet box which is located at the downstream of the flume collects the water flowing through the channel. It is divided into two parts to be used for

84

recirculation as well as feed system. By closing the outlet pipe installed in the lower half and opening the one in the upper half, the entered mixture of water and sediment into the upper half of the outlet box could be recirculated back in to the channel. However, in cases where sediment was supplied at the upstream end of the channel, the sediment entered into the upper half of the outlet box was trapped there to allow clear water enter into the lower half of the outlet box. By opening the outlet pipe installed in the lower half and closing the one in the upper half, the clear water could be returned to the channel.

There is a tilting gate at the downstream end of the flume. The water level in the channel can be adjusted by using the tilting gate. It also serve to protect the channel banks from erosion at downstream reach which is expected in the case of free water fall. A centrifugal pump has the duty of recirculating clear water or water and sediment mixture from the outlet box to the flume channel. The range of discharges which was used for the purpose of the experiments was Q=2-4 l/s.

An electromagnetic flow meter installed in the recirculating line shows the amount of the discharge recirculated to the flume. The discharge can be read in litres per minute from the meter directly.

4.4 Experimental procedure

For each set of experiments, a channel was carved along the centre line of the flume with the help of a wooden plank fixed on the carriage. The slope of the channel was imposed by using the rails and adjusting them to the desired slope. The dimensions of the channel was predicted using the WPB theory, then the carved channel was subjected to the desired discharge and the discharge was kept constant until a stable channel shape in plan was reached. The duration of the experiments was such that the channel would establish a stable shape in plan and cross-section. For the next stage, the channel was drained and the geometry of the channel was measured at selected cross-sections. For series B experiments, the piers were

installed in the channel bed and the experiment was continued without changing the initial imposed parameters. At the end, the channel geometry was measured to assess the interaction effects between bridge piers and stable straight channels. The effects were evaluated by comparing the cross-sections in series A and B.

For series C of the experiments, the abutments were installed in the bed of the developed straight channels. The experiments were continued without changing initial imposed parameters. At the end, the channel geometry was measured to evaluate the interaction effects between abutments and stable straight channels.

The following parameters at appropriate time intervals of the experiments were recorded.

1. Bed level and channel cross-section at appropriate intervals along the channel length.

2. Water surface elevation at appropriate intervals along the channel length.

3. Location of left and right banks at appropriate channel cross-sections.

4. Rate of increase of width with time.

5. Flow discharge in the channel.

6. Sediment concentration using trapped sediments at downstream end of the channel.

7. Velocity measurements in the centre of the channel using Pitot tube (Experiments 32A to 37A).

8. Boundary shear measurements along the channel half width using Preston (1954) method (Experiments 32A to 37A).

According to the above measured quantities calculation of flow velocity, water surface slope, Froude number, and other required parameters was possible.

4.5 Equilibrium channel criterion

For the start of each experiment, the channel slope was set to the required gradient. An initial channel was carved with the required slope in the sand bed.

Plate 4.1 shows a typical channel carved in the sand bed. The water was introduced in to the channel, gradually up to the desired amount. The water surface slope was adjusted by a tilting gate at the downstream end of the flume if necessary. The channel was let to develop until a stable channel plan form was reached.

To decide when a channel has achieved a stable or equilibrium condition has always been difficult. Most previous research indicates that it is a matter of the investigator's judgement. Ackers and Charlton (1970) reported that the experiments were continued until it was judged that a stable channel pattern had formed in at least part of the length of the stream. Schumm and Khan (1972) reported that water was allowed to flow through the initial channel until major channel adjustments were completed and the channel became relatively stable i.e. no further significant changes of channel shape, dimensions, or pattern occurred.

In this work, the criterion for determining if a channel has achieved the equilibrium condition, is based on the rate of channel width increase. It was decided that if the rate of increase of width remains less than 1% per hour for at least 2 to 3 hours, then the channel is treated as having obtained an equilibrium condition. In order to achieve the equilibrium condition, experiments from time duration of 8 up to 25 hours have been carried out. A great deal of time was spent on developing and collecting the data of these channels.

4.6 Development of straight stable channels

For the experiments carried out in series A, the initial valley slope was set approximately equal to the equilibrium slope for a stable straight channel, predicted by the WPB theory. In the experiments, sand feeding was operated by two methods:

A) The same sand as the bed material was fed at the upstream end of the prepared channel. The required rate of sand feeding was according to the initial design in each test. It was fed at a constant rate using the sand feeder.

B) The mixture of water and sediment was recirculated to the channel using the recirculating system.

Typically, after the introduction of water and sediment into the channel, the channel started widening and most of the channels obtained about 90% of the finally developed stable width in the first two hours. Afterwards, the rate of widening was slowed down and in 7 to 8 hours time, the rate of change of width was reduced to less than 1% per hour. This was accepted as the channel having established a stable condition. Plate 4.2 shows a fully developed straight channel at the end of the experiment. Plate 4.3 shows a close shot of the bed profile. As can be seen in Plate 4.3, striations in the channel bed provide some evidence of secondary currents in these channels. Secondary currents are important in hydraulic engineering because these currents affect the primary mean flow field, the friction law, the formation of three dimensional bed configurations such as sand ribbons and three dimensional sediment transport [Vanoni (1946), Karcz (1966), Kinoshita (1967), and Allen (1985)]. The following section will address the characteristics of such phenomena.

4.6.1 The characteristics of observed laboratory secondary currents

More than 100 years ago, river engineers, e.g. Stearns (1883), inferred the existence of secondary currents on the basis of the fact that the maximum velocity occurred well below the free surface in open channels that were not extremely wide. Gibson (1909) examined the pattern of secondary currents and estimated that the velocity of the secondary currents would be about 5% of the mean stream velocity. In addition, Vanoni (1946) suggested that the cellular secondary currents might exist in wide open channels on the basis of the fact that the concentration of suspended sediment varied cyclically in the spanwise direction. This idea was strengthened by Karcz (1966) and Kinoshita (1967). Kinoshita (1967) found from
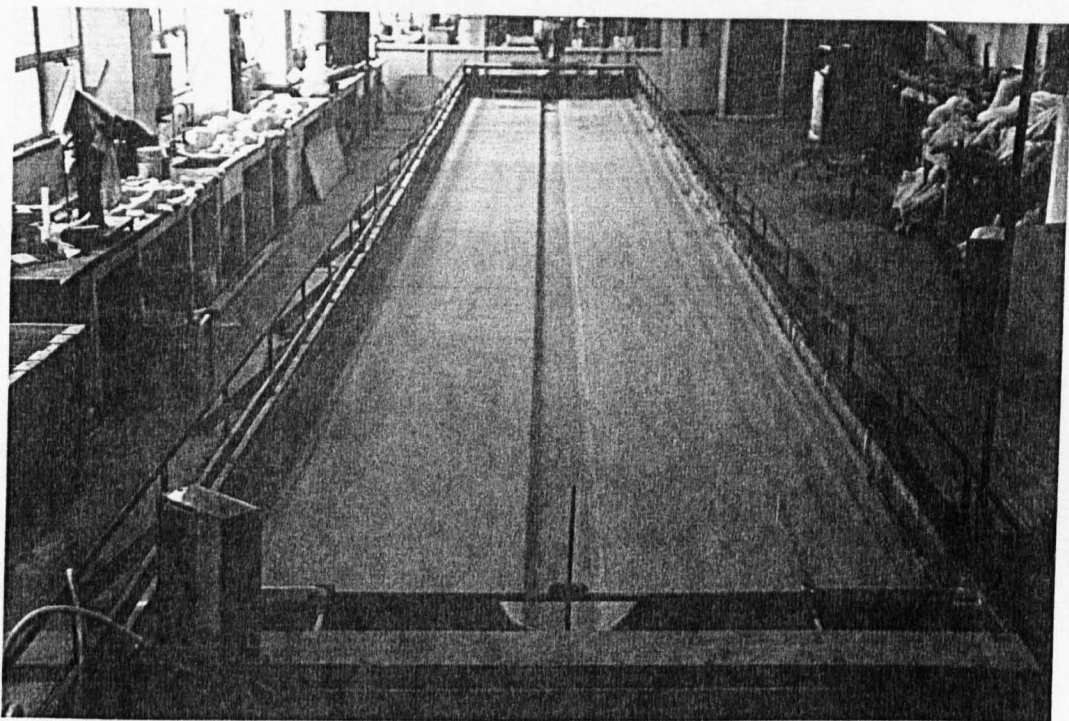
Plate 4.1. Typical carved channel in sand bed.
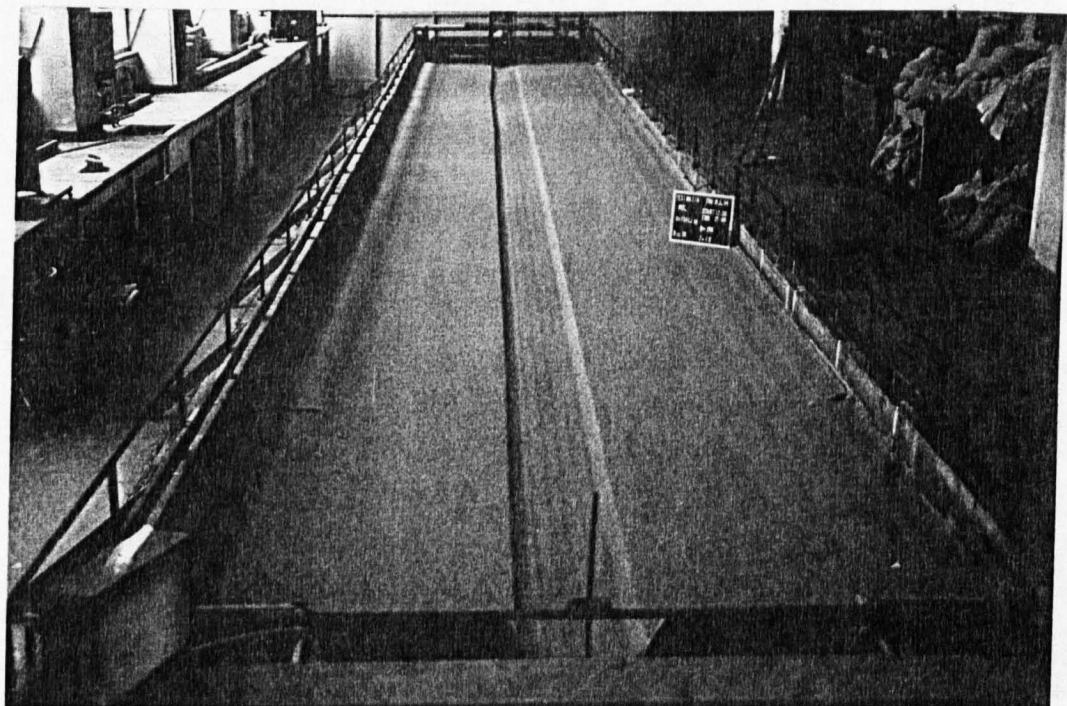
Plate 4.2. A typical developed stable straight channel at the end of experiment.

aerial stereoscopic surveys of flooded rivers that a boil street with high concentration of suspended sediment became a low speed zone and high speed zone in which foams gathered were formed on both sides in spanwise direction, with a spacing of twice the flow depth.

Since Prandtl's time, secondary currents have been known to occur in noncircular duct flows if the solid wall effect is strong. These secondary currents are often called 'corner flows' because they flow from the core toward the corners of duct. In the 1960's, some of the early experimental studies on corner flows in square and rectangular ducts were conducted by means of hot wire anemometers, e.g., Leutheusser (1963), Gessner and Jones (1965). In the 1970's, accurate measurements of corner flows were made possible by the use of a laser Doppler anemometer (LDA), e.g., Melling and Whitelaw (1976). Nezu and Rodi (1985) first conducted accurate measurements of secondary currents in open channel flows by making use of a high power LDA system. They found that the velocity-dip phenomenon, i.e. the maximum velocity in open channel flows appears not at the free surface, but rather just below it, occurs if $\frac{B}{h} \leq \alpha_c = 5$ or slightly larger.

The origin of cellular secondary currents in fluvial channels is referred to non homogeneity of bed roughness, as well as lateral undulations of the bed, which causes nonhomogeneity in the bed shear stress. In turn, this nonhomogeneity of shear stress creates anisotropic turbulence which generates streamwise vorticity and cellular secondary currents. The reverse process may also occur. If cellular secondary currents exist beforehand, longitudinal ridges and troughs are formed even in uniform bed material because of the lateral variation of bed shear stress. In addition, if the bed material is composed of a mixture of sizes, the fine sediment is swept sideways on to ridges of finer material by high shear stress in downflow regions, leaving a strip of coarser sediment exposed to the flow. That is, cellular secondary currents will generate beds consisting of alternating finer and coarser strips. In this way, three dimensional flows and secondary currents in wide fluvial

channels interact with lateral bed conditions. However, the origin of cellular secondary currents and sand ribbons over an initially uniform flat bed has not been elucidated yet. Five possibilities for this initiation mechanism have been proposed.

1. The aspect ratio of channel should be an even number, irrespective of wall properties, thus corresponding to an eigenvalue problem.

2. The existence of a free surface may motivate cellular secondary currents.

3. An initiation of cellular secondary currents may be motivated by the mutual interaction between such pre-existing secondary currents as corner flows and the sand bed.

4. Small disturbances that are always present both on the bed and in the flow itself may provide small driving forces that generate or enhance secondary motions.

5. Coherent motions near the bed like bursting motions may develop in to the outer region and then trigger cellular secondary currents and boil vortices.

Among the five possibilities for the origin of secondary currents, the available information indicates that (3) and (4) are the most likely causes [Nezu and Nakagawa (1993)].

During the experiments in the present study for developing stable straight channels, ridges and troughs were observed in the bed of developed channels. These features provide the evidence of secondary currents' existence in the body of main flow. The present data show that the transverse spacing between the sand ridges is approximately twice the flow depth which is consistent with previous research e.g. Kinoshita (1967).

In some experiments, the presence of the sand ribbons in the bed and the central zone of channels was quite clear up to the end of the tests. Although the sediment used in the experiments was quite uniform, it was possible to distinguish between the finer sediment on ridges and coarser sediment on stripes. This supports the idea that the finer sediments are swept away by high shear stress in downflow regions, leaving a strip of coarser sediment exposed to the flow i.e. secondary currents will generate beds consisting of alternating finer and coarser strips. It also may support

the idea that the presence of the secondary currents and sand ribbons in the bed of the developed channels imply the stability of these channels.

4.7 Description of the experimental data

In this section, details of the methods used regarding the collection of data are explained. The procedure of measurements or the calculations of them are explained. These experimental data mainly include the water discharge, water surface slope, valley slope, sediment concentration, cross-sectional geometry, velocity and shear stress distribution and hydraulic characteristics.

4.7.1 Sediment concentration

There have been different opinions about the sediment concentration index in previous research. In most previous work, sand fed at the channel inlet has been treated as an index of the sediment concentration in the channel. Leopold and Wolman (1957) for calculation of sediment concentration used the sand fed into the channel. Schumm and Khan (1972) also used the amount of sand fed into the channel for calculation of sediment concentration. However, they admitted that this method for estimation of sediment concentration was not accurate because the amount of sand at the channel outlet often exceeded or was less than the amount fed into the channel.

Ackers and Charlton (1970), as an index of sediment concentration, used the sediment concentration measured at the downstream end and averaged over the time span when the channel has established a stable condition.

For the present study, after a number of trials, it was more convincing to use the measured sediment concentration at the downstream end of the channel as the representative value for sediment concentration. Further, Ackers and Charlton's (1970) view for averaging the sediment concentration only over the time span after the channel had fully developed was more reasonable.

For the present work, the concentration is calculated as the mean values of the measured sediment concentrations at the channel outlet. The sediment concentration in the channel was measured at the downstream end by collecting samples of sediments at appropriate time intervals (each 15 or 30 minutes intervals). Fig. A4, in Appendix A, shows the variation of sediment concentration for a typical run. The sediment sampler was weighed before and after the collection of sediment. The difference of the two readings was the wet weight of the sand collected in a fixed time. The relation between dry and wet sand were found by oven drying of a number of samples. The dry weight of the sand collected was obtained by multiplying the wet weight with the coefficient obtained. The dry weight of sand divided by the collection time gave the sediment discharge. The sediment concentration was then calculated by dividing sediment discharge by flow discharge. For the results, see Table A1 in Appendix A.

4.7.2 Channel slope and water surface slope

The slope of the channel could be imposed by adjusting the side rails to the required slope. As the carriage fixed with the screeding board was moved on the side rails to excavate the channel, the carved channel would have the same slope as that of the rails. However, after excavating each channel, the slope was checked using a level and measuring elevation of centre point of the channel in at least every 1m along the channel length. The slope of the best fit line of these measured values was treated as the slope of the carved channel. The water surface slope was measured with the help of point gauges, mounted on the carriage. Water surface levels were recorded at least every 1m along the channel length, after the channel was assumed to have achieved a stable condition. The slope of the best fit line of these measured values was treated as the slope of the water surface. For the results, see Table A1 in Appendix A. Fig. A5, in Appendix A, shows the initial bed and water surface profile for a typical run.

4.7.3 Cross-sectional geometry of the channels

At the end of each run, the bed levels were measured with the help of point gauges to an accuracy of ±0.1mm. A great deal of time and effort was spent on collecting precise bed level measurements. For the results, see Table A2 in Appendix A. Bed level measurements using point gauges proved to be time consuming. In this case an automatic bed level recorder is more efficient.

The water surface levels at these sections were also recorded before the end of each test. The cross-sectional area was calculated using these measured values. The representative cross-sectional area of the channel was then calculated by averaging the cross-sectional areas of at least three channel sections. The variation of individual measurements for the cross-sectional area proved to be less than 2.7% about the mean value.

The water surface width was measured using the point gauges mounted on carriage and the metric scales along the carriage edge. The water surface width was recorded continuously during the run time of the experiments. The water surface width of a channel was considered as stable channel width, if its rate of increase was less than 1% per hour. The average water surface width of the channel was calculated as the average value of at least three representative sections across the channel length. The variation of individual measurements for the water surface width were less than 4.5% about the mean value. The mean depth of the channel was calculated as the cross-sectional area of the channel divided by the mean water surface width. For the results, see Table A1 in Appendix A.

4.7.4 Velocity and bed shear stress distribution

A Pitot-static tube was used to measure the velocity distribution in the developed channels of series A. A Pitot tube, within its range, offers an accurate and convenient way of measuring the magnitude of velocity. Its' effective cross-section

may be assumed small compared with the total cross-section of the stream and it can almost be regarded as a geometrical point. It creates relatively less disturbance

Plate 4.3. Striations in channel bed caused by secondary currents.

in the stream compared with propeller velocity meters. According to Patel (1988) a Pitot-static combination of standard design in conjunction with a properly selected manometer can yield total velocity with almost unsurpassed accuracy, say 0.5% of dynamic pressure and therefore 0.25% of velocity. Patel (1988) stated that difficulties arise at very low velocities (of the order of 1cm/s in water) due to the resolution of the pressure sensing system, and in presence of high turbulence and

high shear, as in the vicinity of a solid surface, corrections can and should be made for these effects but, in practice, they are rarely applied.

In order to measure point velocities aligned with the flow, a Pitot-static tube of outside diameter 2.3mm proved satisfactory as this caused minimal disturbance to the flow and gave adequate damping of fluctuations due to turbulence, therefore no corrections have been made to the velocity measurements for the Pitot displacement, turbulence and other effects. The position of the Pitot tube at any point in the flow depth was obtained by means of a point gauge, which could read up to ±0.1mm. The difference of dynamic and static heads was read with the help of a differential manometer. The differential heads were used to calculate the velocity or the shear stress distribution. The values of local shear stress were calculated using Preston (1954) method. The calibration curves of Patel (1965) were used to convert pressure readings to boundary shear stress. For the results, see Table A3, and A4 in Appendix A.

Hwang and Laursen (1963) examined Preston's shear measurement technique for rough surfaces. They concluded that although certain difficulties remain, it would appear that Preston's technique can be used with rough boundaries. In their work, they experienced a discrepancy of maximum 12% between measurement and analysis, for fully rough flow. Knight and Macdonald (1979) evaluated boundary shear stresses by two methods (1) semi-logarithmic plotting of velocity profile normal to the boundary (2) Preston tube method. In general, both methods gave shear stresses that agreed within $\pm10\%$.

4.8 Chapter summary

In this chapter, the details of the experimental series which have been carried out are explained. The experimental set-up used for the experiments has been described. In addition, the quality and range of variation of the experimental data along with the method of measurement and calculation of them is outlined.

Chapter Five
Self-Formed Laboratory Stable Straight Channels

5.1 Introduction

In this chapter, results of the developed straight channels in the laboratory, series A, are presented. The initial conditions for these channels were estimated using the WPB theory.

In the following sections, cross-sectional geometry, slope, and sediment concentration of these laboratory channels are discussed. In order to assess the applicability of the WPB theory, the results are compared with the theory. The data of Shakir (1992) is also used for the comparison.

The data of present experiments has been used to find the bank profile of developed channels and compare them with recently published models for bank profile predictions of self-formed straight channels. Wherever possible the cross-sectional geometry is also compared with other proposed relationships e.g. Parker (1978), Ikeda (1988). Velocity distribution and shear stress distribution in these channels are also presented.

5.2 Geometric characteristics of the channel

The geometric characteristics of the developed straight channels were calculated by using the measured data in the laboratory. To enable this, a computer program was developed. This program by using the measured bed level points and water level in each cross section computes hydraulic and geometric characteristics of the channel e.g. Froude number, mean velocity, cross-sectional area, water surface width, mean depth, and so on. In the following paragraphs cross-sectional

geometry of the developed straight channels is compared with the WPB [White et al (1981)] theory. For the purpose of comparison, only those data have been used where the developed channel was straight with no bedforms.

5.2.1 Water surface width

The water surface width of the developed straight channels by using observed values of sediment concentrations is compared with WPB theory. The comparison shows that this theory underpredicts the water surface widths. In other words, the observed widths are greater than the calculated widths. The results of this comparison is shown in Fig. 5.1. The observed widths are approximately 46% greater than those calculated using the WPB theory.

5.2.2 Mean depth

For the purpose of comparison, the mean depths are calculated using the WPB theory for the mean values of the observed sediment concentrations. The comparison shows that the WPB theory overpredicts the mean depths consistently at this scale. Thus, the observed mean depths are less than the calculated ones from this theory. The results of this comparison are shown in Fig. 5.2. the mean value of the plotted discrepancy ratio is 1.7 with standard deviation of 0.3.

5.2.3 Cross-sectional area

The cross-sectional area of the developed channels is also compared with those of WPB predictions. For the WPB predictions, the observed mean sediment concentrations in the lab. are used. The results of the comparison are shown in Fig. 5.3. This comparison shows that WPB theory underpredicts the cross-sectional

COMPARISON OF THE OBSERVED AND CALCULATED WATER SURFACE WIDTH
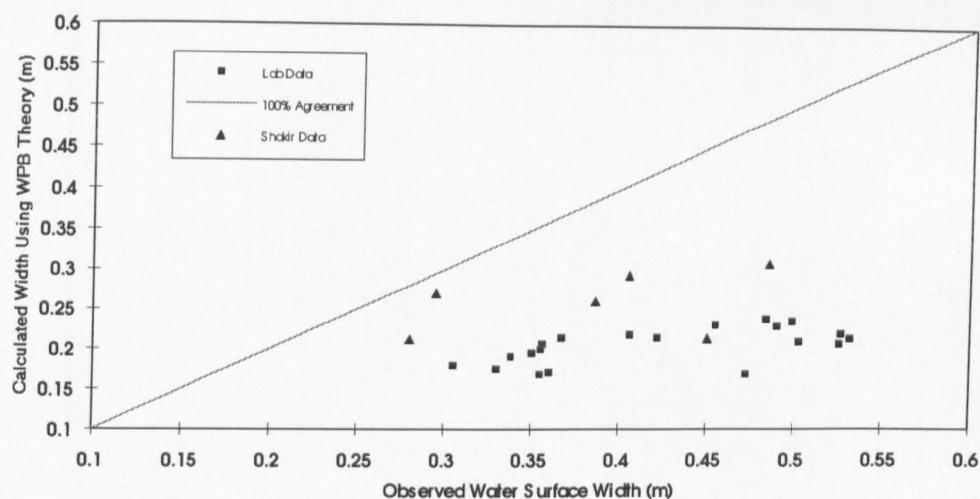
Figure 5.1. Comparison of the observed and calculated water surface widths.

COMPARISON OF THE OBSERVED AND CALCULATED MEAN DEPTHS
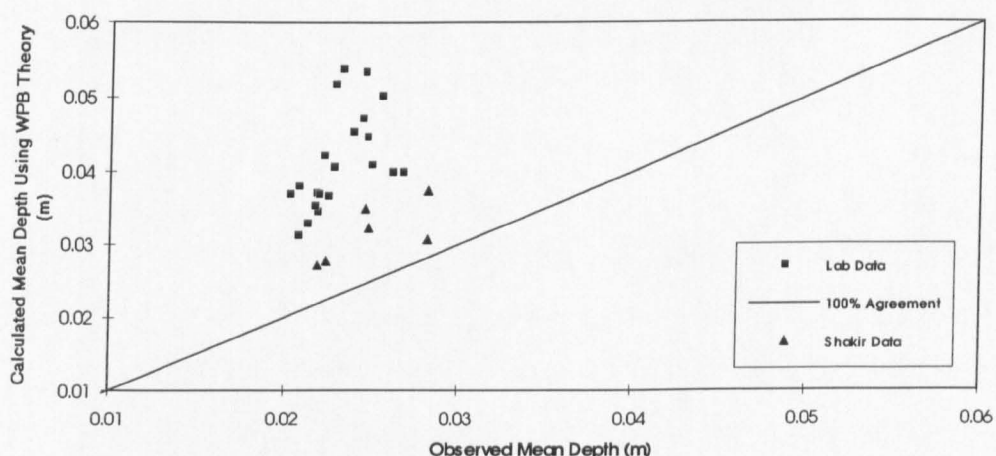
Figure 5.2. Comparison of the observed and calculated mean depths.

areas. The observed cross-sectional areas are approximately 12% greater than the calculated ones using WPB theory.

5.3 Water surface slope

The measured water surface slope of the developed straight channels is compared with the calculated slopes. The calculated slopes were estimated by using the mean values of sediment concentrations measured in the experiments. This comparison reveals that the WPB theory overpredicts the slopes. In other words, the observed slopes are lower than those predicted by the WPB theory. Fig. 5.4 shows the results of this comparison. The mean value of the plotted discrepancy ratios is 1.4 with the standard deviation of 0.3.

It is frequently mentioned in the literature, e.g. Ranga Raju et. al. (1977) that the water surface slope of a stable straight channel is strongly dependent on the sediment concentration of the channel. The WPB theory is used to show the effect of sediment concentration changes on the water surface slope. The effect is shown for the discharge range of 1.0-5.0 l/s and a sediment size of $d_{50} = 1mm$ which is used as bed material. Fig. 5.5. shows that for a given discharge and a sediment size, the slopes are steeper as the sediment concentration increases, which is consistent with observation.

The sensitivity of water slope to sediment concentration indicates that precise prediction of sediment concentration is quite important. In other words, the sediment transport formula in predictions of a rational theory plays an important role. The more precise the sediment transport formula, the more precise is the rational theory predictions. For the design of stable alluvial channels, Babaeyan-Koopaei and Valentine (1995) used the sediment transport maximisation hypothesis of White et. al. (1981) with different combinations of sediment transport and flow resistance equations. They concluded that the success of the method is quite dependent on the equations adopted.

COMPARISON OF THE OBSERVED AND CALCULATED CROSS
SECTIONAL AREAS
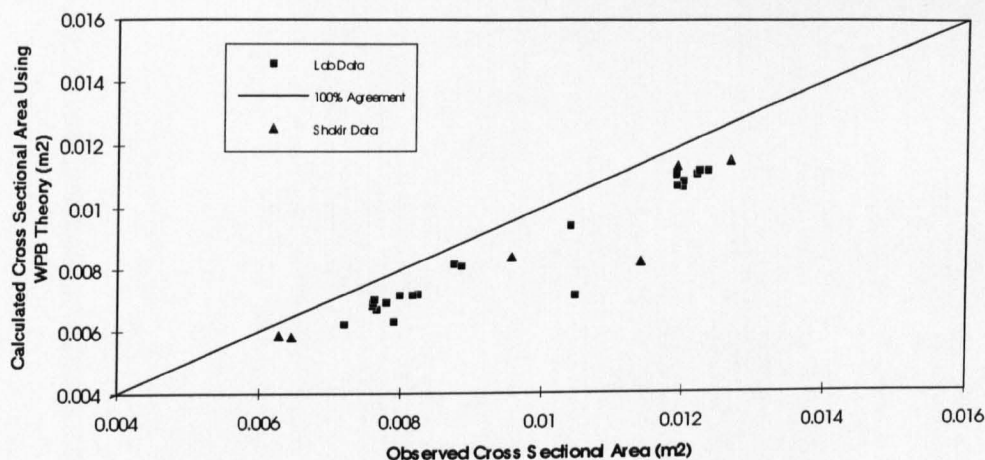
Figure 5.3. Comparison of the observed and calculated cross sectional area.

COMPARISON OF THE OBSERVED AND CALCULATED WATER
SURFACE SLOPES
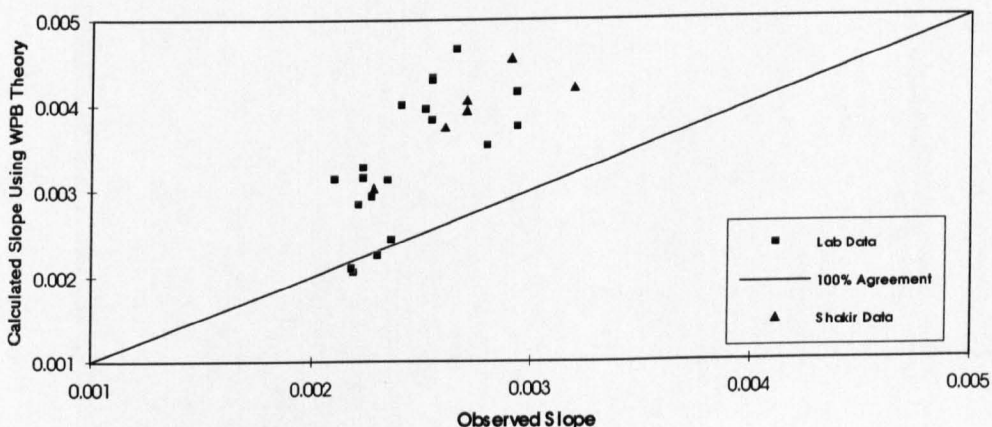
Figure 5.4. Comparison of the observed and calculated water surface slopes.

The WPB theory is based on the Ackers-White sediment transport formula. It has been stated that the Ackers-White (1973) sediment transport formula is under review and modification. Bettess (1991) discussed the impact of the modifications to the equation. He stated that for sediments near the threshold of motion around 0.06 mm, the transport rate is increased by a factor of 10, while for larger sediment mobilities the transport rate is reduced by a factor of up to 10. For coarse sediments around and above 3.6 mm, the modification changes in the transport rate is less than 10%.

According to the above discussion, it is thus clear that the modification of the formula will have a substantial effect on the predictions of the WPB theory.

5.4 Sediment Concentration

The comparison of the measured sediment concentrations in the lab with those calculated from WPB theory has been carried out. The sediment concentrations have been calculated by using observed water surface slopes in the lab. The results of this comparison shows that the WPB theory underpredicts sediment concentrations of the straight stable channels. In other words, the observed sediment concentrations are much higher than the calculated values of sediment concentrations for the observed slopes. The result of the comparison is shown in Fig. 5.6. The observed sediment concentrations are approximately 60% higher than the calculated values of sediment concentrations for the observed slopes. The difference between the observed sediment concentrations and the calculated ones is likely to be because of the sediment transport predictions. It is believed that the difference will be reduced after updating the Ackers-White (1973) sediment transport formula.
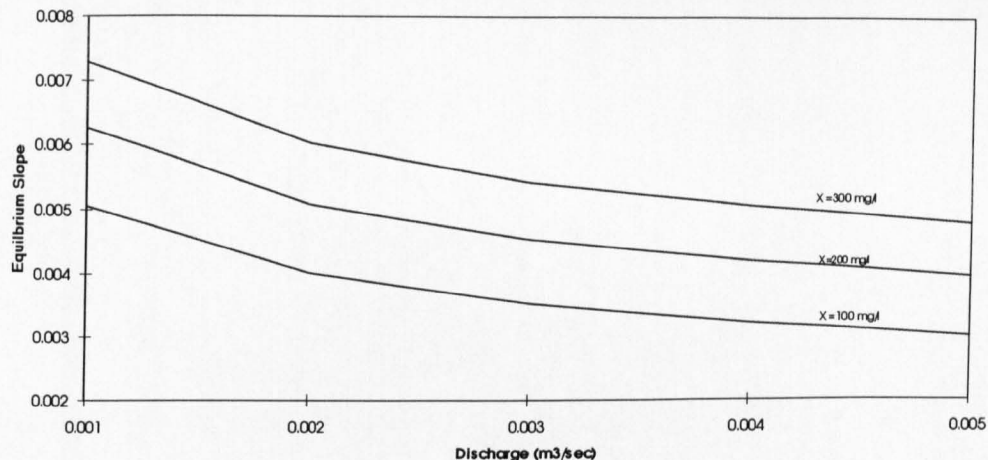
Figure 5.5. Effect of sediment concentration on the slope of stable straight channel.
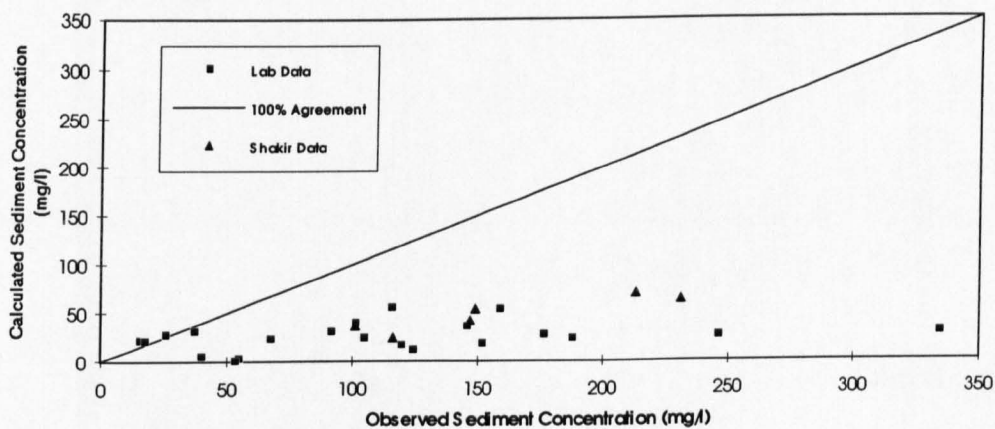
Figure 5.6. Comparison of the observed and calculated sediment concentrations.

5.5 Bank Profile of Self-formed Straight Stable Channels

5.5.1 Introduction

The geometrical dimensions and shape of a straight stable channel is an important issue in design of these channels. For design purposes, it is not only the width and the depth of these channels but also the bank profiles of them which are important.

A simplified model of a natural channel is the flow in a stable self-formed, straight channel composed of uniform material. Such a case has been tackled by an analytical approach of the threshold channel theory. The cross section of a threshold channel is determined such that the grains everywhere on the cross-section are at the threshold of motion. One of the earliest approach of this method is due to Glover and Florey (1951). By assuming the shear stress distribution, they suggested a cosine bank profile for stable channel profiles.

Parker (1978), by taking into consideration the lateral diffusion of downstream momentum due to turbulence, proposed a different approach. He formulated his model according to the method of Lundgren and Jonsson (1964) and solved it in closed form for the bed region. His model assumes that the logarithmic law for rough boundaries is approximately valid over the whole channel depth, that straight channel secondary currents are weak, and that the channel bottom is curving slowly in the bank region.

Ikeda et al. (1988) proposed a mathematical formula for defining stable width and depth of straight gravel rivers. In his analysis, he used the bed shear stress distribution and bank profile equation of Parker (1978).

Diplas (1990), by setting up a series of laboratory experiments for developing self-formed straight channels tested, the validity of the assumptions used to formulate the turbulent diffusion model. He examined the resulting shear stress distribution and its implications. He concluded that the turbulent diffusion model is a more realistic approach to the flow in a straight channel.

Diplas and Vigilar (1992) obtained the cross-section of a threshold channel by numerically solving the coupled equations of turbulent diffusion for the fluid flow (Lundgren and Jonsson 1964; Parker 1978) and force balance applied on a particle resting on the channel boundary (Ikeda 1982). The resulting bank profile is represented by a fifth degree polynomial.

In the following sections, previous research to develop methods to predict bank profiles, stable widths and depths of straight stable channels is reviewed. The data from the present study have been used to shed more light on the applicability of these theories.

5.5.2 Previous Work

Parker (1978) treated the stable channel problem based on the concept of lateral momentum transfer due to turbulent diffusion embodied in the work of Lundgren and Jonsson (1964). He considered the cross section in Fig. 5.1. for the analysis. The channel has width B, constant downstream slope S, centre depth D_C and a perimeter of non-cohesive sand. The channel is divided into an essentially flat central region where $h \geq 0.99 D_c$ and bank regions where $h < 0.99 D_c$. He noted that the extension of the threshold theory to gravel-bed rivers leads to what he termed the "stable channel paradox", that is to say the transport of bed material is incompatible with a stable width. This is because channel widening due to bed load transport and gravity can not be balanced by the lateral diffusion of suspended sediment in gravel-bed streams, since bed material in such streams is, by definition, unsuspendable.
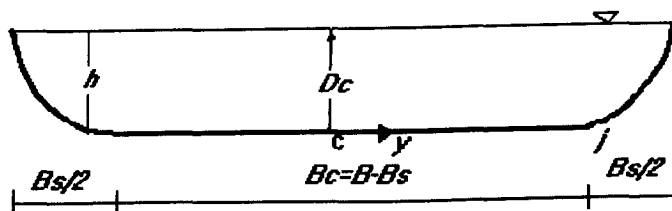
Figure 5.1. Assumed channel geometry.

He proposed a resolution based on the mechanism of turbulent momentum transfer. The downstream velocity, and thus momentum, is greater near the channel centre than near the banks. Parker (1978) postulated that the turbulence induces a net lateral transport of longitudinal fluid momentum from regions of high momentum to regions of low momentum, which yields a lateral redistribution of bed shear stress. He used the concept together with singular perturbation techniques to explain the coexistence of stable banks and mobile beds in straight reaches of coarse gravel rivers. By solving the problem formulated above, Parker (1978) also devised rational regime relations for such reaches. The relations obtained are:

$$R = 0.0553 S^{-1.01} \qquad ; \text{First regime relation} \qquad (5.1)$$

$$R = 0.866 (\frac{\tilde{Q}}{B^*})^{0.83} \qquad ; \text{Second regime relation} \qquad (5.2)$$

$$Q^* = 1.02 \times 10^{-5} R^{0.275} B^* (1 - \frac{4.52}{A}) \qquad ; \text{Third regime relation} \qquad (5.3)$$

in which $R = \dfrac{D_c}{d_{50}}$, D_c is the channel centre depth, d_{50} is the median sediment size, S is the water surface slope, $\tilde{Q} = \dfrac{Q}{d_{50}^2 \sqrt{R_s g d_{50}}}$, Q is the flow discharge, R_S is the submerged specific gravity of sediment (=1.65 for typical river bed material), $B^* = \dfrac{B}{d_{50}}$, $A = \dfrac{B}{B_c}$, $Q^* = \dfrac{Q_s}{d_{50}^2 \sqrt{R_s g d_{50}}}$, Q_S is the volumetric sediment discharge, B is the free surface width.

Ikeda (1981) carried out a series of experiments in two laboratory flumes. In these experiments, he studied the process of widening and hydraulic characteristics of self-formed straight channels with noncohesive sands. He clarified that equilibrium depth and width depend not only on discharge, but also on slope and

bed material. He also concluded that the transverse bed shapes in equilibrium have a universal one in the side bank region regardless of the initial shape, the discharge, and the sand size. In his work, the side bank profile are well-fitted by an exponential function.

Ikeda et al. (1988) presented a model for predicting the depth and width of self-formed straight gravel rivers with actively transported heterogeneous bed material. In his work, he used the bank profile and bed shear stress distribution equation of Parker (1978). The equations obtained for the stable channel depth and width are:

$$D_c = 0.0615 R_s (\log_{10} 19\sigma)^{-2} \sigma d_{50} S^{-1} \tag{5.4}$$

$$B = \frac{Q}{D_c (g D_c S)^{\frac{1}{2}} 5.757 \log_{10}(7.333 \frac{D_c}{\sigma d_{50}})} + [2.571 + \frac{0.8972}{\log_{10}(7.333 \frac{D_c}{\sigma d_{50}})}] D_c \tag{5.5}$$

in which σ is $\frac{d_{90}}{d_{50}}$.

Diplas (1990) conducted laboratory experiments to study various aspects of the mechanics of self-formed, stable, straight alluvial channels in the presence of bed load transport. He quoted the Ikeda (1982) balance of the forces applied to a particle located on a plane-river bank inclined at an angle θ to the horizontal plane. For the solution of the equation a knowledge of the shear-stress distribution in the bank region is essential.

For the shear-stress distribution, Glover and Florey (1951); Stebbings (1963); and Parker (1978), assumed that the shear stress on an element of the

boundary is balanced by the downstream weight component of the water vertically above this element of the channel i.e.:

$$\tau = \rho g D S \cos \theta \qquad (5.6)$$

where D is the vertical depth at the middle of the boundary element, θ is the lateral inclination of this element, S is the water surface slope.

Diplas (1990), by introduction of the equation (5.6) in the force balance equation of Ikeda (1982), gained the well-known cosine bank profile as follows.

$$\frac{D}{D_c} = \frac{1}{1-\mu\beta}[\cos(\mu\sqrt{\frac{1-\mu\beta}{1-\mu\beta}}\frac{y}{D_c}) - \mu\beta] \qquad (5.7)$$

where β is the ratio of hydrodynamic lift and drag forces, and $\mu = \tan\phi$ is the submerged static coefficient of Coulomb friction.

Diplas (1990) used the normal depth method with the Ikeda (1982) force balance equation and developed the following bank profile.

$$\frac{D}{D_c} = 1 - \frac{\mu^2}{1+2\mu^2+\mu\beta}\frac{(y-y_j)}{2D_c^2} \qquad (5.8)$$

Using normal-depth method gives a more accurate estimate of shear-stress distribution. In this method the flow depth is measured at right angles to the boundary, and the force balance yields

$$\tau = \rho g S \frac{D}{\cos\theta} \qquad (5.9)$$

Diplas (1990) concluded that the turbulent-diffusion model is a more realistic approach to the flow in a straight channel. He also proposed that the bank profile obtained from the normal depth method is a better approximation of the actual bank profile than is the cosine profile. However, he admitted that the following exponential profile approximates even closer to the measured bank profiles.

$$\frac{D}{D_c} = 1 - e^{(\frac{-y_T}{D_c})}$$

(5.10)

in which $y_T = \frac{B}{2} - y$, y is lateral distance from the centre of channel on horizontal plane.

Diplas and Vigilar (1992) obtained the cross-section profile of a threshold channel by numerically solving the coupled equations of turbulent diffusion for the fluid flow (Lundgren and Jonsson 1964; Parker 1978) and force balance applied on a particle resting on the channel boundary (Ikeda 1982). He used the turbulent diffusion model to show that neither the cosine, the parabolic, nor the exponential bank profiles are suitable for the threshold channel. He presented the bank profile data points, generated by the numerical model, very closely by a fifth-degree polynomial.

5.6 Data Analysis of Stable Channel Width and Depth

The first regime relation of Parker (1978) is tested in Fig. 5.2. The comparison of the calculated and measured values of D_C shows that the relation underpredicts the values of D_C.

A test of the second regime relation of Parker (1978) is shown in Fig. 5.3. The comparison shows that the relation overpredicts the values of width.
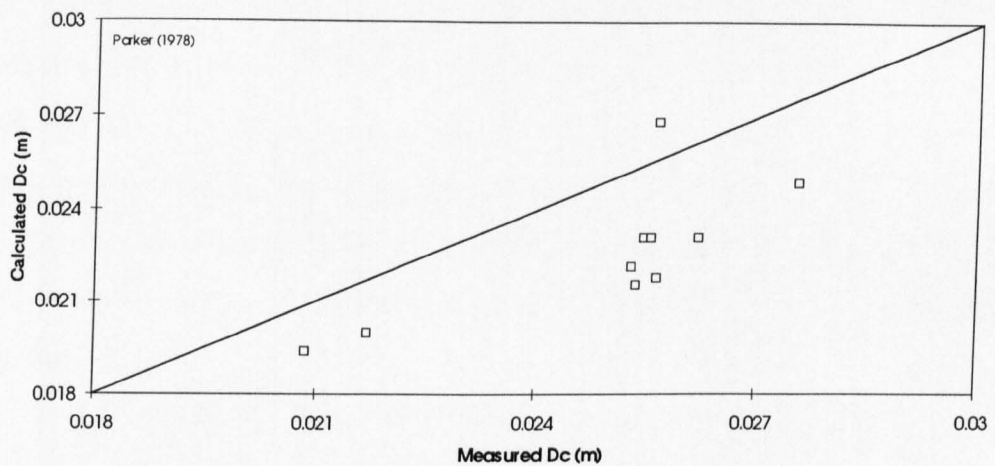
Figure 5.2. The comparison of the calculated channel centre depth (Dc) using Parker's equation (1978) and

the measured values in the lab.
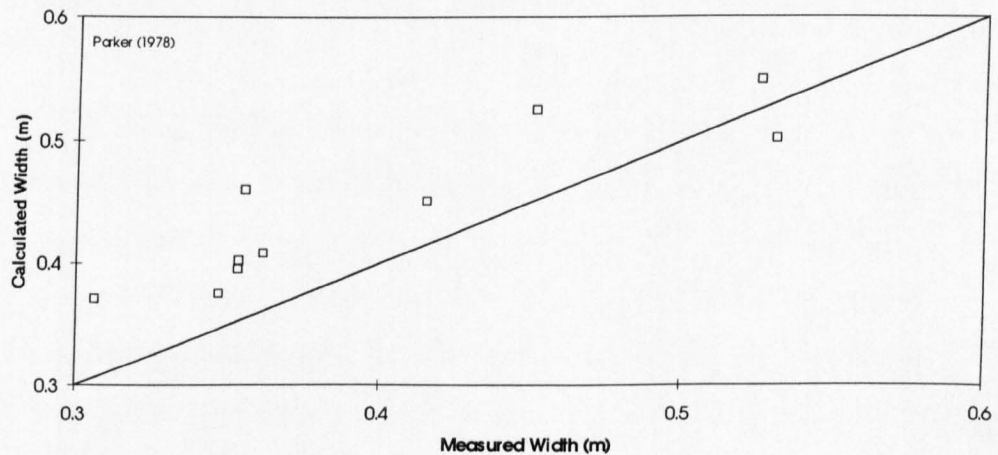
Figure 5.3. The comparison of the calculated width using Parker's equation (1978) and the measured

values of width in the lab.

The equations of Ikeda et al. (1988) for stable channel depth and width were also tested. The graphical presentation of these equations are shown in Fig. 5.4 and Fig. 5.5 respectively. Fig. 5.4 shows that for a constant slope as the bed material size increases the value of the stable channel depth, D_C, will also increase. It also indicates that for a defined size of uniform bed material as the slope increases the stable channel depth, D_C, will decrease. Fig. 5.5 shows that for a constant discharge as the slope increases the stable width also increase. It also indicates that for a constant slope, as the discharge increases, the stable channel width will also increase.

The Ikeda et al. (1988) formula for stable channel depth prediction is tested in Fig. 5.6. The comparison shows that the formula underpredicts the values of stable channel depth.

The test of Ikeda et al. (1988) formula for stable channel width is shown in Fig. 5.7. The comparison shows that the formula overpredicts the values of stable channel width.

5.7 Analysis of Bank Profile Data

The bank profiles predicted from equations 5.7 and 5.9 are compared with the bank profile data obtained from present study. The experiments were carried out with the sediment having an angle of repose equal $32.5°$, and $\beta = 0.85$. The data is also tested with the fifth-degree polynomial of Diplas and Vigilar (1992) in Fig. 5.8. The comparison shows that the fifth-degree polynomial results in a better approximation of the bank profile than that of the one obtained from the normal-depth method and the cosine profile. From Fig. 5.9, it is seen that the following hyperbolic function describes the bank profile even more closely.

Variation of Central Depth with Slope
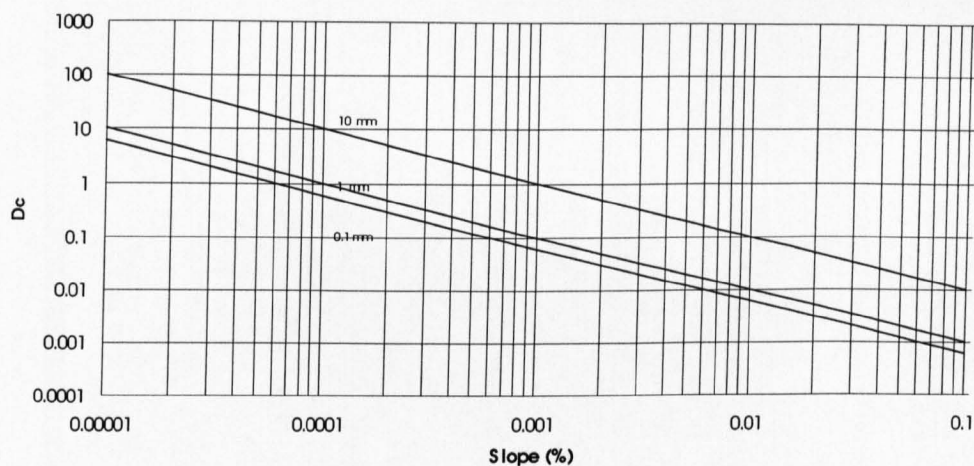
Figure 5.4. Graphical presentation of Ikeda (1988) formula for prediction of centre depth of a

stable channel .
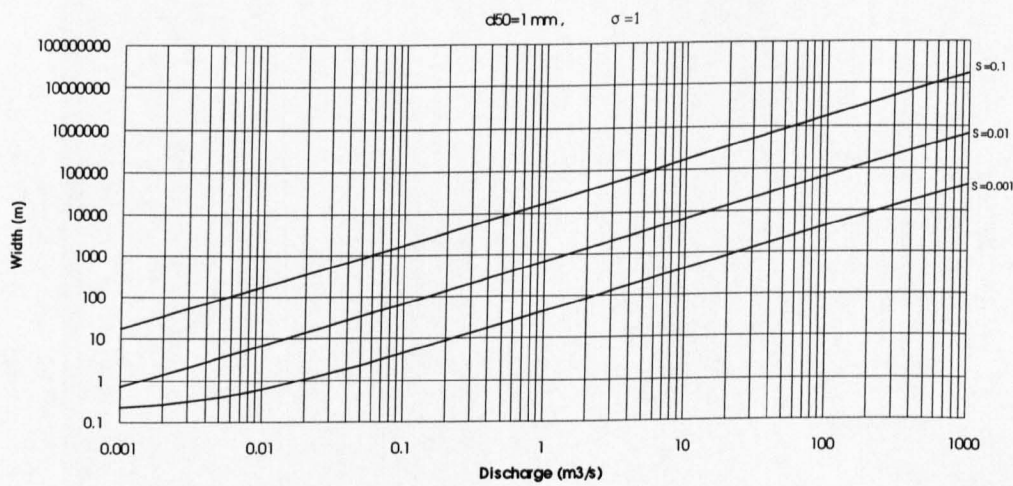
Figure 5.5. Graphical presentation of Ikeda (1988) formula for prediction of a stable channel width.

112
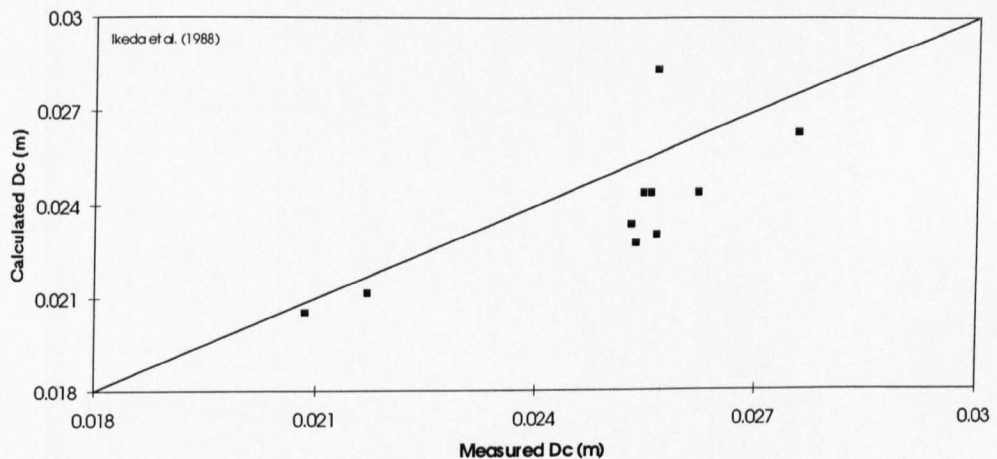
Figure 5.6. The comparison of the calculated *Dc* using Ikeda et al equation (1988) and the measured values

of *Dc* in the lab.
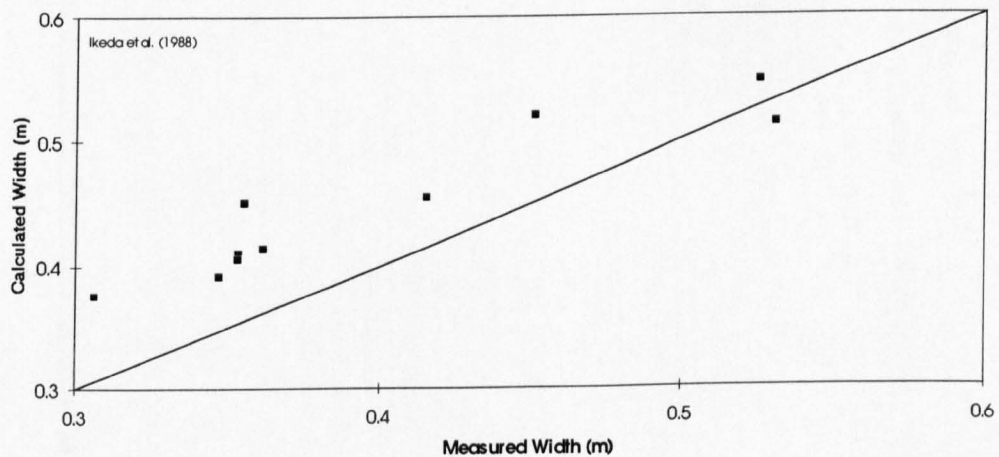
Figure 5.7. The comparison of the calculated width using Ikeda et al equation (1988) and the measured

values of width in the lab.
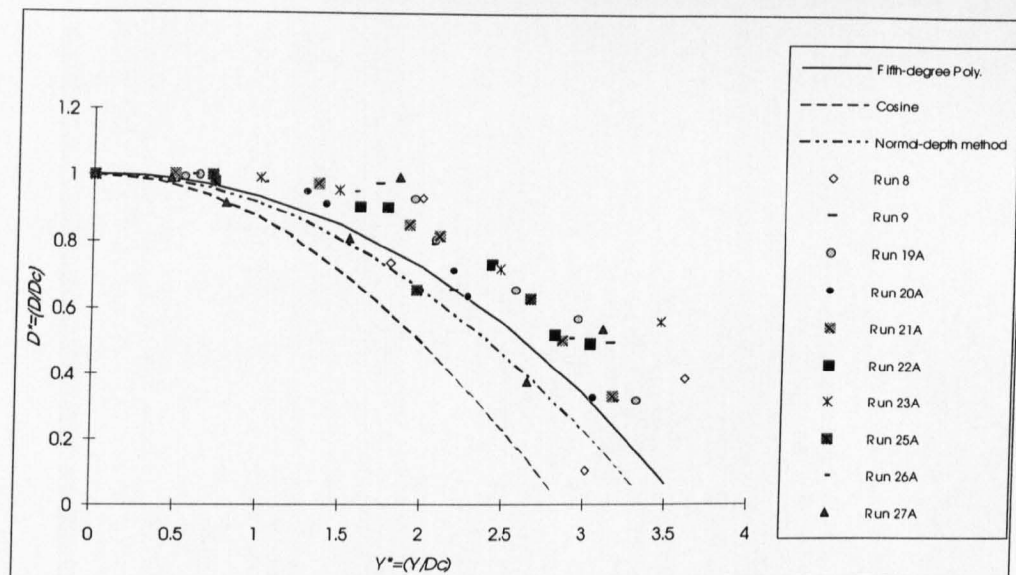
Figure 5.8. Data Comparison with different bank profiles.
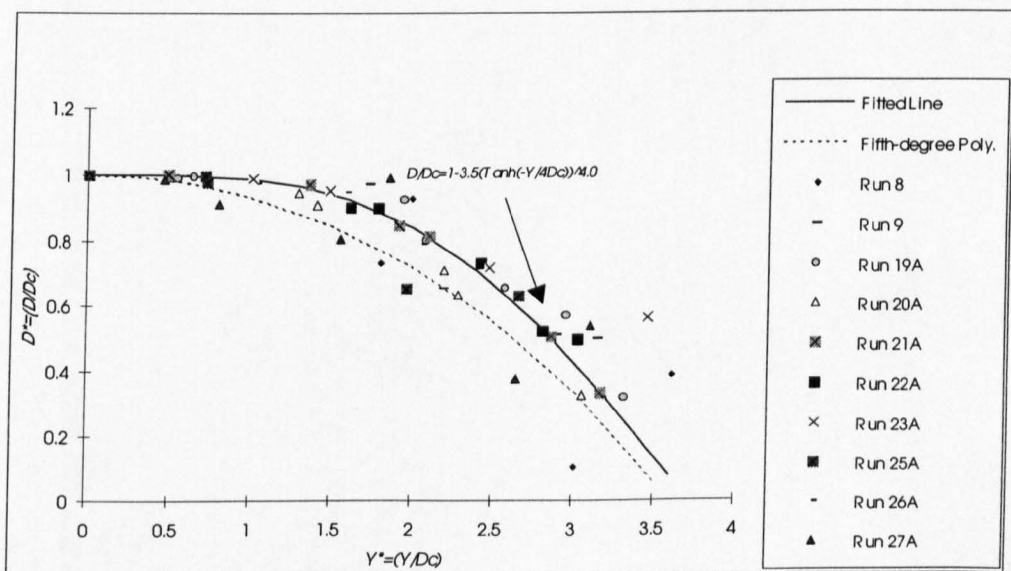
Figure 5.9. Data Comparison with fifth-degree polynomial and the hyperbolic function.

$$\frac{D}{D_c} = 1 - 3.5[\tanh(\frac{-y}{4D_c})]^4 \qquad\qquad (5.11)$$

The experimental data is compared with exponential function of Diplas (1990) in Fig. 5.10. The comparison shows that the function approximates the bank profile quite well but the following equation describes the bank profile even better.

$$\frac{D}{D_c} = \tanh(\frac{y_T}{1.36D_c}) \qquad\qquad (5.12)$$

The non-dimensional presentation of the experimental data is shown in Fig. 5.11. The following equation fits the data.

$$\frac{D}{D_c} = 1 - 111[\tanh(\frac{-y}{0.8B})]^8 \qquad\qquad (5.13)$$
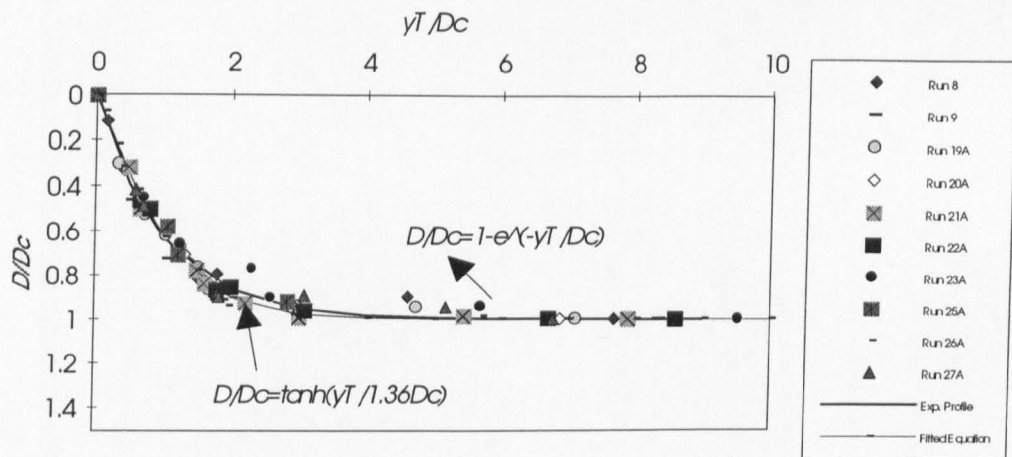
Figure 5.10. Data comparison with the Diplas (1990) exponential bank profile and the fitted hyperbolic

profile.
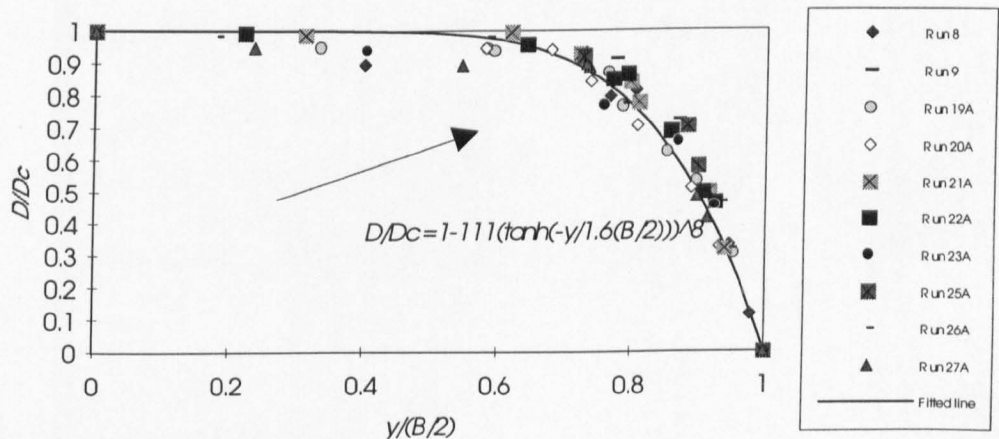
Figure 5.11. Fitted equation to the nondimensional experimental data of bank profile.

5.8 Velocity distribution

The theoretical investigations of Prandtl (1925) and von Karman (1921) on flow through pipes, and the experimental studies of Nikuradse (1933) have led to rational formulae for velocity distribution and hydraulic resistance for turbulent flows over flat plates and in circular pipes. Despite some general similarities between pipe flows and open channel flows, factors like the presence of a free surface, the three dimensional nature of flow, and non-uniform distribution of shear stress along the perimeter, distinguish open channel flow from pipe flow.

Nezu and Nakagawa (1993) divided the flow field in open channels into three subregions:

1) Wall region $[\frac{y}{h} < (0.15 - 0.2)]$. This region corresponds to the "inner layer" of classical boundary-layer treatments where length and velocity scales are $\frac{v}{U_*}$ and U_* respectively.

2) Free surface region $[0.6 < \frac{y}{h} \le 1.0]$. In this region, the turbulent structure is controlled by the outer variables, where length and velocity scales are flow depth, h, and the maximum mainstream velocity U_{max}, respectively.

3) Intermediate region $[(0.15 - 0.2) \le \frac{y}{h} \le 0.6]$. This region is not strongly influenced by either the wall properties or the free surface. The length and velocity scales are y and $\sqrt{\frac{\tau}{\rho}}$, respectively. The intermediate and free surface regions, together are called the 'outer region' or 'outer layer', a region in which viscous effects are negligible.

5.8.1 The law of the wall

The law of the wall governs the wall region; the region in which the characteristic scales of length and velocity are $\frac{v}{U_*}$ and U_*, respectively. Using

Prandtl's (1925) mixing length formulation for turbulent flows leads to the well known formula of "the law of the wall" as follows.

The viscosity dominated region very close to the wall:

$$\frac{U}{U_*} = \frac{yU_*}{\nu} \qquad\qquad \frac{yU_*}{\nu} \le 5 \qquad\qquad (5.14)$$

Outside the viscosity affected area:

$$\frac{U}{U_*} = \frac{1}{\kappa} \ln(\frac{yU_*}{\nu}) + A \qquad\qquad \frac{yU_*}{\nu} > 30 \qquad\qquad (5.15)$$

where A is the integral constant, κ is the von Karman constant, U is the velocity at elevation y, U_* is shear velocity, ν is kinematic viscosity. Although κ=0.4 and A=5.5 were given for pipe flows by Nikuradse (e.g. see Schlichting 1979), the values of κ=0.412 and A=5.29 were recently obtained by Nezu and Rodi (1986) for open channel flows.

The calculated curves of 5.15 are compared with the data of present study in Figs. 5.14, and 5.15. Although the number of data points measured near the wall region, in most cases were limited to two points, a linear regression analysis (i.e. $\frac{U}{U_*} = \alpha \ln(\frac{yU_*}{\nu}) + \beta$) was carried out in the validity region of the law. The regression correlation coefficient for the data was very high for all cases, with an average value of 0.98. The von Karman constant κ and the integral constant then obtained as $\kappa = \frac{1}{\alpha}$, and $A = \beta$. Figs. 5.12, and 5.13 show the resulting values of κ plotted against the Froude number, Fr, and Reynolds number, Re, respectively. No systematic influence of Re or Fr can be recognised from these data. Although one should consider the difficulties and errors which are involved in measuring velocity with Pitot tube (See Section 4.7.4), especially close to mobile bed, One may conclude that the von Karman constant κ is, to good approximation, a universal constant and

does not depend on the Reynolds and Froude numbers. The values of κ overlap well with the universal constant of 0.41, and the reported value of 0.412 by Nezu and Rodi (1986) for open channel flows.

The integral constant A, when plotted against Froude number and Reynolds number, exhibited more scatter than κ. The values decreased with an increase of Reynolds number. Large scatters among the values of A, was also reported by Tominaga and Nezu (1992) over rough beds of steep slope channels.

It can be seen from Figs. 5.14, and 5.15 that in the region of $30 < \frac{yU_*}{\nu} \le 0.6 \frac{hU_*}{\nu}$, the experimental data of present study follow very well the log-law (equation 5.15). In the buffer layer, $5 \le \frac{yU_*}{\nu} \le 30$, the experimental data fail to follow the log-law.

5.8.2 The velocity-defect law

Previous research, e.g. Nezu and Nakagawa (1993), has shown that the log-law 5.15 is valid only in the wall region. In so far as the near-wall region is independent of the flow conditions in many wall bounded shear layers, they have concluded that the established similarity concept of near wall behaviour should be retained: hence, deviations from the standard log-law should not be accounted for by adjusting κ, and A, but rather by adding a wake function $\omega(\frac{y}{h})$, as is customary in boundary layer and closed channel analysis.

$$\frac{U}{U_*} = \frac{1}{\kappa} \ln(\frac{yU_*}{\nu}) + A + \omega(\frac{y}{h})$$ (5.16)

An appropriate wake function, $\omega(\frac{y}{h})$ given empirically by Coles (1956) is described as follows.

$$\omega(\frac{y}{h}) = \frac{2\Pi}{\kappa} \sin^2(\frac{\pi y}{2h})$$ (5.17)

where Π is Coles' wake strength parameter, expressing the strength of the wake function. Although several empirical formulae have been proposed for the outer

region (e.g., Sarma et al. (1983), Coleman and Alonso (1983)), Nezu and Nakagawa (1993) claimed that Coles' wake function appears to be an acceptable extension of the log-law.

The velocity-defect law from 5.16, and 5.17 yields:

$$\frac{U_{max} - U}{U_*} = -\frac{1}{\kappa}\ln(\frac{y}{h}) + \frac{2\Pi}{\kappa}\cos^2(\frac{\pi y}{2h}) \qquad (5.18)$$

If $\Pi = 0$, equation 5.18 reduces to the usual defect law. Therefore, Coles' parameter describes the deviation from the log-law in the outer region.

However, Dean, quoted by Bradshaw (1976), suggested another form for the wake function:

$$\omega(\frac{y}{h}) = \frac{1+6\Pi}{\kappa}(\frac{y}{h})^2 - \frac{1+4\Pi}{\kappa}(\frac{y}{h})^3 \qquad (5.19)$$

This is an empirical function which yields the more realistic result of $\frac{\partial u}{\partial y} = 0$ at $y=h$ for all Π values. As shown in Figs. 5.14, and 5.15, in the outer region, the data of present study for $\frac{U}{U_*}$ deviate from the log-law 5.15. The wake function of Coles, and Dean are added to the log-law to represent this deviation, see Figs. 5.16, and 5.17. The calculated curves of the log-wake law 5.16 for both wake functions describes the flow fairly well in the outer region. In order to confirm which theory describes the flow velocity more accurately, one needs more velocity data points and more precise measurements.

In summary, from the present data, the mean velocity distribution in open channel flows can be predicted in the wall region, with the logarithmic law, and in the outer region with the log-wake law. The von Karman constant, κ, is a universal constant, irrespective of flow type.
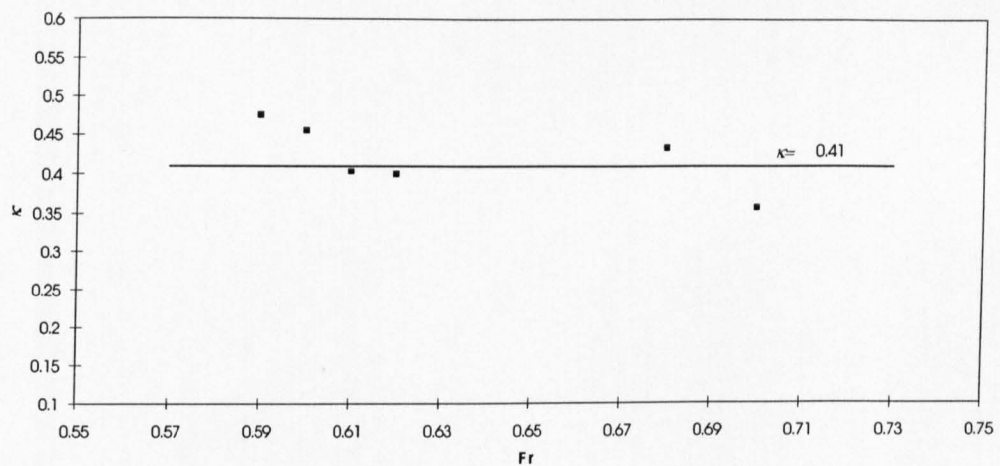
Figure 5.12. The von Karman constant, k, versus Froude number (Data of present study).
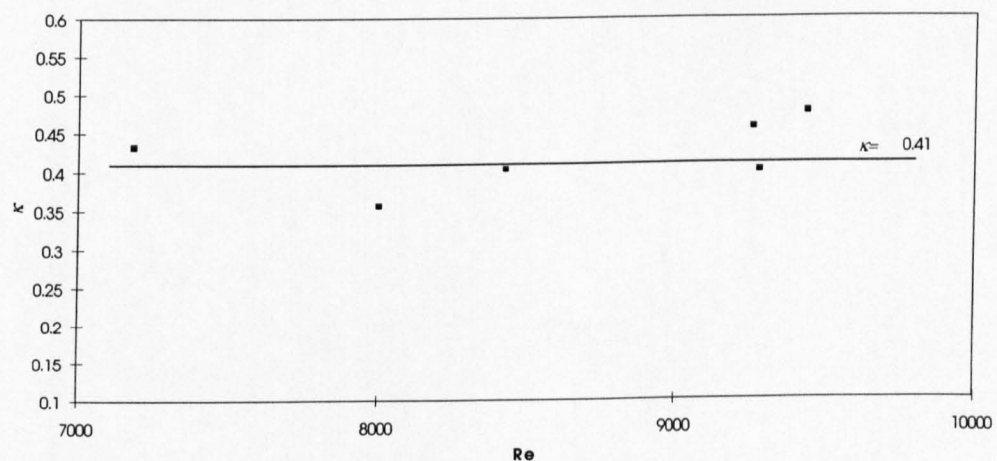
Figure 5.13. The von Karman constant, k, versus Reynolds number (Data of present study).
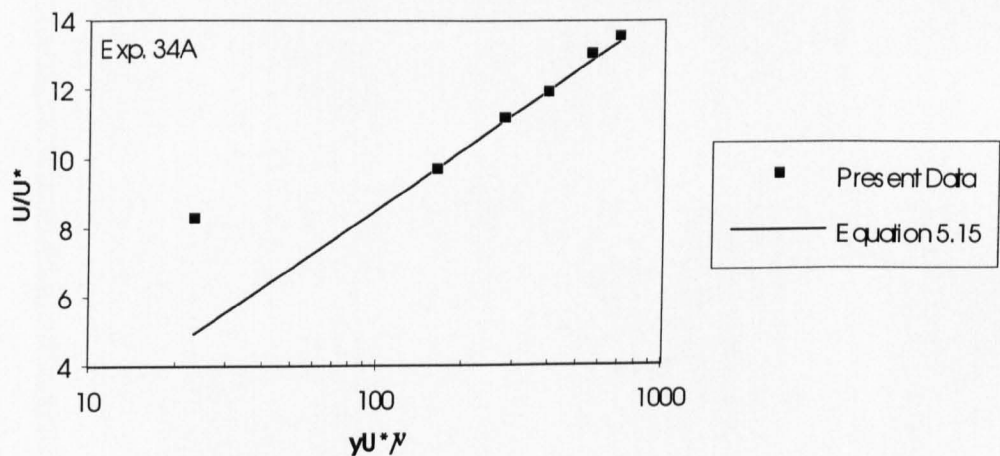
Figure 5.14. $\dfrac{U}{U_*}$ distribution versus $\dfrac{yU_*}{\nu}$.
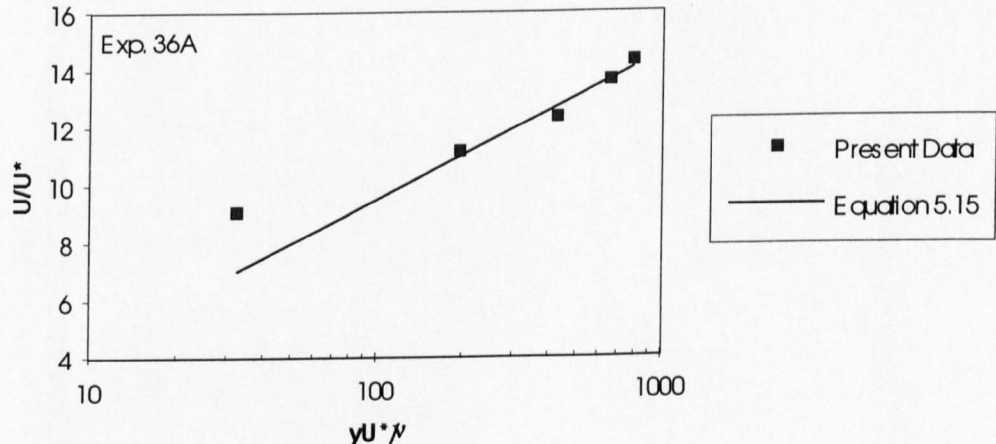
Figure 5.15. $\dfrac{U}{U_*}$ distribution versus $\dfrac{yU_*}{\nu}$.
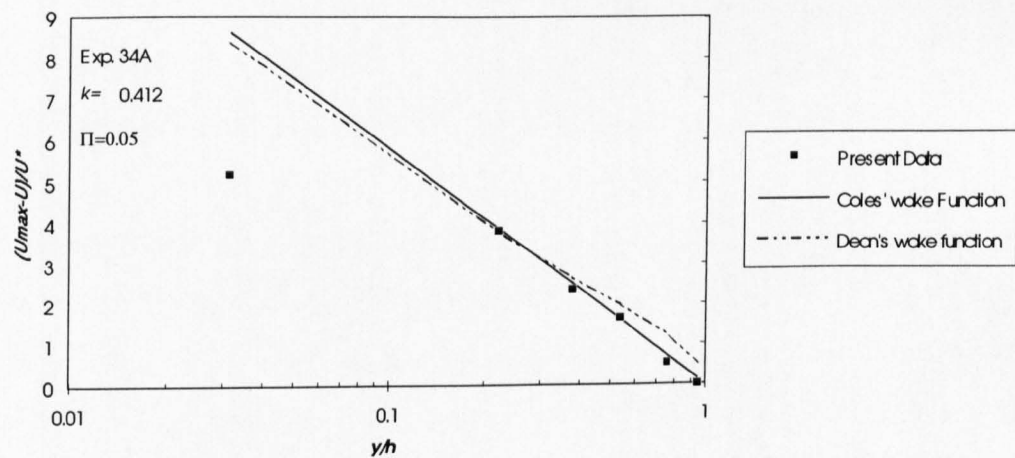
Figure 5.16. The comparison of velocity-defect law with the data of present study.
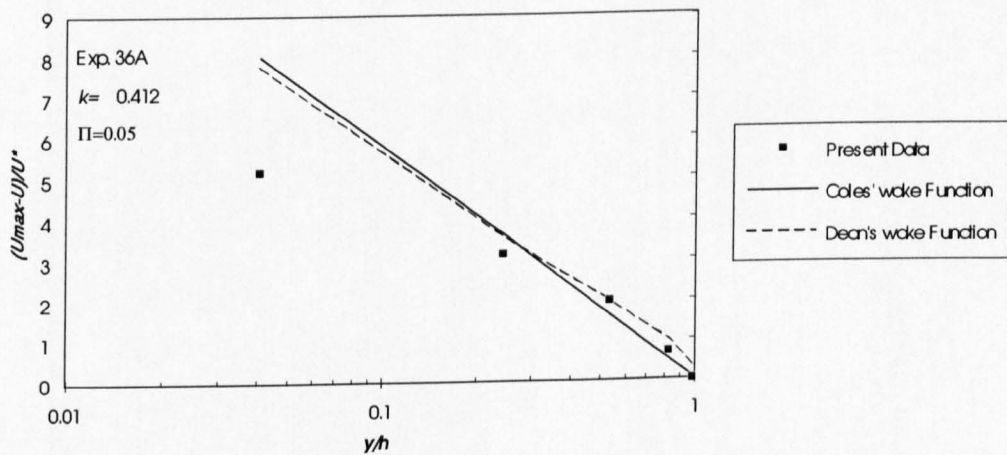
Figure 5.17. The comparison of velocity-defect law with the data of present study.

5.9 Boundary shear stress distribution

In open channel flow with a loose boundary, knowledge of boundary shear stress and its distribution is of significant importance. The distribution of boundary shear stress around the wetted perimeter of an open channel is known to depend on the shape of the cross-section, the structure of the secondary flow currents, and non-uniformity in the boundary roughness. Local or mean boundary shear stress are used extensively in many hydraulic equations concerning sediment transport, resistance, and dispersion problems. Complexities arising from all of the influencing factors, make the theoretical prediction of boundary shear stress distribution difficult, even for straight open channels. However, two dimensional approaches based on averaged parameters have been developed to give the lateral distribution of both velocity and boundary shear stress. These approaches have typically been either numerical, as for example given by Keller & Rodi (1988), or analytical, as given by Shiono & Knight (1988). Shiono & Knight (1988) proposed a solution based on the depth averaged eddy viscosity approach and the momentum equation. The analytical solution was applied to steady uniform flow in a compound channel and the results show that it is capable of predicting certain features of the flow sufficiently accurately for engineering design purposes. Shiono & Knight (1991) improved their analytical solution by including the effects of secondary flow. Consequently a variety of empirical methods have also been proposed to determine local shear stress values with either direct or indirect measurement. When suitable data are not available the mean boundary shear stress may be determined from the energy gradient as follows.

$$\tau_o = \rho g R S_f \tag{5.20}$$

where ρ is the fluid density, g is the gravitational acceleration, R is the hydraulic radius and S_f is the energy gradient.

The measurement of local shear stress on a boundary can be accomplished by direct or indirect methods. In direct methods shear stress on an isolated area must be measured. In indirect methods of measurement either the pressure or the velocity has to be measured and the shear stress computed using knowledge of basic flow mechanics. In the present study the values of local shear stress were calculated using the Preston (1954) method, and the calibration curves of Patel (1965) [See Section 4.7.4].

The transverse distribution of bed shear stress for a typical run is shown in Fig. 5.18. For comparison the graph contains the laboratory data of Nezu et al. (1989), and the field data of Nezu et al. (1993) for open channel flows. The data shows that the measured value of τ_b, increases rapidly with distance from the side wall, and it shows a mild peak followed by a minimum at $x/(B/2) \approx -0.5$. Beyond this position, it increases again and attains a maximum at the central axis.

Fig. 5.19 shows the transverse variation of the measured bed shear stress normalised by its averaged value, $\overline{\tau}_b$, along the whole bed for a typical run where the secondary currents were observed. Of particular significance is an undulation of the bed shear stress $\dfrac{\tau_b}{\overline{\tau}_b}$ in the transverse direction $\dfrac{x}{h}$; where h is mean flow depth, and x is the transverse co-ordinate. As pointed out by Nezu and Nakagawa (1984), the bed shear stress becomes a maximum at the downflow region of secondary current cell, whereas it becomes a minimum at its upflow region. In this manner, the bed shear stress is influenced significantly by the secondary currents, and vice versa. This noticeable feature has been observed in both laboratory duct flow by Knight and Patel (1985) and open channel flow by Nezu and Rodi (1985). It was also computer simulated using the algebraic stress model by Naot and Rodi (1982). The amplitude of the undulation in the bed shear stress is very important in considering various mass transports such as sediment and water quality in rivers.

A useful empirical method for predicting the mean bed and wall shear stresses in smooth and rough rectangular channels was originally proposed by

Knight (1981), using the concept of shear force. The method was modified at the university of Birmingham by Knight and co-workers (1978-1992). The perspective of the shear force method is that the shear force acting on a boundary, per unit length of channel is equal to the mean boundary shear stress $\bar{\tau}_n$, multiplied by the boundary cross-sectional length P_n. The shear force acting on a channels side walls SF_w, and bed SF_b are therefore equal to:

$$SF_w = \bar{\tau}_w P_w \qquad\qquad (5.21)$$

$$SF_b = \bar{\tau}_b P_b \qquad\qquad (5.22)$$

The shear force carried by the side walls or bed can be expressed as a percentage of the total shear force $\%SF$, for example:

$$\%SF_w = \frac{\bar{\tau}_w P_w}{\bar{\tau}_n P_n} \times 100 \qquad\qquad (5.23)$$

Knight et al. (1994) proposed that the percentage shear force carried by the side walls $\%SF_w$, varies exponentially with the bed to walls wetted perimeter ratio $\dfrac{P_b}{P_w}$, in the form:

$$\%SF_w = C_{sf} e^{\alpha} \qquad\qquad (5.24)$$

where α is a function of $\dfrac{P_b}{P_w}$, and C_{sf} is a shape factor as follows.

$$\alpha = -3.23\log(\frac{P_b}{P_w C_2}+1.0)+4.6052 \qquad\qquad (5.25)$$

where C_2 is equal to 1.38.

$$C_{sf} = 1.0 \qquad \text{for} \qquad \frac{P_b}{P_w} < 4.374 \qquad\qquad (5.26)$$
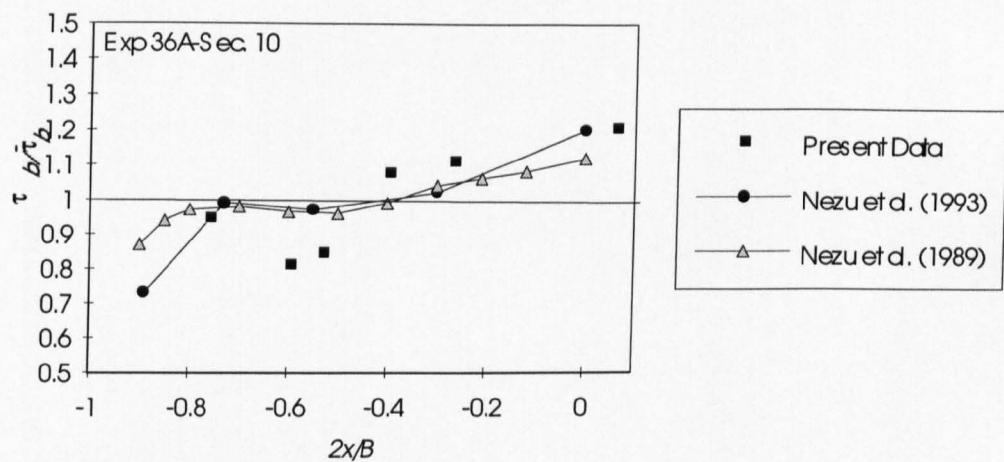
Figure 5.18. Bed shear stress distribution.
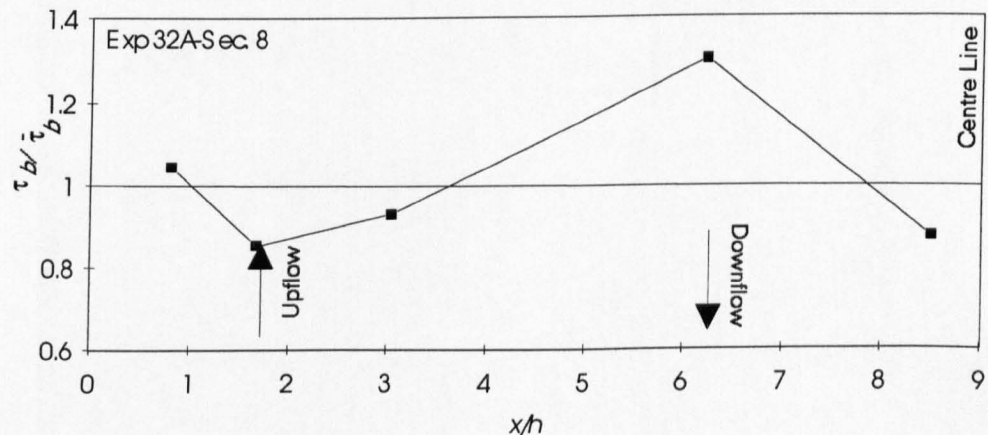
Figure 5.19. Transverse variation of bed shear stress

else

$$C_{sf} = 0.6603(\frac{P_b}{P_w})^{0.28125}$$ (5.27)

Fig. 5.20 shows the equation proposed by Knight et al. (1994) with experimental data from the present study. The agreement between the data and the equation is reasonably good, bearing in mind that the equation is derived by fitting an empirical equation to the data mostly obtained from experiments in flumes with trapezoidal and rectangular sections.
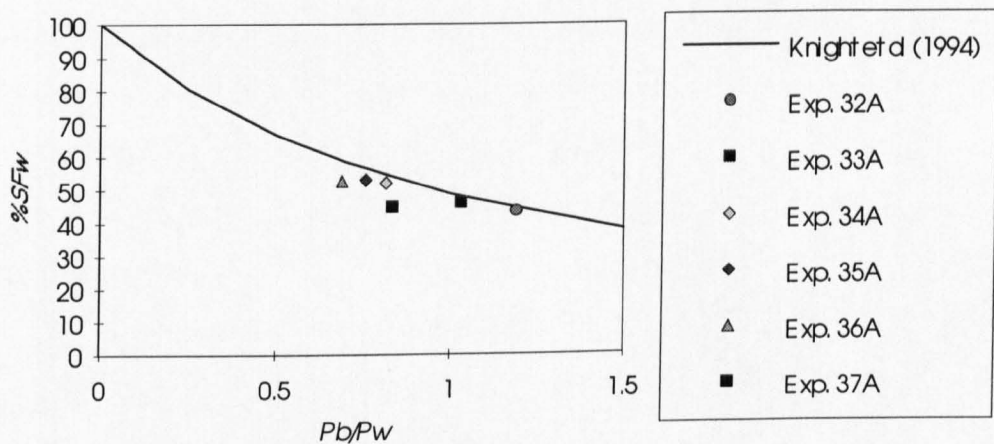
Figure 5.20. Percentage shear force values versus P_b/P_w.

5.10 Chapter Summary

In this chapter, the hydraulic and geometric characteristics of the developed stable straight channels have been discussed. The results are compared with the WPB theory predictions. The results of comparison shows that this theory underpredicts water surface width, cross sectional area, and sediment concentration of these channels. It is also shown that this theory overpredicts mean depth and water surface slopes. This difference is attributed to the estimations of the Ackers-

White (1973) sediment transport formula which is now under review and modification.

Experimental data from the present study is also compared with previous published equations for prediction of the geometry and bank profile of stable alluvial channels. The comparison shows that, for the prediction of bank profile, the fifth-degree polynomial of Diplas and Vigilar (1992) results in a better approximation than that obtained from the normal-depth method and the cosine profile. A hyperbolic function has been fitted to the bank profile data of present study. It is shown that the hyperbolic function approximates the bank profile even more closely than the fifth-degree polynomial indicated by Diplas and Vigilar (1992). The present data for velocity and boundary shear stress distribution are compared with available formulae in the literature. The results show that the velocity distribution predicted in the wall region, with the logarithmic law, and in the outer region with the log-wake law are in good agreement with the experimental data. The von Karman constant has been calculated using a linear regression analysis and the data of velocity distribution from present study. This value has been plotted against Froude and Reynolds Numbers. No systematic influence of Re or Fr on the von Karman value was recognised. It is, therefore, concluded that the von Karman constant κ is, to a good approximation, a universal constant and does not depend on the Reynolds and Froude numbers. In the other words, the von Karman constant, κ, is a universal constant, irrespective of flow type.

The plotted values of transverse distribution of bed shear stress show that the bed shear stress increases rapidly with distance from the side wall and it shows a mild peak followed by a minimum. Beyond this position, the value increases again and attains a maximum at the central axis of the channel. This trend of bed shear stress variation supports the findings of Nezu et. al (1989), and Nezu et. al (1993).

The shear force values from present study are compared with the proposed equation of Knight et. al (1994). The agreement between the experimental data of present study and the equation is good.

129

Chapter Six
The Characteristics of Alternate Bars in Alluvial Channels With Loose Boundaries

6.1 Introduction

Alternate bars are a group of bed forms often observed in alluvial bed rivers at low stages of flow. Their form consists of a series of bars where the crests are on alternate sides of the channel, see Fig. 6.1. Field observation has indicated that where alternate bars form, they are accompanied by considerable scouring at river banks. Much research has shown the close relationship between alternate bar formation and river meandering. The characteristics of these bed forms and their formation are discussed here for their importance and their potential effects on changing the plan shape and stability of straight stable channels.

A great deal of work, by different researchers, on different aspects of alternate bars has been carried out during the past decades, but so far, the experimental study of alternate bars has been limited to experiments in flumes with moveable bed and rigid banks. During the experiments of present study (series A), alternate bars were observed and measured. The measured data have been used to assess the applicability of the available formulae, for prediction of the formation and characteristics of alternate bars in alluvial channels with mobile banks.
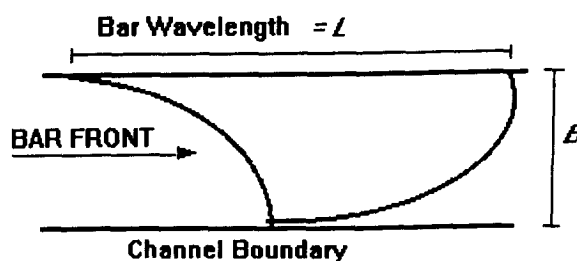
Figure 6.1. Definition sketch of alternate bars (Plan).

6.2 Previous Studies

Chang et al (1971) conducted a series of experiments in a 100ft long and 3ft wide flume. The flume had smooth, rigid walls of sheet metal and a moveable bed. He used three types of sediment: sand, plastic pellets, and expanded clay. Based upon the experimental data, he found that alternate bars were observed when the width-depth ratio of channel flow was greater than 12. He also stated that the dimensionless wavelength, $\dfrac{LS}{h}$, is related to the Froude number of the channel flow. Where L is the bar wavelength, S is the friction slope, and h is the mean depth.

Sukegawa (1972) proposed the equation:

$$\frac{B}{h} = \frac{(\frac{\theta}{\theta_c})^{2.0}}{125S} \qquad (6.1)$$

where B is the channel width and h is the depth of flow. It defines a region of alternate bar formation for $\dfrac{B}{h}$ smaller than this critical value.

Muramoto and Fujita (1978) proposed the following criteria for alternate bar formation.

$$\frac{\frac{h}{d}}{(\frac{B}{d})^{0.67}} < 0.45 \qquad (6.2)$$

$$1 < \frac{\theta}{\theta_c} < 12 \qquad (6.3)$$

where θ is the Shield's parameter, and d is the mean sediment size.

131

Jaeggi (1980) proposed the following equation for upper limit of bar formation.

$$\frac{4\Lambda_D}{\Lambda_M S} = 1 \tag{6.4}$$

where Λ_D is the dune wavelength and Λ_M is the meander wavelength.

Ikeda (1984) conducted a series of experiments in a 15m long and 50cm width flume. He crudely approximated the bar wavelength by

$$L=9B \tag{6.5}$$

Based on the data, he proposed the following equations:

$$L=5(\frac{Bh}{C_f}) \qquad\qquad F<0.8$$

$$\frac{L}{B} = 181C_f(\frac{B}{h})^{0.55} \qquad F\geq0.8 \qquad 4<\frac{B}{h}<70 \tag{6.6}$$

$$\frac{H_B}{h} = 0.0442(\frac{B}{h})^{1.45}(\frac{h}{d})^{-0.45} \qquad F>0.74 \qquad 6<\frac{B}{h}<40$$

where $C_f = \frac{ghS}{U^2}$, H_B is the bar height. He also proposed a linear relationship between the maximum scour depth, S^*, and bar height as follows.

$$S^*=0.75H_B \tag{6.7}$$

Jaeggi (1984) carried out a series of experiments in a 25m long and 0.3m wide flume. He used natural sands with mean grain sizes of 0.52, 1.8, 4.0 mm and PVC granulate of cylindrical shape with mean diameter of 3.0 mm. He used his data and the data of Chang et al. (1971) to establish a new criterion for alternate bar

formation. His proposed equation for upper limit of alternate bar formation is given by:

$$\frac{\theta}{\theta_c} = 2.93 \ln \frac{BS}{(s-1)d\theta_c} - 3.13(\frac{B}{d})^{0.15}$$ (6.8)

He introduced a more general expression for defining the lower limit of alternate bar formation which is:

$$\frac{\theta}{\theta_c} = (\frac{d_{90}}{d_m})^{0.67}$$ (6.9)

where d_m is the mean grain size. He also defined a minimum condition for the slope at which alternate bar formation will occur. This criterion is:

$$\text{Slope} > \frac{\exp[1.07(\frac{B}{d_m})^{0.15} + M]}{12.9\frac{B}{d_m}}$$ (6.10)

where M is a parameter which is a function of sediment grading and varies from 0.34 (uniform material) to 0.7 (widely graded material). This equation has been compared with the data of present study, see Fig. A2 in Appendix A. According to this criterion, most of the data are in the region in which alternate bar formation is not possible. The reason may be due to the fact stated by Bathurst and Cao (1986) that Eq. 6.10 does not set limits to the region of formation of bars in general but only to three dimensional bars in particular.

Jaeggi (1984) proposed an equation for scour depth, S, as follows:

$$S = 0.76\Delta_{AB} = \frac{B}{6(\frac{B}{d})^{0.15}}$$ (6.11)

where Δ_{AB} is the total height of alternate bar.

Chang (1985) proposed a criteria for alternate bar formation in straight alluvial bed channels with rigid banks following a rational approach, based upon the condition which initiates meandering in a confined channel. He, therefore,

133

hypothesised that alternate bars may develop if the stable width is less than the channel width between the rigid banks or in other words,

$$B_s < B \tag{6.12}$$

where B_s is the stable width of alluvial stream, and B is the channel width between rigid banks.

The analysis of alternate bars in straight channels has also been tackled by analytical studies. The most recent ones belong to Blondeaux and Seminara (1985), Colombini et al. (1987).

Blondeaux and Seminara (1985) worked on the stability analysis of the formation of alternate bars in straight channels. The stability analysis provides dispersion relationships which allow two curves to be built. The curves typically exhibit two characteristic points, which are found to correspond to critical or threshold conditions for the formation of alternate bars.

Colombini et al. (1987), by using a weakly non-linear analysis, proposed a theory for prediction of a finite amplitude of the alternate bars in a straight alluvial channel. They used their theory to develop an equation for dimensionless maximum bar height estimation as follows.

$$\frac{H_B}{h} = b_1 (\frac{\beta - \beta_c}{\beta_c})^{\frac{1}{2}} + b_2 (\frac{\beta - \beta_c}{\beta}) \tag{6.13}$$

where $\beta = \frac{B}{2h}$, β_c is the critical value of β for the formation of alternate bar, b_1 and b_2 are parameters that depend on θ, β_c, and $\frac{d_{50}}{h}$.

Yalin and Silva (1991) explained the formation of alternate bars on the basis of horizontal bursts, which occur in an open channel. They found that the length of alternate bars, namely $6B$, is but the length of horizontal burst producing them.

They proposed the following two criteria for separating alternate bars from multiple bars and dunes.

$$\frac{B}{h} = 26.46(\frac{h}{d})^{\frac{1}{3}}$$
(6.14)

$$\frac{B}{h} = 0.215\frac{h}{d}$$
(6.15)

Garcia and Nino (1993) conducted a series of experiments in two flumes one with 20m long, 0.9m wide and the other 50m long, 1.8m wide. The sediment median size was 0.53 mm. By confining the flume width, they developed one straight and three meandering channels with 0.4m width. They used the experimental data to analyse recently developed linear and non-linear theoretical models for the formation, geometrical properties, and migration characteristics of alternate bars. They indicated that the experimental data of wavelength, celerity, and critical conditions for the formation of alternate bars in their straight channel is in agreement with predictions of the Blondeaux and Seminara (1985) linear theory of free bars.

They concluded that the closure relationships employed in the theoretical analysis play a fundamental role in the accuracy of the prediction. They also found that the observed wavelength of well developed bars tends to be underestimated by the linear theory.

6.3 Experimental Study

So far, experimental study of alternate bars has been limited to experiments in flumes with moveable bed and rigid banks. It is the aim of this section to consider the applicability of the available formulae, for prediction of the formation

and characteristics of alternate bars in alluvial channels with loose banks. During the experiments of present study (series A), alternate bars were observed and measured. The measured data have been used to assess the applicability of the available formulae. In these experiments channels with loose banks have been developed in the regime flume. The channel model was allowed to develop freely while all hydraulic parameters were kept constant. The experiment was stopped when the channel and bed forms gained a state of equilibrium.

6.4 Data Analysis

The data obtained in the laboratory, has been used to investigate the applicability of available formulae in the literature (For the experimental results, see Table A5 in Appendix A). This comparison is concerned with the criteria of alternate bars formation, bar wavelength, and bar height and scour depth. The following paragraphs describe the results of this comparison.

6.5 Criteria For Alternate Bar Formation

The laboratory data has been compared with the Chang et al. (1971), Yalin and Silva (1991) criteria for alternate bar formation. The results of this comparison are shown in Fig 6.1. The experimental data are located in the defined region for alternate bar formation and therefore satisfy the criteria of both researchers. The criterion of Muramoto and Fujita (1978) is compared with the data in Fig. 6.2. The comparison shows that most of the data are located below the upper limit criterion. Therefore the data mostly satisfy their criterion.

The Colombini et al. (1987) criterion is also compared with the data in Fig. 6.3. The data fall in the region defined for alternate bar formation and therefore satisfy their criterion.

The Jaeggi (1984) criterion has been compared with the data in Fig. 6.4 which shows that all the data are located below the upper limit criterion and satisfy this criterion.

6.6 Bar Wavelength

The experimental data for the bar wave lengths have been compared with JSCE (Japanese Society of Civil Engineers) committee (1974), and Ikeda's (1984) crudely approximated bar wavelength formula. Fig. 6.5 shows the results of this comparison. It shows that the data from the present study mostly fall between the two lines. In other words, $6B < L < 9B$, where B is channel width and L is bar wavelength.

The Ikeda (1984) formula for bar wavelength prediction has also been examined by the present data. The result is shown in Fig. 6.6. It shows that this formula underpredicts the bar wave length by an average amount of 14%.

6.7 Bar Height and Scour Depth

The present data for bar height has been compared with the Ikeda (1984) formula for bar height prediction. Fig. 6.7 shows that this formula overpredicts the data by an average amount of 8%.

The data also has been compared with predictions of the Jaeggi (1984) formula. The comparison in Fig. 6.8. shows that this formula underpredicts the bar height by an average amount of 13%.

Alternate Bar Formation Criteria
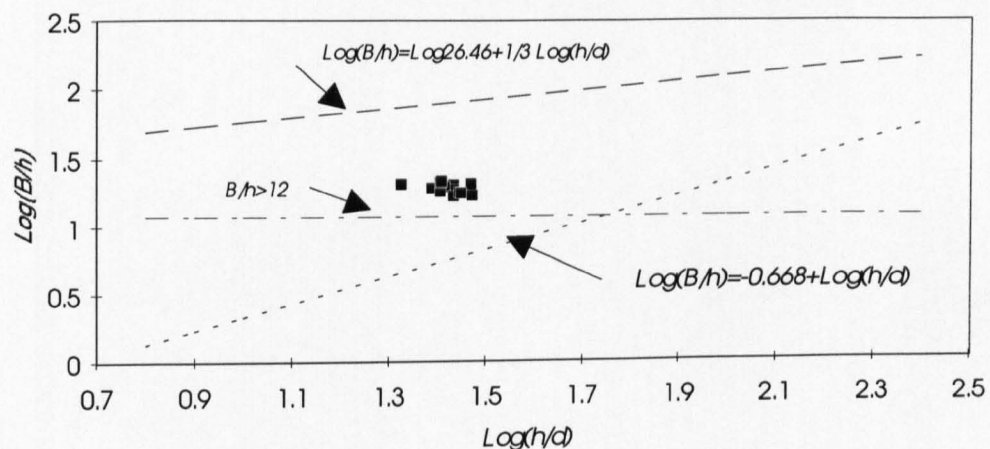
Figure 6.1. Comparison of the lab. data with Chang (1971), and Yalin and Silva (1992) criteria.

Alternate Bar Formation Criteria
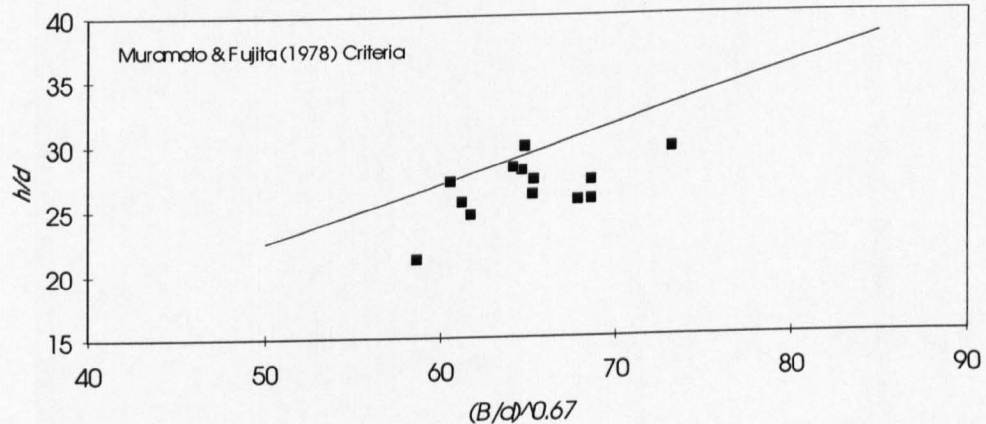
Figure 6.2. Comparison of lab. data with Muramoto and Fujita (1978) criteria.
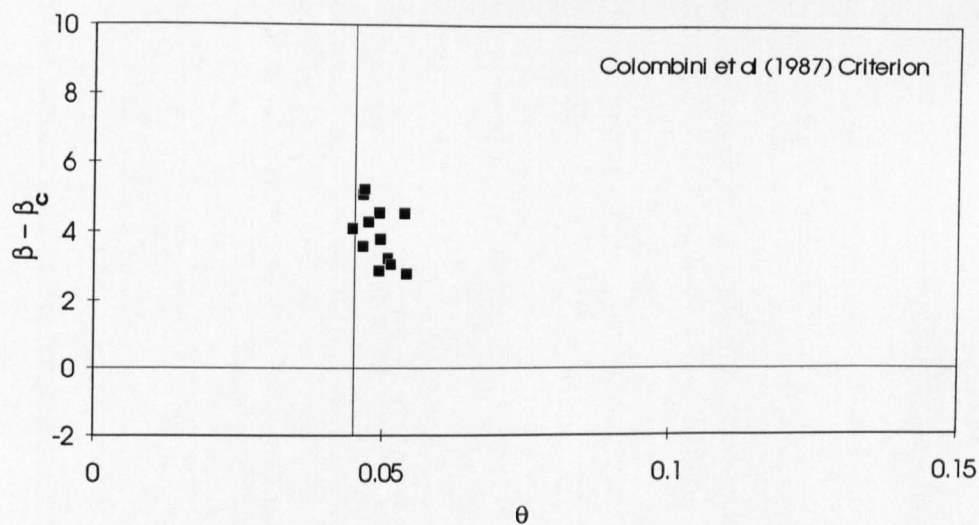
Figure 6.3. Comparison of lab. data with Colombini et al (1987) criteria.
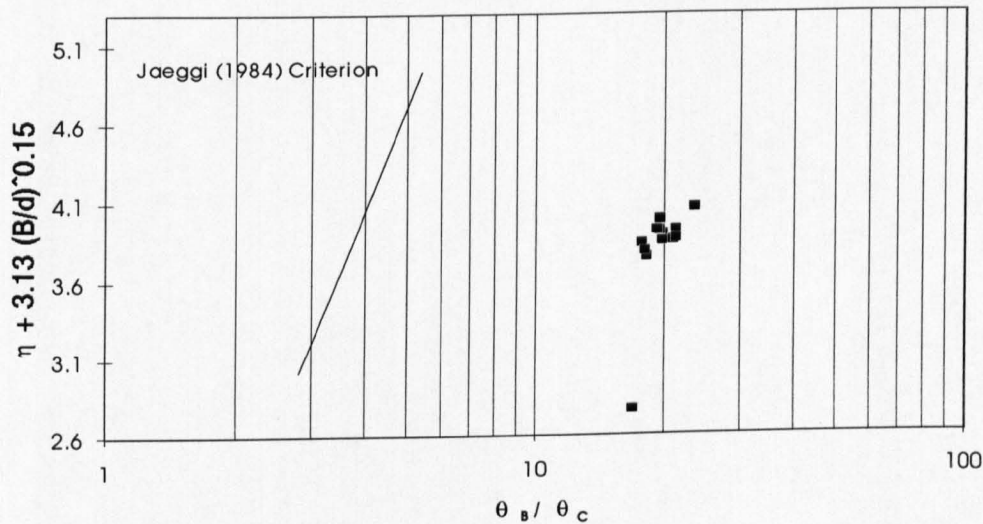
Figure 6.4. Comparison of lab. data with Jaeggi (1984) criteria.

The Colombini (1987) formula for dimensionless bar height calculation has also been compared with the data in Fig. 6.9. The formula overpredicts the dimensionless bar height. The average value of the discrepancy ratio for dimensionless bar height is 2.16.

The data for maximum scour depth is compared with the Ikeda (1984) formula. The results are shown in Fig. 6.10. As the most of the data falls above the proposed line, it implies that $S^* > 0.75H_B$, where S^* is scour depth and H_B is bar height.

Relation Between Channel Width and Wave Lenght of the Bars
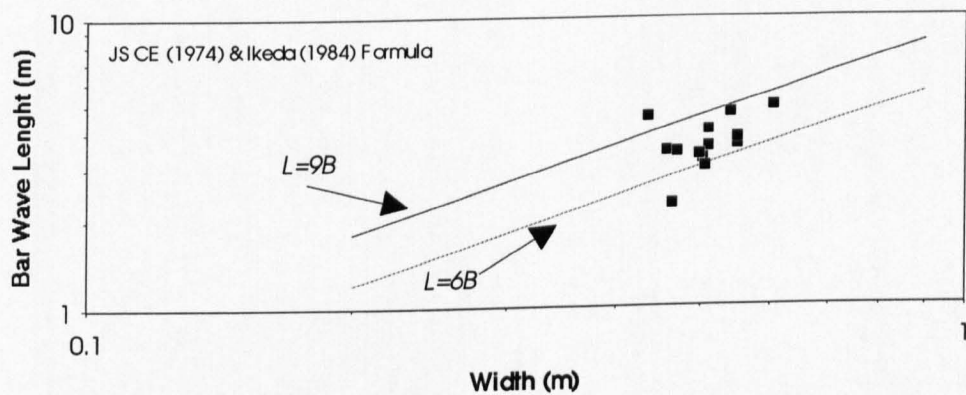
Figure 6.5. Comparison of the lab. data with JSCE (1974) and Ikeda (1984) formula.

Comparison Between Observed And Calculated L /B
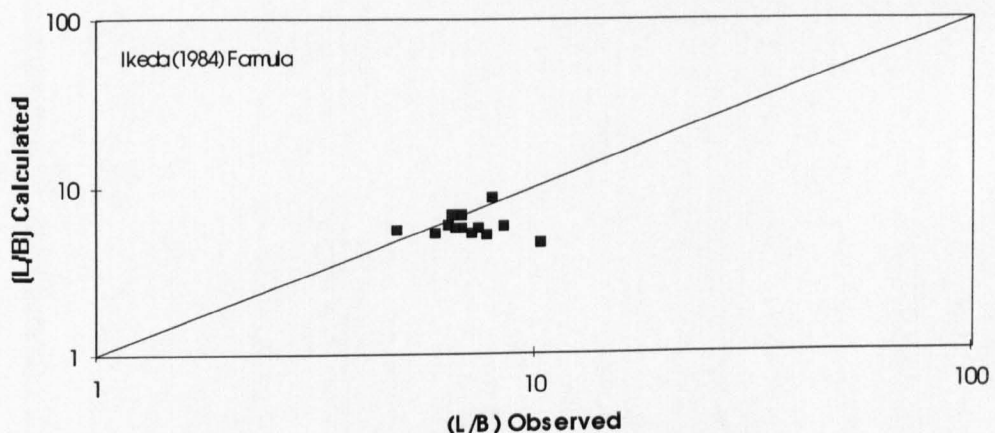
Figure 6.6. Comparison of the lab. data with Ikeda (1984) formula.
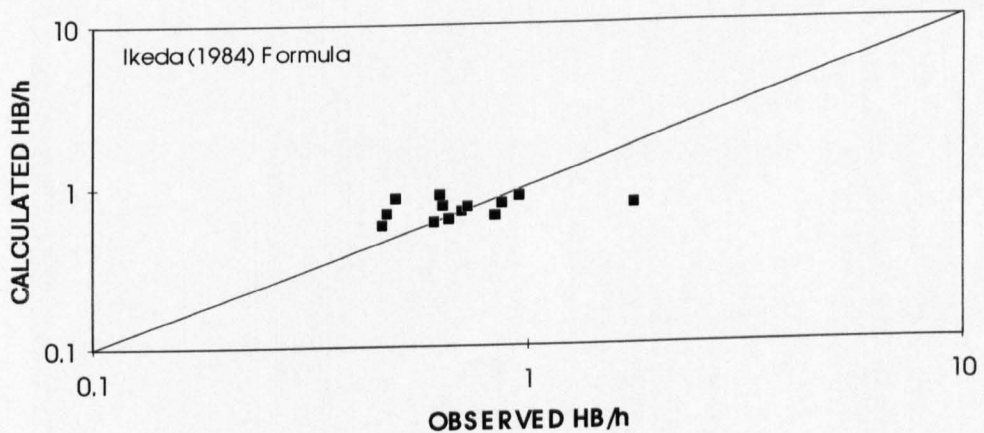
Figure 6.7. Comparison of the lab. data with Ikeda (1984) formula.
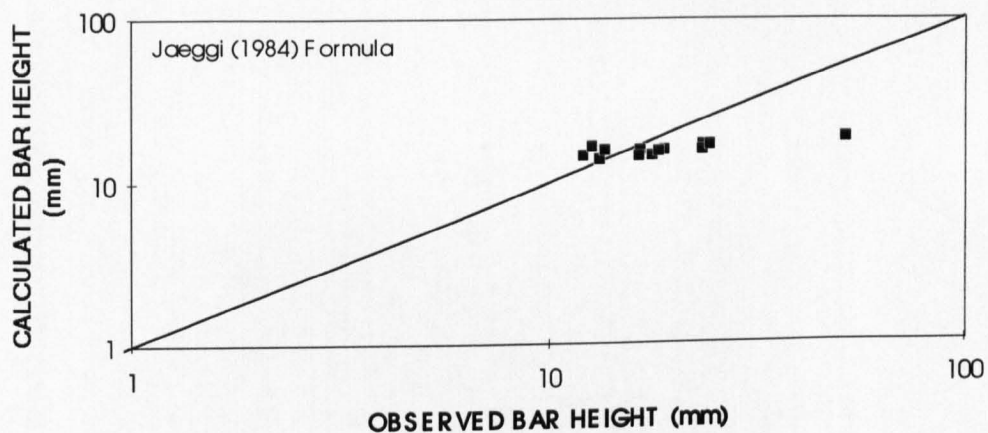
Figure 6.8. Comparison of the lab. data with Jaeggi (1984) formula.
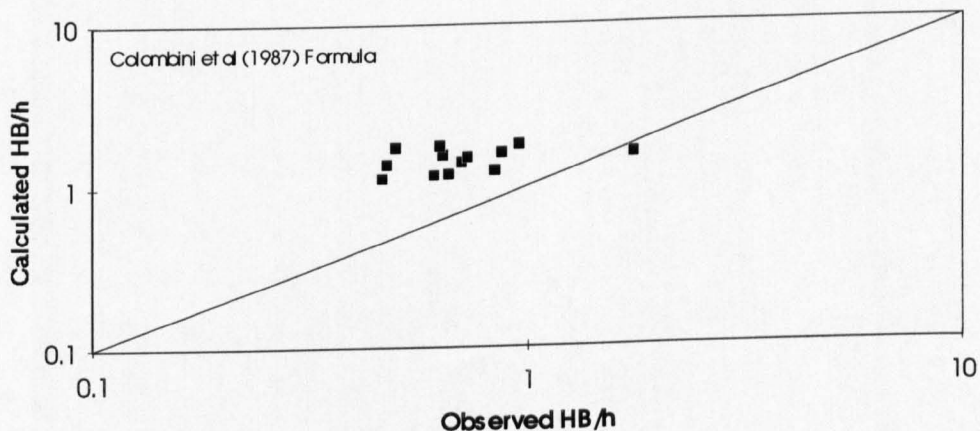
Figure 6.9. Comparison of the lab. data with Colombini (1987) formula.

142
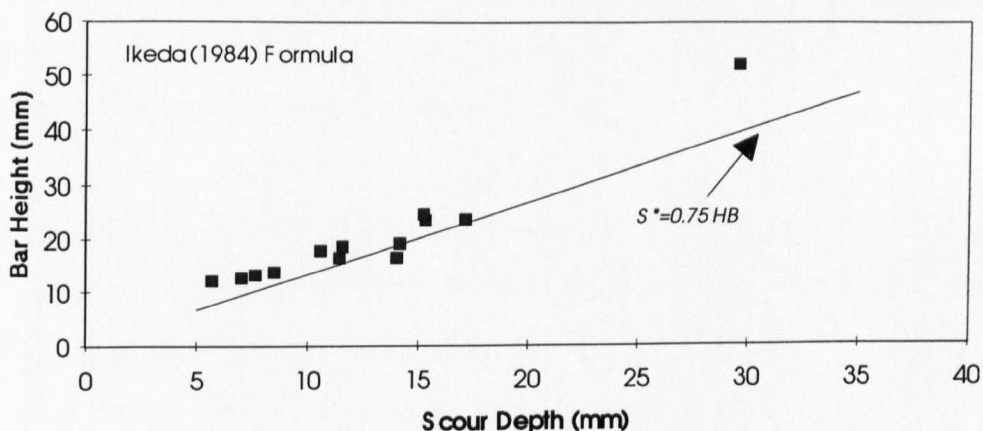
Figure 6.10. Comparison of the lab. data with Ikeda (1984) formula.

6.8 Chapter summary

The available formulae in the literature have mostly resulted from experiments on alluvial channels with fixed walls. In order to investigate their applicability to real alluvial channels, a series of experiments have been carried out. The results have been compared with existing formulae. The comparison shows that the present data is in good agreement with the Chang (1971), Yalin and Silva (1991), Muramoto and Fujita (1978), Colombini et al. (1987), and Jaeggi (1984) criteria for alternate bar formation. The present data shows that the bar wavelength, *L*, is *6B < L < 9B*. It also shows that the Ikeda (1984) formula for dimensionless bar wavelength prediction underpredicts this parameter by an average amount of 14%.

The comparison of present data with Ikeda (1984) formula for dimensionless bar height prediction shows that this formula overpredicts the dimensionless bar height by an average amount of 8%. It also has been found that the Jaeggi (1984)

143

formula underpredicts the bar height by an average amount of 13%. In the case of the Colombini et al. (1987) formula, it shows that the average discrepancy ratio for dimensionless bar height is 2.16. The comparison with the maximum scour depth formula of Ikeda (1984) proposes that $S^* > 0.75H_B$.

The published formulae for characteristics of alternate bars in channels with rigid banks give satisfactory predictions for those with loose banks. In order to derive more precise formulae more laboratory and field measurements of alternate bars, in channels with loose banks, are necessary.

Chapter Seven
Interaction of Bridge Piers with Laboratory Channels

7.1. Introduction

Extensive studies on scour around isolated bridge piers have been carried out in the past. As a result, scour formulae have been developed for the prediction of local scour depth. There also have been several preliminary studies of scour around pier groups but none of them give a complete treatment of the problem. Hanna (1978) showed that scour for a pile group was less than 20% greater than scour at a single pier when the spacing exceeded five pier diameters. Despite all the previous work there is still a need for bridge scour research. The experiments in the previous research have been carried out in laboratory flumes with fixed wall. However a regime flume, in which the experiments of present study have been carried out, has moveable bed and banks and represents the field situation more closely. It is the aim of this study to consider recently published formulae for scour depth prediction and the effect of pier spacing on pier groups. The time variation of scour depth and topography of scour has also been considered.

7.2. Previous Studies

As it has been reviewed before, the Colorado State University's (CSU) equation (1975) has the following form:

$$\frac{d_s}{y_o} = 2.0 K_1 K_2 (\frac{b}{y_o})^{0.65} F_r^{0.43} \tag{7.1}$$

where the variables are the same as defined in chapter 2. Different values of K_1 and K_2 are given in Table 7.1.

Table 7.1. K_1, and K_2 values.

Type of pier	K_1
Square nose	1.1
Round nose	1.0
Circular cylinder	1.0
Sharp nose	0.9
Group of cylinders	1.0

Angle	$\frac{L}{b}=4$	$\frac{L}{b}=8$	$\frac{L}{b}=12$
0	1.0	1.0	1.0
15	1.5	2.0	2.5
30	2.0	2.5	3.5
45	2.3	3.3	4.3
90	2.5	3.9	5.0
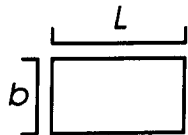
(a) Square nose   (b) Cylinder

Figure 7.1. Pier shapes.

In FHWA (1991) report, the CSU equation is recommended as it encloses all the points when it is compared with field data measurements.

Breusers et al.'s (1977) recommended equation has the following form:

$$\frac{d_s}{b} = [2.0 Tanh(\frac{y_o}{b})][f_1(\frac{U}{U_c})][f_2(Piershape)][f_3(\alpha,\frac{l}{b})] \qquad (7.2)$$

where the variables are the same as defined in chapter 2

Melville and Sutherland's (1988) proposed design method, which is based on envelope curves drawn to experimental data derived mostly from laboratory experiments, has the following form:

$$\frac{d_s}{b} = K_1 K_y K_d K_\sigma K_s K_\alpha \qquad (7.3)$$

146

where the K values are the same as defined in chapter 2.

They considered each parameter individually and for design purposes they recommended the following expressions for the indicated parameters.

$$K_y = 1.0 \qquad \text{for} \qquad \frac{y}{D} > 2.6 \qquad (7.4)$$

$$K_y = 0.78 \left(\frac{y}{D}\right)^{0.255} \qquad \text{for} \qquad \frac{y}{D} < 2.6 \qquad (7.5)$$

$$K_d = 1.0 \qquad \text{for} \qquad \frac{D}{d_{50}} > 25 \qquad (7.6)$$

$$K_d = 0.57 \log\left(2.24 \frac{D}{d_{50}}\right) \qquad \text{for} \qquad \frac{D}{d_{50}} < 25 \qquad (7.7)$$

For flow intensity and sediment gradation effects they discussed different situations for bed armouring and concluded that the best form for flow intensity parameter is $\frac{[\,U-(U_a-U_c)\,]}{U_c} < 1.0$, in which the difference $(U_a\text{-}U_c)$ reflects the influence of sediment grading so for all σ_g values and design purposes, they recommended the following expressions for K_I :

$$K_I = 2.4 \left|\frac{U-(U_a-U_c)}{U_c}\right| \qquad \text{for} \qquad \left|\frac{U-(U_a-U_c)}{U_c}\right| < 1 \qquad (7.8)$$

$$K_I = 2.4 \qquad \text{for} \qquad \left|\frac{U-(U_a-U_c)}{U_c}\right| > 1 \qquad (7.9)$$

where U_a is the mean approach flow velocity to characterise the limiting armour condition for scour calculation and is equal to 0.8 U_{ca}, U_{ca} is the mean flow velocity beyond which no armour layer can form, U is the mean approach flow velocity, and U_c is the mean approach velocity at threshold condition.

A selection of shape factors K_S is given in Table 2. of their publication which apply to piers aligned with the flow and are based on $K_S = 1.0$ for cylindrical piers. For $K\alpha$ they recommended the alignment factor given by Laursen (1958).

Gao et al. (1993) summarised the development and verification of scour equations based on laboratory studies and a great number of field data that were used in China. The equation used for live bed scour around a pier is:

$$d_s = 0.46 K_\xi b^{0.6} y_o^{0.15} d_{50}^{-0.07} [\frac{U - U_c'}{U_c - U_c'}]^\eta \tag{7.10}$$

which U_c is the critical velocity for initiation of motion of the bed material.

$$U_c = [\frac{y_o}{d_{50}}]^{0.14} [17.6 \frac{\rho_s - \rho}{\rho} d_{50} + 0.000000605 \frac{10 + y_o}{d_{50}^{0.72}}]^{0.5} \tag{7.11}$$

which ρ_s and ρ are the density of the sediment particles and water, respectively. d_{50} is the mean sediment diameter, in m and U_c in m/s. U_c' is the initial velocity and given by:

$$U_c' = 0.645 (\frac{d_{50}}{b})^{0.053} U_c \tag{7.12}$$

η is a power related to bed load.

$$\eta = [\frac{U_c}{U}]^{9.35 + 2.23 \log d_{50}} \tag{7.13}$$

which y_o is the depth of approach flow, b is the pier width projected to flow direction, and K_ξ reflects the influence of pier shape and flow attack angle to scour depth.

7.3. Data Comparison

The data obtained from the present study are compared with the CSU (1975) equation. This equation is the most commonly used pier scour equation in the United States. Fig 7.2 shows that the calculated scour depths by the CSU (1975) equation are higher than the measured data, therefore it is a conservative equation. It also shows that the equation is not very sensitive in scour depth prediction, as it turns to predict more and less the same scour depth for the range of measured data.

Breusers et al's (1977) recommended relation for scour depth prediction is also compared with the data in Fig. 7.3. This equation appears to underpredicts the scour depth. For safety reasons, in design practice, it is undesirable to underpredict scour depth, therefore the use of this equation is not recommended for design purposes.

Melville and Sutherland's (1988) design method for local scour is examined in Fig. 7.4. The results show that the method overpredicts the scour depth. The overprediction of the scour depth is due to this fact that the equation is intended to be used for design purposes and therefore to be an envelope curve for scour depth prediction.

The data comparison with Gao et al's (1993) equation is shown in Fig. 7.5. It shows that the equation overpredicts the scour depth. Due to the fact that it is a part of "Code of Investigation and Design of Highway Bridge Crossing" in China and is proposed for design purposes, it is a conservative equation. Thus it may include safety factors.
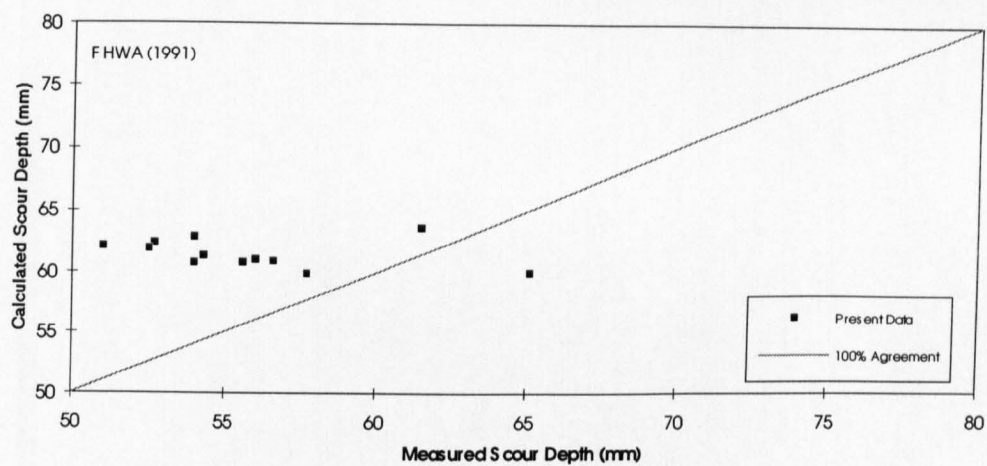
Figure 7.2. Data comparison with CSU (1975) equation.
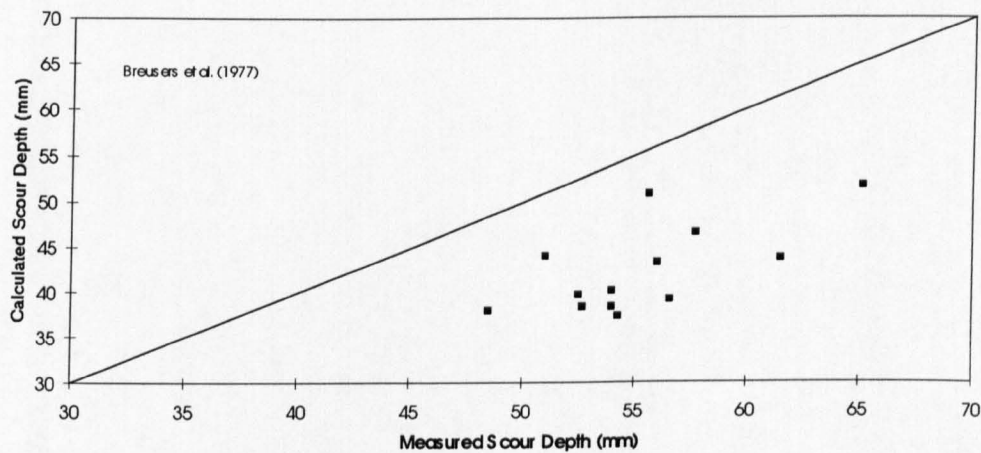
Figure 7.3. Data comparison with Breusers et al. (1977) equation.

150
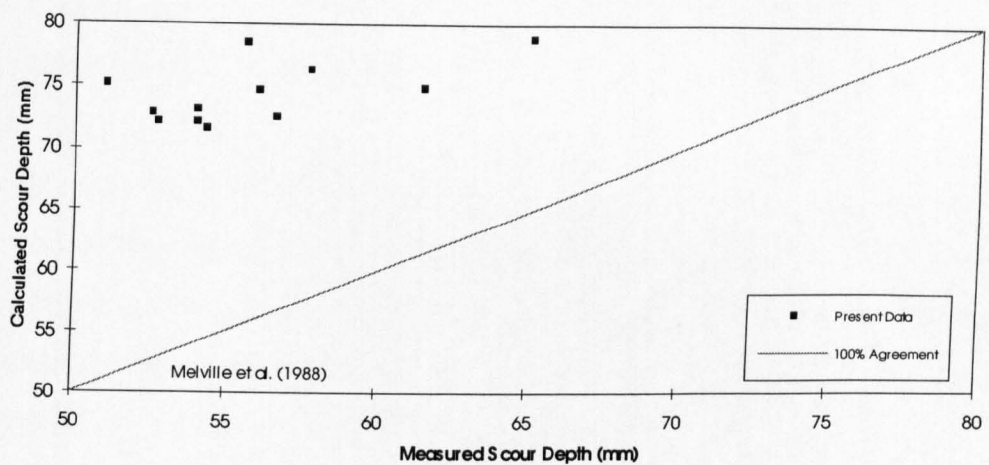
Figure 7.4. Data comparison with Melville et al. (1988) equation.
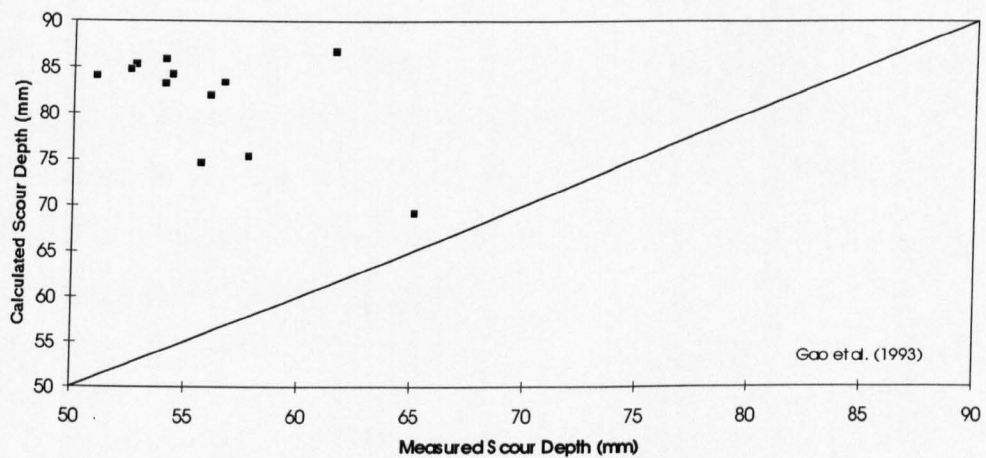
Figure 7.5. Data comparison with Gao et al. (1993) equation.

From the equations, which have been compared with the data from present study, the CSU equation gives the best prediction. The difference is attributed to the fact that these formulae are based on limited data and have not been developed by taking into consideration the mechanism of local scour. It may also be due to the fact that laboratory flumes do not represent the real situation in the field. A "regime" flume, in which the present experiments were carried out, represents the field situation more closely than a standard laboratory flume. It is also notable that the temporal variation of scour depth has a practical significance, as the peak discharge of the flood does not last long enough to scour up to its full potential. Therefore, it is believed that the maximum scour depth should be calculated from the temporal variation of scour depth rather than empirical relations fitted to laboratory data. This issue has been addressed in section 7.6.

7.4. Pier groups

Among the reviewed formulae for scour depth, none of them consider the effect of pier spacing. In fact there is little information on the effects of spacing on scour depth. In this note a further factor, K_{ps}, is introduced which considers the effect of pier spacing. K_{ps} is a function of x (the pier centre line spacing), and b (pier diameter) as shown in Fig. 7.6.
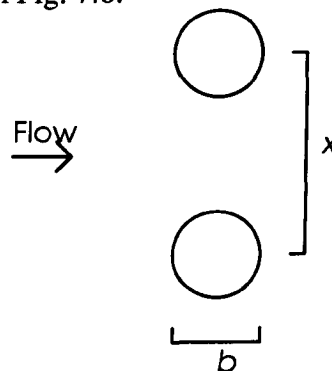
Figure 7.6. Definition Sketch.

K_{ps} is define by :

$$K_{ps} = \frac{d_s}{d_{si}}$$ (7.18)

which d_s is the maximum scour depth for pier groups and subscript i, refers to the isolated pier.

As the spacing between the piers increases, one would expect K_{ps} converge toward unity i.e. the scour depth will not be affected by pier spacing. As pier spacing decreases the flow will be accelerated by the contraction produced by the piers. Hanna (1978) conducted a series of experiments on pier groups. On the basis of his observations, he commented that when piers are placed transverse to the flow, each will have, except at very close spacing, it's own 'horseshoe vortex'. As pier spacing is decreased, the inner arms of the 'horseshoe vortices' will be compressed. This causes velocities within the arms to increase with a consequent increase in scour depth.

7.5. Experimental set-up

In order to isolate the effect of pier spacing on scour depth, the results of series B of the experiments have been used. Circular piers were used for the experiments. The pier groups were set transverse to the flow with the pier spacing of $\frac{x}{b} = 2.0$ and 4.0, see Fig. 7.6. All the experiments were in a live bed condition where $\frac{U}{U_c} > 1$. Fig. 7.7. shows the variation of K_{ps} with pier spacing for the data of present study, Hanna (1978), and Vittal et al (1994). This variation can be well represented by the envelope curve formula as follows.

153
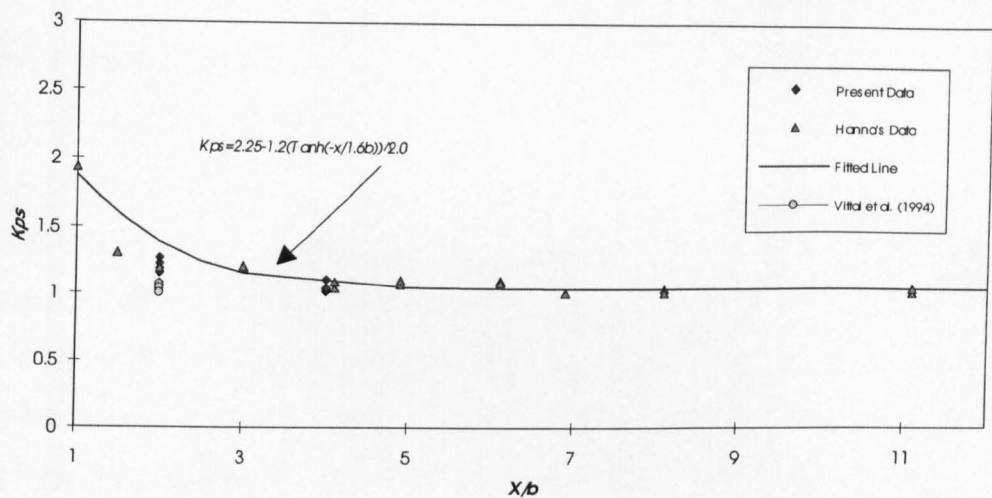
Figure 7.7. Variation of K_{ps} with pier spacing.

$$K_{ps} = 2.25 - 1.2(Tanh(\frac{-x}{1.6b}))^{2.0} \tag{7.19}$$

Pier spacing coefficient, K_{ps}, which have been derived for transverse flow condition can be used with the previously introduced scour equations to account for the pier spacing effect on scour depth.

7.6 Temporal variation of scour depth around bridge piers

7.6.1 Introduction

The estimation of the depth of scour at a bridge pier in an alluvial stream is required for the safe and economical design of the bridge pier and its foundation. Most scour research has been carried out for clear water conditions, in which relationships for the maximum scour depth in steady flow have been developed. However, the flow in a river during a flood is unsteady, and discharge changes can be rapid. As the maximum flood discharge may not last long enough to develop the full scour depth, therefore time is an important factor in the scour process. Thus, the hydraulic design of foundations based on computations of maximum scour depth for the design discharge can be uneconomical. Therefore, it is believed that the maximum scour depth should result from the temporal variation of scour depth rather than empirical relations fitted to laboratory data.

Several investigators have studied the temporal variation of scour depth, e.g. Shen et al (1965), Nakagawa and Suzuki (1975), Hjorth (1977), Ettema (1980), Islam (1986), and Kothyari (1989,1992,1993). The following paragraphs describe the details of a mathematical model which is proposed to describe temporal variation of scour depth around circular bridge piers in clear-water and live-bed scour.

7.6.2 Basic assumptions of the model

The horseshoe vortex has been considered as the prime agent causing scour. Baker (1978,1980) studied the characteristics of the horseshoe vortex. He considered the simplest possible type of vortex system, consisting of just one vortex around a cylindrical obstacle on a plane bed in a channel flow. He

expressed the circulation around the vortex core on the plane of symmetry, Γ_o as follows.

$$\Gamma_o = k_1 (2\pi r_o U) \qquad\qquad (7.16)$$

where r_o is the radius of the vortex core on the plane of symmetry, U is the surface flow velocity, and k_1 is a constant.

Kothyari (1989) using the experimental data of Baker (1978), Qadar (1980), Muzzamil et al (1989), with the data of his study developed the following relationship for the diameter of primary vortex.

$$\frac{D_v}{Y} = 0.28(\frac{b}{Y})^{0.85} \qquad\qquad (7.17)$$

where b is the pier diameter, and Y is the approach flow depth.

As a scour hole forms beneath the vortex system, the system sinks in to the scour hole. Baker (1980) assumed that the vortex system within the scour hole may be represented by a circular forced vortex of radius r and maximum circulation Γ. Then

$$\Gamma = 2\pi r V \qquad\qquad (7.18)$$

where V is the tangential velocity at the edge of the vortex. He assumed that the radius of this vortex is given by:

$$r = r_o + k_2 d_s \qquad\qquad (7.19)$$

where r_o is the vortex radius on a flat bed, d_s is the scour depth, and k_2 is a constant during the scouring process.

Further by assuming $\Gamma = \Gamma_o$, he derived the following equation for tangential velocity at the edge of the vortex.

$$V = k_1 r_o U (r_o + k_2 d_s)^{-1} \tag{7.20}$$

Baker (1980), by considering the applied forces of the flow within the vortex system on an idealised sediment particle at the equilibrium scour depth found the tangential vortex velocity at the equilibrium scour depth as follows.

$$V_c = \sqrt{\frac{8}{3} \frac{Cos(60-\alpha)}{\sqrt{3}C_D + C_L}(\frac{\rho_s}{\rho}-1)gd} \tag{7.21}$$

where α is the slope of scour hole, C_D is the drag coefficient, C_L is the lift coefficient, d is the sediment size.

Obviously the scour would cease when V tends to V_c, the critical velocity for removing the material from the scour hole.

Paintal (1971) developed a stochastic model of bed load transport. He discussed that the time t^* required, through which the hydrodynamic forces should act on a single particle to move it, may be expressed by:

$$t^* = \frac{C_2 d}{p_{o,t} U_{*,t}} \tag{7.22}$$

where

$$U_{*,t} = \sqrt{\frac{\tau_{p,t}}{\rho_f}} \tag{7.23}$$

where C_2 is a constant, d is the sediment size, $p_{o,t}$ is the average probability of movement of the particle at time t, and $U_{*,t}$ is the shear velocity at time t.

According to Paintal (1971) and Kothyari (1989), the relationship for $p_{o,t}$ is given as:

$$p_{o,t} = 0.45(\frac{\tau_{p,t}}{\Delta\gamma_s d})^{3.45} \qquad \text{for} \qquad (\frac{\tau_{p,t}}{\Delta\gamma_s d}) \le 0.25 \qquad (7.24)$$

$$p_{o,t} = 1.0 \qquad \text{for} \qquad (\frac{\tau_{p,t}}{\Delta\gamma_s d}) > 0.25 \qquad (7.25)$$

where $\Delta\gamma_s = \gamma_s - \gamma, \gamma_s$ and γ are the specific weights of the sediment and the fluid respectively. Kothyari (1989) on the basis of experimental data determined the value of C_2 to be 0.05.

In order to convert the velocity value to shear velocity Bray's (1979) equation has been used. This equation has been used in order to demonstrate the methodology and technique of the model. An investigation needs to be carried out in order to derive a more precise equation.

7.6.3 Computational steps for clear-water scour

On the basis of above considerations, the following scheme shows the computational steps of the proposed model for determination of temporal variation of scour depth in clear water scour.

1. For known values of flow characteristics and pier diameter, calculate the diameter of primary vortex.

2. Calculate tangential velocity at the vortex edge at $t=0$ setting $d_s=0$.

3. Find the shear velocity using Bray's (1979) equation.

4. Using step 3 and equations 7.22 to 7.25 find the value of t^*.

5. Scour depth d_s, after time t^* is equal to d.

6. The changed value of tangential velocity at vortex edge due to development of scour hole is computed using 7.20 and setting d_s equal to d.

158

7. The new value of t^*, which is now the time for the scour depth to increase from d_s to $d_s + d$ is computed using equations 7.22 to 7.25.

8. Steps 2 to 7 are repeated until the value of $V \leq V_c$.

The computations are stopped when the value of the tangential velocity at the vortex edge is less than the critical value for removing the sediment from the scour hole.

In present study the value of $C_2 = 0.05$, as recommended by Kothyari (1989), was used. For the values of k_1 and k_2, Baker (1980) stated that k_1 can be considered to be constant at all flow conditions. He stated that k_2 relates the vortex radius to the scour depth. At a fixed value of the scour depth d_s, the dimensions of the scour hole are largely controlled by the value of the angle of repose of the sediments, and not by the flow conditions. The angle of repose of the sediment in fact varies only with the sediment size and shape. Since the vortex radius is determined by the scour hole dimensions, for any one sediment k_2 will be constant.

The experimental data of Kothyari (1989), Ettema (1980), Chabert and Engeldinger (1956) were used for estimating the values of constants k_1 and k_2. The values of k_1 and k_2 were estimated so that the difference between the calculated and observed values of scour depth would be minimum. Figs. 7.12 to 7.17 show the comparison between the temporal variation of scour depth calculated from the model and the data of Chabert and Engeldinger (1956), Ettema (1980), and Kothyari (1989). The comparison is based on the same data set that has been used for the calibration of the model. For the Chabert and Engeldinger's (1956) data, and Ettema's (1980) data, the agreement with the proposed model is reasonable. The data of Kothyari (1989) shows some differences especially at the beginning of the scour process.
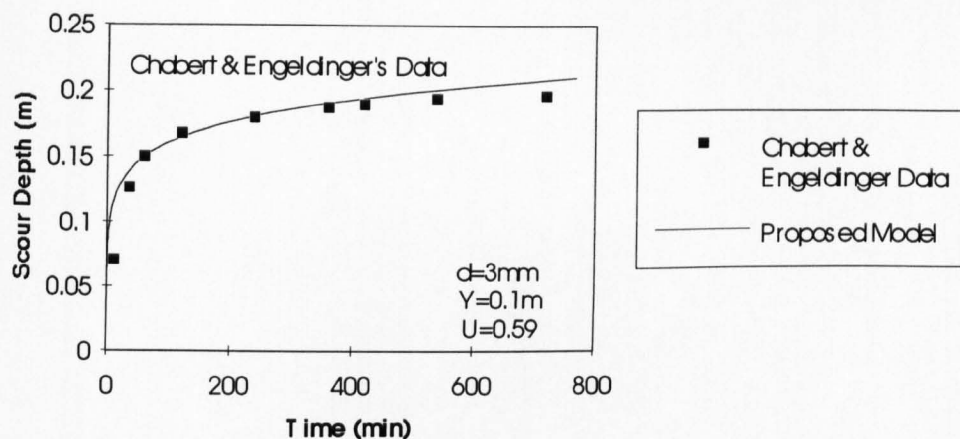
Figure 7.12. The comparison between the temporal variation of scour depth
calculated from the model and the data of Chabert & Engeldinger (1956).
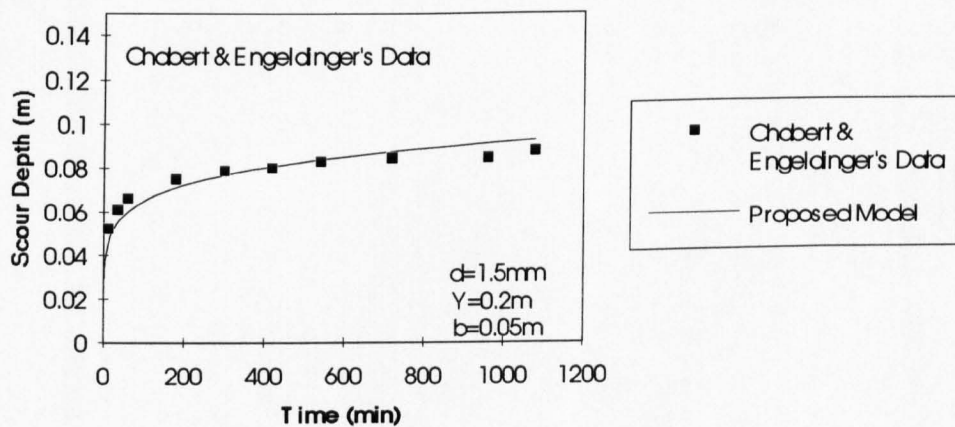
Figure 7.13. The comparison between the temporal variation of scour depth
calculated from the model and the data of Chabert & Engeldinger (1956).
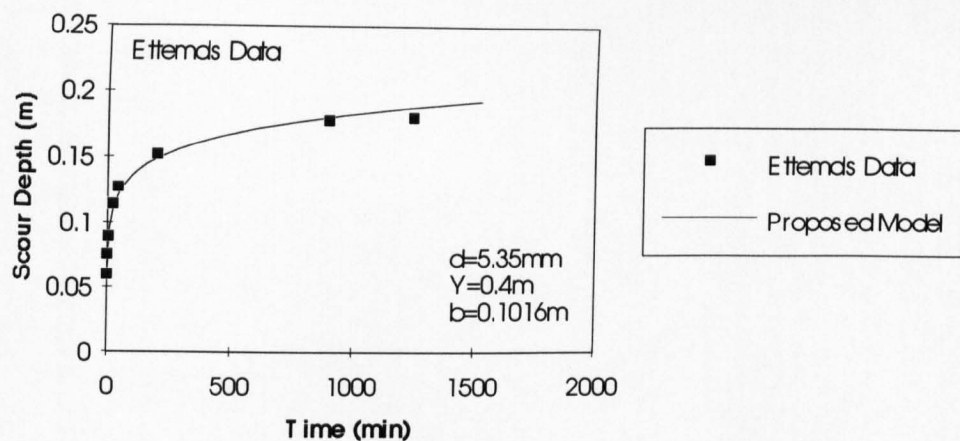
Figure 7.14. The comparison between the temporal variation of scour depth
calculated from the model and the data of Ettema (1980).
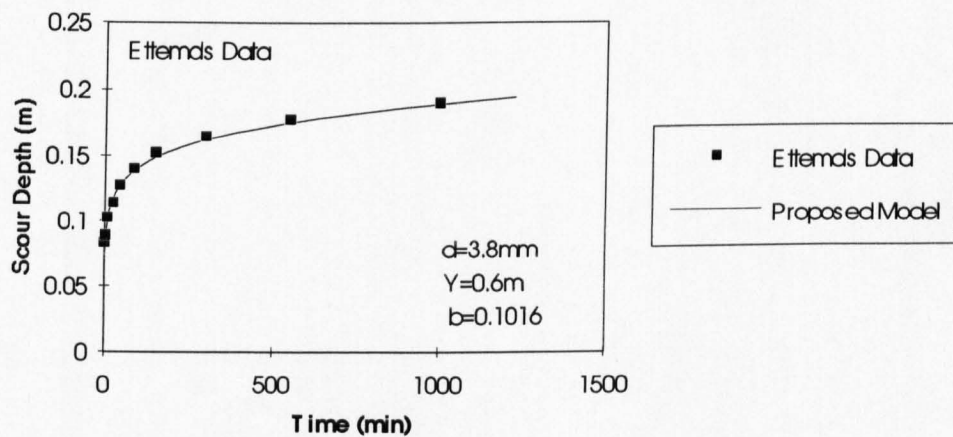
Figure 7.15. The comparison between the temporal variation of scour depth
calculated from the model and the data of Ettema (1980).

Scour Depth with Time
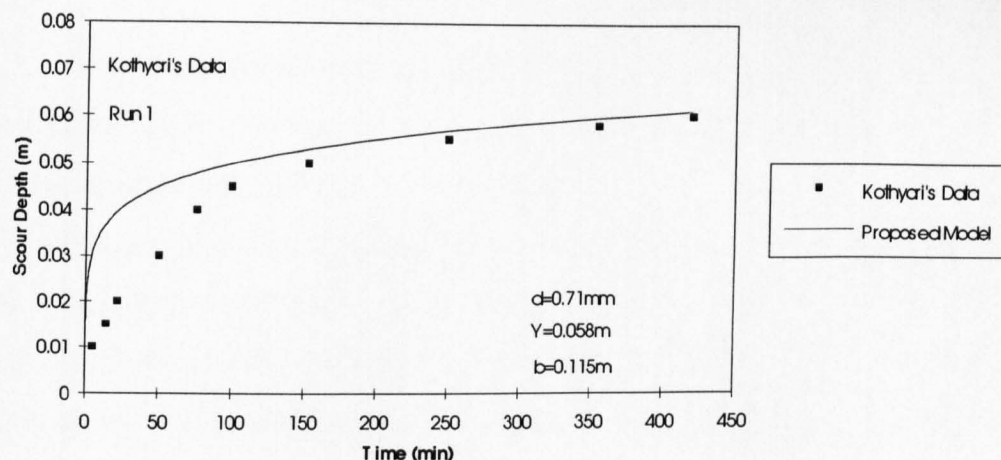
Figure 7.16. The comparison between the temporal variation of scour depth calculated from the model and the data of Kothyari (1989).

Scour Depth with Time
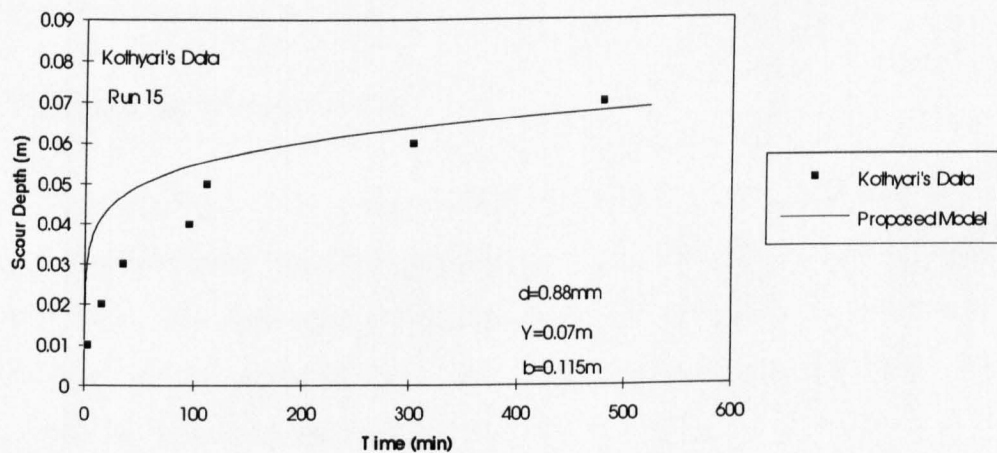
Figure 7.17. The comparison between the temporal variation of scour depth calculated from the model and the data of Kothyari (1989).

7.6.4 Computational steps for live-bed scour

While scour occurs at bridge piers, sediments are fed into the scour hole from upstream. The sediment load entering the scour hole can be computed using an appropriate sediment transport formula.

In order to compute the variation of mean scour depth with time, the sediment load entering in to the scour hole during time t^* was computed using the Engelund-Hansen (1967) sediment transport formula. Hence the net scoured depth at the end of time period t^* is equal to the sediment size minus the deposition due to incoming sediment load.

The temporal variation of scour depth, using the above approach, was compared with the live bed scour data of Chabert and Engeldinger (1956), and Kothyari (1989). Table 7.2 shows the range of data used for comparison with the model of present study. Figs. 7.18 to 7.21 shows the comparison results. The comparison is based on the same data set that has been used for the calibration of the model. A study of the plotted results reveals that the proposed model produces satisfactory results.

7.7 Geometry of scour hole

For blunt nosed piers, the scour hole is in the shape of an inverted cone with a stability angle equal to the angle of repose of the grains. Bonasoundas (1973) found that the shape of the final scour hole, in plan was similar to a semi-circle on the upstream and a semi-ellipse on the downstream face. He expressed the volume of the scour as:

$$V_s = 13b^2 d_s \tag{7.26}$$

where V_s is the volume of scour hole, b is the pier width, and d_s is the scour depth.

Chang (1987) treated the area of scour hole in front of a pier as a semi-circular shape while the area at the back of pier as a semi-elliptic shape. Using dimensional analysis and the data of his study, he proposed the following formula.

$$\frac{A_s}{L^2} = 8.8(\frac{U}{\sqrt{gL}})^{1.36}(\frac{d_{50}}{L})^{-0.36} \tag{7.32}$$

Table 7.2 Range of Experimental Data, and Variables

No	Variable	Range
1	Flow Depth, Y	0.058m-0.6m
2	Flow Velocity, U	0.265m/s-1.18m/s
4	Sediment Size, d_{50}	0.52mm-5.35mm
5	Pier Diameter, b	0.05m-0.17m
6	k_1	4.5
7	k_2	0.32-1.1
8	C_2	0.05

7.7.1 Top width of scour hole

Knowledge of the top width of scour holes at piers and abutments is important in determination of the extent of riprap needed as a scour countermeasure and to determine whether the scour holes overlap or not. If the scour holes overlap at a bridge crossing the local scour holes will not be independent from the influence of adjacent piers or abutments and the holes may be much deeper than predicted by existing formulae.

The top width of a scour hole W_s depends on a number of parameters among them the most important are:

$$W_s = f(d_s, \phi, b_s) \tag{7.33}$$

S cour Depth with T ime
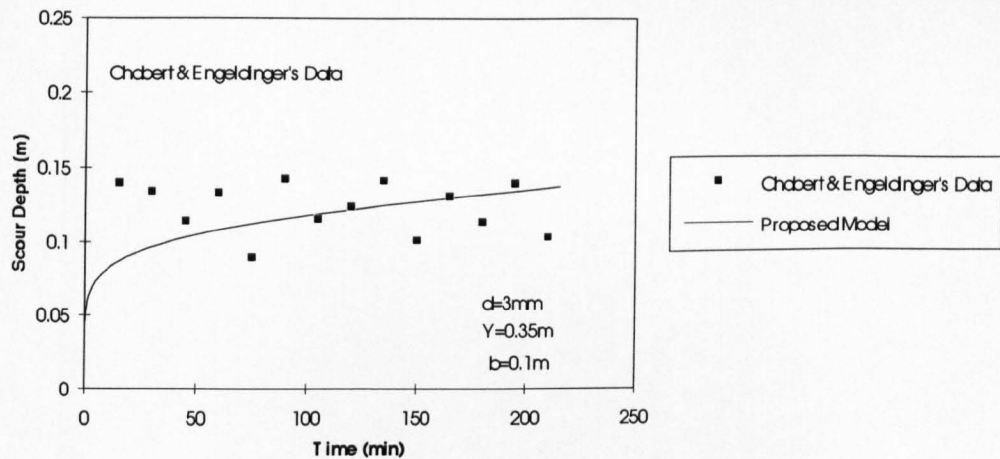
Figure 7.18. The comparison between the temporal variation of scour depth
calculated from the model and the data of Chabert & Engeldinger (1956).

S cour Depth with T ime
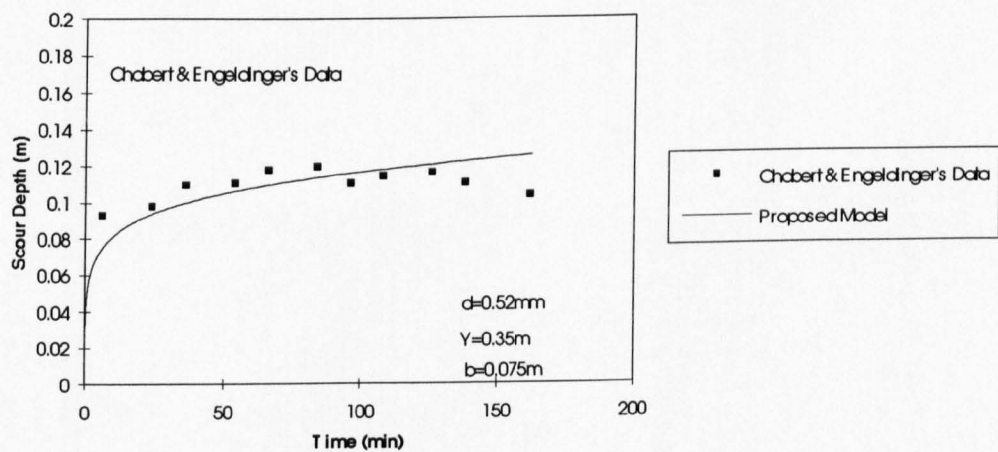
Figure 7.19. The comparison between the temporal variation of scour depth
calculated from the model and the data of Chabert & Engeldinger (1956).
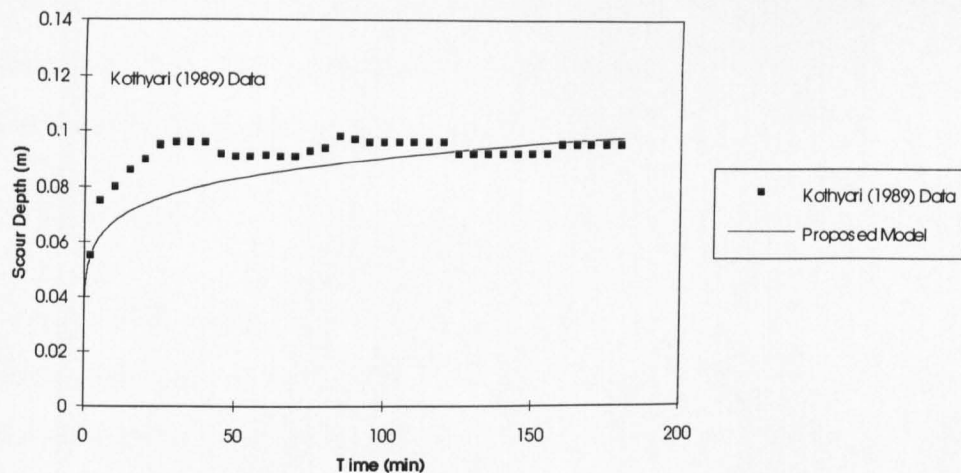
Figure 7.20. The comparison between the temporal variation of scour depth calculated from the model and the data of Kothyari (1989).
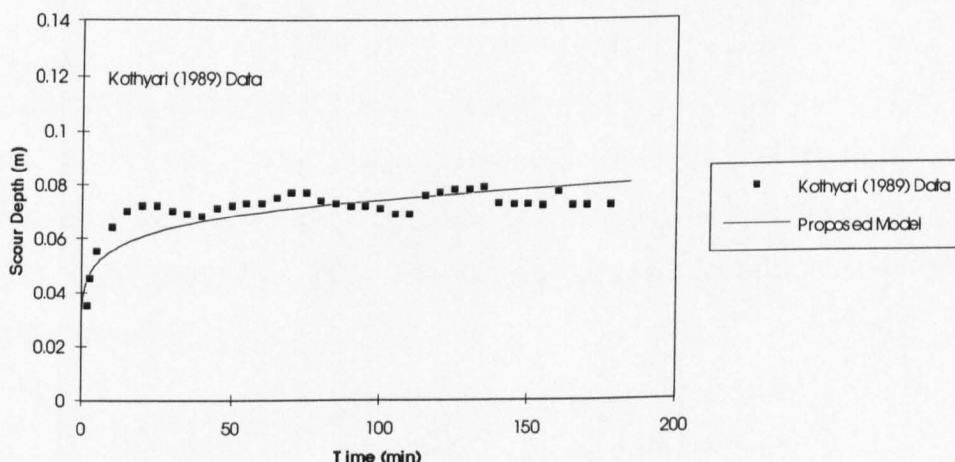
Figure 7.21. The comparison between the temporal variation of scour depth calculated from the model and the data of Kothyari (1989).

where d_s is the scour depth, ϕ is the angle of repose of the bed material, and b_s is the bottom width of the scour hole (See Fig. 7.22).

Richardson et al (1991) stated that the top width of the scour hole measured from the side of a pier could be expressed as follows:

$$W_s = d_s (ACot\phi + B) \tag{7.34}$$

where A and B are constants.

The data of present study with the data of Abed (1991) has been used to determine the top width of scour holes. Fig. 7.23 shows the best fit equation.

$$W_s = 1.36(d_s Cot\phi + b_s) - 0.04 \tag{7.35}$$

Fig 7.24 shows the best fit equation of bottom width b_s, against d_s.

$$b_s = 0.316 d_s - 0.003 \tag{7.36}$$

Combining equations 7.35 and 7.36 gives the final equation.

$$W_s = d_s (1.36Cot\phi + 0.43) - 0.044 \tag{7.37}$$

In the present study, the measured angle of scour holes at upstream of the pier had a mean values of 34.3^o with a standard deviation of 1.3^o. This value is very close to the angle of repose of the material used in the experiments. Therefore, values of the angle of repose of material in the air can be used for calculation of scour hole width.
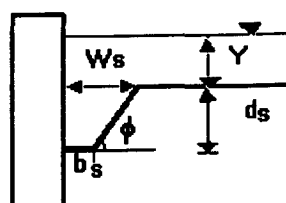
Figure 7.22. Scour hole geometry.

167
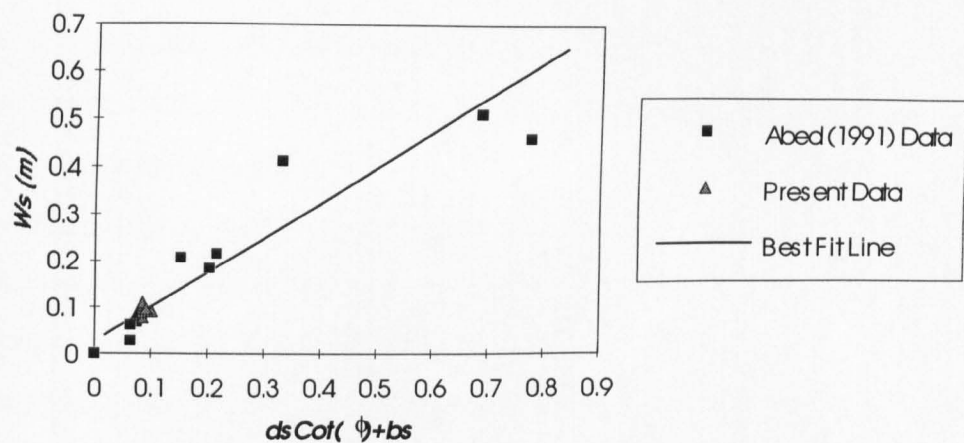
Figure 7.23. Top width of scour hole.
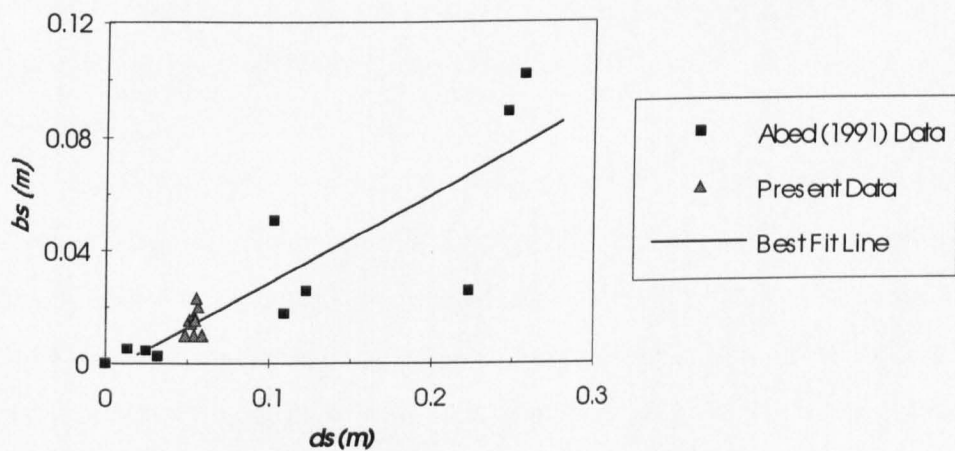
Figure 7.24. Bottom width of scour depth against scour depth.

7.8 Interaction of the channels with piers

After development of stable straight channels, the piers were set up in the channel bed. Necessary precautions were taken, during the introduction of piers into bed, in order not to disturb the bed. This was successfully achieved by using hollow sharp edge cylindrical pipes for the piers. Afterwards, water was introduced gradually up to the same initial value for the development of straight channels. After introduction of the flow, the scour initiated near the piers at approximately 70° to 80° from the stagnation point. Then scouring was extended rapidly on the upstream edge of the scour initiation points until they were extended around the upstream face of the piers. Once the scouring process was initiated, the dominant erosion mechanism for the development of the scour hole was a combination of downflow at the upstream face of the pier and the horseshoe vortex.

Scouring continued under the arms of the horse shoe vortex. While the scour depressions at the sides of the piers deepened, the side slopes developed into the scour hole. The scour hole grow with time under the action of the horseshoe vortex. It increased in diameter and the rate of scouring decreased with time.

Additional sediment was transported by the arms of the horseshoe vortex. As more sediment was eroded from the sides of the piers, a sediment mound formed downstream of the piers. The sediment mound migration and enlargement of downstream cross-section was continuous. In the meantime wake vortices resulting from flow separation at the sides of the piers, aided the erosion process by transporting the scoured particles downstream of the piers.

Although the scouring process did not stop completely, it's intensity reduced considerably after a few hours. When there were no further significant changes of channel shape, around and downstream of the piers, it was accepted that the interaction process has attained an equilibrium condition.

Normally after 7 to 8 hours, the changes in channel shape were insignificant, and the experiments were stopped and the measurements were carried out. Plate 7.1 shows a typical channel with piers at the end of experiment.
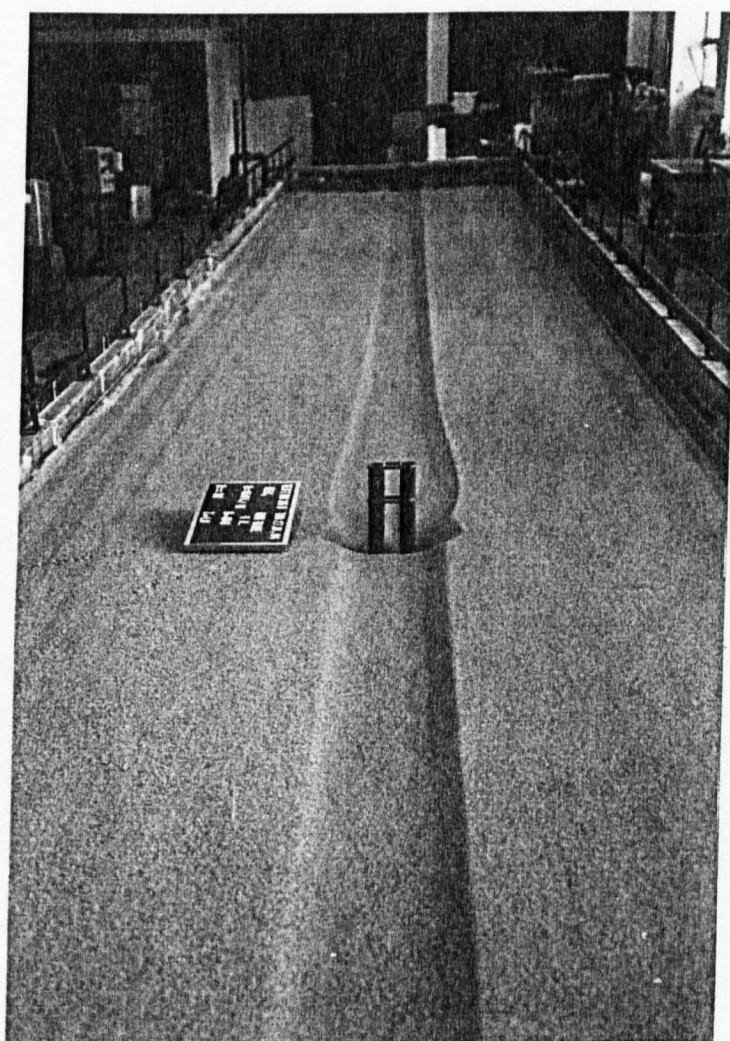
Plate 7.1. Typical channel with piers at the end of experiment.

7.9. Topography of pier scour

The scour pattern caused by introducing bridge piers in the bed of developed straight channels are shown in Figs. 7.25 to 7.30. This pattern shows that the channels are mostly intact upstream of the channel and beyond the upper edge of scour hole.

During the experiments the backwater effect caused by the piers in the upstream part of channel was observed. The upstream depth increased due to backwater effect. Increased depth caused velocity reduction and sediment deposition. During the experiments no abrupt change in channel geometry was observed upstream due to backwater effects. The most abrupt change in channel bed and bank was because of scour hole formation. The scour shape upstream of the pier was semi-circular in plan for a single pier. For pier groups, the plan shape was of interfered semi-circles, see Fig. 7.24. As the pier spacing increase the upstream plan geometry tends toward two individual semi-circle shape. The scour shape upstream of piers was in the shape of an inverted frustum of semi-circle cone with side angle very close to the angle of repose of bed material.
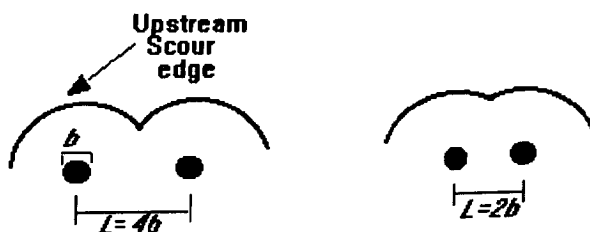
Figure 7.24. Upstream plan geometry of scour hole for pier groups.
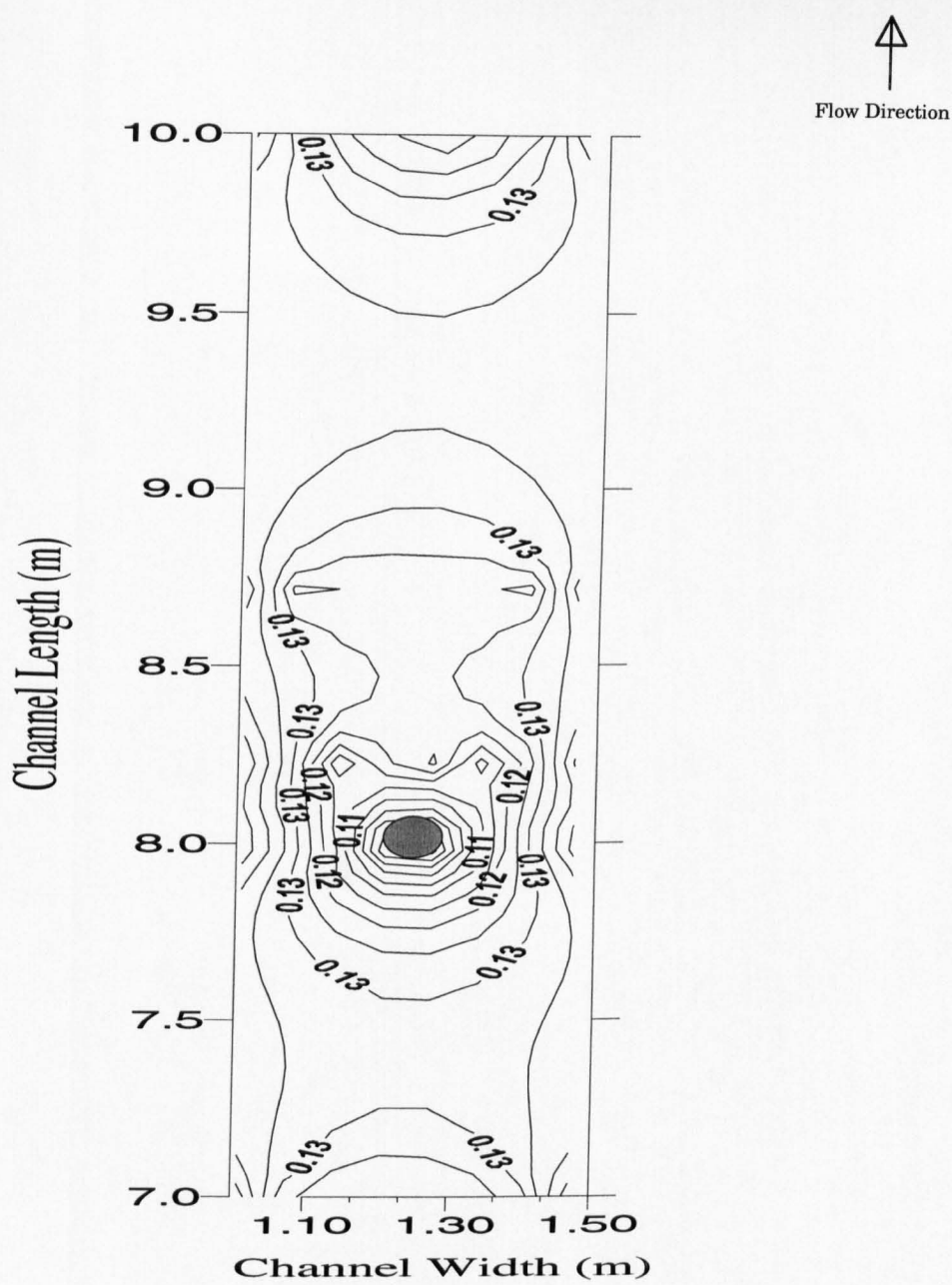
Figure 7.25. Typical scour topography for single pier.
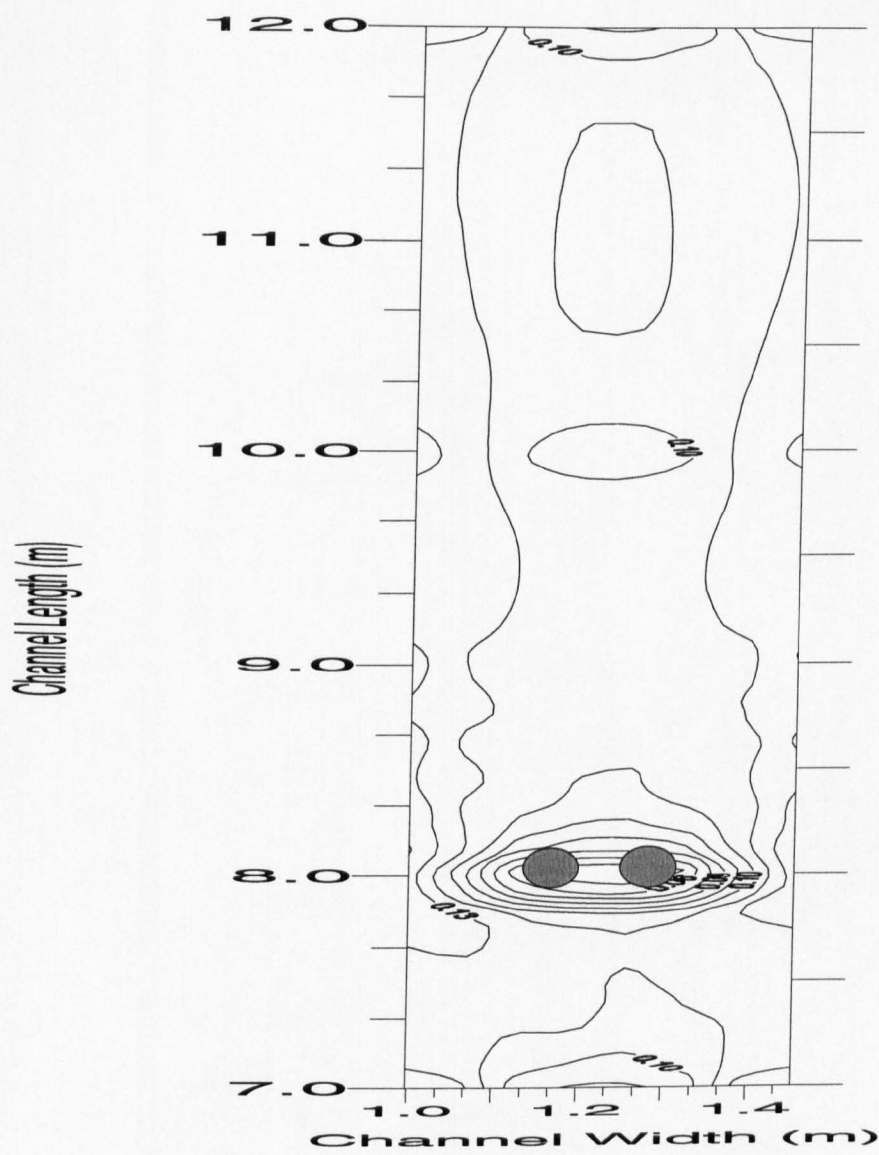
Figure 7.26. Typical scour topography for double piers (L=2b).
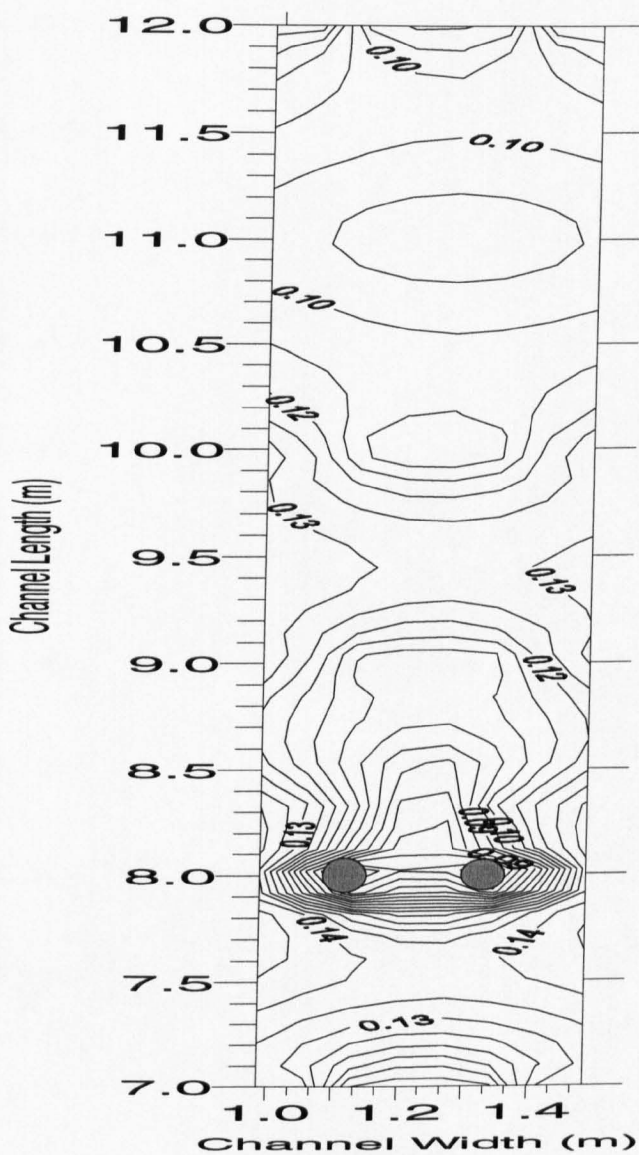
Figure 7.27. Typical scour topography for double piers (L=4b).
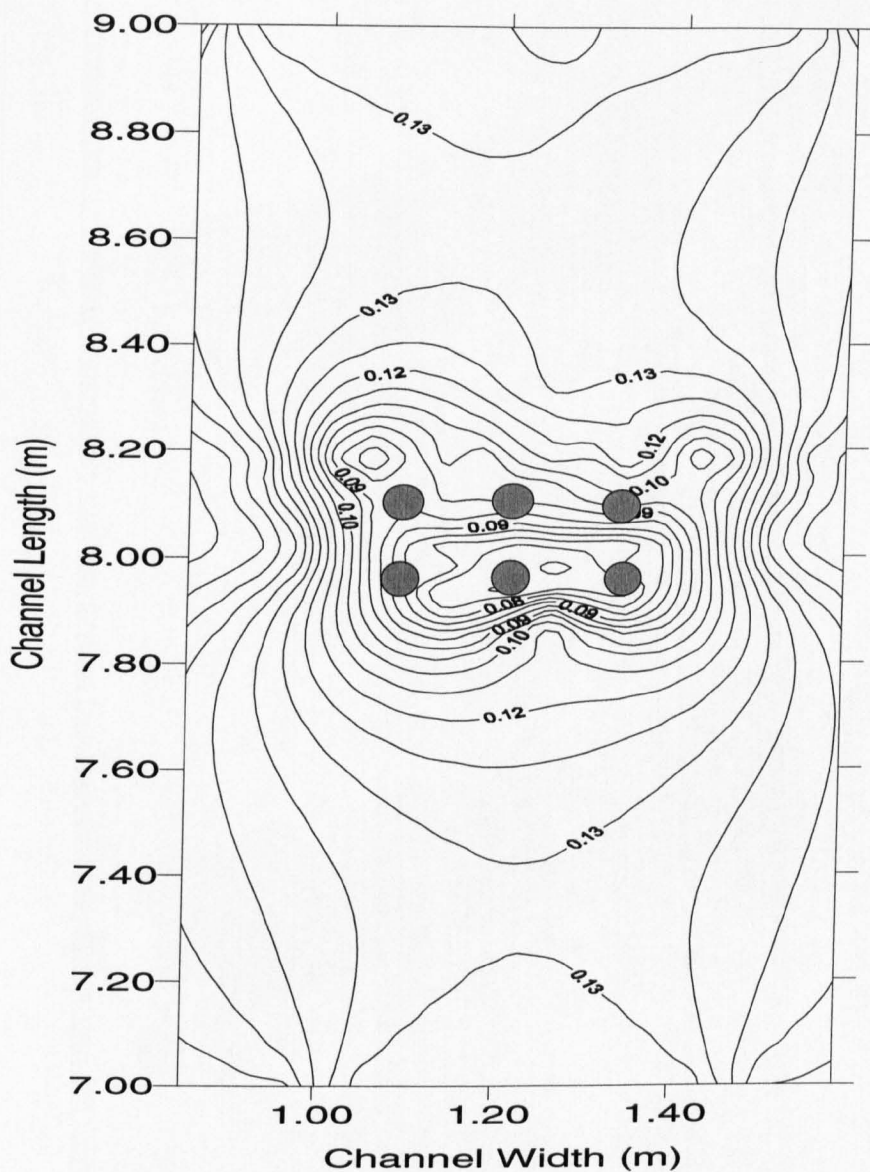
Figure 7.28. Scour topography for group of six piers (L=2b).
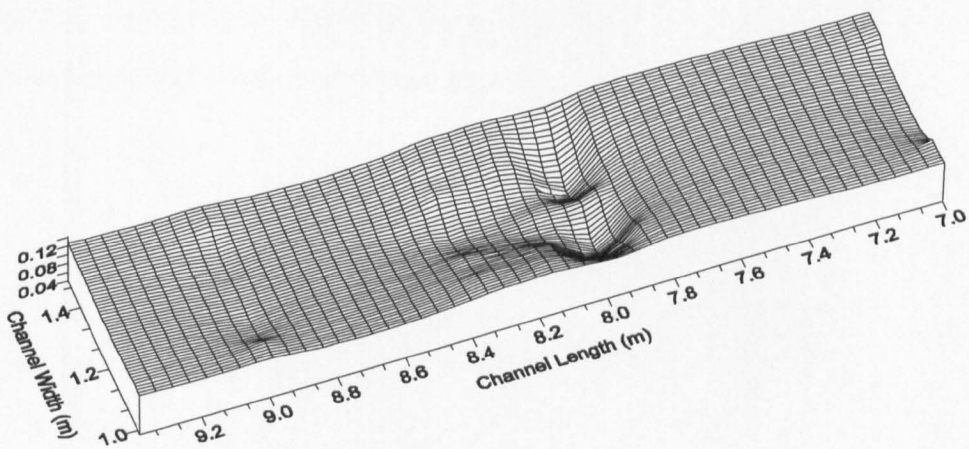
(b)
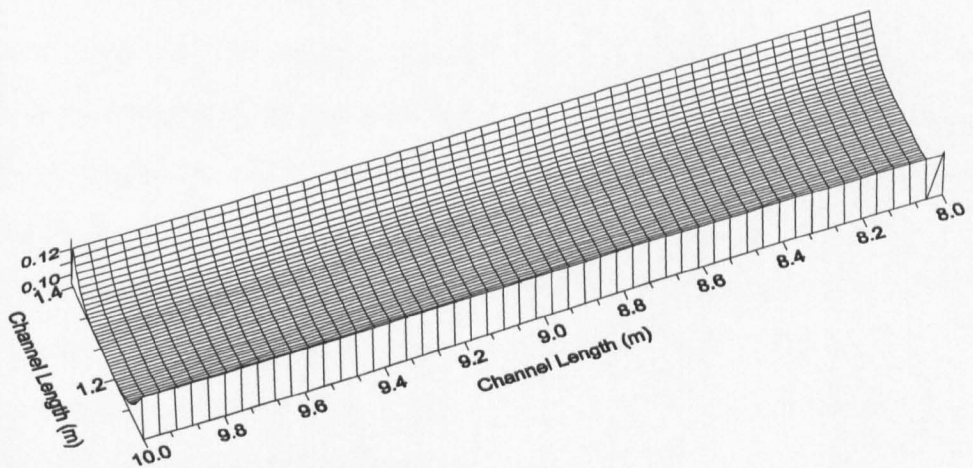
(a)

Figure 7.29. Three dimensional channel demonstration (a) before pier installation (b) after pier installation.

As the channel passes through the centreline of the piers, the scour plan shape is not any longer semi-circular. The cross-section changes to a W shape with rounded edges, where the trough represents the scoured bed and the crest represents deposited material, see Fig. 7.31.
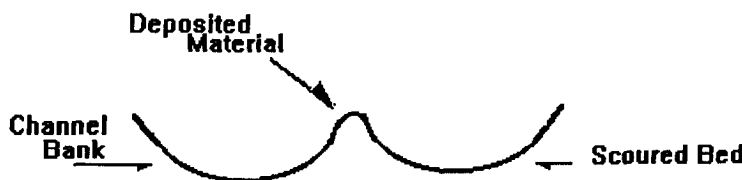
Figure 7.31. Channel downstream cross-section.

For all the experiments an increase in channel width downstream of the piers was observed. This increase in width was a result of scoured materials which were transported downstream by the arms of horseshoe vortex. The channel downstream width increased to a maximum value and decreased afterwards, see Fig. 7.32. In order to relate the downstream width increase to the percent of blockage, the two values were plot against each other. No unique relation was found to relate these two parameters for all cases. However, the trend of variation in data shows that, for single piers, as the percent of blockage increases, the width increase also increases.
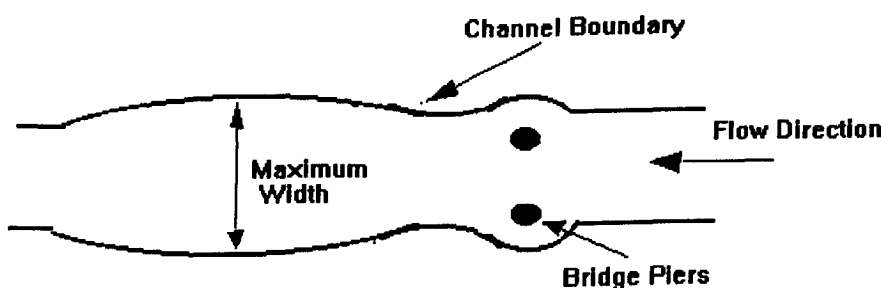
Figure 7.32. Channel boundary plan.

For piers with spacing equal to two pier diameters, the trend of variation seems to follow the same trend as for single piers. For situations that the pier spacing has been equal to four pier diameters, the width increase has been less than 17%. See Fig. A3 in Appendix A.

Time variation of channel width increase downstream of piers has been plotted for a typical case, see Fig. 7.33. The plotted time variation shows that the rate of channel widening is high in the first hour of the experiment. This rate decreases during the progress of the experiment so that after the first two hours the rate of change fell well below 5% per hour. The channel cross-section at the pier centreline has been plotted in Figs. 7.34 and 7.36. The graph shows the changes before and after pier installation. The channel cross-section downstream of piers is also compared for the indicated case in Figs. 7.35 and 7.37.
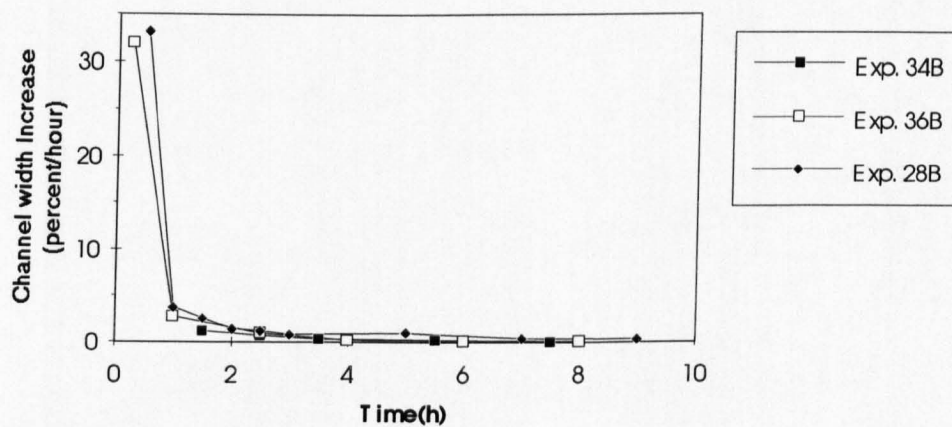
Figure 7.33. Time variant of channel width increase downstream of the piers.

178
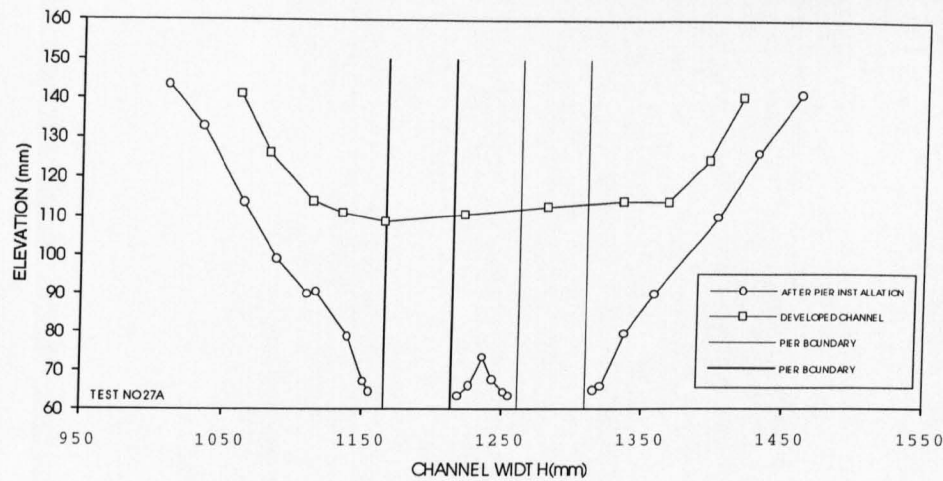
Figure 7.34. Channel cross-section changes at centreline of the piers.
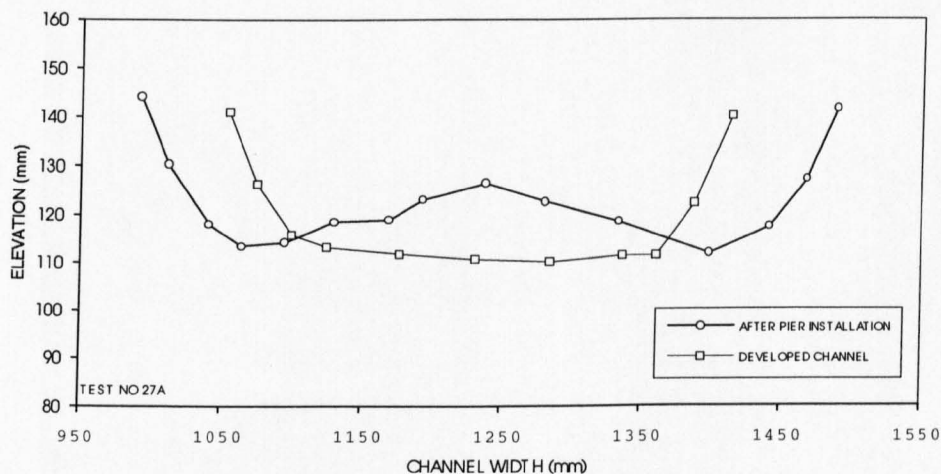
Figure 7.35. Channel cross-section changes downstream of the piers.

179
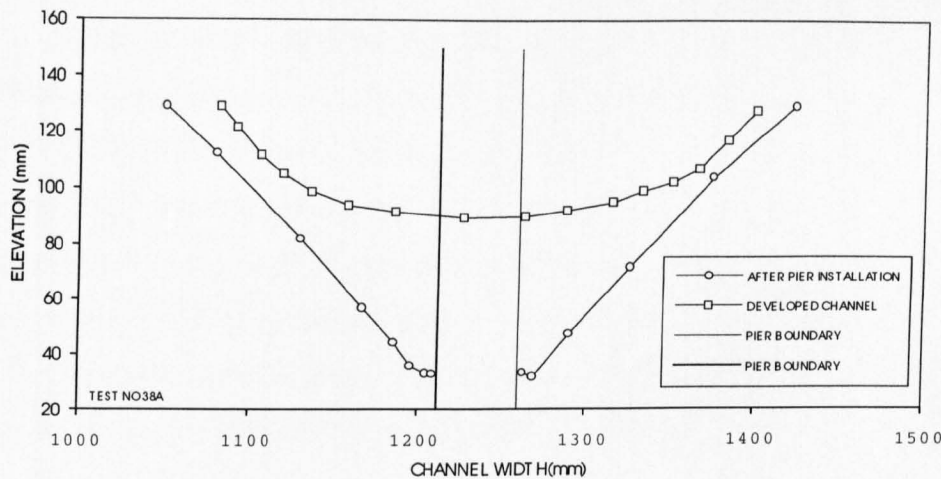
Figure 7.36. Channel cross-section changes at centreline of the piers.
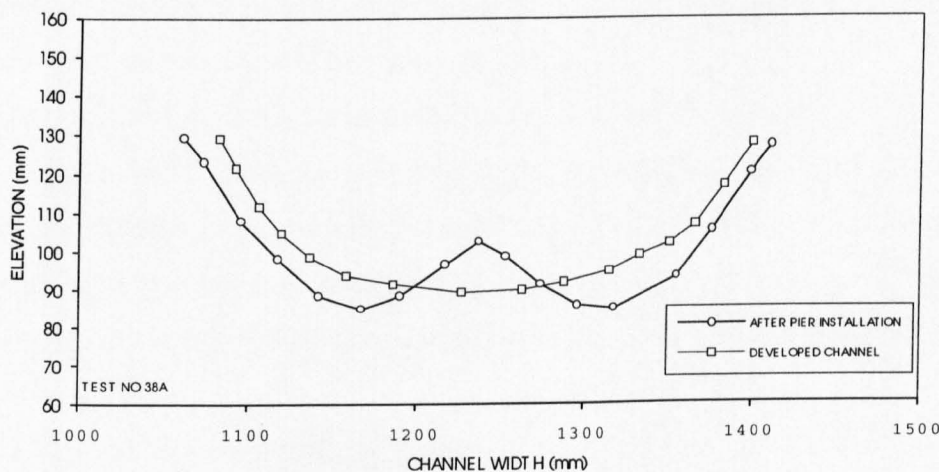
Figure 7.37. Channel cross-section changes downstream of the pier.

7.10. Chapter summary

Experimental data from the present study is compared with recently published equations for scour depth prediction. The comparison reveals that the CSU (1975), Melville and Sutherland (1988), and Gao et. al (1993) equations mostly overpredict the data. The difference is attributed to the fact that these formulae are obtained from experiments carried out in laboratory flumes with fixed walls. The data of present study is obtained from experiments carried out in a flume with mobile banks. This case is closer to the real field situation. Among the equations used for the comparison, the CSU equation predicts the scour depth data of present study more closely.

The effect of pier spacing on scour depth is also considered. A pier spacing coefficient, K_{ps}, has been derived which can be used with scour equations to account for the effect of pier spacing on scour depth.

A mathematical model has been proposed to predict the temporal variations of scour depth in clear water and live bed scour. The computed results of the model have been compared to the available data. The comparison shows that the results are satisfactory for most conditions.

In present investigation, the measured angle of scour holes at the upstream side of the pier had a mean value of 34.3^o with a standard deviation of 1.3^o. This supports the findings of previous research, e.g. Melville (1975) that the angle of scour holes upstream of the pier is close to the angle of repose of the bed material. An equation has been proposed to calculate the top width of scour hole.

Investigation of scour topography due to interactions of piers and developed straight channels reveals that the main abrupt change in channel bed and bank is because of scour hole formation. An increase in channel width downstream of piers is observed, i.e. the width increases to a maximum value and then decreases. The rate of this increase is high in the first hour of the experiments and reduces afterwards.

Chapter Eight
Interaction of Abutments with Laboratory Channels

8.1. Introduction

Scour around abutments has been extensively studied in the past. Several studies of abutment scour have been carried out at Auckland University by Wong (1982), Tey (1984), Kwan (1984,1988), and Kandasamy (1985,1989). These studies employed laboratory flumes which were rectangle in cross-section and had smooth fixed walls. In natural field situations, channels are non rectangle with mobile banks. Also in field situation, overbank flow occurs frequently at the design flow rate and the lateral flow distribution is nonuniform. For these reasons, predictive abutment scour equations from laboratory flume studies tend to estimate excessive abutment scour when these equations are applied to the actual field situation.

The experiments in the present study have been carried out in a regime flume where the experimental conditions are very close to the field situation. It is the aim of this section to consider recently published formulae for abutment scour prediction and test them using the data from this work.

8.2. Previous studies

Liu et al (1961) for the prediction of local equilibrium scour depth in a live bed condition in sand at a vertical wall abutment with no overbank flow when the flow is subcritical developed the following equation.

$$\frac{d_s}{y_o} = 2.15(\frac{a}{y_o})^{0.4} F_r^{0.33} \qquad (8.1)$$

where d_s is the equilibrium depth of scour, y_o is the average upstream flow depth in the main channel, a is the abutment length, and F_r is the upstream Froude number. Liu et al's equation is for a dune bed configuration. Therefore, it is recommended, for a dune bed configuration in the natural stream the scour given by their equation are for equilibrium scour and for maximum scour the values must be increased by 30%. For plane bed and antidune flow there is no equation given, but it is suggested that Liu et al's equation could be used as given unless the antidunes would be occurring at the abutment. If antidunes exist or there is the possibility that they might break at the abutment then the scour depth given by their equation may be increased by 20%.

Laursen (1980), considering the relative magnitude of the bed shear stresses to the critical shear stress for the bed material of the stream, suggested the following relationship for live bed scour at vertical abutments.

$$\frac{a}{y_o} = 2.75\frac{d_s}{y_o}[(\frac{d_s}{11.5y_o}+1)^{1.7} - 1.0] \qquad (8.2)$$

which in a simplified form is:

$$\frac{d_s}{y_o} = 1.5(\frac{a}{y_o})^{0.48} \qquad (8.3)$$

Scour values given by Laursen's equations are for vertical wall abutments. He suggested the following multiplying factors for other abutment types for small encroachment lengths.

Abutment Type	Multiplying Factor
45 degree wing wall	0.9
Spill-through	0.8

The Laursen's equations are based on sediment transport relations. They predict maximum scour and include contraction scour. It is recommended that the maximum value of the $\frac{d_s}{y_o}$ ratio in the equation be taken as 4.0 because his equations are open ended and field observations admitted that scour never exceed $4y_o$.

Froehlich (1989) analysed 170 live-bed scour measurements in laboratory flumes and obtained the following scour prediction equation.

$$\frac{d_s}{y_o} = 2.27 K_1 K_2 (\frac{a'}{y_o})^{0.43} F_r^{0.61} + 1.0 \qquad (8.4)$$

where d_s is the scour depth, y_o is the flow depth at abutment, K_1 is the shape coefficient of abutment, K_2 is the skewness coefficient of abutment, a' is the length of abutment projected normal to flow, F_r is the Froude number of flow upstream of abutment.

Abutment Type	K_1
Vertical Abutment	1.0
Vertical Abutment with wing walls	0.82
Spill-through Abutment	0.55

Angle of Abutment and flow	K_2
90	1.0
60	0.95
30	0.87

Melville (1992) quoted a large number of experimental data on abutment scour and proposed a design method for maximum scour depth. His method which depends on empirical correction factors for abutment shape, alignment and length, and flow depth, classifies abutments as short or long. According to the method, the equilibrium scour depth, d_s, at an abutment can be written as:

$$d_s = 2K_s L \qquad\qquad \frac{L}{y} < 1 \qquad\qquad (8.5)$$

$$d_s = 2K_s^* K_\theta^* (yL)^{0.5} \qquad\qquad 1 \le \frac{L}{y} \le 25 \qquad\qquad (8.6)$$

$$d_s = 10K_\theta y \qquad\qquad \frac{L}{y} > 25 \qquad\qquad (8.7)$$

where L is the length of abutment perpendicular to the flow, K_S is the abutment shape factor, y is the flow depth, K_θ is the abutment alignment factor. The values of K_s^*, and K_θ^* are given as follows.

$$K_s^* = K_s \qquad\qquad \frac{L}{y} \le 10 \qquad\qquad (8.8)$$

$$K_s^* = K_s + (1 - K_s)(0.0667\frac{L}{y} - 0.667) \qquad 10 < \frac{L}{y} < 25 \qquad\qquad (8.9)$$

$$K_s^* = 1 \qquad\qquad \frac{L}{y} \ge 25 \qquad\qquad (8.10)$$

The shape factor values, K_S, given in the following table.

Abutment Shape	K_S
Vertical plate, narrow vertical wall	1.0
Vertical wall with semicircular end	0.75
45° wing wall	0.75
Spill-through (H:V) : (0.5:1)	0.6
(1:1)	0.5
(1.5:1)	0.45

$$K_\theta^* = K_\theta \qquad\qquad \frac{L}{y} \geq 3 \qquad\qquad (8.11)$$

$$K_\theta^* = K_\theta + (1 - K_\theta)(1.5 - 0.5\frac{L}{y}) \qquad\qquad 1 < \frac{L}{y} < 3 \qquad\qquad (8.12)$$

$$K_\theta^* = 1 \qquad\qquad \frac{L}{y} \leq 1 \qquad\qquad (8.13)$$

Palaviccini (1993) presented a model to predict local abutment scour. His model is based on a large number of laboratory experiments over the past half century. The predictor model is based on dimensionless ratios whose coefficients are determined using least squares regression analysis and nonlinear optimisation.

In his method, the determination of both clear water or live bed approach conditions use Kilgore, et al. (1993) relationship for incipient motion. It is as follows:

$$\theta = 88.05 - 4.37F^2 \qquad\qquad (8.14)$$

where $\theta = \text{Arctan}(1/S)$, F is the approach flow Froude number, and S is the Shields' number $= \dfrac{S_f y}{(s-1)d_{50}}$.

The local abutment scour prediction model for $F<1$ is:

$$\frac{(y+d_s)}{y_e} = 1.23 F^{2.06} X^{0.78} M^{-2.65} \tag{8.15}$$

where M is the conveyance ratio, $X = \dfrac{(y^\alpha w^\beta)}{x^{\alpha+\beta}}$, for the live bed condition $x = d_{50}$, $\alpha = 0.74$, $\beta = 0.07$ and for the clear water condition $x = d_{84}$, $\alpha = 0.77$, $\beta = 0.15$. w is the width of the abutment/embankment in the flow direction.

Palaviccini (1993) claimed that the abutment model is operational for $F<1$ and statistically superior to and more realistic than other published models. He also concluded that the model should be checked with prototype scale data.

8.3. Contraction Scour

This kind of scour can result from a contraction of the flow or change in downstream control of the water surface elevation. It occurs when the flow area of a stream is decreased from normal, either by a natural contraction, or by a bridge or abutment. With decrease in flow area, there is an increase in average velocity and bed shear stress through the contraction. Hence, there is an increase in erosive forces in the contraction and more bed material is removed from the contracted reach than is transported in to the reach. This results in lowering the natural bed elevation which is called contraction scour.

Contraction scour equations basically are derived by using the principle of sediment transport conservation i.e. the fully developed scour in the bridge cross-section reaches equilibrium when sediment transported into the contracted section equals sediment transported out in a live bed scour situation.

Laursen (1960) derived a live bed contraction scour equation based on his simplified transport function and several other simplifying assumption. His equation where there is no over bank flow and the main channel narrows either naturally or due to the bridge piers or the abutment obstructing part of the main channel are recommended in the following form by Richardson et al (1991).

$$\frac{y_2}{y_1} = (\frac{W_{c_1}}{W_{c_2}})^{K_1}$$

(8.16)

where y_1 is the average depth in the main channel, y_2 is the average depth in the contracted section, W_{c_1} is the bottom width of the main channel, W_{c_2} is the bottom width of the contracted section, and K_1 is a factor depends on the mode of bed material transport. This factor is 0.59 when the material in transport mostly are bed material.

8.4. Data Comparison

The data obtained from the present study are compared with previously introduced methods for local scour prediction at abutments. The values of contraction scour are calculated using the Laursen (1960) equation. The comparison with Liu et al (1961) shows that the equation mostly overpredicts the scour depth. Fig 8.1 shows the comparison results. This may be due to the fact that Liu et al's experiments were made in a rectangular laboratory flume with a sand bed and they did not represent many of the conditions in the field.

The relation which Laursen (1980) recommended for scour depth prediction is also compared with the data in Fig. 8.2. This equation overpredicts the scour depth used for comparison. The Froehlich (1988) live bed scour formula is tested in Fig. 8.3. The results show that the method overpredicts the scour depth. This is due to the fact that the Froehlich's equation includes a safety factor which makes the prediction of scour depth greater than the measured value.

The data comparison with Melville (1992) design method is shown in Fig. 8.4. It shows that the method overpredicts the scour depth. The Palaviccini (1993) predictor model is compared with the data in Fig. 8.5. From the equations compared with the data of present study, the Laursen (1980) equation gives the best prediction. The difference is attributed to the fact that all of the formulae are based on experimental data where the experiments have been carried out in laboratory flumes. In laboratory flumes, the approaching flow is essentially uniform, having a transverse velocity profile which is nearly the same at all locations across the flume. In contrast, in a "regime" flume, where the present experiments were carried out, abutments intercept flow on the banks where flow is not uniformly distributed. In a standard laboratory flume, scour occurs at the end of the abutment. This is, in part, due to contracted flow and subsequent increased flow velocity. It is also due to the forced flow returning to the opening in the vicinity of the abutment end. However in a "regime" flume, the flow may return to the channel in a less concentrated manner. When this occurs the magnitude of the turbulent eddies and vortexes generated by the converging flow at the abutment is diminished, reducing the erosive velocities and turbulence which cause local scour.
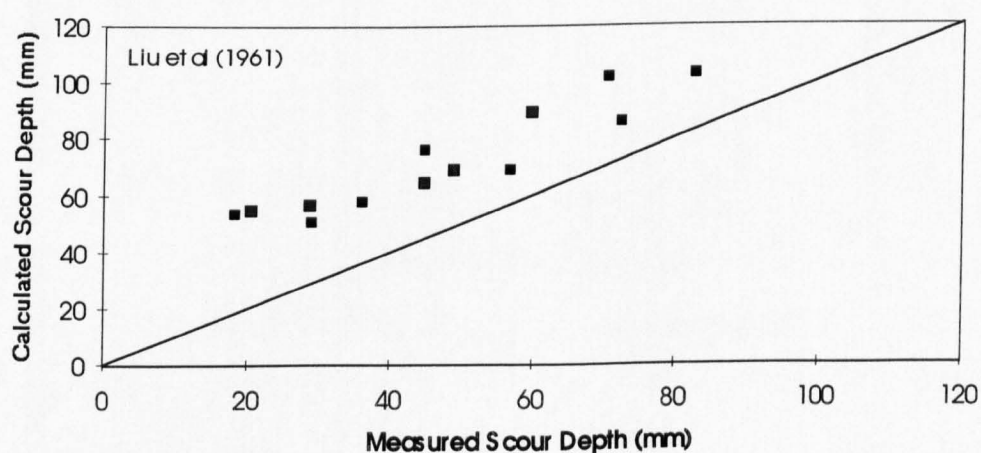
Figure 8.1. Data comparison with Liu et al (1961) equation.

189
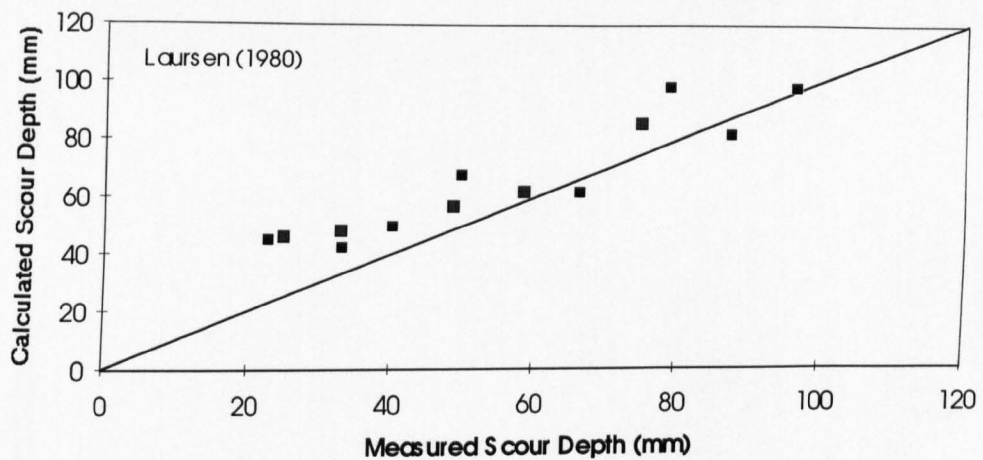
Figure 8.2. Data comparison with Laursen (1980) equation.
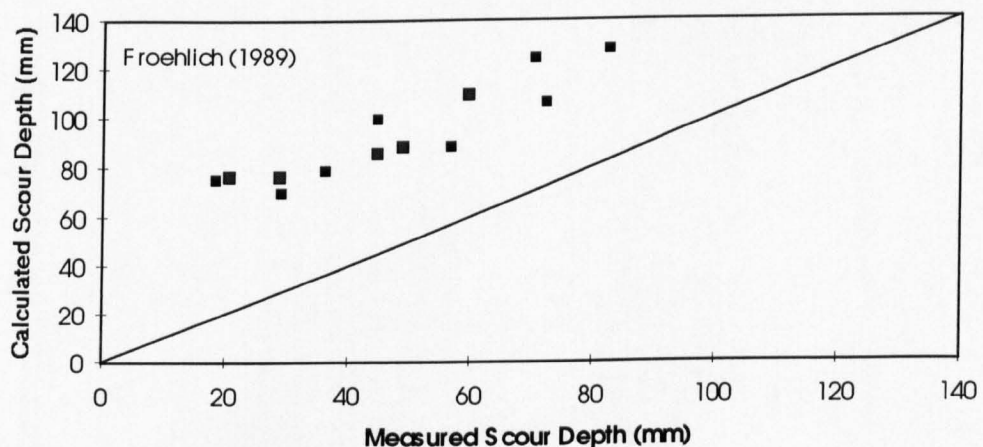
Figure 8.3. Data comparison with Froehlich (1988) equation.
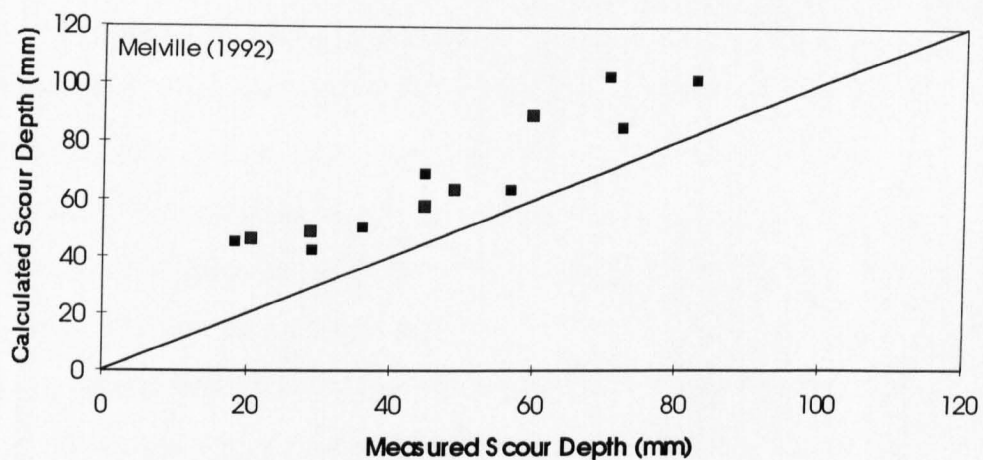
Figure 8.4. Data comparison with Melville (1992) equation.
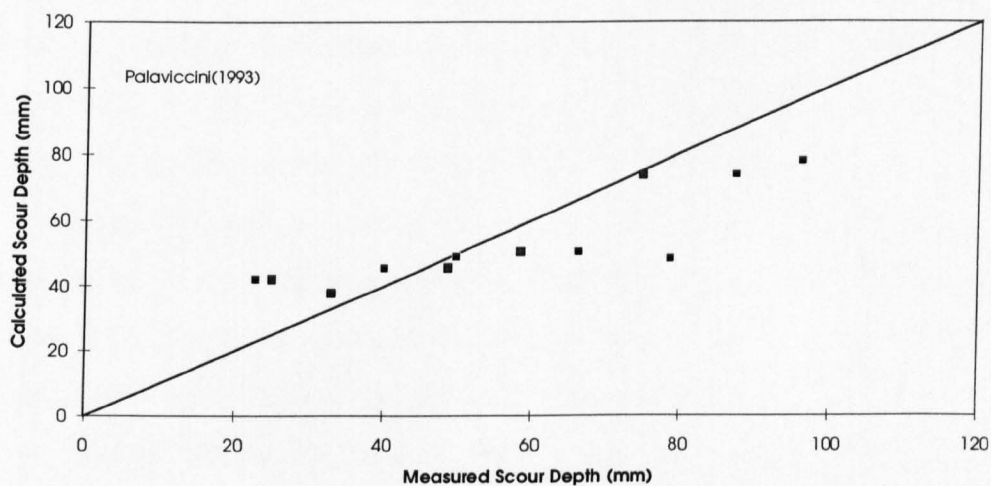
Figure 8.5. Data comparison with Palaviccini (1993) equation.

8.5 Interaction of the channels with the abutments

For series C of the experiments, the abutments were set up in the channel bed. Necessary precautions were taken, during the introduction of abutments into bed, in order not to disturb the bed. This was successfully achieved by using hollow sharp edge abutments with vertical wall. Water was then introduced gradually up to the required value. After introduction of water, the flow was deviated around the abutment leading to an increase in the velocity of the flow in the vicinity of abutment head and a higher bed shear stress. The scour was initiated at abutment head and was developed rapidly on the face of the abutment. Soon after the initial phase of scour, the downflow and primary vortex was formed. The vortex action became increasingly more dominant in eroding and extending the boundaries of the scour hole as the scour hole developed. Fig. 8.6 shows section view of the primary vortex.

Sediments were transported and piled up near the downstream lip of the hole. The piled sediment progressively pushed further downstream as the scour processed, resulting in enlargement of downstream cross section. The wake vortices resulted from flow separation at the abutment head aided scour process by entraining and transporting the scour material downstream of abutment.

As the flow was diverted around the abutment head, a region of slowly circulating water ahead of the abutment and adjacent to the channel bank was formed. This circulating water, which is referred as "dead water region", continuously scoured the channel bank as the experiment was progressing.

Although the scouring process did not seem to cease completely, it's intensity reduced considerably after a few hours. When there was no significant changes of channel shape, around the abutment, it was accepted that the interaction process has attained an equilibrium condition. Afterwards the experiment was stopped and the bed level measurements were carried out. Plate 8.1 shows a typical channel with abutment at the end of experiment.

Wake vortex

abutment

Dead
region

Primary
vortex

Channel
bank

Flow

(a)

Abutment

Primary
vortex

channel bed
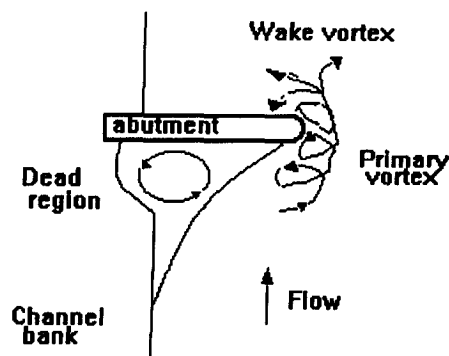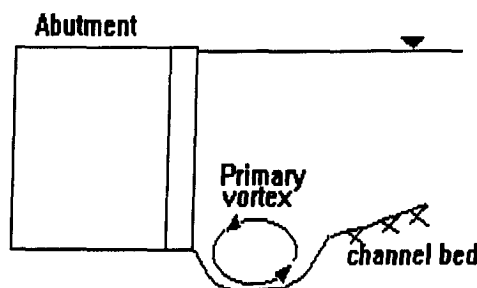
(b)

Figure 8.6. (a) Plan view of abutment showing the dead water region (b) Section view of the principal
vortex.
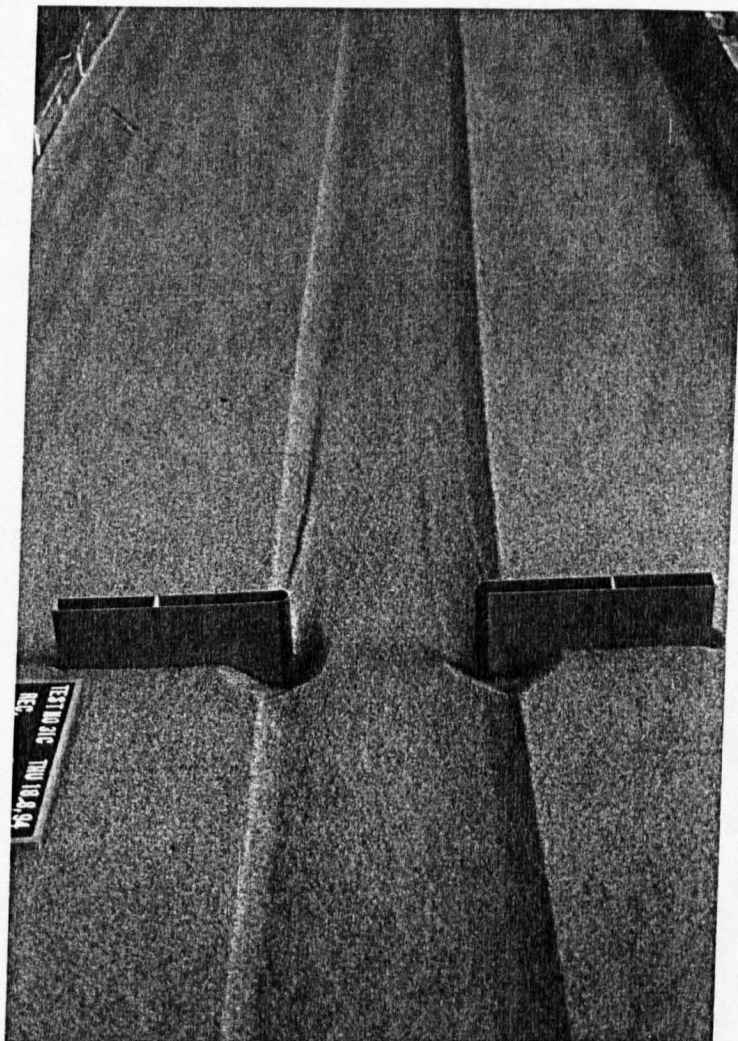
Plate 8.1. Typical channel with abutment at the end of experiment.

194

8.6. Topography of abutment scour

The scour topography caused by introducing abutments in the bed of developed straight channels are shown in Figs. 8.8 to 8.10. The topography shows that the channels are mostly intact upstream of the channel except in the area close to the abutment. The main change in channel bed and bank is because of local scour hole formation. The channel bank upstream of the abutments were mainly scoured because of slowly circulating water ahead of them. This circulating water which forms adjacent to the channel wall is referred to as the dead water region. See Fig. 8.7.
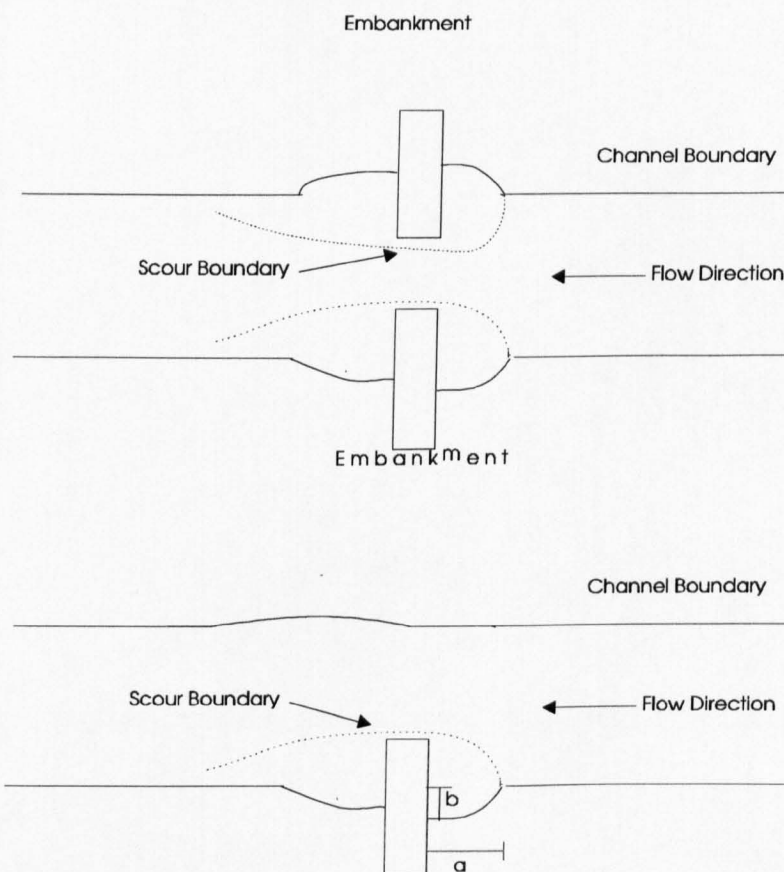
Figure 8.7. Channel boundary plan.
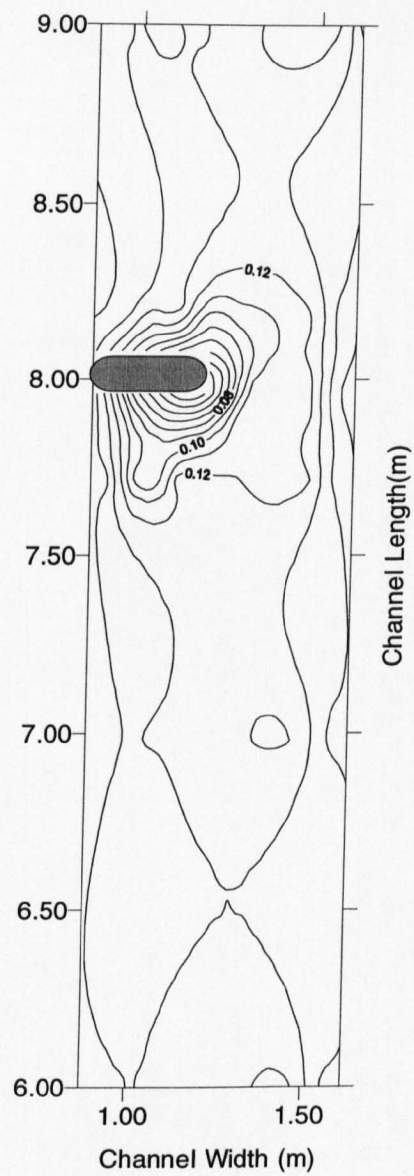
Figure 8.8. Typical scour topography for abutment at one side of channel.
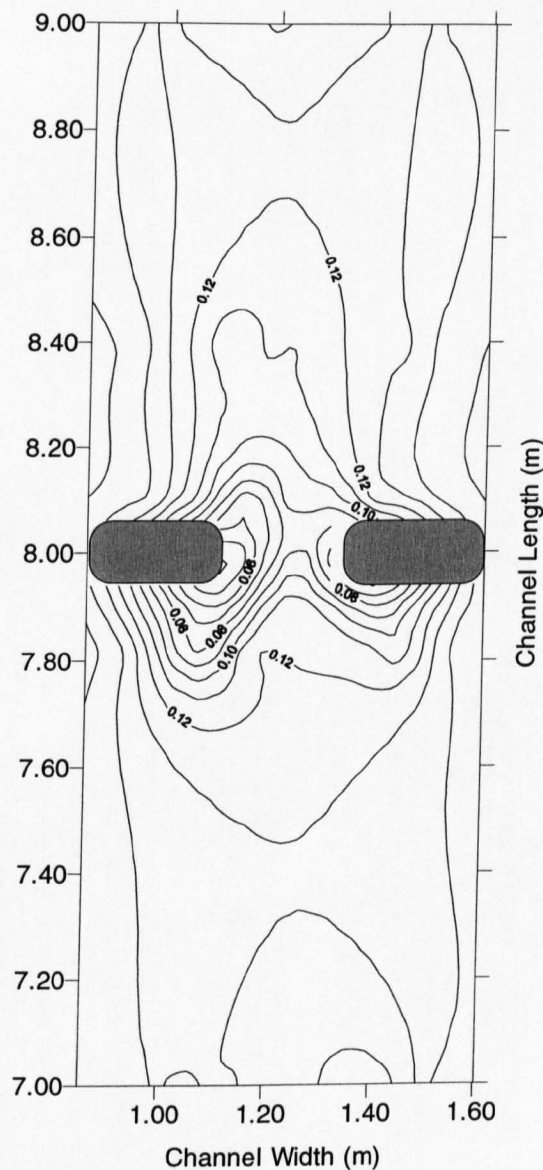
Figure 8.9. Typical scour topography for abutment at both sides of channel.
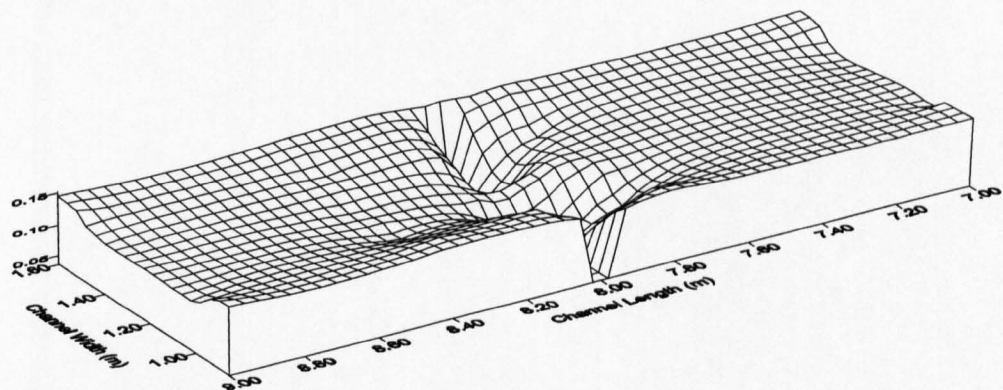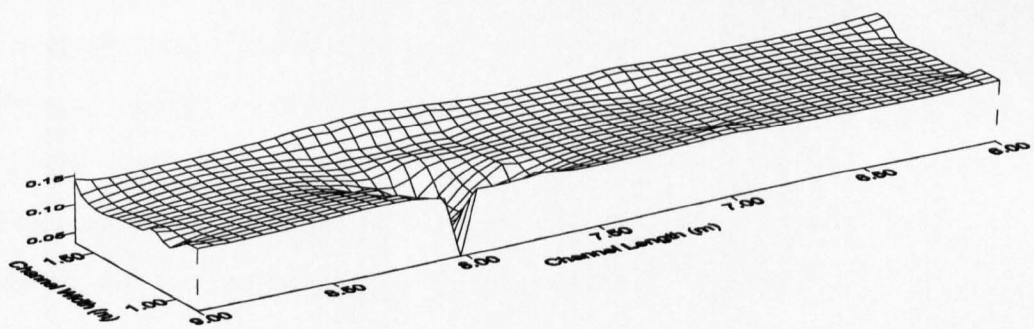
Figure 8.10. Three dimensional channel demonstration for (a) abutment one side (b) abutment both sides of the channel.

In order to measure the scoured bank region ahead of abutment two length parameters, e.g. a and b, have been used, see Fig. 8.7. The values of a was in the range of $2b < a < 3b$. The variation of b is plotted against abutment length, L, and flow depth, y_o in Fig 8.11. The plotted values shows as the dimensionless abutment length increases the value of b/y_o also increases. The best fit line of the indicated variation is shown by equation 8.15. The bank downstream of abutment was also scoured as the flow was diverted around the abutment head. Figs. 8.12 to 8.17 show typical channel cross-sections at abutment centreline and downstream of abutment for cases of abutment at one side and two sides of channel.

$$\frac{L}{y_o} = 1.1105(\frac{b}{y_0}) - 1.008 \tag{8.17}$$
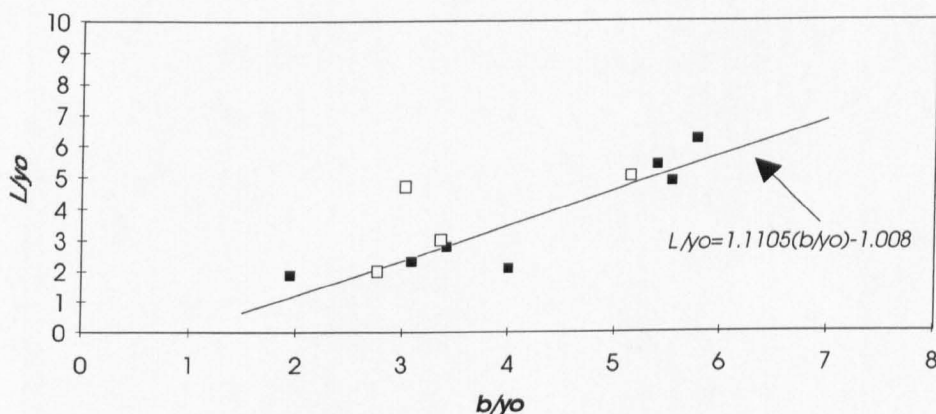
Figure 8.11. Variation of L/yo against b/yo.
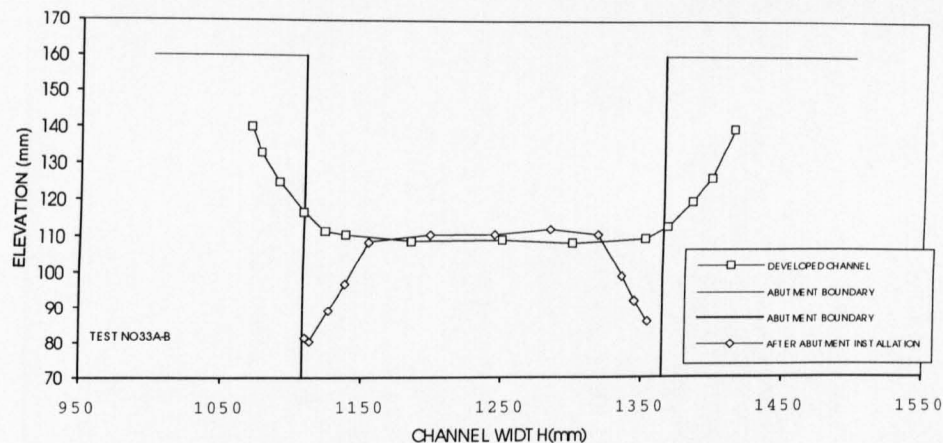
Figure 8.12. Channel cross-section changes at abutment centreline.
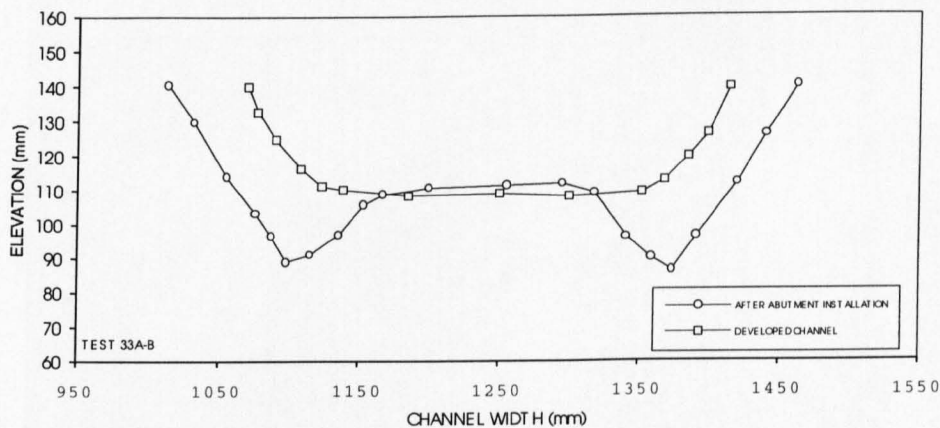
Figure 8.13. Channel cross-section changes downstream of abutment.
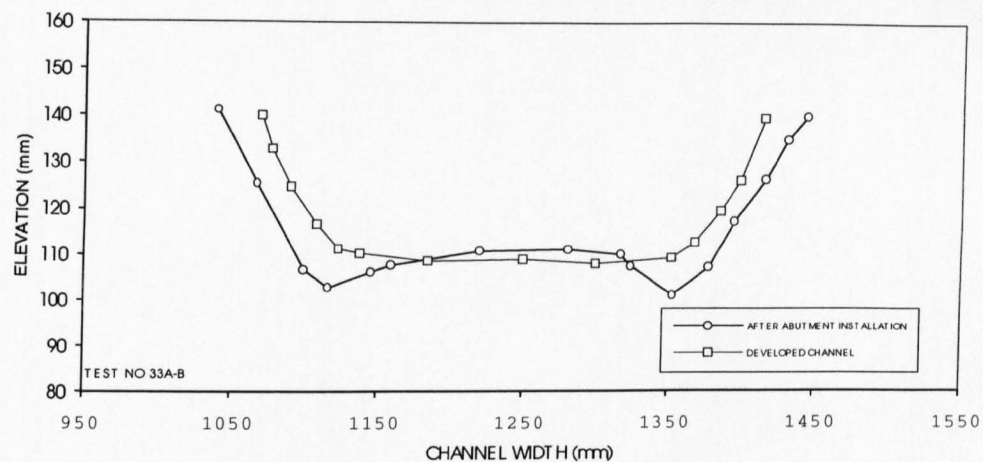
Figure 8.14. Channel cross-section changes downstream of abutment.

CHANNEL CROSS SECTION CHANGES AT SECTION NO 8
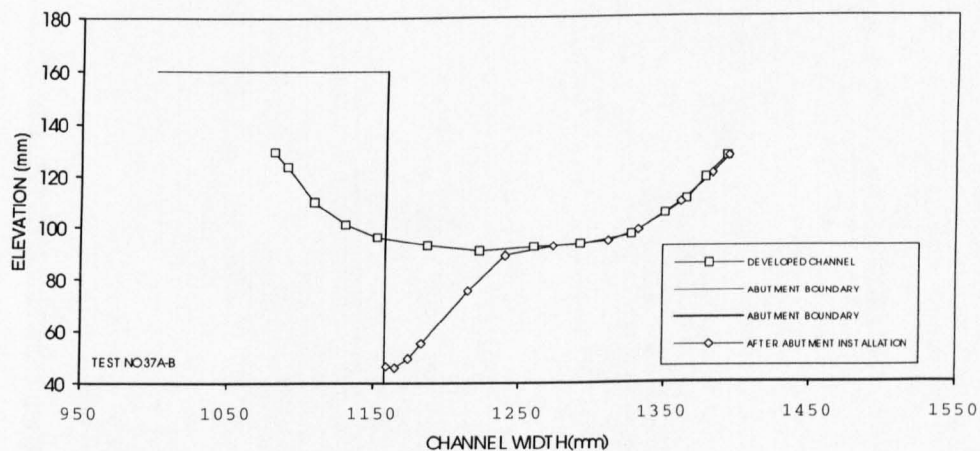
Figure 8.15. Channel cross-section changes at abutment centreline.
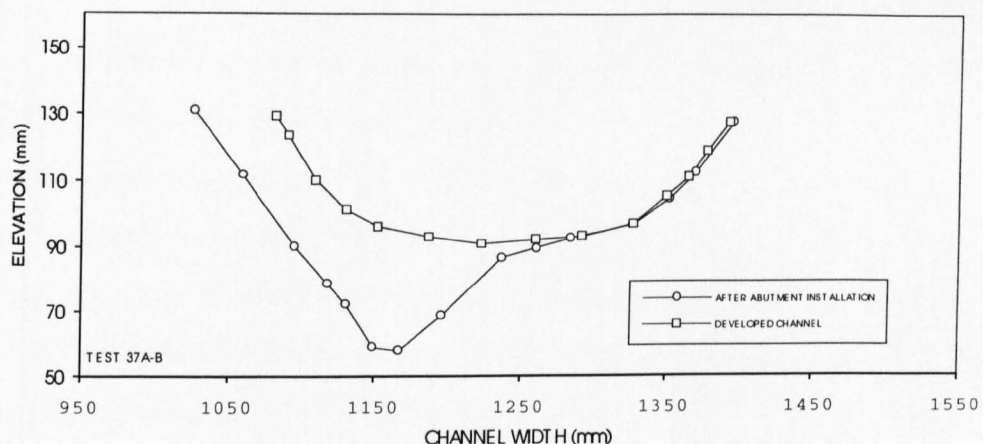
Figure 8.16. Channel cross-section changes downstream of abutment.

CHANNEL CROSS SECTION CHANGES AT SECTION NO 8.48
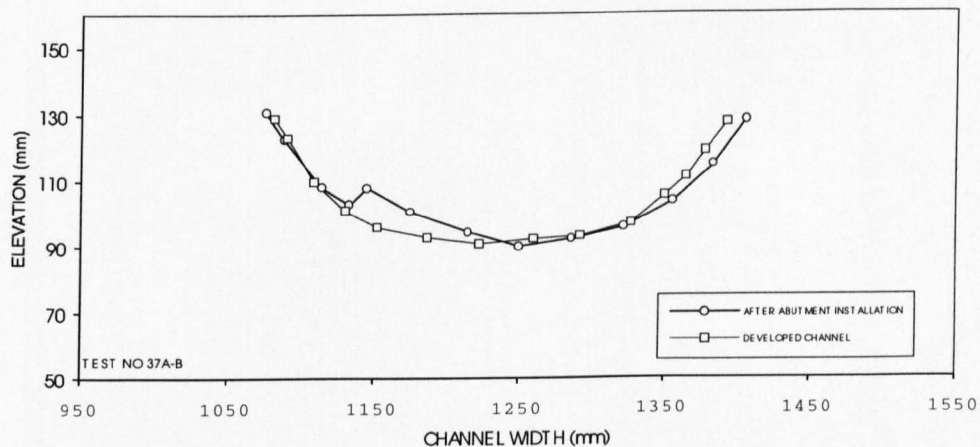
Figure 8.17. Channel cross-section changes downstream of abutment.

8.7. Chapter summary

Experimental data is compared with recommended equations in the FHWA Hydraulic Engineering Circular No. 18 (HEC-18)(1991), Melville's (1992) design method, and Palaviccini (1993). All the equations appear to overpredict the scour depth. The reason is due to the fact that these equations are mostly based on the physical model studies in laboratory flumes. The data of present study is obtained from experiments carried out in a regime flume. The latter is more close to the real field situation.

From the comparison, the equations that predict the data most closely are Laursen's (1980), and Palaviccini's (1993) equation respectively.

Scour topography due to interaction of abutments and developed straight channels has also been demonstrated and described. This reveals that the main change in channel bed and bank is because of abutment local scour hole formation. The channel bank upstream of the abutment was mainly scoured because of slowly circulating water ahead of the abutment. An equation is proposed to calculate the scoured bank region ahead of abutment.

Chapter Nine
Conclusions and Recommendations for Future Work

9.1 Summary

This study was primarily intended to examine the development of self-formed straight channels in the laboratory and the effect of introduced hydraulic structures, e.g. bridge piers or abutments to the beds of these channels. An experimental study has been carried out to achieve the aim. Three groups A, B, and C of experiments were designed and carried out.

The first series, i.e. series A of these experiments, was designed to develop straight stable channels in the laboratory. The results of this series of experiments have been used to investigate the geometrical characteristics of straight stable channels. The recorded laboratory data have also been used to investigate the ability of the White, Paris, and Bettess (WPB) theory to predict the geometry of these channels.

Series B was designed to test the interaction between straight stable channels and bridge piers. In this series of experiments the developed straight stable channels of series A were used as a basis for these experiments. Bridge piers were then located in the bed of the developed channels. Without changing the imposed conditions, i.e. discharge, sediment load etc., the channels were allowed to develop freely, until the rates of change in bed and banks of these channels were insignificant.

The last series of the experiments, i.e. series C, was conducted to study the changes which occurred in the developed channels when abutments were introduced. The abutments used for the purpose of this study were vertical walls with a semicircular nose. In this series of experiments, the developed straight stable channels of series A were used again as the first part of the

experiments. Then, the abutments were located in the bed of the developed channels. With these abutments in place, the channels were again allowed to develop freely until the rates of change in bed and banks of the channels were insignificant. From these results, the following conclusions are drawn.

9.2 Conclusions

1. The effect of combining different formulae for the predictions of channel dimensions using the maximisation of sediment transport hypothesis was tested in chapter three. The results show that the predictions of the method are dependent on the equations adopted. That is, the use of different sediment transport and flow resistance equations may lead to different predictions. Among the different combinations considered, those which provided the best agreement with the data were the Brownlie (1982) formulae.

2. The predictions of the White, Paris, Bettess (WPB) theory have been compared with the data from present study in chapter five. The results show that the WPB theory seems to be a useful tool for prediction of the hydraulic and geometric dimensions of stable straight channels. However, this theory underpredicts water surface width, cross-sectional area, and sediment concentration of the laboratory channels for the range of applied discharges. It is also shown that this theory overpredicts mean depth and water surface slopes. This difference may be due to the Ackers-White (1973) sediment transport formula which is now under review. It may also be due to scale effects involved in the laboratory data.

3. The present study shows that, for the prediction of bank profile, the fifth-degree polynomial of Diplas and Vigilar (1992) results in a better approximation than that obtained from the normal-depth method and the cosine profile. A hyperbolic function, equation 5.11, has been fitted to the bank profile data of present study. It is also shown that the hyperbolic function

approximates the bank profile even closer than the fifth-degree polynomial indicated by Diplas and Vigilar (1992)

4. The present study, for velocity distribution, in the wall region, is in good agreement with the logarithmic law, and with the log-wake law in the outer region. See Figs. 5.14-5.17. It is, therefore, concluded that these two laws can predict velocity distribution in alluvial open channels with reasonable accuracy.

5. The von Karman constant has been calculated using a linear regression analysis from velocity distribution data of this study. This value has been plotted against Froude and Reynolds Numbers. See Figs 5.12 and 5.13. No systematic influence of Re or Fr on the von Karman value was observed. It is, therefore, concluded that the von Karman constant (κ) is, to a good approximation, a universal constant and does not depend on the Reynolds and Froude numbers. In the other words, the von Karman constant, κ, is independent of flow type.

6. The values of bed shear stress distribution, Fig 5.18, show that the bed shear stress increases rapidly with distance from the side wall and a mild peak is followed by a minimum. Beyond this position, the value increases again and attains a maximum at the central axis of the channel. This trend of bed shear stress variation supports the findings of previous research, e.g. Nezu et. al (1989), and Nezu et. al (1993).

7. The agreement between the shear force values from the present study and the equation of Knight et. al (1994) is good, bearing in mind that the equation is derived by fitting an empirical equation to the data mostly obtained from experiments in flumes with trapezoidal and rectangular sections.

8. During the present study where stable straight channels were developed, ridges and troughs were observed in the beds of the channels. These features provide evidence of secondary currents in the body of main flow. The data show that the transverse spacing between the sand ridges is approximately

twice the flow depth which is consistent with previous research, e.g. Kinoshita (1967).

9. This investigation shows that the present study is in good agreement with the Chang (1971), Yalin and Silva (1991), Muramoto and Fujita (1978), Colombini et al. (1987), and Jaeggi (1984) criterion for alternate bar formation. It is therefore concluded that these criteria give reasonable predictions for alternate bar formation in channels with loose banks.

10. This study shows that the bar wave length, *L*, is *6B < L < 9B*. It also shows that the Ikeda (1984) formula for dimensionless bar wavelength prediction underpredicts this parameter by an average amount of 14%. The Ikeda (1984) formula for dimensionless bar height prediction overpredicts the dimensionless bar height by an average amount of 8%. The Jaeggi (1984) formula underpredicts the bar height by an average amount of 13%. In the case of the Colombini et. al (1987) formula, it shows that the average discrepancy ratio for dimensionless bar height is 2.16. The difference between the predicted values and the measured values is attributed to the fact that these formulae are based mainly on experiments in alluvial channels with fixed walls rather than loose banks.

11. A comparison between the present data and available equations for scour depth prediction reveals that the CSU (1975), Melville and Sutherland (1988), and Gao et. al (1993) equations mostly overpredict the scour depth. The difference is attributed to the fact that these formulae are obtained from experiments carried out in fixed wall laboratory flumes. This study concerned a free bank channel which is closer to the real field situation.

12. The effect of pier spacing on scour depth was also considered. A pier spacing coefficient, K_{ps}, equation 7.19, has been derived which can be used with scour equations to account for the effect of pier spacing on scour depth.

13. A mathematical model, section 7.6, has been proposed to predict the temporal variations of scour depth in clear water and live bed scour. The

computed results of the model have been compared with available data. The comparison shows that the results are satisfactory for most conditions.

14. Knowledge of the top width of scour holes at piers and abutments is important in determining the extent of riprap needed as a scour countermeasure and to determine whether the scour holes overlap or not. An equation, equation 7.37, has been proposed to calculate the top width of scour holes.

15. In the present investigation, the measured angle of scour holes at the upstream side of the pier had a mean value of $34.3°$ with a standard deviation of $1.3°$. This supports the findings of previous research, e.g. Melville (1975) that the angle of scour holes upstream of the pier is close to the angle of repose of the bed material.

16. Investigation of scour topography due to interactions of piers and developed straight channels reveals that the main abrupt change in channel bed and bank is because of scour hole formation. An increase in channel width downstream of piers is observed, i.e. the width increases to a maximum value and then decreases afterwards. The rate of this increase is high in the first hour of the experiments and reduces afterwards.

17. This investigation reveals that the Laursen (1980), Froehlich (1988), Melville (1992), and Palaviccini (1993) equations for local scour prediction at abutments overpredict the scour depth. The reason is probably that these equations are mostly based on physical model studies in laboratory flumes with fixed walls. The present study acquired data from experiments carried out in a "regime" flume. The latter is closer to the real field situation.

18. Scour topography due to the interaction of abutments and developed straight channels reveals that the main change in channel bed and bank is due to abutment local scour hole formation. The channel bank upstream of abutments was mainly scoured because of slowly circulating water ahead of the abutment. An equation (8.17) is proposed to calculate the scoured bank region ahead of the abutment. This equation has been derived using laboratory data from the

present study. It gives an estimation of the scoured area. However, its' applicability to the field should be tested.

9.3 Recommendations for future work

1. The experiments conducted in this study for the development of straight stable channels were carried out for a limited range of discharge and for only one sediment size. An extensive programme of laboratory experiments using a wide range of discharge and different sediment sizes of bed material is recommended.

2. The effect of non-uniform sediments on the development of these channels is an important subject and needs attention.

3. An investigation needs to be carried out to examine the bank profile of self-formed straight channels for a wider range of flow discharge and different sediment sizes.

4. More accurate laboratory data, using Laser Doppler Anemometer (LDA), is needed to examine the velocity and boundary shear stress distribution in these channels.

5. Research is needed to study bank effects on the development of straight stable channels.

6. Time variation of bed scour due to the presence of bridge structures in the channels needs more research. The discharge used for the experiments was constant during each run. However the flow in a river during a flood is unsteady and discharge changes with time are rapid. Work is needed to focus on scour variation during an unsteady flow.

7. Laboratory data in the literature for live bed scour variation with time for bridge structures is limited, and the field data is almost unavailable. Extensive research is necessary to collect these kinds of data.

References

Abdu, M. I. (1993) "Effect of sediment gradation and coarse material fraction on clear water scour around bridge piers" Ph.D. Dissertation, Civil Eng. Dept., Colorado State Univ., Fr. Collins, Colorado.

Abed, L. (1991) "Local scour around bridge piers in pressure flow" Ph.D. Dissertation, Civil Eng. Dept., Colorado State Univ., Fr. Collins, Colorado.

Ackers, P. (1964) "Experiments on small streams in alluvium" Proc. ASCE, JHD, 90, HY4, pp 1-37.

Ackers, P., and White, W. R. (1973) "Sediment transport : new approach and analysis" ASCE, JHD, 99, HY11, pp 2041-2060.

Ackers, P., and Charlton, F.G. (1970a) "Meander geometry arising from varying flows" Journal of Hydrology 11 North Holland Publishing co., Amsterdam pp 230-252.

Ackers, P., and Charlton, F.G. (1970b) "The geometry of small meandering streams" Proc. ICE, supplement XII, paper 7328 S, pp. 289-317.

Ackers, P., and Charlton, F.G. (1970c) "The slope and resistance of small meandering channels" Proc. ICE, supplement XV, 1970, paper 7362S.

Allen, J. R. L. (1985) "Principles of physical sedimentology" George Allen & Unwin.

Arunachalam, K. (1965) "Scour around bridge piers" Journal of the Indian Roads Congress, Vol. 29, No. 2, pp 189-210.

Babaeyan-Koopaei K., and Valentine, E. M. (1995) "Experimental assessment of a rational regime theory" XXVI Th. congress of Int. Association for Hydraulic Research, Hydra 2000, Sept., London.

Babaeyan-Koopaei K., and Valentine, E. M. (1995) "Experimental study of the characteristics of alternate bars in a flume with loose banks" The Second Int. Conference on Hydro-Science and Eng., Vol. II, Part B, pp. 2029-2036, Beijing, China.

Babaeyan-Koopaei K., and Valentine, E. M. (1995) "A rational regime theory : different combinations of formulae" The Second Int. Conference on Hydro-Science and Eng., Vol. II, Part B, pp. 2037-2044, Beijing, China.

Baker, C. J. (1978) " Vortex flow around the bases of obstacles" Ph.D. thesis, University of Cambridge, Cambridge, UK.

Baker, C. J. (1980) "Theoretical Approach to Prediction of Local Scour Around Bridge Piers " Journal of Hydraulic Research, Vol. 18, No. 1, pp 1-12.

Baker, R. E. (1986) "Local scour at bridge piers in nonuniform sediment" Report No. 402, School of Engineering, University of Auckland, Auckland, New Zealand.

Basak, V. (1975) "Scour at square piers" Devlet su isteri genel mudulugu, Report No. 583, Ankara.

Bata, G. (1960) "Erozija Oko Novosadskog Mostovskog Stuba (Serbian) (Scour around bridge piers)" Inst. Za Vodoprivreder, Jaroslav Cerai Beozard Yugoslavia.

Bathurst, J. C., and Cao, H. H. (1986) Discussion on "Formation and effects of alternate bars" by Jaeggi, M. N. R., Proc. ASCE, Vol. 112, HY11, pp. 1101-1103.

Bettess, R. (1991) "Updated sediment transport theory" Research Focus, No. 7 (October Volume).

Bettess, R., and White, W. R. (1987) "Extremal hypothesis applied to river regime" Sediment Transport in Gravel Rivers, edited by C. R. Thorne, J. C. Bathurst and R. D. Hey, John Wiley & Sons.

Blench, T. (1957) "Regime behaviour of canals and rivers" Butterworth, London.

Blench, T. (1965) "Mobile bed Fluviology" University of Alberta Press.

Blondeaux, P., and Seminara, G. (1985) "A unified bar-bend theory of river meanders" J. Fluid Mech., Vol. 157, pp. 449-470.

Bonasoundas, DR. ING., (1973) "Flow structure and scour problem at circular bridge piers" Report No. 28, Oskar V. Miller Institute, Munich Technical University.

Bradshaw, P. (1976) "Turbulence" Topics in applied physics, Springer Verlag.

Bray, D. I. (1975) "Representative discharge for gravel bed rivers in Alberta, Canada" Journal of Hydrology, Vol. 27, pp 143-153.

Bray, D. I. (1979) "Estimating average velocity in gravel bed rivers" Proc. ASCE, Vol. 105, HY9, pp. 1103-1122.

Breusers, H. N. C. (1965) "Scour around drilling platforms" Journal of Hydraulic Research, I.A.H.R, Vol. 19, pp 276.

Breusers, H. N. C., Nicollet, G. and Shen, H. W. (1977) "Local scour around cylindrical piers" Journal of Hydraulic Research, Vol. 15, No. 3, pp 211-252.

Breusers, H. N. C., and Raudkivi, A. J. (1991) "Scouring" Hydraulic Structures Design Manual Series No 2, A. A. Balkema, Rotterdam.

Brownlie, W. R., (1982) "Prediction of Flow Depth and Sediment Discharge in Open Channels " PhD. Thesis, California Institute of Technology, Pasadena, California.

Callander, R. A. (1966) "Research in loose boundary hydraulics at Auckland University" Reprint from Journal of Hydrology (N. Z.) Vol. 5, No. 2, pp 111-121, Published by New Zealand Hydrological Society.

Chabert, J., and Engeldinger, P. (1956) "Etude des Affouillements Autour des Piles de Ponts (Study of scour around bridge piers) " Laboratoire National D'Hydrauligue 6, Quai Watier, Chatou, France.

Chang, H. H. (1980a) "Stable alluvial canal design" Proc. ASCE, JHD, Vol.106, HY5, pp. 873-891.

Chang, H. H. (1980b) "Geometry of gravel streams" Proc. ASCE, JHD, Vol.106, HY9, pp. 1443-1456.

Chang, H. H. (1985) "Formation of alternate bars" Proc. ASCE, JHD, Vol.111, HY11, pp. 1412-1420.

Chang, S. Z. (1987) "The area of scour hole around bridge piers" AIT Master thesis No. WA-87-9, Bangkok, Thailand.

Chang, Y., Simons, D. and Woolhiser, D.A., (1971) "Flume Experiments on Alternate Bar Formation", Proc., ASCE, Waterways Division, Vol. 97, No. WW1, pp. 155-165.

Chee, R. K. W. (1982) "Live bed scour at bridge piers" Report No. 290, School of Engineering, University of Auckland, Auckland, New Zealand .

Chiew, Y. M. (1984) "Local scour at bridge piers" Thesis presented to the University of Auckland, at Auckland, New Zealand, in partial fulfilment of the requirements for the degree of Doctor of Philosophy in Engineering .

Chiew, Y. M., and Melville, B.W. (1987) "Local scour around bridge piers" Journal of Hydraulic Research, Vol. 25, No. 1, pp 15-26.

Chin, C. O. (1985) "Stream bed armouring" Eng. Report No. 403, Dept. of Civil Eng., University of Auckland, N.Z.

Chitale, S.V. (1962) "Discussion of scour at bridge crossings" Trans. ASCE, Vol. 127, part 1, p. 191.

Coleman, N. L., and Alonso, C. V. (1983) "Two dimensional channel flows over rough surfaces" J. Hydr. Eng., ASCE, Vol. 109, pp 175-188.

Coleman, N. L. (1971) "Analysing laboratory measurements of scour at cylindrical piers in sand beds" Proc. 14th Congress I.A.H.R., Vol. 3, pp 307-313.

Coles, D. (1956) "The law of the wake in the turbulent boundary layer" J. Fluid Mech., Vol. 1, pp 191-226.

Colombini, M., Seminara, G. and Tubino, M. (1987) "Finite-amplitude Alternate Bars" Journal of Fluid Mechanics, Vol. 181, pp. 213-232.

Cunha, L.V. (1970) Discussions on "Local scour around bridge crossings" by Shen, H.W., Schneider, V. R., and Karaki, S. S., JHD, Proc. ASCE., Vol. 96, HY8, pp 1742-1747.

Dabkowski, S. L., (1991) "Mean Flow Depth in Sandy Bed River" XXIV IAHR Congress, Spain, pp. A353-A359.

Dalton, C., and Masch, F. D. (1964) "Drag forces in velocity gradient flows" Tech. Rep. No. 04-6402, Hydraulic Engineering Laboratory, Dept. of Civil Engineering, The University of Texas, Austin.

Davies, T. R. H., and Sutherland, A. J. (1980) "Resistance to flow past deformable boundaries" Earth Surf. Proc., Vol. 5. pp. 175-179.

Davies, T. R. H. (1980) "Bedform spacing and flow resistance" J. Hydr. Div., ASCE, Vol. 106, HY3, pp. 423-433.

Diplas, P., and Vigilar, G. (1992) "Hydraulic geometry of threshold channels" J. Hydr. Eng., ASCE, Vol. 118, HY4, pp 597-614.

Diplas, P. (1990) "Characteristics of self-formed straight channels" J. Hydr. Eng., ASCE, Vol. 116, HY5, pp 707-728.

Duboys, M. P. (1879) "Le Rhone et les Rivieres a Lit affouillable" Mem. Doc., Pont et chaussees, ser. 5., Vol. XVIII.

Einstein, H. A. (1950) "The bed load function for sediment transportation in open channel flows" U.S. Dept. of Agric., Tech. Bull. 1026, 70P.

Engelund, F., and Hansen, E. (1967) "A monograph on sediment transport in alluvial streams" Teknisk vorlag, Copenhagen, Denmark.

Ettema, R. (1980) "Scour at bridge piers" Report No. 216, School of Engineering , Univ. of Auckland, Auckland, New Zealand.

Farias, H. D. (1991) "A unified approach to extremal hypotheses for morphology of stable alluvial channels" Student Paper Competition, XXIV IAHR Congress, Madrid, pp S13-S22.

Federal Highway Administration (FHWA) (1991) "Evaluating scour at bridges" Hydr. Eng. Circular No. 18, FHWA-IP-90-017, Washington, D.C.

Froehlich D. C. (1989) "Abutment scour prediction" Paper presented at the 68th annual TRB meeting, Washington D.C.

Froehlich D. C. (1988) "Local scour at bridge abutments" Proc. of the National conference on Hyd. Eng., ASCE, New Orleans, pp 13-18.

Froehlich D. C. (1987) "Analysis of onsite measurements of scour at piers" Proc. of the National conference, Hyd. Div., ASCE, pp 534-539.

Gao, D., Posada, G. L., and Nordin C. F. (1993) "Pier scour equations used in China" Proc. of the 1993 National Conf. on Hyd. Eng., pp 1031-1036, San Francisco, California.

Garcia, M. and Nino, Y. (1993) "Dynamics of Sediment Bars in Straight and Meandering Channels : Experiments on the Resonance Phenomenon" J. of Hyd. Res., Vol. 31, No 6, pp. 739-761.

Garde, R. J. (1961) "Local bed variation at bridge piers in alluvial channels" University of Roorkee Research Journal, Vol. 4, No. 1, pp 101-116.

Garde, R. J., and Rangaraju, K. G. (1991) "Mechanics of Sediment Transportation and Alluvial Stream Problems " second reprint, Wiley eastern limited, New Delhi, India.

Gessner, F. B., and Jones, J. B. (1965) "On some aspects of fully developed turbulent flow in rectangular channels" J. Fluid Mech., Vol. 23, 689-713.

Gibson, A. H. (1909)"On the depression of the filament of maximum velocity in a stream flowing through an open channel" Proc. Royal Soc. of London, Series A, Vol. 82, pp 149-159.

Gill, M. A. (1968) "Rationalisation of lacey's regime equations" Proc. ASCE, JHD, 94, HY4, pp 983-995.

Glover, R. E., and Florey, Q. L. (1951) "Stable channel profiles" US. Bureau of Reclamation, Washington, D.C.

Goldstein, S. (1965) "Modern developments in fluid mechanics" Dover Publications Inc., Vol. 1 and 2, pp 55-62.

Hancu, S. (1971) "Sur le calcul des affouillements locaux dans la zone des piles de ponts " Proc. 14th IAHR Congress, Paris, Vol. 3, pp 299-313.

Hanna C. R. (1978) "Scour at pile groups" Report No. 78-3, Dept. of Civil Eng., School of Eng., University of Canterbury, New Zealand.

Henderson, F. M. (1961) "Stability of alluvial channels" Proc. ASCE, JHD, 87, HY6, pp. 109-138.

Hjorth, P. (1977) " A stochastic model for progressive scour" Proc. of IAHR Symp. on stochastic hydraulics, Univ. of Lund, Lund, Sweden.

Hjorth, P. (1975) "Studies on the nature of local scour" Dept. of Water Resources Engineering, Lund Institute of Technology, Bulletin Series A, No. 46.

Hwang, Li-San, and Laursen, E. M. (1963) "Shear measurement technique for rough surfaces" J. Hyd. Div., ASCE, Vol. 89, HY2, pp 19-37.

Ikeda, S., Parker, G., and Kimura, Y. (1988) "Stable width and depth of straight gravel rivers with heterogeneous bed materials" Water Resour. Res., Vol. 24, pp 713-722.

Ikeda, S., (1984) "Prediction of Alternate Bar Wavelength and Height" J. of Hydraulic Eng., ASCE, Vol. 110, HY4, pp. 371-386.

Ikeda, S., (1982) "Incipient motion of sand particles on side slopes" J. Hydr. Div., ASCE, Vol. 108, HY1, pp. 95-113.

Ikeda, S., (1981) "Self-formed straight channels in sandy beds" J. Hydr. Div., ASCE, Vol. 107, HY4, pp 389-406.

Inglis, C. C. (1949) "The behaviour and control of rivers and canals" C.W.I.N.R.S., Poona, Res. Publication No. 13.

Islam, M. L., Grade, R. J., and Ranga-Raju, K. G. (1986) "Temporal variation of local scour" Proc. of IAHR Symposium on Scale Effects in Modelling Sediment Transport Phenomenon, Toronto, Canada.

Jaeggi, M. N. R., (1994) Discussion of "Dynamics of Sediment Bars in Straight and Meandering Channels : Experiments on the Resonance Phenomenon" by Garcia, M. and Nino, Y., Journal of Hydraulic Research, Vol. 32, No 4, pp. 632-635.

Jaeggi, M. N. R., (1984) "Formation and Effects of Alternate Bars" J. of Hydraulic Eng., ASCE, Vol. 110, HY2, pp. 142-156.

Jaeggi, M. N. R., (1980) discussion of "Steepness of sedimentary dunes" by Yalin, M. S., and Karahan, E., J. of Hyd. Eng., ASCE, Vol. 106, HY1, pp. 230-233.

Jain, S.C., and Fischer, E. E. (1979) "Scour around circular bridge piers at high Froude numbers" Report FHWA-RD-79-104, Available through NTIS, Springfield, VA 22161.

Jain, S.C., and Fischer, E. E. (1980) "Scour around bridge piers at high flow velocities" JHD, Proc. ASCE., Vol. 106, HY11, pp. 1827-1842.

Jones, J. S. (1984) "Comparison of Prediction Equations for Bridge Pier and Abutment Scour" Transportation Research Record, Vol. 950, No. 2, pp 202-209.

Jones, J. S. (1989) "Laboratory studies of the effects of footings and pile groups on bridge scour" Proc., Bridge Scour Symp., Report No. FHWA-RD-90-035 , FHWA, Washington, D.C.

JSCE Task Committee on the Bed Configuration and Hydraulic Resistance of Alluvial Streams (1974) : The bed configuration and roughness of alluvial streams. (In Japanese). Proceeding , JSCE, No. 210, Feb.

Kandasamy, J. K. (1985) "Local scour at skewed abutments" Report No. 375, Dept. of Civil Eng., School of Eng., Auckland Univ., New Zealand.

Kandasamy, J. K. (1989) "Abutment scour" Report No. 458, Dept. of Civil Eng., School of Eng., Auckland Univ., New Zealand.

Karcz, I. (1966) "Secondary currents and the configuration of a natural stream bed" J. Geophys. Res., Vol. 71, pp 3109-3116.

Keller, R. J. and Rodi, W. (1988) "Prediction of flow characteristics in main channel flood plain flows" J. Hyd. Res., Vol. 26, pp 425-441.

Kellerhals, R. (1967) "Stable channels with Gravel-Paved beds" J. Waterways Harb. Div., ASCE., Vol. 93, WW1, pp 63-84.

Kennedy, R. G. (1895) "The prevention of silting in irrigation canals" paper No. 2826, Proc. ICE, Vol. 119, London.

Kilgore, R. T., and Young, G. K. (1993) "Riprap incipient motion and Shield's parameter" Proc. of the 1993 National Conf. on Hyd. Eng., pp 1552-1557, San Francisco, California.

Kinoshita, R. (1967) "An analysis of the movement of flood waters by aerial photography; Concerning characteristics of turbulence and surface flow" Photographic Surveying, Vol. 6, pp 1-17 (in Japanese).

Knezevic, B. (1960) "Contribution to research work of erosion around bridge piers" Translation is filed at Eng. Research Centre, Colorado State University, Fort Collins, Colorado (No. I.D. 67-11).

Knight, D. W., Yuen, K. W. H., and Al- Ahmad, A. A. I. (1994) "Boundary shear stress distributions in open channel flow", Mixing and Transport in the Environment, John Wiley & Sons Ltd, Beven, Chatwin, and Millbank (eds.), pp. 51-87.

Knight, D. W., and Patel, H. S. (1985) "Boundary shear in smooth rectangular ducts" J. Hyd. Eng., ASCE, Vol. 111, pp 29-47.

Knight, D. W. (1981) "Boundary shear in smooth and rough channels" J. Hyd. Div., ASCE, Vol. 107, HY7, pp 839-851.

Knight, D. W., and Macdonald, A. (1979) "Open channel flow with varying bed roughness " J. Hyd. Div., ASCE, Vol. 105, pp 1167-1183.

Kothyari, U. C. (1989) "Scour around bridge piers" Ph.D. Thesis, Dept. of Civil Eng., Univ. of Roorkee, India.

Kothyari, U. C., Garde R. J., and Ranga-Raju K. G. (1992) "Temporal variation of scour around circular bridge piers" J. Hyd. Eng., ASCE, Vol. 118, HY8, pp 1091-1106.

Kwan, T. F. (1984) "Study of abutment scour" Auckland Univ., Civil Eng. Dept., Report No. 328.

Kwan, T. F. (1988) "A study of abutment scour" Auckland Univ., Civil Eng. Dept., Report No. 451.

Lacey, G. (1929-1930) "Stable channels in alluvium" Minutes of Proc. ICE, 229, pp 259-384.

Lacey, G. (1958) "Flow in alluvial channels with sandy mobile beds" Proc. ICE, Vol. 9, pp 145-164.

Lagasse, P. F., Schall, J. D., Johnson, F. D., Richardson, E. V., Richardson, J. R., and Chang, F. F. M.(1990) "Stream stability at highway structures" Hydraulic Engineering Circular No. 20, FHWA, Dept. of Transportation, Washington, D.C.

Lane, E. W. (1953) "Progress report on studies on the design of stable channels by the Bureau of reclamation " Proc. ASCE, Vol. 79, separate no. 280.

Larras, J. (1963) "Profonders maximales d'erosion des fonds mobiles autor des piles en riviere "Annales des ponts et Chausses, Vol. 133, No. 4, pp 411-424.

Laursen, E. M. (1980) "Predicting scour at bridge piers and abutments" General Report No. 3, Arizona Dept. of Transportation, Phoneix, Arizona.

Laursen, E. M. (1960) "Scour at bridge crossings" Proc. ASCE, Vol. 86, HY2, pp. 39-54.

Laursen, E. M. (1958) "Scour at bridge crossings" Iowa Highway Research Board, Bulletin No. 8.

Laursen, E. M., and Antonas, N. J. (1980) "Scour and backwater at a progressively encroaching abutment" Engineering Experiment Station, College of Engineering, Arizona Univ., Report No. 2.

Laursen, E. M., and Toch, A. (1956) "Scour around bridge piers and abutments" Iowa Highway Research Board, Bulletin No. 4, 60 pp.

Leopald, L. B., and Wolman, M. G. (1957) "River channel patterns: Braided, Meandering, and straight" US Geol. Survey, Prof. Paper 282-B.

Leutheusser, H. J. (1963) "Turbulent flow in rectangular ducts" J. Hyd. Div., ASCE, Vol. 89, HY3, pp 1-19.

Lindley, E. S. (1919) "Regime Channels" Proc. Punjab Engineering Congress, Vol. 7.

Liu, U. K., Chang, F. M., and Skinner, M. M. (1961) "Effect of bridge constriction on scour and backwater" Engineering Research Centre, Colorado State Univ., Report No. CER 60, HKL 22.

Lundgren, H., and Jonsson, G. I. (1964) "Shear and velocity distribution in shallow channels" J. Hyd. Div., ASCE, Vol. 90, HY1, pp 1-21.

Mahmood, K., et al. (1979) "Selected equilibrium state data from ACOP canals" Civil, Mechanical and Environmental Engineering Dept., Report No. EWR-79-2, George Washington Univ., Washington D. C.

Maza Alvarez, J. A., and Sanches Bribiesca, J. L. (1964) "Contribueion al Estudio de la Socavacion local en Pilas de Puente" Universidad Nacional Autonoma de Mexico, Facultad de Ingenieria Publication Numero 84.

Melling, A., and Whitelaw, J. H. (1976) "Turbulent flow in a rectangular duct" J. Fluid Mech., Vol. 78, pp 289-315.

Melville, B. W., and Ettema R. (1993) "Bridge abutment scour in compound channels" Proc. of the 1993 National Conf. on Hyd. Eng., pp 767-772, San Francisco, California.

Melville, B. W. (1992) "Local scour at bridge abutments" J. of Hyd. Eng., ASCE, Vol. 118, HY4, pp. 615-631.

Melville, B. W., and Sutherland, A.J. (1988) "Design method for local scour at bridge piers" J. Hyd. Eng., ASCE, Vol. 114, HY10, pp. 1210-1226.

Melville, B. W. (1984) "Live bed scour at bridge piers" J. of Hyd. Eng., Vol. 110, No. 9, ASCE, pp. 1234-1247.

Melville, B. W. (1975) "Local scour at bridge sites" Report No. 117, Univ. of Auckland, Auckland, New Zealand.

Muramoto, Y., and Fujita, Y., (1978) "The Classification of Meso-Scale River Bed Configuration and the Criteria of its Formation" Proceedings of the 22nd Japanese Conference on Hydraulics, pp. 275-282.

Muzzamil, M., K. Gupta, Gangadharaiah, T., and Subranya, K. (1989) "Vorticity characteristics of scouring horseshoe vortex" Proc. of 3rd Int. Workshop on Alluvial River Problems, Roorkee, India.

Naot, D., and Rodi, W. (1982) "Calculation of secondary currents in channel flow" J. Hyd. Div., ASCE, Vol. 108, HY8, pp. 948-968.

Nakagawa, H., and Suzuki, K. (1975) "An application of stochastic model of sediment motion on local scour around a bridge pier" Proc. of 16th congress, IAHR, Sao Paulo, Brazil, Vol. 2., pp. 228-235.

Neil, C. R. (1973) "Guide to bridge hydraulics" Univ. of Toronto Press, Torento.

Neil, C. R. (1964) "River-bed scour, a review for engineers" Canadian Good Roads Assoc., Tech. Pub. No. 23.

Nezu, I., and Nakagawa, H. (1993) "Turbulence in open channel flows" IAHR Monograph, A.A.Balkema, Rotterdam.

Nezu, I., and Nakagawa, H. (1984) "Cellular secondary currents in straight conduit" J. Hyd. Eng., ASCE, Vol. 110, pp. 173-193.

Nezu, I., Nakagawa, H., and Rodi, W. (1989) "Significant difference between secondary currents in closed channels and narrow open channels" Proc. of 23rd IAHR congress, Ottawa, pp A125-A132.

Nezu, I., and Rodi, W. (1986) "Open channel flow measurements with a laser Doppler anemometer" J. Hyd. Eng., ASCE, Vol. 112, pp. 335-355.

Nezu, I., and Rodi, W. (1985) "Experimental study on secondary currents in open channel flow" Proc. of 21st IAHR congress, Melbourne, Vol. 2, pp 115-119.

Nikuradse, J.(1933) "Stromungsgezetze in Rauhen Rohren" Vein Deutscher Ingenieure, Forschumgasheft 361, Translated as National Advisory Committee for Aeronautics Technical Manual 1292, Nov. 1950.

Paintal, A. S. (1971) " A stochastic model of bed load transport" J. of Hyd. Res., IAHR, Vol. 9, No. 4, pp. 91-109.

Palaviccini, M. (1993) "Scour predictor model at bridge abutments" Ph.D. Dissertation, Dept. of Civil Eng., School of Engineering, The Catholic University of America, Washington D. C.

Parker, G. (1978) "Self-formed straight rivers with equilibrium banks and mobile bed. Part 2. The gravel river" J. Fluid Mech., Vol. 89, pp. 127-146.

Patel, V. C. (1988) "An introduction to measurement of velocity" Discharge and velocity measurements, A. Muller (ed.), Balkema, Rotterdam, pp. 81-93.

Patel, V. C. (1965) "Calibration of the Preston tube and limitations on its use in pressure gradients" J. Fluid Mech., Vol. 23, pp. 185-208.

Prandtl, L. (1925) "Uber die ausgebildete turbulenz" ZAMM, Vol. 5, pp.136.

Preston, J. H. (1954) "The determination of turbulent skin friction by means of pitot tubes" J. Roy. Aeronaut. Soc., Vol. 58, pp. 109-121.

Qadar, A. (1980) "The vortex scour mechanism at bridge piers" Ph.D. Thesis Aligarh Muslim Univ., Aligarh, India.

Ranga-Raju K.G., Dhandapani K. R. and Kandap D. M., (1977) "Effect of Sediment Load on Stable Sand Canal Dimensions" Journal of the Water-way, Port, Coastal and Ocean Divisions, ASCE, Vol. 103, No. WW2, pp. 241-249.

Raudkivi, A. j. (1986) "Functional trends of scour at bridge piers" J. Hyd. Eng., ASCE, Vol. 112, pp. 1-13.

Raudkivi, A. J. (1990) "Loose Boundary Hydraulics" third edition, Pergamon press, Oxford, England.

Raudkivi, A. J., and Ettema, R. (1982) "Scour at bridge piers" 3rd Congress of the Asian and Pacific Division (A.P.D.) of the International Association for Hydraulic Research (I.A.H.R.) pp. 277-285.

Raudkivi, A. J., and Sutherland, A. J. (1981) "Scour at bridge crossings" Road Research Unit bulletin 54, Wellington, New Zealand.

Richardson, E. V., Harrison, L. J., and Davis, S. R. (1991) "Evaluating scour at bridges" Hydr. Engrg. Circular No. 18:FHWA-IP-90-017, Dept. of Transportation, FHWA, Washington, D.C.

Richardson, E. V., Simons, D. B., and Julien, P. Y. (1990) "Highways in the River Environment" FHWA-HI-90-016, Dept. of Transportation, Washington, D.C.

Roper, A. T. (1965) "The Wake Region of a Circular Cylinder in a Turbulent layer" Msc Thesis, Colorado State University, Fort Collins, Colorado.

Sarma, K. V. N., Lakshminarayana, P., and Rao, N. S. L. (1983) "Velocity distribution in smooth rectangular open channels" J. Hyd. Eng., ASCE, Vol. 109, pp. 270-289.

Schlichting, H. (1979) "Boundary layer theory" 7th edition, McGraw Hill.

Schumm, S. A., and Khan, H. R. (1972) "Experimental study of channel patterns" Geol. Soc. of America Bulletin, Vol. 83, pp. 1755-1770.

Shakir, A. S. (1992) "An experimental investigation of channel plan forms" Thesis presented to the Newcastle University, at Newcastle, England, in partial fulfilment of the requirements for the degree of Doctor of Philosophy in Engineering.

Shakir, A. S., and Valentine, E. M. (1992) "Characteristics of braided laboratory channels" Conference on Braided Rivers Form, Process and Economic Applications, London.

Shen, H.W., Ogawa, Y, and Karaki, S. (1963) "Time variation of bed deformation near bridge piers" Proc. 10th Congress I.A.H.R., Paper No. 3.14.

Shen, H.W., Schneider, V. R., and Karaki, S. (1966) "Mechanics of local scour" Colorado State University Report CER66, HWS-VRS-SK22.

Shen, H.W., Schneider, V. R., and Karaki, S. (1969) "Local scour around bridge piers" Proc. ASCE., Vol. 95, HY6, pp. 1919-1940.

Shiono, K., and Knight, D. W. (1988) "Two dimensional analytical solution for a compound channel" Proc. 3rd Int. Symp. on Refined Flow Modelling and Turbulence Measurements, Tokyo, Japan, pp. 591-599.

Shiono, K., and Knight, D. W. (1991) "Turbulent open channel flows with variable depth across the channel" J. Fluid Mech., Vol. 222, pp. 617-646.

Simons, D. B., and Richardson E. V. (1966) "Resistance to flow in alluvial channels" US Geol. Survey Prof. paper 422-j .

Simons, D. B. (1957) "Theory and design of stable channels in alluvial material" Ph.D. thesis, Colorado state Univ., USA.

Skolds, D. M., and Strum,T. W. (1986) "Alluvial Stream bed Adjustment in a Laboratory Model" Third International Symposium on River Sedimentation, The Univ. of Mississippi, pp. 235-244.

Song, C. C. S., and Yang, C. T. (1980) "Minimum stream power: theory" J., Hyd., Div., ASCE, Vol. 106, HY9, pp. 1477-1487.

Stearns, F. P. (1883) "On the current meter, together with a reason why the maximum velocity of water flowing in open channels is below the surface" Trans. of ASCE, Vol. 12, No. 216, pp. 331-338.

Stebbings, J. (1963) "The shape of self-formed model alluvial channels" Proc., ICE, Vol. 25, pp. 485-510.

Stevens, M. A., and Nordin, C.F. (1990) "First step away from Lacey's regime equations" ASCE, JHD, Vol. 116, HY11, pp. 1422-1425.

Sukegawa, N. (1972) "Criterion for alternate bar formation" Memoris of the School of Science and Engineering, No. 36, Waseda University, Japan.

Tey, C. B. (1984) "Local scour at bridge abutments" Ms. Thesis, Auckland Univ., School of Eng., Report No. 329, Auckland, New Zealand.

Tison, L. J., (1940) "Erosion autour des piles de ponts en riviere" Annales des Travaux publics de Belgigue, Vol. 41, No. 6, pp 813-871.

Tison, L. J. (1960) "Discussion of scour at bridge crossings" ASCE, JHD, Vol. 86, HY9, Part I.

Tominaga, A., and Nezu, I. (1992) "Velocity profiles in steep open channel flows" J. Hyd. Eng., ASCE, Vol. 118, pp. 73-90.

Transportation Research Board, (1970) "Scour at bridge waterways" National Co-operative Highway Research Program (NCHRP), Synthesis of Highway Practice 5, Washington, D. C.

Valentine, E. M. (1986) "Application to braided rivers of the Wallingford regime theory" Proc. of the gravel bed rivers workshop, Hydrology Centre, Public. No. 9, Christchurch.

Valentine, E. M., and Shakir A. S. (1992) "River channel planform : An appraisal of a rational approach" Eighth Congress of the Asia and Pacific Division of IAHR, Poona, India.

Vanoni, V. A. (1946) "Transportation of suspended sediment by water" Trans. of ASCE, Vol. 111, pp. 67-133.

Vittal, N., Kothyari, U. C., and Haghighat, M. (1994) "Clear water scour around bridge pier group" J. Hyd. Eng., ASCE, Vol. 120, HY11, pp. 1309-1318.

Wang, S., White, W. R., and Bettess, R. (1986) "A Rational Approach to River Regime" Third International Symposium on River Sedimentation, Mississippi, pp. 167-176.

White, W. R., Paris, E., and Bettess, R. (1980) "The frictional characteristics of alluvial streams : a new approach" Proc. ICE, Part 2, 69, pp737-750.

White, W. R. (1975) "Scour around bridge piers in steep streams" Proc. 16th Congress I.A.H.R., Sao Paulo, Vol. 2, pp. 279-284.

White, W. R., Paris, E., and Bettess, R. (1981) "River Regime Based on Sediment Transport Concepts " HRS, Report No. IT 201, Wallingford, England.

White, W. R., Paris, E., and Bettess, R. (1981) "Tables for the design of stable Alluvial Channels " HRS, Report No. IT 208, Wallingford, England.

White, W. R., Bettess, R. and shiqiang, W. (1987) "Frictional characteristics of alluvial streams in the lower and upper regimes" Proc. ICE, Part 2, 83, pp 685-700. and Discussion on pp. 577-581, ICE, part 2, 85 (1988).

Wong, W. H. (1982) "Scour at bridge abutments " Ms. Thesis, Auckland Univ., School of Eng., Report No. 275, Auckland, New Zealand.

Yalin, M.S. and Silva, A. M. F. (1991) "On the Formation of Alternate Bars", Sand Transport in Rivers, Estuaries and the Sea, A. A. Balkema Publishers, Soulsby and Bettess (eds.), USA, pp. 171-178.

Yang, C. T. (1976) "Minimum unit stream power and fluvial hydraulics " Proc. ASCE, JHD, Vol. 102, HY7, pp 919-934.

Yang, C. T. (1971) "Potential energy and stream morphology" Water Res. Research, Vol. 7, pp. 311-322.

Yang, C. T., and Song, C. C. S. (1979) "Theory of minimum rate of energy dissipation" Proc. ASCE, JHD, Vol. 105, HY7, pp. 769-784.

Young, G. K., Palaviccini, M., and Kilgore, R. T. (1993) "Scour prediction model at bridge abutments" Proc. of the 1993 National Conf. on Hyd. Eng., pp. 755-760, San Francisco, California.

Addendum and errata:

(1) The parameters x, and B in Fig. 5.18 correspond to the transverse co-ordinate and channel width respectively. Therefore the value of 2x/B=0 corresponds to the channel centre and the value of 2x/B=-1 corresponds to the channel bank end.

(2) In order to measure shear stress distribution across the channel section, the Pitot-static tube described in section 4.7.4 was used. The difference of dynamic and static heads was read on a differential manometer. The differential heads were used to calculate the shear stress distribution using the Preston (1954) method, and the calibration curves of Patel (1965). [See section 4.7.4]

(3) The bar height and scour depth were calculated as a result of bed level measurements carried out with the help of point gauges described in section 4.7.3. The bar wavelength were measured using metric scale along the length of the flume [See section 4.7.3].

(4) Nezu and Rodi (1986) reported that, when their data were fitted by the log-law, up to $\frac{yU_*}{v} \cong 0.6\frac{hU_*}{v}$, the linear regression of $\frac{U}{U_*}$ versus $\frac{yU_*}{v}$ was as good as in the case for the wall region i.e. $\frac{yU_*}{v} \leq 0.2\frac{hU_*}{v}$. In the present study, as the number of data points measured in the validity area of equation 5.15 were limited, due to small flow depth, the regression analysis was carried out for the extended range reported by Nezu and Rodi (1986), i.e. $30 < \frac{yU_*}{v} \leq 0.6\frac{hU_*}{v}$, and the values of κ, and A were evaluated.

The effect of roughness on the von Karman constant, κ, was examined by Tominaga and Nezu (1992). They demonstrated that κ is a universal constant irrespective of roughness size.

(5) The Bray (1979) equation, which is used in the mathematical model of temporal variation of scour depth (Section 7.6.2), is as follows:

$$\frac{U}{U_*} = \sqrt{8}[0.248 + 2.36\log(\frac{y}{d_{50}})]$$

where U is the average velocity, U_* is the shear velocity, y is the flow depth, and d_{50} is the mean bed material size.

(6) In chapter 5, two sets of figures appear as Figs. 5.1 to 5.6. The first set corresponds to the sections 5.1 to 5.4. The second set corresponds to the sections 5.5 to 5.6.

APPENDIX A :   **EXPERIMENTAL RESULTS**

TABLE A1 : Straight stable channels (Experimental Results).

Test No	Run Time (h)	Carved channel slope	Q (l/s)	B_m (mm)	D_m (mm)	A_m (mm²)	WS_m	X (mg/l)
1	12	0.0028	4.0	496.1	24.8	12265.2	0.002539	527.9
2	12.5	0.0028	4.0	606.5	21.6	13090.1	0.002975	709.9
3	12.5	0.0028	4.0	550.7	23.3	12783.2	0.002701	222.2
4	9.25	0.0028	4.0	511.4	23.9	12192.3	0.002562	105.5
5	8.5	0.0027	4.0	511.1	22.5	11462.5	0.002683	91.4
6	9.0	0.0027	3.0	435.4	19.9	8671.4	0.00283	____
7	11.0	0.0028	3.0	421.8	20.8	8751.4	0.002928	159.0
8	8.0	0.0027	2.0	306.1	18.5	5673.8	0.003023	____
9	9.25	0.0029	2.5	354.9	20.3	7204.0	0.002931	101.3
10	8.5	0.0028	3.5	456.9	22.9	10461.4	0.002808	150.6
11	8.5	0.003	3.5	470.3	21.8	10243.0	0.00284	130.8
12	8.5	0.0029	3.5	464.4	22.8	10585.7	0.002763	130.9
13	9.0	0.003	3.5	473.0	22.2	10478.8	0.002796	115.7
14	8.5	0.0028	4.0	503.8	23.9	12037.2	0.002739	112.7
15	8.75	0.0029	4.0	514.1	23.2	11870.7	0.002869	87.6
16	9.0	0.0028	4.0	529.4	22.6	11898.5	0.002720	____
17	9.0	0.003	4.0	566.3	21.2	11976.6	0.002875	____
18	8.0	0.0029	4.0	578.7	21.0	12097.9	0.003100	125.8

A_m =   Measured channel cross-sectional area
B_m =   Measured channel width
D_m =   Measured channel depth
WS_m =   Measured water surface slope
X   =   Measured sediment concentration (Average)

TABLE A1 : Straight stable channels (Experimental results) (Cont.).

Test No	Run Time (h)	Carved channel slope	Q (l/s)	B_m (mm)	D_m (mm)	A_m (mm²)	WS_m	X (mg/l)
19A	8.0	0.0024	2.5	367	20.8	7657.4	0.00275	334.6
20A	8.5	0.0024	2.5	356	21.3	7596.9	0.00269	246.4
21A	9.0	0.0024	3.0	406	21.8	8857.0	0.00254	176.8
22A	8.0	0.0025	3.5	455	22.8	10408.8	0.00254	145.9
23A	8.0	0.0026	4.0	527	25.5	11898.7	0.00236	37.1
24A	8.0	0.0027	4.0	532	22.8	12191.8	0.00230	25.8
25A	8.0	0.0026	4.0	526	23.2	12226.6	0.00219	15.6
26A	9.0	0.0025	2.5	355	21.9	7790.2	0.00265	188.1
27A	8.5	0.0026	2.5	350	21.7	7609.2	0.00254	152.0
28A	10.0	0.0024	4.0	484	24.7	11991.9	0.00223	104.8
29A	8.5	0.0024	4.0	490	24.4	12005.3	0.00221	67.6
30A	8.0	0.0025	4.0	499	23.9	11912.6	0.00234	91.7
31A	16.0	0.0026	4.0	503	24.5	12351.2	0.00218	17.7
32A	14.0	0.0026	2.5	360	22.0	7908.0	0.00251	119.8
33A	8.0	0.0026	2.5	338	22.5	7627.5	0.00240	124.5
34A	25.0	0.0021	2.5	330	25.0	8245.3	0.00227	39.9
35A	8.0	0.0020	2.5	305	26.1	7985.3	0.00223	54.9
36A	8.0	0.0019	2.5	305	26.8	8178.6	0.00210	53.4
37A	8.5	0.0016	2.5	305	26.9	8214.8	0.00202	41.5
38A	8.5	0.0017	2.5	307	26.9	8243.8	0.00199	37.4
39A	20.0	0.0018	2.5	316	26.3	8317.4	0.00203	36.5

TABLE A2 : Bed Level Measurements*** (Experimental results).
All numbers are in mm.

'TEST NO.7 - 19MAY93'		'TEST NO.8- 21MAY93'		'TEST NO.9- 25MAY93'		'TEST NO.13- 16JUN93'	
'SECTION 7 *'		SECTION 8 '		SECTION 8 '		'SECTION 5 '	
1003**	147**	1074	143.8	1059	144.2	998	146.3
1022	131.8	1091	131.5	1078	127.9	1016	131
1041	123.9	1119	116.9	1107	118.2	1046	120.6
1108	118.7	1164	110.3	1152	117.5	1087	117.9
1183	117.6	1244	112.9	1208	117.9	1176	118
1291	123.5	1312	115.2	1267	115.5	1257	117.3
1350	125.9	1371	117.3	1322	113.3	1328	117.3
1400	123.6	1400	127	1378	114.6	1403	115.4
1423	130.8	1417	140.9	1406	122.3	1456	120
1447	144.7	' SECTION10'		1434	141.1	1485	129.7
' SECTION 9 '		1082	141.1	' SECTION10'		1506	145
1031	145.5	1101	123.5	1062	142.9	' SECTION 7 '	
1055	129.9	1130	113.4	1093	122	1011	145
1081	122.2	1200	111	1136	113.1	1040	126.5
1167	121.1	1264	110.4	1188	112.1	1058	120.4
1272	117.8	1331	110	1269	114.8	1110	116.9
1358	115	1377	119	1339	116.5	1166	116
1418	120.8	1410	140.2	1381	116.9	1260	116
1447	132.9	' SECTION12'		1405	125	1372	118
1463	145	1079	142.5	1430	141.8	1424	120
' SECTION 11'		1102	125.7	' SECTION 12'		1453	127.8
1038	146.5	1125	114	1063	142.6	1479	143.7
1060	131.5	1183	108.6	1085	125.1	' SECTION 9'	
1110	116.8	1264	108.3	1113	116	1003	145.7
1181	116.1	1345	109.6	1183	112.8	1021	130
1252	117.4	1379	120.1	1253	112	1043	121
1343	118	1410	140.6	1318	111.6	1066	116.5
1408	120.6			1369	113.5	1139	116.1
1432	128.8			1402	123.5	1240	114.7
1465	145.3			1428	141	1365	115.7
' SECTION 13'						1416	118.9
1022	147.5					1450	128.1
1050	129.9					1475	143.9
1100	120.5						
1209	118.9						
1317	119.8						
1396	122.5						
1427	132.2						
1450	145						

*Each section is 1m apart. e.g. The distance between section 8 and 10 is 2m.

**The numbers in the first and second column correspond to transverse location along the channel width, and bed elevation respectively.

***Only those data have been given here where the developed channel was straight with no bedforms.

TABLE A2 : Bed Level Measurements (Experimental results) (Cont.)

TEST NO.19A-9MAR94	TEST NO.20A-18MAR94	TEST NO.21A-28MAR94	TEST NO.22A-7APR94	TEST NO.23A-28APR94	TESTNO.24A-5MAY94
'SECTION 8'	'SECTION 8'	'SECTION 8'	'SECTION 8'	'SECTION 8'	'SECTION 6'
1063 146.8	1059 145	1032 146.1	1013 148.1	968 149.9	954 147.3
1078 133.3	1088 125.4	1052 132.8	1035 132.3	996 132	977 133.5
1096 125.2	1115 116.9	1078 121.1	1050 126.4	1040 123.3	1012 121.2
1108 121.6	1143 114.3	1096 117.3	1070 122.2	1141 120.1	1049 116
1145 117.1	1204 113.6	1144 116.3	1115 119.5	1265 116.1	1160 120.1
1208 115.8	1259 112.6	1203 115.2	1198 118.1	1345 118.6	1307 121
1258 115.6	1317 112.4	1303 115.8	1293 118.5	1431 119.6	1442 120
1310 117	1365 114.4	1365 115.6	1388 119.4	1468 126.4	1488 132.5
1357 117.3	1388 120.4	1401 119.5	1422 121.8	1506 146.5	1516 146
1388 119	1410 130.2	1425 128.2	1448 131.4	'SECTION 10'	'SECTION 8'
1412 127.5	1430 144.1	1446 144	1471 145.8	969 149.2	968 147.1
1437 145.7	SECTION 10'	'SECTION 10'	SECTION 10'	1000 130.8	994 131.5
'SECTION 10'	1057 144.6	1034 145	1020 146.7	1037 120.7	1030 120.2
1054 146.3	1072 134	1048 134.5	1029 139	1075 120.1	1147 115.9
1063 137.7	1090 123.6	1065 124.5	1046 129.4	1143 121.4	1272 115.8
1080 127.9	1109 116.9	1081 119.2	1071 120.5	1262 116	1364 119.1
1100 120.8	1156 113.1	1109 117.1	1153 116.3	1378 115.2	1430 120.2
1138 117.7	1198 112.4	1155 117	1246 117.7	1441 119.5	1467 125.8
1183 117	1246 111.8	1224 114.6	1327 117	1477 131.4	1491 136.1
1230 115	1285 112.1	1316 111	1397 118.6	1499 146.1	1507 146
1280 113.9	1320 112.3	1373 114.6	1430 124.1	SECTION 12	SECTION10
1340 114.3	1355 113.3	1404 122.7	1455 135.5	962 150.6	977 146
1378 119	1381 119.4	1427 132.3	1466 145.3	990 131.7	986 138
1396 124	1405 128.2	1442 143.3	SECTION 12'	1032 120.3	1012 125
1413 132.7	1426 143	'SECTION 12'	1010 148.2	1100 117	1064 122.5
1424 144	'SECTION 12'	1036 145.2	1026 136	1202 120.5	1152 121.3
'SECTION 12'	1057 144.5	1053 133.5	1051 125.5	1298 123.6	1272 116.1
1058 145.6	1080 130.2	1066 127.8	1069 121	1386 123.9	1367 109.5
1071 135.8	1107 119.6	1096 119.3	1127 118.8	1440 123.9	1433 113.3
1088 126.7	1125 116.2	1134 114.8	1191 118.5	1470 128.6	1475 127.3
1112 119.1	1157 114.8	1224 115.2	1291 119.6	1493 137.3	1500 145.4
1143 116.4	1210 114.1	1315 117.7	1385 121.7	1507 146.7	
1175 115.1	1272 114.4	1368 117.8	1415 122.3		
1218 115.6	1322 115	1396 118.2	1442 128.5		
1253 116.3	1358 115.5	1422 127.2	1460 136.7		
1288 116.7	1381 118.8	1442 137.3	1472 145.3		
1330 117.8	1411 129.1	1452 145.2			
1370 118.5	1431 143.7				
1388 120.3					
1408 126.5					
1427 138.5					
1436 145.7					

A4

TABLE A2 : Bed Level Measurements (Experimental results) (Cont.).

'TEST NO.25A-11MAY94'	'TEST NO.26A-16MAY94'	'TEST NO.27A-19MAY94'	'TEST NO.28A-6JUN94'	'TEST NO.29A-21JUN94'
SECTION 8'	'SECTION 8'	'SECTION 8'	'SECTION 8'	'SECTION 8'
969 145.7	1059 142.9	1061 141	992 146	990 144.1
1003 126.9	1073 130.6	1082 126.1	1001 138.1	1010 130.8
1049 118.2	1113 114.9	1113 114	1012 131.1	1038 120.4
1162 117.9	1185 112.6	1134 111	1032 121.5	1075 113.2
1271 115.5	1272 113.7	1165 108.8	1052 116	1140 111
1365 112.7	1343 113.9	1222 110.5	1096 111.9	1235 112.8
1439 114.8	1379 119	1281 112.5	1161 113.1	1323 116
1476 123.7	1400 126	1335 113.9	1220 114.8	1388 118.9
1511 144.1	1420 141	1367 113.8	1283 116	1423 119.3
'SECTION 10'	'SECTION 10'	1396 124.3	1380 118.3	1452 124.3
970 145.3	1051 143.9	1419 140.3	1426 119.5	1474 132.9
1000 127.8	1075 125.7	'SECTION 10'	1452 127	1487 142.6
1045 116.2	1105 114.8	1054 141	1466 132.8	'SECTION 10'
1099 114.1	1169 112	1075 126.2	1481 144.7	1003 143.1
1124 117.2	1240 111.4	1100 115.9	'SECTION 10'	1018 132
1190 116.6	1314 112.9	1125 113.3	1001 144.6	1034 126
1330 112.6	1360 114.3	1177 111.9	1017 131.9	1053 119.2
1410 115	1389 123.8	1231 110.7	1043 122	1094 115
1453 120.5	1416 141	1285 110.1	1071 119	1169 113.5
1481 131.1	'SECTION 12'	1337 111.5	1122 117.8	1273 114.2
1500 142.4	1052 143	1361 111.5	1191 115.3	1393 112.8
'SECTION 12'	1075 125.8	1388 122.1	1267 113	1436 114.5
967 145.8	1108 115.9	1414 140	1358 111.4	1458 122.5
996 128.1	1187 112.9	'SECTION 12'	1403 113.3	1477 130.7
1036 118	1282 113.6	1053 143.8	1433 117.2	1495 142.5
1089 114.1	1340 114.7	1073 128.7	1456 125.6	'SECTION 12'
1170 115.2	1370 116.1	1099 117.5	1475 135.6	1010 143.2
1290 118.8	1394 124.1	1114 114.9	1485 145.4	1022 134.6
1371 120	1420 141.3	1142 112.9	'SECTION 12'	1046 124
1440 118.3		1174 112.5	995 145.1	1067 118
1470 128		1199 111.9	1009 135.2	1116 119.8
1496 142.1		1228 112.3	1028 126.6	1182 117.6
		1253 111	1054 119.6	1285 113
		1283 112.8	1105 116.2	1378 113.5
		1310 112.3	1190 115.5	1422 115.2
		1342 114	1282 116.6	1454 121.1
		1365 115	1356 117.3	1476 129.5
		1388 122.3	1414 118.6	1499 143.2
		1418 140	1441 122	
			1463 130.4	
			1476 136.1	
			1487 145.1	

TABLE A2 : Bed Level Measurements (Experimental results) (Cont.)

'TEST NO.30A-20JUL94'		'TEST NO.31A-10AUG94'		'TEST NO.32A-5SEP94'		'TEST NO.33A-19SEP94'		'TEST NO.34A-6OCT94'		'TEST NO.35A-18OCT94'	
'SECTION 8'		'SECTION 8'		'SECTION 8'		'SECTION 8'		'SECTION 8'		'SECTION 8'	
981	144.2	993	142	1058	141.7	1070	139.8	1068	127.8	1083	129.1
1002	131.6	1009	132.1	1066	134.9	1077	132.7	1076	121.6	1095	120.1
1037	117.5	1021	126.9	1076	127.6	1090	124.7	1084	115.9	1118	107.6
1071	111.8	1047	117.4	1092	120.2	1108	116.5	1098	108.4	1142	99
1126	112.3	1080	116.9	1106	115.1	1123	111.2	1117	101	1175	94.4
1190	115	1148	115.6	1121	113.2	1138	110.2	1130	97.5	1226	93.7
1295	118.1	1243	113.3	1140	111.6	1185	108.5	1150	95.5	1263	93.7
1381	120.1	1331	112.7	1170	112	1250	108.9	1182	94.1	1306	97.1
1423	121.9	1391	113.8	1200	112	1300	108	1234	93.6	1335	98.3
1450	125.5	1428	115.7	1224	112.3	1352	109.2	1285	94.1	1354	105.2
1472	133.1	1451	121	1250	111.8	1368	112.6	1314	95.3	1372	112.3
1488	144	1475	130	1270	111.7	1385	119.4	1334	96.4	1395	126.4
'SECTION 11'		1491	141.9	1300	112.4	1399	125.9	1352	99.5	'SECTION 10'	
1002	145.3	SECTION 10'		1344	113.3	1415	139.3	1373	106.4	1086	129.4
1019	134.7	987	143	1372	113.5	'SECTION 10'		1385	111.9	1097	121.7
1046	124.3	1001	133.7	1387	116.7	1068	140	1396	118.3	1114	110.7
1094	124.1	1026	121.5	1404	122.8	1076	131.7	1408	125.4	1137	102
1148	122.6	1050	114.2	1416	129.1	1092	121.3	'SECTION 10'		1150	97.3
1206	119.9	1117	111.4	1424	135	1110	114.5	1069	127.8	1181	94.1
1283	115.2	1213	113.3	1429	139.5	1127	109.2	1084	118.8	1225	93.4
1347	109.7	1340	116.7	'SECTION 10'		1153	108	1098	111	1288	93.8
1385	106.8	1413	118.7	1053	141.1	1190	108.2	1110	105.3	1316	94.6
1414	106.4	1440	119	1059	136.6	1250	107.5	1133	98.2	1336	99.1
1455	116.5	1478	129.9	1074	125.6	1297	108.4	1157	95.3	1362	107
1477	125.3	1489	138	1087	120.4	1331	109.9	1200	93.2	1379	116
1507	143.3	1498	142.2	1105	113.4	1354	109.2	1239	93.1	1396	127.8
'SECTION 13'				1121	113.3	1372	112.8	1278	94	'SECTION 12'	
1001	145.3			1167	110	1393	122.6	1311	93.9	1084	130
1024	131.5			1212	110.4	1405	129.7	1330	95.9	1095	121.8
1057	120.2			1288	110.6	1413	138.3	1350	99	1117	107.9
1096	113.1			1343	112.4	'SECTION 12'		1368	105.1	1144	99
1135	110			1362	112.3	1065	141.2	1385	113	1168	94.3
1177	112.2			1377	115.2	1077	130.7	1406	125.7	1218	90.8
1243	117.1			1390	120.3	1099	119.9	'SECTION 12'		1262	91.1
1305	120.9			1403	125.8	1117	112.9	1072	128.6	1307	93.5
1373	121.8			1415	134.1	1175	110.5	1089	116.9	1339	99.5
1425	122.2			1422	140	1232	110.1	1115	104.2	1369	111.1
1456	126.8			'SECTION 12'		1282	111	1133	97.9	1394	127.5
1481	135			1056	141.2	1327	110.6	1151	93.6		
1496	144.2			1066	133.4	1357	110.6	1182	92.8		
				1086	122.5	1383	118.2	1222	91.7		
				1111	114.2	1400	124.6	1267	91.7		
				1164	113.1	1419	139.1	1278	90.8		
				1209	112.8			1311	92.6		
				1253	112.3			1337	94.8		
				1297	112.1			1360	101.1		
				1337	111.7			1375	107.8		
				1365	113.2			1390	115		
				1378	115.8			1408	125.4		
				1400	123.7						
				1413	132						
				1423	140.7						

TABLE A2 : Bed Level Measurements (Experimental results) (Cont.)

'TEST NO.36A-26OCT94'		'TEST NO.37A-23NOV94'		'TEST NO.38A-5/12/94'		'TEST NO.39A-13/12/94'	
'SECTION 8'		**'SECTION 8'**		**'SECTION 8'**		**'SECTION 8'**	
1080	127.2	1081	129.3	1082	129	1078	127.5
1088	123.5	1090	123.5	1092	121.5	1088	122.3
1102	113.5	1109	110.1	1106	111.7	1102	113.4
1118	105.1	1130	101.3	1119	105	1116	106
1135	100	1152	96.2	1136	98.8	1137	99.3
1156	94.9	1187	93	1158	93.9	1162	93.5
1179	93	1223	90.8	1186	91.7	1185	91.8
1223	91	1260	92.2	1227	89.5	1213	90
1266	90.2	1292	93.2	1263	90	1260	89.7
1287	91.3	1327	97	1288	92	1292	91
1318	94.9	1350	105.3	1315	94.9	1316	94.1
1340	100.3	1365	110.9	1333	98.9	1340	99.3
1364	108.2	1378	118.6	1351	102	1364	106.6
1376	114.7	1393	127.3	1366	106.8	1375	111.7
1394	127	**'SECTION 10'**		1383	116.7	1387	118
'SECTION 10'		1080	130.5	1400	127.4	1404	126
1084	128.5	1093	122.2	**'SECTION 10'**		**'SECTION 10'**	
1093	122.9	1106	113	1081	129.3	1080	127.8
1109	111.5	1125	104.3	1092	121.4	1095	117.4
1131	102.1	1148	97.3	1113	107.6	1113	108.2
1154	95.5	1169	94.9	1127	102	1140	99
1176	93.3	1212	92.8	1148	96.7	1160	94.2
1213	92.3	1259	92.4	1178	91.9	1190	91.5
1268	91.8	1290	92.9	1218	92.8	1220	91.1
1306	92	1314	94.6	1259	92.2	1249	91.9
1328	95.3	1339	100.9	1288	92	1290	91.3
1352	103.7	1358	108.8	1316	92.5	1320	94.5
1367	110.4	1380	122.3	1347	101.1	1340	98.9
1376	115.1	1390	128.8	1363	108.2	1360	105.3
1390	125.5	**'SECTION 12'**		1380	117.4	1379	114.2
1396	127.5	1083	130	1395	127.3	1398	126
'SECTION 12'		1099	118.3	**'SECTION 12'**		**'SECTION 12'**	
1088	127.2	1127	104.4	1083	129.2	1079	128
1097	120.7	1157	96.6	1097	120	1099	115.4
1105	114.7	1202	92.3	1112	109.8	1113	107
1123	105.3	1247	92.3	1133	101	1140	99.5
1144	97.7	1295	93	1157	94.2	1162	93.6
1172	92.8	1324	95.9	1185	91	1200	91.8
1198	91.4	1350	104.5	1233	89.6	1245	90.5
1239	90.3	1372	113.5	1269	90.2	1290	90.6
1281	91.7	1394	128.4	1299	91.4	1316	92.5
1314	92.8			1322	93.6	1340	97.7
1335	97.5			1345	100.5	1357	104
1357	105.5			1370	110	1381	114.6
1377	114			1384	119.2	1398	125
1395	127			1396	127.8	1405	126.8

A7

TABLE A3 : Velocity Measurements using Pitot tube (Channel Centre).

Exp. 32A -Section 8 (5/9/94)		Exp. 33A-Section10 (19/9/94)	
Transverse Location =1.25 m Water Level =137.3mm		Transverse Location =1.25m Water Level =134.9mm	
Location Point (mm)	Velocity (m/s)	Location Point (mm)	Velocity (m/s)
131	0.42	132	0.38
121.5	0.38	125	0.39
117.9	0.36	120	0.37
114.6	0.32	115	0.33
112.5	0.27	110	0.30
		107.7	0.25

Exp. 34A -Section 10 (7/10/94)		Exp. 35A-Section10 (17/10/94)	
Transverse Location =1.25 m Water Level =124.7mm		Transverse Location =1.25m Water Level =127mm	
Location Point (mm)	Velocity (m/s)	Location Point (mm)	Velocity (m/s)
94	0.22	125	0.35
100	0.26	120	0.35
105	0.30	110	0.33
110	0.32	100	0.26
117	0.35	95	0.21
123	0.36		

Exp. 36A -Section 10 (25/10/94)		Exp. 37A-Section10 (23/11/94)	
Transverse Location =1.25 m Water Level =126.1mm		Transverse Location =1.23m Water Level =127.5mm	
Location Point (mm)	Velocity (m/s)	Location Point (mm)	Velocity (m/s)
93	0.24	94	0.21
100	0.30	100	0.27
110	0.33	110	0.31
120	0.36	120	0.34
125.5	0.38	126	0.34

Note: The bed elevation is given in table A2.

TABLE A4 : Bed Shear Measurements along half the channel width.

Exp. 32A-Section 8			Exp. 33A-Section 10		
Transverse Location (m)	Elevation (mm)	Shear Stress (N/m²)	Transverse Location (m)	Elevation (mm)	Shear Stress (N/m²)
1.25	112.5	0.405	1.25	107.7	0.368
1.2	112.5	0.604	1.2	107.6	0.322
1.13	113	0.431	1.15	108.7	0.322
1.1	119	0.396	1.125	112	0.341
1.081	128.3	0.484	1.094	125.5	0.256

Exp. 34A-Section 10			Exp. 35A-Section 10		
Transverse Location (m)	Elevation (mm)	Shear Stress (N/m²)	Transverse Location (m)	Elevation (mm)	Shear Stress (N/m²)
1.25	94	0.304	1.25	95	0.285
1.2	93	0.153	1.2	95	0.313
1.15	96.5	0.313	1.16	97.2	0.216
1.13	100	0.236	1.14	104	0.246
1.11	107.5	0.256	1.12	125.5	0.332
1.095	114.5	0.195			

Exp. 36A-Section 10			Exp. 37A-Section10		
Transverse Location (m)	Elevation (mm)	Shear Stress (N/m²)	Transverse Location (m)	Elevation (mm)	Shear Stress (N/m²)
1.25	93	0.350	1.1	121.7	0.081
1.2	93	0.322	1.12	109.5	0.106
1.18	94	0.313	1.15	99.7	0.206
1.16	98	0.246	1.18	95.2	0.174
1.15	100	0.236	1.23	94	0.285
1.125	109.5	0.275			

Note: The bed elevation, and the channel cross-section are given in table A2.

Table A5. Characteristics of Alternate Bars (Experimental Results).

Test. No.	Bar Wavelength (m)	Bar Height (mm)	Bar Maximum Scour Depth (mm)
2	4.88	52.0	29.6
3	3.56	23.6	17.2
4	3.50	19.1	14.2
5	4.00	16.6	14.04
6	4.50	13.3	7.64
10	3.40	16.5	11.48
11	3.38	17.8	10.61
12	2.25	12.1	5.70
14	3.20	23.4	15.35
15	3.30	18.5	11.61
16	3.00	13.7	8.52
17	4.60	12.7	7.05
18	3.75	24.5	15.3

Note: The bar wavelength values are for one representative bar measured in the channel according to the definition of bar wavelength shown in Fig. 6.1.

TABLE A6 : Pier scour (Experimental results).

Test No	Q (l/s)	Pier set up	Max. scour depth (left pier) (mm)	Max. scour depth (right pier) (mm)
19B	2.5	Single	54.3	N/A
20B	2.5	Single	52.7	N/A
21B	3.0	Single	52.5	N/A
22B	3.5	Single	54.0	N/A
23B	4.0	Single	48.5	N/A
24B	4.0	Double (L=2d)	56.0	57.5
25B	4.0	Double (L=4d)	51.0	54.0
26B	2.5	Double (L=4d)	54.0	54.9
27B	2.5	Double (L=2d)	56.6	55.1
28B	4.0	Six pier (L=2d)	61.5	59.3
34B	2.5	Double (L=4d)	57.7	58.7
36B	2.5	Double (L=2d)	65.1	67.7
38B	2.5	Single pier	55.6	N/A

TABLE A7 : Abutment scour (Experimental results).

Test No	Q (l/s)	Abutment set up	Max. scour depth (left abutment) (mm)	Max. scour depth (right abutment) (mm)
29C	4.0	One side of channel	78.7	N/A
30C	4.0	Both sides of channel	87.4	74.8
31C	4.0	Both sides of channel	40.0	48.6
32C	2.5	Both sides of channel	66.2	58.4
33C	2.5	Both sides of channel	33.1	32.9
35C	2.5	Both sides of channel	22.7	24.9
37C	2.5	One side of channel	49.7	N/A
39C	2.5	One side of channel	96.3	N/A

BED MATERIAL SIEVE ANALYSIS
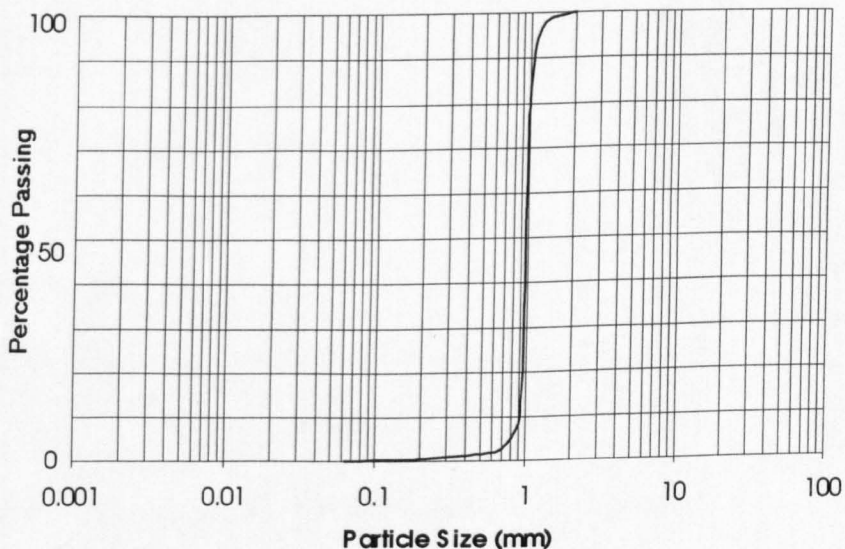
Figure A1. Particle size distribution of the bed material.
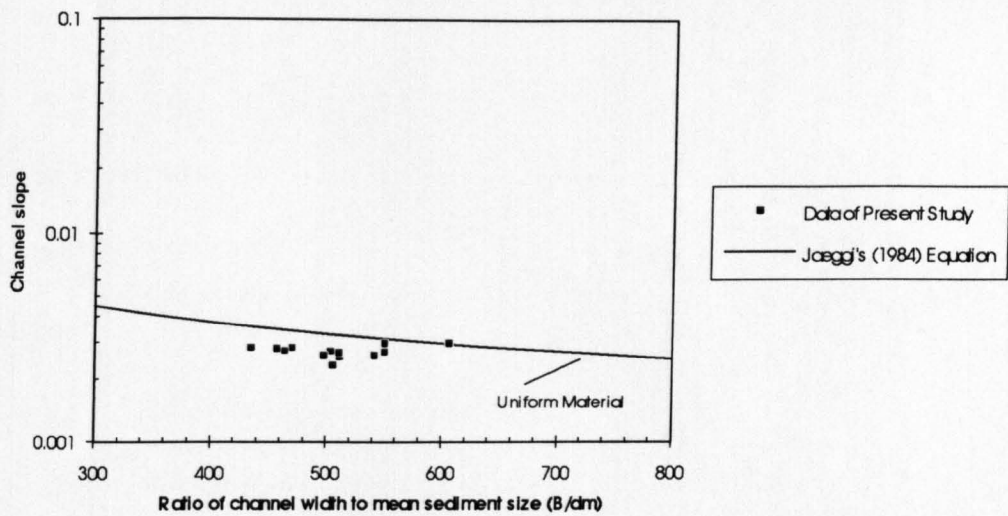
Figure A2. Comparison of Jaeggi's (1984) Criterion for development of alternate bars with the data of present study.
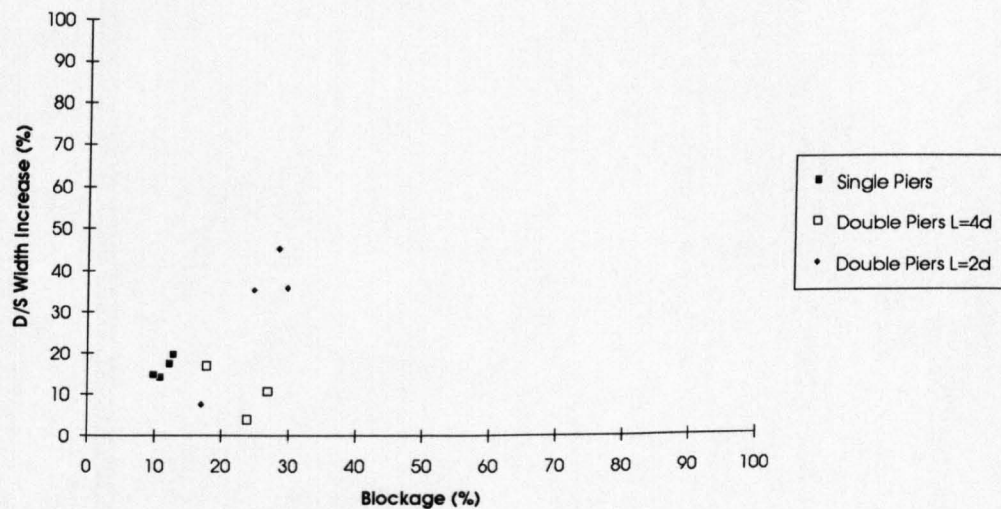

Figure A3. Pier blockage (%) against channel downstream width increase (%).
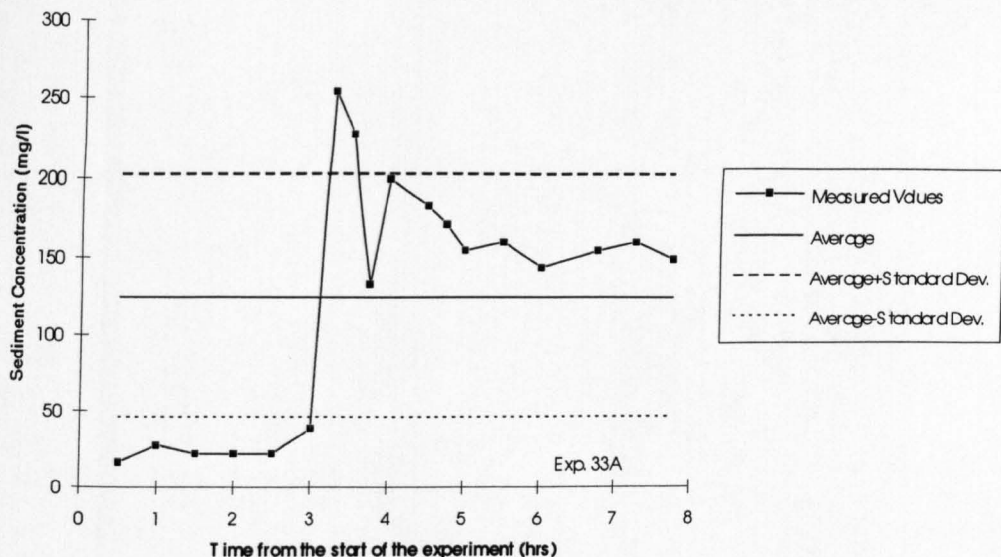
Figure A4. Time series of sediment concentration for a typical experiment.
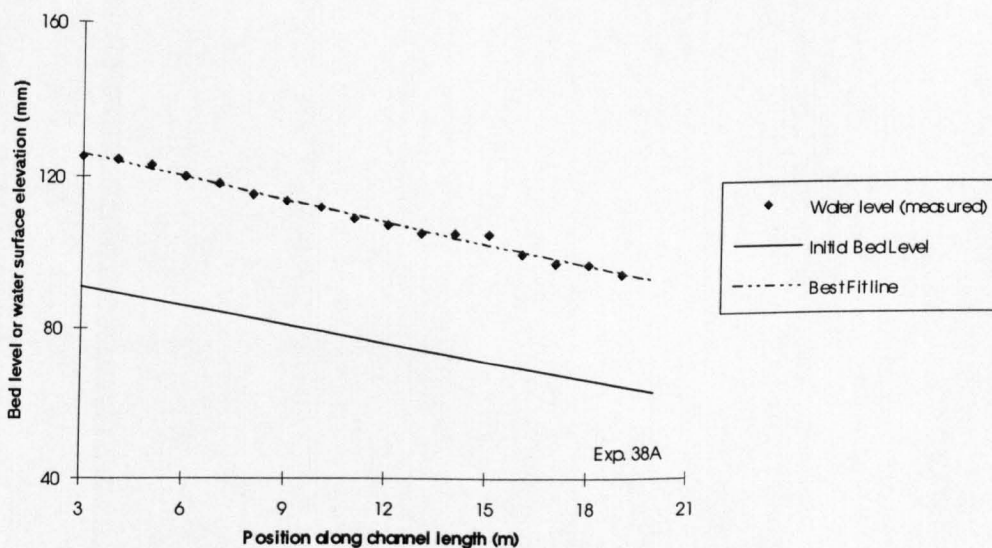
Figure A5. Water surface and initial bed profile for a typical experiment.